THE UNIVERSITY OF HULL

DEVELOPMENT OF PORPHYRIN-ANTIANGIOGENIC ANTIBODY IMMUNOCONJUGATES FOR PHOTODYNAMIC THERAPY

A thesis submitted for the Degree of Doctor of Philosophy in the University of Hull

by

Aaron Bullous, MChem

December 2010

Acknowledgements

I would like to convey my deepest gratitude to my supervisor Dr Ross Boyle, for his advice and support during my research project. My thanks go to all the students and personnel I have shared laboratory space with throughout the project, for general advice, encouragement and interesting conversations. Among them, I would especially like to express my appreciation to Dr Cristina Alonso and Dr Chris Welch, for their continuous help and support. I would also like to thank Dr Steve Archibald and Carol Kennedy for providing chemicals, glassware and equipment throughout the project. Finally, I would like to acknowledge the generous funding of this project by the European Commission (FP6-2005-LIFESCIHEALTH-7).

Abstract

Photodynamic therapy is a novel cancer treatment, involving the combination of light, photosensitiser and molecular oxygen to produce cytotoxic species. Currently, commercially available photosensitisers, including Photofrin® and Foscan®, only exhibit a passive selectively towards cancerous tissue. Therapeutically, this results in a variety of unfavourable characteristics, obstructing PDT from becoming a more viable cancer treatment. Research has been directed towards improving the pharmacokinetic and biodistribution profiles of photosensitisers, which can be achieved by conjugating the photosensitiser moiety to a biomolecule which has affinity for the diseased tissue; these 3rd generation photosensitisers include photoimmunoconjugates.

Three synthetic routes were developed, with the aim of producing novel bioconjugatable porphyrins, which could be subsequently conjugated to cysteine residues expressed by a suitable monoclonal antibody (SIP(L19)).

Two cationic, thiol reactive photosensitisers were synthesised and successfully conjugated to SIP(L19) in a reproducible manner, affording well defined immunoconjugates, which retained both the immunoreactivity of the antibody moiety and the photoactivity of the photosensitiser. The effect of the length and hydrophilicity of the linker connecting the photosensitiser and bioconjugatable group was investigated, and it was observed that the photoactivity of the immunoconjugate was enhanced using a longer, hydrophilic chain.

Synthetic routes leading to the production of bioconjugatable porphyrin dimers, and photosensitisers from symmetrical porphyrin, were developed, but failed to yield final products.

Contents

Chapter 1: Introduction……...1

1.1 Photodynamic therapy……...1

1.1.1 Photochemistr……2

1.1.3 Photosensitisers……...5

1.2 Antibodies and associated fragments……7

1.2.1 SIP(L19)……..9

1.2.2 Strategies for conjugating photosensitisers to monoclonal antibodies……..10

1.2.2.1 Carbodiimide coupling……11

1.2.2.2 Activated esters……...15

1.2.2.3 Reductive amination……26

1.2.2.4 Isothiocyanate conjugation……..29

1.2.2.5 Maleimide conjugation……32

1.2.2.6 Acryloyl conjugation……...34

1.2.3 Conjugations using polymeric linkers……35

1.2.3.1 Dextran……35

1.2.3.2 Polyvinyl alcohol……38

1.2.3.3 Polylysine……41

1.2.3.4 *N*-(2-hydroxypropyl)methacrylamide……45

1.3 Cysteine reactive functionalities……50

1.3.1 Maleimide……...50

1.4 Synthetic overview……53

Chapter 2: Functionalisation of symmetrical porphyrins……54

2.1 Introduction……...54

2.2 Porphyrins……..54

2.3 Porphyrin synthesis……56

2.3.1 Adler-Longo porphyrin synthesis……...56

2.3.2 Lindsey porphyrin synthesis……...59

2.4 Functionalising the β-position of a symmetrically substituted porphyrin…….61

2.4.1 Halogenation……...61

2.4.2 Nitration……..61

2.4.3 Formylation……63

2.5 Synthetic strategy……..67

2.5.1 2-Formyl-5,10,15,20-tetraphenylporphyrin (3)……..69

2.6 Reductive Amination……70
2.6.1 Reductive amination synthetic strategy……..71
2.6.2 Attempted reductive aminations involving alkyl diamines……71
2.6.3 Reductive amination reaction involving aniline……76
2.6.4 Reductive aminations involving aryl amine derivatives……77
2.6.5 Reductive amination using methyl 4-aminobenzoate……83
2.7 Formylation of porphyrins bearing water solubilising functionalities in the meso-positions……...92
2.7.1 Attempted formylation of tetra(4-pyridyl)porphyrin (12)……..94
2.7.2 Attempted formylation of tetra(3,5-dimethoxyphenyl)porphyrin (14)……...95
2.8 Summary / further work……95
Chapter 3: Synthesis of immunoconjugate bearing a linker between photosensitiser and targeting moiety……...96
3.1 Introduction……...96
3.2 Synthesis of unsymmetrical porphyrins……97
3.2.1 Mixed condensation porphyrin synthesis……...97
3.2.2 MacDonald porphyrin synthesis..……99
3.2.3 Polymer supported synthesis of mono-functionalised porphyrin……101
3.3 Porphyrins bearing amino functionalities……103
3.4 Porphyrins bearing carboxyl functionalities……107
3.5 Synthetic strategy involving addition of SMCC to 5-(4-aminophenyl)-10,15,20-tri-(4-pyridyl)porphyrin (17)……110
3.5.1 Attempted addition of SMCC to 5-(4-aminophenyl)-10,15,20-tri-(4-pyridyl)porphyrin (17)……...112
3.6 Synthetic strategy involving synthesis of porphyrin bearing an alkyl chain terminating with a maleimide bioconjugatable group……...113
3.6.1 Synthesis of 5-(4-((6-*tert*-butylcarbamate)hexyl-1-amino-*N*-carbonyl)phenyl)10,15,20-tri-(4-pyridyl)porphyrin (20)……...114
3.6.2 Synthesis of 5-(4-(6-(4-(*N*-maleimidomethyl)cyclohexane-1-amido)hexyl-1-amino-*N*-carbonyl)phenyl)-10,15,20-tri-(4-pyridyl)porphyrin (21)……..120
3.6.3 Synthesis of 5-(4-(6-(4-(*N*-maleimidomethyl)cyclohexane-1-amido)hexyl-1-amino-*N*-carbonyl)phenyl)-10,15,20-tri-(4-*N*-methyl-pyridyniumyl)porphyrin triiodide (22)……..123
3.7 Synthesis of photosensitisers PS3 and PS4……125
3.8 Photoimmunoconjugates……126

3.8.1 Photoimmunoconjugate preparation……126
3.8.1 Conjugation to SIP(L19)……..127
3.8.2 Photoimmunoconjugate characterisation……..127
3.8.3 Photoimmunoconjugate Immunoreactivity……..131
3.8.4 Photoimmunoconjugate photoactivity……..132
3.9 Summary / further work……..134
Chapter 4: Preparation of immunoconjugate bearing a PEG linker……..135
4.1 Introduction……135
4.2 Polyethylene glycol (PEG)……..135
4.3 Properties of PEGs……...136
4.4 Porphyrins functionalised with PEG moieties……138
4.5 Synthetic strategy: synthesis of a hydrophilic porphyrin bearing a PEG chain terminating in a maleimide group……..143
4.5.1 Synthesis of 5-(4-(23-(*tert*-butylcarbamate)-3,6,9,12,15,16,21-heptaoxadocosyl-1-amino-*N*-cabonyl)phenyl)-10,15,20-tri(4-pyridyl)porphyrin (23)……145
4.5.2 Synthesis of 5-(4-(23-(4-(*N*-maleimidomethyl)cyclohexane-1-amido)-3,6,9,12,15,18,21-heptaoxadocosyl-1-amino-*N*-cabonyl)phenyl)-10,15,20-tri(4-pyridyl)porphyrin (24)……...149
4.5.3 Synthesis of 5-(4-(23-(4-(*N*-maleimidomethyl)cyclohexane-1-amido)-3,6,9,12,15,18,21-heptaoxadocosyl-1-amino-*N*-cabonyl)phenyl)-10,15,20-tri(4-*N*-methyl-pyridyniumyl)porphyrin triiodide (25)……..153
4.6 Photoimmunoconjugates……155
4.6.1 Photoimmunoconjugate characterisation……..156
4.6.2 Photoimmunoconjugate characterisation……..158
4.7 Summary / further work……..160
Chapter 5: Towards a bioconjugatable porphyrin dimer……...161
5.1 Introduction……161
5.2 Porphyrin dimers……161
5.2.1 Porphyrin dimer synthetic aims……161
5.2.2 Suzuki coupling……163
5.2.3 Click chemistry……168
5.3 Trans-substituted porphyrins……...174
5.4 Synthetic strategy: porphyrin dimer via Suzuki coupling……...176

5.4.1 Synthesis of 5-(4-acetamidophenyl)-10,20-di-(4-pyridyl)-15-(4-bromophenyl)porphyrin (27)……178
5.4.2 Attempted synthesis of (5-(4-(4,4,5,5-tetramethyl-1,3,2-dioxaborinan-2-yl)phenyl)-10,15,20-tri-(4-pyridyl)porphyrinato) zinc(II)……181
5.5 Synthetic strategy: porphyrin dimer by click coupling……...188
5.5.1 Synthesis of (5-(4-acetamidophenyl)-10,20-di-(4-pyridyl)-15-(4-((trimethylsilyl)ethynyl)phenyl)porphyrinato) zinc(II) (34)……190
5.5.2 Synthesis of (5-(4-azidophenyl)-10,15,20-tri-(4-pyridyl)porphyrinato) zinc(II) (35)……194
5.5.3 Attempted synthesis of 5-(4-((4-trimethylsilyl)-1,2,3-triazole)phenyl)-10,15,20-tri-(4-pyridyl)porphyrin……..198
5.6 Summary/further work……199
Chapter 6: Experimental……200
6.1 Synthesis of 5,10,15,20-tetraphenylporphyrin (1)……...202
6.2 Synthesis of (5,10,15,20-tetraphenylporphyrinato)copper(II) (2)……...203
6 .3 Synthesis of 2-formyl-5,10,15,20-tetraphenylporphyrin (3)……..204
6.4 Attempted synthesis of tert-butyl(3-((5,10,15,20-tetraphenylporphyrin-2-ylmethyl)amino)propyl)carbamate……205
6.5 Attempted synthesis of tert-butyl(12-((5,10,15,20-tetraphenylporphyrin-2-ylmethyl)-amino)dodecyl)carbamate……208
6.6 Synthesis of (2-formyl-5,10,15,20-tetraphenylporphyrinato)copper(II) (4)…...209
6.7 Attempted synthesis of tert-butyl(3-((((5,10,15,20-tetraphenylporphyrinato)copper(II))-2-ylmethyl)-amino)propyl)carbamate…….210
6.8 Attempted synthesis of tert-butyl(12-((((5,10,15,20-tetraphenylporphyrinato)copper(II))-2-ylmethyl)-amino)dodecyl)carbamate……..211
6.9 Synthesis of phenyl-(5,10,15,20-tetraphenylporphyrin-2-ylmethyl)amine (5)...212
6.10 Synthesis of succinimidyl-4-aminobenzoate (6)……...213
6.11 Synthesis of tert-butyl(3-(4-aminobenzamido)propyl)carbamate (7)……214
6.12 Synthesis of tert-butyl(12-(4-aminobenzamido)dodecyl)carbamate (8)……...215
6.13 Attempted synthesis of tert-butyl(3-(4-((5,10,15,20-tetraphenylporphyrin-2-ylmethyl)-amino)benzamido)propyl)carbamate……216
6.14 Attempted synthesis of tert-butyl(12-(4-((5,10,15,20-tetraphenylporphyrin-2-ylmethyl)-amino)benzamido)dodecyl)carbamate……..217

6.15 Attempted synthesis of tert-butyl(3-(4-((((5,10,15,20-tetraphenylporphyrinato)copper(II))-2-ylmethyl)-amino)benzamido)propyl)carbamate……218
6.16 Attempted synthesis of tert-butyl(12-(4-((((5,10,15,20-tetraphenylporphyrinato)copper(II))-2-ylmethyl)-amino)benzamido)dodecyl)carbamate……...219
6.17 Synthesis of methyl 4-((((5,10,15,20-tetraphenylporphyrinato)copper(II))-2-ylmethyl)amino)benzoate (9)……220
6.18 Synthesis of methyl 4-((5,10,15,20-tetraphenylporphyrin-2-ylmethyl)amino)benzoate (10)……..221
6.19 Synthesis of 4-((5,10,15,20-tetraphenylporphyrin-2-ylmethyl)amino)benzoic acid (11)……223
6.20 Synthesis of 5,10,15,20-tetra-(4-pyridyl)porphyrin (12)……...224
6.21 Synthesis of (5,10,15,20-tetra(4-pyridyl)porphyrinato) copper(II) (13)……...225
6.22 Attempted synthesis of 2-formyl-5,10,15,20-tetra(4-pyridyl)porphyrin……...226
6.23 Synthesis of 5,10,15,20-tetra(3,5-dimethoxyphenyl)porphyrin (14)……227
6.24 Synthesis of (5,10,15,20-tetra(3,5-dimethoxyphenyl)porphyrinato) copper(II) (15)……228
6.25 Attempted synthesis of 2-formyl-5,10,15,20-tetra(3,5-dimethoxyphenyl)porphyrin……..229
6.26 Synthesis of 5-(4-acetamidophenyl)-10,15,20-tri(4-pyridyl)porphyrin (16)….230
6.27 Synthesis of 5-(4-aminophenyl)-10, 15, 20-tri-(4-pyridyl)porphyrin (17)……231
6.28 Attempted synthesis of 5-(4-((N-maleimidomethyl)cyclohexane-1-amido)phenyl)-10,15,20-tri(4-pyridyl)porphyrin……..232
6.29 Synthesis of 5-(4-carboxyphenyl)-10,15,20-tri-(4-pyridy)porphyrin (18)……233
6.30 Synthesis of 5-(4-(succinimidyl-N-oxycarbonyl)phenyl)-10,15,20-tri-(4-pyridyl)porphyrin (19)……...234
6.31 Synthesis of 5-(4-((6-tert-butylcarbamate)hexyl-1-amino-N-carbonyl)phenyl)10,15,20-tri-(4-pyridyl)porphyrin (20)……..235
6.32 Synthesis of 5-(4-(6-(4-(N-maleimidomethyl)cyclohexane-1-amido)hexyl-1-amino-N-carbonyl)phenyl)-10,15,20-tri-(4-pyridyl)porphyrin (21)……..237
6.33 Synthesis of 5-(4-(6-(4-(N-maleimidomethyl)cyclohexane-1-amido)hexyl-1-amino-N-carbonyl)phenyl)-10,15,20-tri-(4-N-methyl-pyridyniumyl)porphyrin triiodide (22)……..239

6.34 5-(4-(23-(tert-butylcarbamate)-3,6,9,12,15,16,21-heptaoxadocosyl-1-amino-N-cabonyl)phenyl)-10,15,20-tri(4-pyridyl)porphyrin (23)……241
6.35 5-(4-(23-(4-(N-maleimidomethyl)cyclohexane-1-amido)-3,6,9,12,15,18,21-heptaoxadocosyl-1-amino-N-cabonyl)phenyl)-10,15,20-tri(4-pyridyl)porphyrin (24)……243
6.36 5-(4-(23-(4-(N-maleimidomethyl)cyclohexane-1-amido)-3,6,9,12,15,18,21-heptaoxadocosyl-1-amino-N-cabonyl)phenyl)-10,15,20-tri(4-N-methyl-pyridyniumyl)porphyrin triiodide (25)……..245
6.37 Synthesis of 5-(4-pyridyl)dipyrromethane (26)……246
6.38 Synthesis of 5-(4-acetamidophenyl)-10,20-di-(4-pyridyl)-15-(4-bromophenyl)porphyrin (27)……247
6.39 Synthesis of 5-(4-bromophenyl)-10,15,20-tri-(4-pyridyl)porphyrin (28)…….249
6.40 Synthesis of (5-(4-bromophenyl)-10,15,20-tri-(4-pyridyl)porphyrinato) zinc(II) (29)……250
6.41 Synthesis of 5-(4-iodophenyl)-10,15,20-tri-(4-pyridyl)porphyrin (30)…….251
6.42 Synthesis of (5-(4-iodophenyl)-10,15,20-tri-(4-pyridyl)porphyrinato) zinc(II) (31)……252
6.43 Attempted synthesis of (5-(4-(4,4,5,5-tetramethyl-1,3,2-dioxaborinan-2-yl)phenyl)-10,15,20-tri-(4-pyridyl)porphyrinato) zinc(II)……253
6.45 Synthesis of 4-((trimethylsilyl)ethynyl)benzaldehyde (32)……...257
6.46 Synthesis of 5-(4-acetamidophenyl)-10,20-di-(4-pyridyl)-15-(4-((trimethylsilyl)ethynyl)phenyl)porphyrin (33)……258
6.47 Synthesis of (5-(4-acetamidophenyl)-10,20-di-(4-pyridyl)-15-(4-((trimethylsilyl)ethynyl)phenyl)porphyrinato) zinc(II) (34)……260
6.48 Synthesis of (5-(4-azidophenyl)-10,15,20-tri-(4-pyridyl)porphyrinato) zinc(II) (35)……261
6.49 Synthesis of 5-(4-azidophenyl)-10,15,20-tri-(4-pyridyl)porphyrin (36)……...262
6.50 Attempted synthesis of 5-(4-((4-trimethylsilyl)-1,2,3-triazole)phenyl)-10,15,20-tri-(4-pyridyl)porphyrin……263
References……264

Schemes

Scheme 1: Hematoporphyrin carbodiimide coupling. 12
Scheme 2: General NHS activated ester strategy for bioconjugates involving chlorin e_6 or Verteporfin®. 16
Scheme 3: TrTAPP conjugation to an antibody by the NHS-activated ester approach. 22
Scheme 4: TrTAPP conjugation to modified antibody. 23
Scheme 5: Modification of Foscan® and conjugation to mAb using TFP activated ester strategy.' 24
Scheme 6: Reductive amination reaction between derivatised chlorin e_6 and oxidised antibody. 26
Scheme 7: Coupling of thiolated antibody to a maleimido porphyrin. 33
Scheme 8: Bioconjugation involving the acryloyl functionality. 34
Scheme 9: Synthesis of dextran immunoconjugates.' 36
Scheme 10: Synthesis of immunoconjugate using polyvinyl alcohol as a polymeric linker. 39
Scheme 11: Cationic and anionic lysine based immunoconjugates. 42
Scheme 12: Synthesis of chlorin e_6 monoethylenediamine-HPMA-co-polymer 1-IgG. 45
Scheme 13: Synthesis of chlorin e_6 monoethylenediamine-HPMA-co-polymer 2-IgG_{ox}. 46
Scheme 14: Synthesis of chlorin e_6 monoethylenediamine-HPMA-co-polymer 2-Fab'. 47
Scheme 15: Synthesis of chlorin e_6 monoethylenediamine-HPMA-co-polymer 2-IgG. 48
Scheme 16: Formation of HPMA co-polymer immunoconjugate. 49
Scheme 17: Synthesis of 5,10,15-tris(4-methoxycarbonylphenyl)-20-(4-(2-(3-maleimido)propionamido)phenyl)porphyrin. 51
Scheme 18: Mechanism for the formation of a porphyrin using Adler-Longo conditions. 58
Scheme 19: Examples of symmetrical porphyrins synthesised under Adler-Longo condtions.' 59
Scheme 20: Porphyrins synthesised under Lindsey condtions. 60
Scheme 21: Nitration of the copper(II) complex of TPP. 62
Scheme 22: Nitration of tetraheteroarylporphyrins. 62
Scheme 23: Optimised formylation reaction conditions. 64
Scheme 24: Formation of porphyrin-fullerene dyad. 64

Scheme 25: Modified Horner-Wadsworth-Emmons reactions of 2-formyl TPP. 65
Scheme 26: Reductive amination of the nickel(II) complex of 2-formyl TPP. 66
Scheme 27: Reductive amination of 2-formyl TPP. 66
Scheme 28: Reductive amination synthetic strategy for mono functionalisation of porphyrins. 68
Scheme 29: Illustration of the reductive amination reaction. 70
Scheme 30: Attempted reductive amination employing alkyl diamines. 75
Scheme 31: Reductive amination of 3 with aniline. 76
Scheme 32: Attempted reductive aminations using 3 and 4 with aryl linkers. 77
Scheme 33: Synthetic strategy involving methyl 4-aminobenzoate. 84
Scheme 34: Hypothetical mechanisms for base cleavage of 10 leading to the formation of 3. 89
Scheme 35: Attempted formylation reactions involving porphyrins with water solubilising groups in the *meso*-positions. 93
Scheme 36: Examples of unsymmetrical porphyrins synthesised using Adler-Longo conditions.' 98
Scheme 37: Unsymmetrical porphyrins synthesised using Lindsey conditions.' 99
Scheme 38: Example of MacDonald porphyrin synthesis. 99
Scheme 39: Theoretical synthesis of multifunctional porphyrin using 2+2 carbinol strategy. 100
Scheme 40: Porphyrins synthesised using the carbinol intermediate.' 101
Scheme 41: Polymer supported synthesis of mono-functionalised porphyrin. 102
Scheme 42: Amino porphyrins from acetamido,' nitro, and phthalimide analogues. ... 104
Scheme 43: Synthesis of porphyrin-corrole adduct. 106
Scheme 44: DCC coupling of porphyrin and phosphonate derivatives. 108
Scheme 45: Reaction between *N*-hydroxysuccinimide activated porphyrin and PEG derivative. 109
Scheme 46: Synthetic strategy involving addition of SMCC to 5-(4-aminophenyl)-10,15,20-tri-(4-pyridyl)porphyrin. 111
Scheme 47: Synthesis of hydrophilic porphyrin bearing an alkyl chain terminating with a maleimide group. 114
Scheme 48: Synthesis of 5-(4-maleimidophenyl)-10,15,20-tri-(4-*N*-methyl-pyridiniumyl)porphyrin triiodide (PS4). 125
Scheme 49: Porphyrin-peptide conjugates. 139
Scheme 50: PEGylated 5,10,15,20-tetra(4-hydroxyphenyl)porphyrin. 140

Scheme 51: PEGylation of 5,10,15,20-tetra(2,3,4,5,6-pentafluorophenyl)porphyrin derivatives. 141
Scheme 52: Synthesis of porphyrin dimer with PEG connection. 142
Scheme 53: Synthesis of the hydrophilic porphyrin bearing a PEG chain terminating with a maleimide group..... 144
Scheme 54: Porphyrin dimer synthesis. 165
Scheme 55: Synthesis of bis(5-4-(5,15-dimesitylporphyrinatozinc(II)-10-yl)phenyl)dipyrro)palladium (II). 166
Scheme 56: Evaluation of different reaction conditions for the synthesis of a porphyrin dimer. 171
Scheme 57: Syntheses of a porphyrin-thiaporphyrin adduct..... 173
Scheme 58: Proposed synthesis of porphyrin dimer using Suzuki coupling. 177
Scheme 59: Attempted Suzuki coupling involving 31. 183
Scheme 60: Attempted boronation of 29. 187
Scheme 61: Proposed synthesis of porphyrin dimer using ‘click’ chemistry. 189
Scheme 62: Synthesis of 36..... 196
Scheme 63: Attempted ‘click’ reaction..... 198

Figures

Figure 1: Modified Jablonski diagram illustrating PDT photochemistry.’..... 2
Figure 2: Photofrin® and Foscan®. 6
Figure 3: Schematic representation of antibodies and related fragment. 7
Figure 4: Structure of palladium(II) coproporphyrin. 14
Figure 5: Hydrophilic photosensitiser bearing an isothiocyanate group..... 29
Figure 6: Dual functional porphyrins. 53
Figure 7: Porphyrin nomenclature. 54
Figure 8: Retro-synthesis of porphyrin. 56
Figure 9: TPP reaction stoichiometry. 57
Figure 10: Range of adducts produced via reductive amination of 2-formyl TPP. 67
Figure 11: Crude ^{1}H NMR of suspected *tert*-butyl(3-((5,10,15,20-tetraphenylporphyrin-2-ylmethyl)amino)propyl)carbamate. 74
Figure 12: ^{1}H NMR and ^{13}C NMR spectrum’s of compound 6. 79
Figure 13: Mass spectrum of 9. 85
Figure 14: ^{1}H NMR spectrum of 10. 87

Figure 15: ^{1}H NMR spectrum of compound 11. 91
Figure 16: Representation of porphyrins produced during a mixed condensation porphyrin synthesis. 97
Figure 17: ^{1}H NMR spectrum of 20. 117
Figure 18: ^{1}H NMR COSY of 20. 118
Figure 19: ^{1}H NMR spectrum of 21. 122
Figure 20: ^{1}H NMR spectrum of 22. 124
Figure 21: Hydrophilic porphyrins used for conjugations with SIP(L19) 126
Figure 22: SDS-PAGE of SIP(L19), PS4-SIP(L19) and 22- SIP(L19). 128
Figure 23: MALDI-TOF/TOF spectra for (A) SIP(L19), (B) 22-SIP(L19)..... 129
Figure 24: Size exclusion chromatography profile of SIP(L19) and 22-SIP(L19). 130
Figure 25: BIAcore analysis of photoimmunoconjugates and SIP(L19). 132
Figure 26: *In vitro* photocytotoxicity assay of photoimmunoconjugates on LM fibroblasts. 133
Figure 27: Illustrations of the PS4-SIP(L19) and 22-SIP(L19)..... 134
Figure 28: Hydroxide initiated anionic ring-opening polymerisation of ethylene oxide. 135
Figure 29: PEGylated TPP derivatives. 138
Figure 30: ^{1}H NMR spectrum of 23. 147
Figure 31: ^{1}H NMR spectrum of 24. 150
Figure 32: Aliphatic section of the 2D COSY of 24. 151
Figure 33: ^{1}H NMR spectrum of 25. 154
Figure 34: Hydrophilic photosensitisers PS3, 22 and 25. 155
Figure 35: MALDI-TOF/TOF spectra for (A) SIP(L19), (B) 25-SIP(L19)..... 156
Figure 36: Size exclusion chromatography profile of SIP(L19) and 25-SIP(L19). 157
Figure 37: Phototoxicity of photoimmunoconjugates and SIP(L19) on antigen-positive (LM fibroblasts) and antigen-negative (CHO-S, HEK293T) cell lines. 159
Figure 38: *In vitro* phototoxicity assay of PS4-SIP(L19) (black ▲), 22-SIP(L19) (red ■) carried out on LM fibroblasts using MTS assay. 160
Figure 39: Retro-synthesis of bioconjugatable porphyrin dimer. 162
Figure 40: Suzuki catalytic cycle. 163
Figure 41: Suzuki couplings involving metal complexes of 5-(4-bromophenyl)-10,15,20-(4-pyridyl)porphyrin. 167
Figure 42: Click catalytic cycle. 169
Figure 43: Scrambling of poly-pyrrolic intermediate. 175

Figure 44: ^{1}H NMR spectrum of 27. 180
Figure 45: Mass spectrum of 27. 180
Figure 46: ^{1}H NMR and ^{11}B NMR of spectra of suspected (5-(4-(4,4,5,5-tetramethyl-1,3,2-dioxaborinan-2-yl)phenyl)-10,15,20-tri-(4-pyridyl)porphyrinato) zinc(II). 186
Figure 47: ^{1}H NMR spectrum of 34. 193
Figure 48: ^{1}H NMR spectrum of 35. 195
Figure 49: ^{1}H NMR spectrum of 36. 197

Tables

Table 1: Reaction conditions used for the synthesis of 20. 116
Table 2: Reaction conditions used for the synthesis of 23. 145
Table 3: Attempted Suzuki coupling reactions involving bis(pinacolato)diborane and 29. 182
Table 4: Attempted Suzuki coupling reactions involving bis(pinacolato)diborane and 31. 184
Table 5: Attempted boronation reactions involving 29 or 31 and bis(pinacolato)diborane. 255

Abbreviations

AcOH	acetic acid
AIBN	azobisisobutyronitrile
$AlPcS_4$	aluminium tetrasulfophthalocyanine
$AlPcS_4A_1$	aluminium tetrasulfophthalocyanine monosulfonamide product
Boc	*tert*-butyloxycarbonyl
BSA	bovine serum albumin
cmAb	chimeric monoclonal antibody
COSY	homonuclear correlation spectroscopy
DABCO	1,4-diazabicyclo(2,2,2)octane
DCC	*N,N'*-dicyclohexylcarbodiimide
DCM	dichloromethane
DDQ	2,3-dichloro-5,6-dicyanobenzoquinone
DEAD	diethyl azodicarboxylate

DIEA	*N,N'*-diisopropylethylamine
DMAP	4-dimethylaminopyridine
DMF	*N,N'*-dimethylformamide
DMSO	dimethylsulfoxide
DNA	deoxyribonucleic acid
EDB	extra domain B
EDCI/EDC	1-ethyl-3-(3-dimethylaminopropyl) carbodiimide
EDTA	ethylenediaminetetraacetate
EGFR	epidermal growth factor receptor
ELISA	enzyme-linked immunosorbent assay
EtOH	ethanol
FMP	2-fluoro-1-methyl pyridinium toluene-4-sulfonate
FPCL	fibroblast-populated collagen lattice
HEPES	(4-(2-hydroxyethyl)-1-piperazineethanesulfonic acid
HMBC	heteronuclear multiple bond coherence
HMPA	*N*-(2-hydroxypropyl)methacrylamide
HOBt	hydroxybenzotriazole
HPLC	high performance liquid chromatography
HRMS	high resolution mass spectrometry
IgG	immunoglobulin G
IUPAC	international union of pure and applied chemistry
mAb	monoclonal antibody
mal	maleimide
MeI	methyl iodide
MeOH	methanol
mmAb	murine monoclonal antibody
MRSA	methicillin-resistant *Staphylococcus aureus*
MTS	(3-(4,5-dimethylthiazol-2-yl)-5-(3-carboxymethoxyphenyl)-2-(4-sulfophenyl)-2H-tetrazolium)
NEt_3	triethylamine
NHS	*N*-hydroxysuccinimide
NMR	nuclear magnetic resonance
PBS	phosphate buffered saline
PDT	photodynamic therapy
PEG	polyethylene glycol

PVA	polyvinyl alcohol
ROS	reactive oxygen species
RT	room temperature
scFv	single chain fragment variable
SDS	sodium dodecyl-sulphate
SDS-PAGE	sodium dodecyl-sulphate polyacrylamide gel electrophoresis
SIAB	*N*-succinimidyl(4-iodoacetyl)aminobenzoate
SIP	small immune protein
SMBS	sulfo-*m*-maleimidobenzoyl-*N*-hydroxysuccinimide ester
SMCC	4-(*N*-maleimidomethyl)cyclohexanecarboxylic acid *N*-hydroxysuccinimide ester
SMP	*N*-succinimidyl-3-maleimidopropionate
SPR	surface plasmon resonance
TBTA	tris((1-benzyl-1H-1,2,3-triazol-4-yl)methyl)amine
TBTU	*O*-(benzotriazol-1-yl)-*N*,*N*,*N'*,*N'*-tetramethyluronium tetrafluoroborate
TCEP	tris(2-carboxyethyl)phosphine
TDP	1,1-thiocarbonyldi-2,2`-pyridone
TEA	triethylamine
TFA	trifluoroacetic acid
TFP	tetrafluorophenol
THF	tetrahydrofuran
TLC	thin layer chromatography
TOF	time of flight
TPP	5,10,15,20-tetraphenylpoprhyrin
TrTAPP	5-(2-*N*-triphenylmethylaminophenyl)-10,15,20-tri(2-aminophenyl)porphyrin
UV	ultra violet

Chapter 1: Introduction

1.1 Photodynamic therapy

Photodynamic therapy (PDT) is a therapeutic concept, which combines a light activated drug; known as a photosensitiser, visible light and molecular oxygen, leading to the formation of reactive oxygen species (ROS), which can adversely affect surrounding cells.[1,2] PDT has been utilised for the treatment of certain cancers, including lung cancer,[3] tumours of the head and neck,[4] as well as some non-malignant conditions such as macular degeneration,[5] microbial infections,[6] atherosclerosis[7] and psoriasis.[8]

The PDT treatment involves the administration of the photosensitiser to the patient, topically, orally or via intravenous injection, depending on which photosensitiser is being used, and the condition being treated.[4,9] The photosensitiser distributes non-specifically around the body, and is preferentially retained within rapidly dividing tissues including neoplastic tissues and skin.[10,11] A time interval is therefore required for the photosensitiser to accumulate in the target tissue and reach the optimum tumour to peritumoural ratio. The time period is dependent on the biodistribution and pharmacokinetic profile of the photosensitiser used, for example, it typically takes 48-72 hours for the maximal tumour to peritumoural tissue ratio to be achieved for Photofrin®, whereas it takes 96 hours for Foscan®.[11] The photosensitiser is then activated with a wavelength of light which corresponds to an absorption peak of the chromophore. Once activated, a photochemical reaction occurs between the photosensitiser in its excited state and molecular oxygen, leading to the formation of cytotoxic ROS. Oxidative damage to a variety of cellular components occurs, which adversely affects the structure and function of the cell, ultimately inducing cell death.[2]

The PDT therapeutic effect is dependent on the light dose, the photosensitiser concentration within the target tissue and the availability of oxygen. To achieve cell death the potency of PDT effect must surpass a certain threshold level. Patients remain photosensitive until the photosensitiser has cleared from the body, and this time period is dependent on the photosensitiser being used.[12] Following treatment, if there is damage to surrounding healthy tissue, it usually heals within 2-3 months.[9]

1.1.1 Photochemistry

The photochemical processes which transpire during PDT, can be illustrated using a modified Jablonski diagram, as depicted in Figure 1.[2,10]

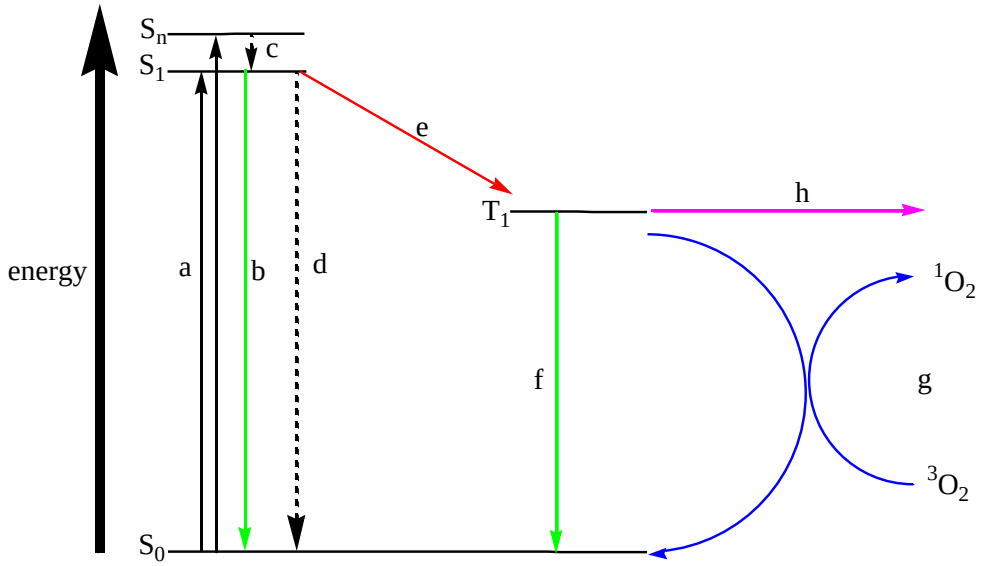

a = absorption
b = fluorescence
c = internal conversion
d = nonradiative decay
e = intersystem crossing
f= phosphorescence
g = Type II reaction (singlet oxygen formation)
h = Type I reaction

Figure 1: Modified Jablonski diagram illustrating PDT photochemistry.[2,10]

Photosensitisers are administrated while in the singlet ground state (S_0), and once irradiated with a wavelength of light corresponding to one of its absorption bands, the chromophore absorbs energy (**a**) and reaches a short lived (10^{-12}-10^{-9}seconds) excited singlet state (S_n). The excited photosensitiser can then lose the absorbed energy by relaxing to lower energy levels. The excited chromophore can return to its ground state by a variety of mechanisms: by simultaneous emission of a photon, a process formerly known as fluorescence (**b**); by collisions with surrounding molecules and/or vibrational relaxation, a phenomena known as internal conversion (**c**); or by colliding with other molecules, causing either the release of thermal energy or the molecule dissociating or fragmenting (**d**). Another process by which the photosensitiser can lose some of the absorbed energy is by a mechanism known as intersystem crossing (**e**), which involves the excited singlet state being converted into an excited triplet state (T_1), by inversion of the spin of one electron; a process which is formerly forbidden by the spin selection

rule, as it involves a net change in spin for the transition. The photosensitiser in the excited triplet state can also lose its energy radiatively by emission of a photon, a mechanism called phosphorescence (**f**), or by interacting with other molecules within its sphere of influence. Since the lifetime of the excited triplet state is considerably longer than the excited singlet state, 10^{-3}-10^{-1}seconds as opposed to 10^{-12}-10^{-9} seconds, there is a greater probability that the photosensitiser in the triplet state can diffuse to, and interact with other molecules within its immediate vicinity, leading to the generation of cytotoxic species, via either a type I or type II reaction.[2,10,13]

Type I reactions occur when the chromophore (T_1) interacts with an organic substrate, causing a redox reaction, resulting in the photosensitiser being reduced, and the substrate oxidised. The reduced photosensitiser can interact with molecular oxygen, producing super oxide anions, which are subsequently used to create the highly reactive hydroxide radicals. Additionally, the excited photosensitiser can also react with super oxide radicals, generating super oxide anions, which subsequently produce hydroxide radicals [2,12,13] Generally, Type I reactions are prominent if there is a high photosensitiser concentration, low oxygen concentration, a high singlet state acceptor substrate concentration, and polar surroundings; due to inhibition of the reverse redox reaction and stabilization of the radicals produced.[13]

The type II photochemical reaction occurs between the excited photosensitiser (T_1) and ground state oxygen ($^3O_2$). $^3O_2$ has two outer electrons which are unpaired and are located in the π_{2px*} and π_{2py*} anti-bonding orbitals. When a magnetic field is applied, these electrons can be parallel; aligned up or aligned down; or anti-parallel, giving ground state oxygen three possible electron configurations, known as a triplet state.[2] Oxygen has low lying excited states, 95 and 158 kJ mol^{-1} above the triplets state, thus the chromophore (T_1) can transfer sufficient energy to $^3O_2$, causing a change in the electronic configuration of the π-antibonding orbitals.[14] The increase in degeneracy causes an inversion of one of the oxygen outer electrons, causing both of the outer electrons pairing up in the π_{2px*} orbital. Oxygen in this excited state only has one possible electron configuration, a singlet state ($^1O_2$).[2] An individual photosensitiser can typically afford 10^3-10^5 molecules of $^1O_2$ before it is degraded via photobleaching or other processes.[14] $^1O_2$ is thought to be the primary cytotoxic agent in PDT and is so highly reactive that its lifetime is only 10-100 μs in organic solutions, however in an aqueous environments the lifetime was estimated to be 2 μs, as the energy of waters oxygen-hydrogen stretching is approximately the same as the excited state energy of singlet oxygen.[2,12] Due to the high reactivity and short lifetime of singlet oxygen, the

oxidative damage is restricted to an area equivalent to the thickness of a cell membrane.[2] Type II reactions are favoured in hydrophobic environments, due to the increased solubility and longer lifetime of the singlet oxygen species.[13]

The cytotoxic species produced during PDT can cause photo-oxidation to nearly all proteins, and certain cellular structures, including: nuclei, endoplasmic reticulum, lysosomes, mitochondria or plasma membrane. Oxidative damage to these cell organelles can disrupt the normal functioning of the cell, inducing cell death by either apoptosis or necrosis.[2,12,13,15,16] ROS can also target the tumours neovasculature, causing thrombosis, haemorrhaging and blood stasis, depriving the tumour of oxygen and nutrients, resulting in infarction.[2,17] Furthermore, when the tumour is exposed to oxidative stress, an influx of phagocytes, including neutrophils and macrophages occurs. The accumulation of macrophages in cancerous tissues can induce PDT-mediated lysis and enhances the accumulation of tumour necrosis factors, increasing the concentration of nutrophils in the blood. Neutrophils can aid damage to tumour stroma, making the cancerous cells more susceptible to cytotoxic species, as well as being a source of immunoregulatory factors, which induce inflammation.[18]

1.1.3 Photosensitisers

Photosensitisers can absorb light of a specific wavelength, transforming it into energy, which is transferred to a substrate or molecular oxygen, leading to the production of ROS. Thus a good photosensitiser should absorb light efficiently, forming a high quantum yield of photosensitiser in the excited triplet state. The excited triplet state should also be relatively stable, increasing the probability of reacting with either oxygen or a suitable substrate. Compounds that have the ability of to form excited triplet states generally posses conjugated systems, hence porphyrin type structures have been utilised as photosensitisers.[19]

Porphyrin derivatives are aromatic tetrapyrrolic macrocycles consisting of four pyrrolic subunits connected by methine bridges. The porphyrin nucleus has a total of 22 π electrons, with 18 π electrons in direct conjugation in compliance with Hückels 4n+2 rule of aromaticity.[19,20] Free base porphyrins have a UV/visible spectrum consisting of one intense absorption band, referred to as the Soret band, at 380-430 nm, and four less intense signals, known as the Q bands at higher wavelengths.[21]

The optical properties of different porphyrin derivatives are dependent on the functional groups that are present on the porphyrin core.[22] Porphyrins absorb photons efficiently at wavelengths corresponding to their absorption peaks, leading to high excited triplet state yields, which efficiently produce ROS.[2]

The first generation photosensitisers were derived from hematoporphyrin, e.g. Photofrin®, shown in Figure 2. The synthesis of Photofrin® was achieved by treating hematoporphyrin derivative with 5 % sulphuric acid in acetic acid, under ambient conditions. Following neutralisation with aqueous base, a complex mixture of oligomers and dimers were produced, which were connected by ether and/or ester linkages. The active oligomer forms (Photofrin®) were isolated by either high performance liquid chromatography (HPLC) or size exclusion chromatography.[12] Due to the nature of the synthesis, Photofrin® exhibited inconsistent batch-to-batch preparations, leading to inconsistent biological studies.[23] Furthermore, patients remained photosensitive for 4-6 weeks post treatment, and the optical properties of Photofrin® were not ideal. Therefore, second generation photosensitisers were developed to circumvent these unfavourable characteristics.[24]

While irradiating a photosensitiser, light can be absorbed by endogenous chromophores, such as haemoglobin, or by microscopic cellular structures, including cell organelles, resulting in the loss of direction by the light beam.[15] Human tissue transmits light most

efficiently in the red region of the electromagnetic spectrum (> 600 nm). A 630 nm light source will penetrate tissues up to 0.5 cm, whereas at 700 nm this increases to 1.5 cm; thus the second generation photosensitisers, such as Foscan® (Figure 2), had longer activation wavelength (652 nm).[4] In comparison to Photofrin®, Foscan® also exhibited other favourable properties: chemically purity, reduced photosensitivity (2 weeks) and increased photoactivity; Photofrin® had a singlet quantum yield of 0.5, whereas Foscan® had a yield of 0.87.[24]

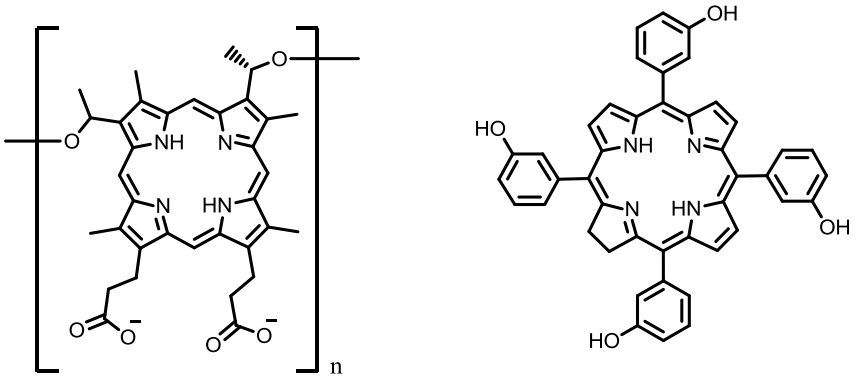

Photofrin® Foscan®

Figure 2: Photofrin® and Foscan®.[19]

Although not fully understood, first and second generation photosensitisers exhibit a passive selectively towards cancerous tissue, an effect that has been attributed to the morphology of the tumour neovasculature, and subsequent retention of the photosensitiser. Non-covalent interactions between photosensitiser and serum components, including low density lipoproteins have also been implicated.[17,25] Therapeutically this results in a variety of unfavourable characteristics; the time required to reach the optimal tumour to peritumoural ratio is extensive; the tumour to peritumoural ratio for photosensitisers is low, potentially leading to damage to the healthy surrounding tissue; and a high dose of photosensitiser is necessary to obtain a satisfactory therapeutic.[12,19]

Research has therefore been directed towards improving the pharmacokinetic and biodistribution profiles of photosensitiser and thus addressing these undesirable features preventing PDT from becoming a more viable cancer treatment.

Passive targeting vehicles such as oil dispersions, hydrophilic polymer-photosensitiser conjugates, or encapsulation of the photosensitiser inside a drug delivery vehicle, such as nanoparticles or liposomes, attempt to enhance the retention of the construct, and

thence photosensitiser, within the neoplastic tissue.[13,26] Another method for augmenting the desired selectivity involves the formation of bioconjugates; in this case the photosensitiser is covalently attached to a biomolecule that is metabolically associated with, or recognised by, the diseased tissue. The biomolecules used to produce these "third generation" PDT agents include albumin, lipoproteins, transferrin, insulin, epidermal growth factor and steroids.[26,27,28]

This particular research project involves the production of photosensitiser bioconjugates formed from another class of biomolecule, antibodies and antibody fragments.

1.2 Antibodies and associated fragments

Certain antibodies and antibody fragments,[27] (Figure 3) have the ability to bind to specific antigens associated with cancerous tissue, thus the production of photosensitiser-antibody bioconjugates or "photo-immunoconjugates" is an attractive targeting strategy.

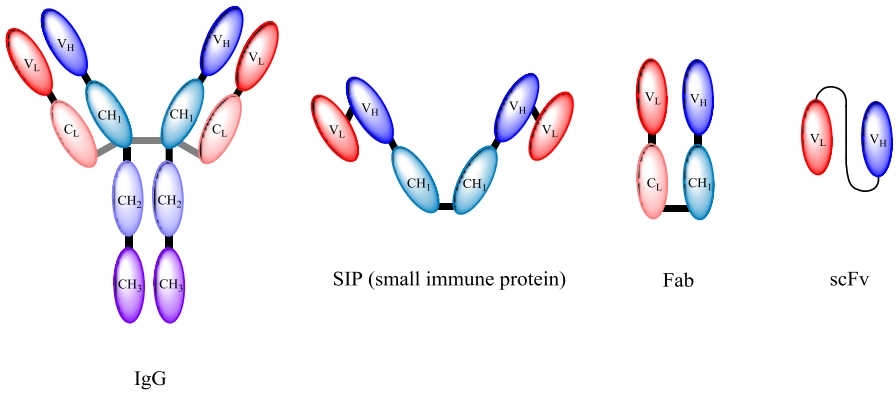

Figure 3: Schematic representation of antibodies and related fragment.[27]

Hydridoma technology developed by Köhler and Milstein[29] enabled the production of monoclonal antibodies (mAb), specific to a selected antigen. The procedure involves production of a hydridoma cell line, via the fusion of spleen cells from immunised mice, with murine myeloma cells. Screening of the hydridoma cells identified the antigen positive clone, which was subsequently propagated to afford the desired antibody.[30] Another screening method, phage display, produces antibodies with a higher antigen affinity. Once the antigen positive phage has been identified, the isolation of the DNA from the phage genome and recombinant DNA technology generates the antibody.[31] The different antibody formats can be produced from either proteolytic cleavage of the

intact antibody, or using recombinant DNA technology.[32] These techniques have facilitated the production of numerous antibody forms, each with their own unique characteristics.[33,34]

Intact IgG, the largest antibody format (160-170 kDa), contains more lysine residues, available for conjugations, than the associated fragments; therefore the loading of photosensitisers should statistically occur more in areas remote from the antigen recognition region. In contrast, single chain fragments (scFv; 25 kDa), the smallest antibody format, contain more limited lysine sites for conjugations, thus photosensitiser loading is more likely to occur at the antigen binding region, hindering immunoreactivity.[27]

The pharmacokinetic profiles of different antibody formats are significantly different *in vivo*.[35,36] The intact mAb exhibits slow blood clearance, leading to accumulation in vital organs. Additionally, due to the size of the mAb, in combination with the physiological barriers of the tumour,[37] poor diffusion of the mAb throughout the tumour mass results. Conversely, the smaller scFv format has a rapid blood clearance; therefore it does not accumulate in organs so prominently. The small immune protein (SIP) format has enhanced tumour retention, faster blood clearance and reduced accumulation in vital organs, compared to the whole mAb. Once conjugated, the biodistribution profile of the antibody, or fragment, should be transferred to the photosensitiser.

Tumours are highly heterogeneous in nature, with the expression of antigens being inconsistent throughout the tumour mass, therefore immunoconjugate can also be unevenly distributed, resulting in an inconsistent photodynamic action throughout the tumour.[28]

Immunoconjugates using internalising antibodies represents another strategy for enhancing the photodynamic effect. By delivering the photosensitiser directly into the tumour cells, reactive oxygen species are formed closer to sensitive organelles within the cell, resulting in an enhanced phototoxic effect.[38]

1.2.1 SIP(L19)

Generally, immunoconjugate enhanced selectivity is only observed for a particular condition, as the target antigen is usually specific to a certain malignancy. Hence, it would be desirable to produce a range of antibodies targeting antigens which are expressed by a variety of cancerous tissues. The formation of the tumour neovasculature by the proliferation of new blood vessels is a process associated with many solid aggressive tumours. Therefore, if an immunoconjugate bore an antibody targeting antigens associated with angiogenesis, it could enable the treatment of a variety of cancerous conditions. A recent example of this strategy involves the L19 antibody, which targets the extra domain B (EDB) of fibronectin. EDB fibronectin is expressed during the angiogenic process and is undetectable in most normal tissue, except during tissue remodelling.[36]

A study was conducted over a 144 hour period, evaluating the pharmacokinetic profiles of radiolabeled L19 antibody in the $(ScFv)_2$, SIP and IgG formats, employing SK-MEL-28 tumour bearing mice. The SIP(L19) exhibited a 2-5 fold more favourable % ID/g in tumours, in comparison to the $(ScFv)_2$L19. The % ID/g for the IgG(L19) consistently increased throughout the experiment, reaching 11.22 % ID/g after 144 hours. However, the % ID/g tumour-organ ratios showed that IgG(L19) accumulated to a greater extent in the organs tested, and SIP(L19) exhibited the most favourable tumour-peritumoural ratios, thus the SIP format was deemed the most suitable for producing conjugates.[36]

The 80 kDa SIP(L19) is a homo-dimer composed of two scFv fused to the human ϵ_{s2}-CH4 domain of the human IgE, with the two CH4 domains covalently attached via a disulphide linkage.[39] It has been reported that the mild reducing agent: tris(2-carboxyethyl)phosphine hydrochloride (TCEP), can reduce a C-terminal cysteine expressed by an engineered scFv, without destabilising the fragment by reducing the intra-domain disulphide bridges.[40] Therefore, TCEP could be used to reduce SIP(L19) disulphide linkage, leading to the expression of two thiol groups remote from the antigen binding site, which could be used for site-specific, stoichiometrically controlled conjugations. The reduced SIP(L19) fragment was selected for this research project.

1.2.2 Strategies for conjugating photosensitisers to monoclonal antibodies

Antibodies and related fragments express certain amino acid residues and oligosaccharides that can be used to form covalent bonds with photosensitisers exhibiting complementary functionalities. Once conjugated, a successful photo-immunoconjugate must at least retain, or ideally enhance, both the photoactivity of the photosensitiser moiety and the immunoreactivity profile of the antibody.

Conjugation of a photosensitiser to an antibody can however be problematic for a variety of reasons. Lysine residues are heterogeneously distributed throughout the antibody, thus conjugations are not regioselective, resulting in possible binding of the photosensitisers in close proximity to each other, and potentially quenching excited states. Conjugation may also occur in the recognition site, thus inhibiting targeting activity. Furthermore, the amount of photosensitiser per antibody cannot be accurately controlled, often resulting in a complex mixture of photo-immunoconjugates with inconsistent batch to batch preparations; although using consistent reagent concentrations and reaction times can lead to a certain degree of reproducibility. Cysteine residues within the antibody are connected together in an oxidised form, and some of these disulphide bridges can be reduced using mild conditions; yielding reactive thiol groups in specific regions remote from the binding site. Due to the relatively low percentage of cysteine residues, only a limited amount of photosensitiser can be directly loaded on to the antibody in this way. As an alternative to direct coupling to lysine or cysteine residues, oligosaccharide moieties present in the Fc domain can be oxidised, producing formyl functionalities which can then participate in conjugation reactions. The reactions associated with these formyl groups; reductive amination or formation of a hydrazone linkage, are however relatively slow reactions. Additionally, as with coupling to cysteine residues, the photosensitiser loading is restricted due to the limited availability of the formyl functionalities.

The structural features required of the photosensitiser can also represent challenges for the bioconjugation procedure. Antibodies are generally stable in an aqueous environment and become denatured when exposed to many organic solvents. Hence the photosensitiser must be sufficiently hydrophilic to facilitate the conjugation reaction and preventing substantial aggregation of the photosensitiser under aqueous conditions. Rendering the photosensitiser hydrophilic also reduces non-covalent binding to hydrophobic regions of the antibody. Additionally, some photosensitisers derived from naturally occurring porphyrins, such as hematoporphyrin and chlorin e_6, contain

multiple functional groups, in this case carboxylic acids, leading to cross-linking and inconsistent preparations. Considerations of all these potential problems need to be addressed, in order to synthesise successful photo-immunoconjugates. There has been a variety of coupling strategies reported for synthesising photosensitiser-antibody conjugates:

1.2.2.1 Carbodiimide coupling

The carbodiimide strategy relies on activation of carboxyl groups present on the photosensitiser using a carbodiimide reagent, and subsequent coupling with amino groups expressed by the antibody. An innovative report by Mew *et al.*[41] investigated the potential of photo-immunoconjugates by conjugating hematoporphyrin to mAbs, including anti-myosarcoma M1 (anti-M1) targeting DBA/2J myosarcoma. Hematoporphyrin is a relatively hydrophobic molecule; therefore a mixture of dimethylformamide and water was used as an appropriate reaction medium. A carbodiimide reagent, 1-ethyl-3-(3-dimethylaminopropyl) carbodiimide-HCl (EDCI) was added to the hematoporphyrin solution causing activation of the carboxyl functionalities. Anti-myosarcoma mAb in distilled water was subsequently added, resulting in coupling between carboxyl groups present on the photosensitiser and amino groups present on the antibodies; the environmental pH was monitored and maintained between 6 and 7 (Scheme 1). Monoethanolamine was used to quench the residual EDCI and the mixture was dialyzed against phosphate buffered saline (PBS). The conjugate was freeze dried, re-dissolved in PBS and passed through a Sephadex G-25 column using PBS as eluent, thus removing unbound photosensitiser which was retained at the top of the column. The final conjugate did however possess extensive non-covalently bound hematoporphyrin, indicated by thin layer chromatography (TLC), due to hydrophobic interactions between photosensitiser and mAb. *In vivo* studies of the anti-M1-hematoporphyrin conjugate with mice bearing M1 tumours showed significant reduction (95 %) in tumour growth upon irradiation with broad band light, whereas the tumour was unaffected by individual treatment with hematoporphyrin and mAb. Experiments using a different tumour type (C57BL/6J lymphoma EL4) with the anti-M1-hematoporphyrin conjugate and a non-specific antibody-hematoporphyrin conjugate with M1 tumours, demonstrated that the antibody conjugates were only selective towards complementary antigens.

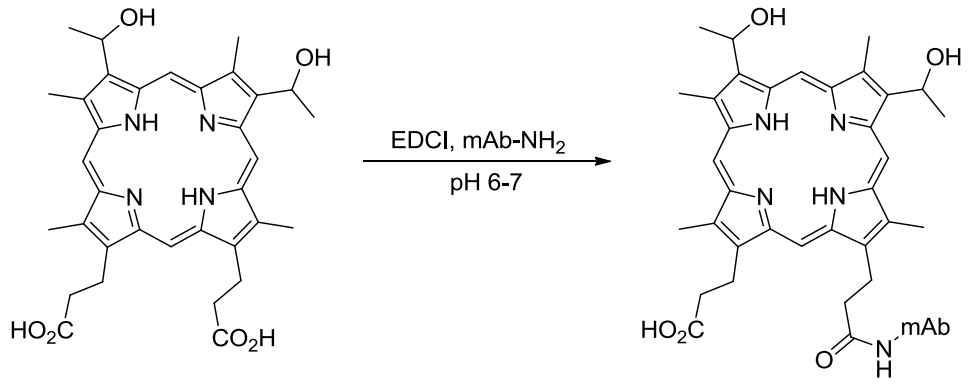

Scheme 1: Hematoporphyrin carbodiimide coupling.[41]

These findings prompted further studies from the same research group.[42] Hematoporphyrin was conjugated to the CAMAL-1 (mAb which specifically targets the leukaemia related CAMAL antigen), and L1210 (irrelevant antibody) mAbs, via an EDCI methodology. The concentration of hematoporphyrin (mg / mg of mAb), was determined spectrophotometrically, and found to be CAMAL-1-hematoporphyrin (0.26) and L1210-hematoporphyrin (0.172). *In vitro* experiments were preformed using three cell lines; antigen positive WC4 and WC6 expressing CAMAL, and antigen negative WC2. Fluorescence microscopy was used to confirm that the CAMAL-1-hematoporphyrin labels the WC6 cell line while L1210-hematoporphyrin does not, by comparing the fluorescent spectra of the cell line pre- and post-labelling. The photo-immunoconjugates capability to kill these labelled cells upon irradiation with light was then analysed. It was found that CAMAL-1-hematoporphyrin had the ability to eradicate a substantial number of cells when the hematoporphyrin concentration was 1.2 ng/10^6 cells, whereas concentrations of 240 ng/10^6 cells for L1210-hematoporphyrin and 120 ng/10^6 cells for hematoporphyrin were required to obtain a similar therapeutic response. The cell lines were also treated with each of the conjugates; when the concentration of hematoporphyrin was 12 ng/10^6 cells; the antigen positive cell lines were destroyed, while the WC2 control cell line was not. The carbodiimide strategy was utilized to couple hematoporphyrin to the monoclonal antibody 45-2D9, which has an affinity towards the cell surface glycoprotein expressed by 45-342 cells.[43] A pre-activated hematoporphyrin solution, formed by the reaction of hematoporphyrin with EDCI dissolved in dimethylsulfoxide, was added to a solution of antibody in PBS. After a short time period, the reaction mixture was placed on a gel permeation column and the product was eluted with PBS. The conjugate exhibited a certain degree of precipitation, which could be problematic for characterisation and activity studies, therefore the final purification step involved passing the conjugate through a 0.22 µm filter to remove

precipitate. Spectrophotometric studies revealed that there were considerable batch to batch variations as the number of hematoporphyrin molecules per antibody molecule varied from 4.2-39.5. *In vivo* kinetic and toxicity studies using nude mice bearing 45-342 tumours were performed. The kinetic experiments involved treatment with hematoporphyrin and hematoporphyrin-45-2D9, then harvesting the tumour and skin tissues after 24, 48 and 72 hours. The mice treated with hematoporphyrin exhibited no photosensitiser accumulation in the skin and the optimum concentration was observed after 24 hours corresponding to 0.09 ng hematoporphyrin/mg of tissue. The hematoporphyrin-45-2D9 conjugate had a maximum concentration of 0.98 ng/mg of tissue, after 72 hours. The conjugate also accumulated in the skin, to the level of 0.23 ng/mg of tissue after 24 hours and 0.42 ng/mg of tissue after 48 hours, but the conjugate was absent after 72 hours. The carbodiimide (EDCI) approach has also being used to produce hematoporphyrin conjugates with a-PNAr-I mAbs, targeting gastric cancer cells.[44] Purification of the immunoconjugate was attempted by dialyzing the reaction mixture against 0.01M PBS, pH 7.4, at 4 ^{o}C for 48 hours followed by passing the resulting solution through a Sephadex G-25 column equilibrated with PBS; despite the purification attempt, TLC revealed the presence of non-covalently bound hematoporphyrin. The immunoreactivity and photochemical properties of the conjugate was not significantly compromised, as indicated by ELISA and comparison of the generation of photoproducts following He-Ne laser irradiation between hematoporphyrin and hematoporphyrin-a-PNAr-I. *In vivo* studies involving the administration of hematoporphyrin and hematoporphyrin-a-PNAr-I at a concentration of 0.2 mg/kg body weight to nude mice bearing a human gastric cancer xenograft in combination with light irradiation was conducted. Tumour regression of 10 % for hematoporphyrin and 90 % for hematoporphyrin-a-PNAr-I was observed, thus verifying the enhanced potency exhibited by the conjugate at a concentration of 0.2 mg/kg of body weight.

An article by Linares *et al.*[45] has demonstrated that the carbodiimide conjugation methodology can also be used to synthesise chlorin e_6 conjugates by a modification of the Mew *et al.*[41] procedure. The antibodies selected for conjugation were anti-IL-2R and anti-IL-2R Fab, targeting the multichain interleukin-2-receptor (IL-2R) associated with various cancers including cutaneous T-cell lymphoma and T-cell leukaemia. The report describes the synthesis of immunoconjugates using either hematoporphyrin or chlorin e_6 conjugated to anti-IL-2R mAb, in addition to hematoporphyrin conjugated to anti-IL-2R Fab. UV-visible spectroscopy was used to determine the photosensitiser/antibody molar

ratios: the hematoporphyrin-anti-IL-2R (14.5) contained more photosensitiser in comparison to both chlorin e_6-anti-IL-2R (3.43) and hematoporphyrin-anti-IL-2R Fab (5). Sodium dodecyl sulfate polyacrylamide gel electrophoresis (SDS-PAGE) revealed that each of the antibody conjugates contained less than 1 % unconjugated photosensitiser, while the anti-IL-2R Fab conjugate contained up to 4 %. *In vivo* photolysis experiments with TIB-152 T-leukaemia cells expressing the IL-2R receptor verified that chlorin e_6 conjugate was more effective than the analogous hematoporphyrin conjugate. There was fewer photosensitisers per antibody for hematoporphyrin-anti-IL-2R Fab in contrast to hematoporphyrin-anti-IL-2R, thus a higher concentration of hematoporphyrin-anti-IL-2R Fab was required to reduce TIB-152 cell viability, even though the hematoporphyrin-anti-IL-2R Fab conjugate diffuses to the receptor more efficiently. These findings illustrate the importance of loading multiple photosensitiser units on to antibodies.

The carbodiimide strategy has been used to conjugate palladium(II) coproporphyrin (Figure 4) to rabbit anti-human ferritin antibodies.[46] The photosensitiser was dissolved in a dilute potassium hydroxide solution and hydrochloric acid was used to adjust the acidity of the solution to pH 6. EDCI was dissolved in water and sodium phosphate buffer was added. The activated photosensitiser was added in either 50 or 200 molar excess, relative to the antibody, in a sodium bicarbonate solution (pH 8.3). The crude conjugate was then loaded on to a Sephacryl S-200 column and eluted with sodium borate (pH 8.5). The loading ratio was dependent on the molar ratio of photosensitiser used: 50 molar excess of photosensitiser produced conjugate with 0.3 porphyrin molecules/antibody and 200 molar excess created conjugate with 1.0 porphyrin molecules/antibody.

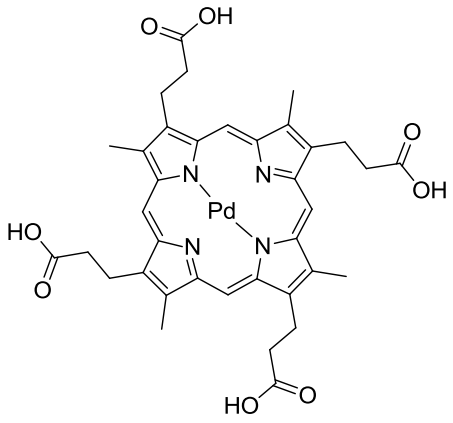

Figure 4: Structure of palladium(II) coproporphyrin.[46]

Although the versatility of the carbodiimide coupling strategy has been demonstrated, and produces conjugates with promising biological results; carbodiimide coupling has the disadvantage that it requires the *in situ* formation of a reactive intermediate, and can also result in substantial loss of photosensitiser as the *N*-acyl urea derivative.[47]

1.2.2.2 Activated esters

Due to inherent problems with direct carbodiimide coupling to form photo-immunoconjugates, research involving carbodiimide agents has been directed towards derivatising photosensitiser as activated esters, which can be isolated and purified before conjugation. The most common method involves the transformation of carboxyl functionalities present on the photosensitiser into *N*-hydroxysuccinimide esters via treatment with *N*-hydroxysuccinimide (NHS) in the presence of dicyclohexylcarbodiimide (DCC), and subsequent coupling with amino functionalities expressed by the antibody (Scheme 2).

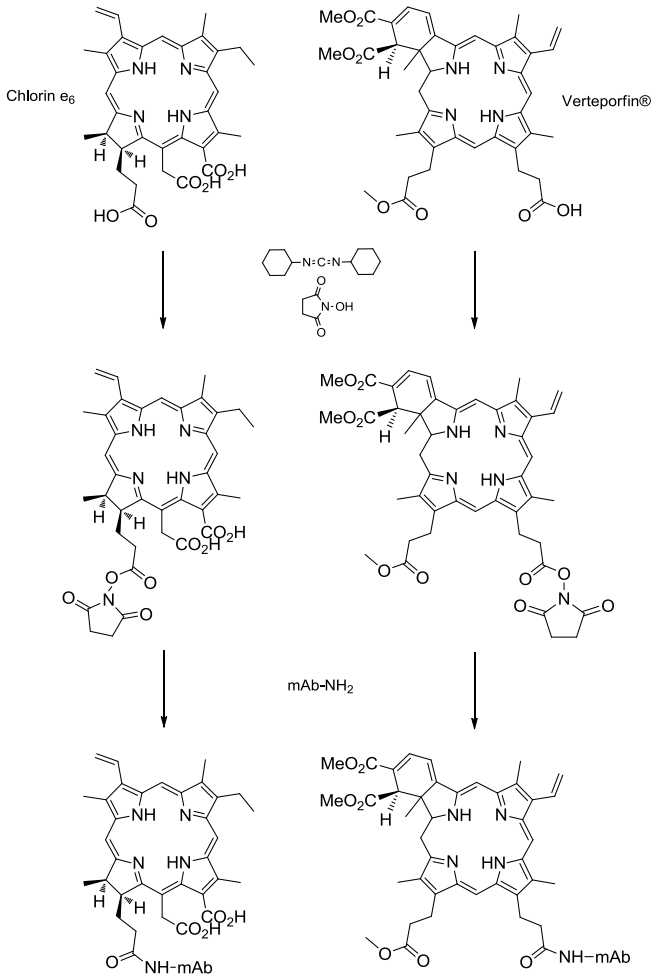

Scheme 2: General NHS activated ester strategy for bioconjugates involving chlorin e_6 or Verteporfin®.

Martsez *et al.*[46] investigated both the direct carbodiimide (previously described) and activated ester strategies for conjugating palladium(II) coproporphyrin to a mouse monoclonal antibody IgG2a and rabbit anti-human ferritin antibodies. The palladium(II) coproporphyrin bearing NHS activated ester was dissolved in dimethylformamide and added in a range of molarities between 5 and 100 excess, to the antibody in sodium borate buffer solutions of differing pH (7.4, 7.8 or 8.5), while ensuring that the overall dimethylformamide concentration was 13 % in all the conjugation mixtures. Glycine in sodium borate buffer was added to quench the reactions and each resulting mixture was passed through a Sephacryl S-200 column and eluted with sodium borate buffer (pH 8.5). The conjugation reaction produced both the monomeric conjugate and aggregates, with yields of both increasing directly with increasing photosensitiser/IgG molar ratios. The pH of the conjugation medium also influenced the reaction, increasing the pH from 7.4 to 8.5 resulted in more covalently bound photosensitiser, however the formation of aggregates was also more prominent. Thus the optimised conditions to synthesise

monomeric conjugates, was addition of a 10-40 molar excess of photosensitiser to the antibody in a buffer solution at pH 7.4. The monomeric conjugates did not contain any significant amount of unbound photosensitiser as indicated by gel permeation chromatography. A study to establish how the direct carbodiimide coupling and NHS activated ester methodology influenced the binding efficiency of monomeric conjugates to the target antigen, revealed that the immunoreactivity of the conjugates formed by the carbodiimide reaction had been compromised. However the conjugate formed via the activated ester exhibited enhanced antigen affinity, which was attributed to an increase in the conformational mobility of the derivatised antibody.

Synthesis of a chlorin e_6-anti-EGFR mAb (C225) conjugate was achieved using a NHS activated ester strategy as reported by Soukos *et al.*[48] Chlorin e_6 was treated with NHS and DCC in anhydrous dimethylsulfoxide and the resulting chlorin e_6-NHS ester was reacted with C225 dissolved in a sodium bicarbonate buffer solution (pH 9.3). The conjugate was dialyzed against phosphate buffer to remove the unconjugated photosensitiser and stored in the presence of horse serum to prevent conjugate aggregation. The loading of chlorin e_6 was limited by the tendency to form aggregates when more than 5 molecules of photosensitiser were added to an individual mAb; the loading ratio was 4.8 molecules chlorin e_6 per C225 as calculated by UV-visible spectroscopy. The chlorin e_6-C225 conjugate was tested *in vivo* employing hamsters expressing papillary tumours; following a typical PDT treatment, the expression of EGFR was reduced, as indicated by immunophotodiagnosis.

Fabbrini *et al.*[49] have used bis(triethanolamine)Sn(IV)chlorin e_6 to form conjugates with SIP and scFv formats of the L19 antibody, which shows affinity for the EDB domain of fibronectin. The bis(triethanolamine)Sn(IV)chlorin e_6-(SIP)L19 immunoconjugate was produced by two different methodologies. One procedure involved isolation of bis(triethanolamine)Sn(IV)chlorin e_6-NHS and progressive additions of the activated photosensitiser to the antibody in carbonate buffer (pH 8.5). The bis(triethanolamine)Sn(IV)chlorin e_6-NHS was synthesised by DCC mediated reaction between NHS and bis(triethanolamine)Sn(IV)chlorin e_6 dissolved in anhydrous dimethylformamide; the reagents stoichiometry relative to the photosensitiser was used to control whether monoesterification or triesterification of the photosensitiser occurred. To terminate the conjugation reaction, tris(hydroxymethyl)aminomethane was used to quench un-reacted bis(triethanolamine)Sn(IV)chlorin e_6-NHS ester; dialysis and gel permeation chromatography was used to purify the immunoconjugate. The other procedure used to produce bis(triethanolamine)Sn(IV)chlorin e_6-(SIP)L19, as well as

the scFv(L19) conjugate, involved *in situ* formation of bis(triethanolamine)Sn(IV)chlorin e_6-NHS ester, resulting from carbodiimide coupling (EDCI) of sulfo-NHS to bis(triethanolamine)Sn(IV)chlorin e_6 suspended in phosphate buffer (pH 6), followed by the addition of antibody in phosphate buffer (pH 8.5). Exhaustive dialysis and gel permeation chromatography yielded the purified conjugate. The conjugates formed by the *in situ* production of bis(triethanolamine)Sn(IV)chlorin e_6-NHS ester exhibited an average loading ratio of 2:1 (photosensitiser:antibody) for both conjugates as determined by UV-visible spectroscopy, with no detectable non-covalently bound photosensitiser, as indicated by SDS-PAGE. Affinity chromatography showed that the immunoreactivity of the conjugates was mostly retained after conjugation, at 84 % for bis(triethanolamine)Sn(IV)chlorin e_6-(SIP)L19 and 82 % bis(triethanolamine)Sn(IV)chlorin e_6-(ScFv)L19 in comparison to the corresponding un-conjugated antibody fragments. *In vivo* experiments treating mice bearing FE8 sarcoma with bis(triethanolamine)Sn(IV)chlorin e_6-(SIP)L19 and bis(triethanolamine)Sn(IV)chlorin e_6-(ScFv)L19 conjugates, once they had reached comparable tumour:blood ratios, demonstrated that the bis(triethanolamine)Sn(IV)chlorin e_6-(SIP)L19 reduced tumour mass to a greater extent in comparison with bis(triethanolamine)Sn(IV)chlorin e_6-(ScFv)L19. Further *in vivo* studies comparing bis(triethanolamine)Sn(IV)chlorin e_6-(SIP)L19 as a single PDT treatment, with a three dose PDT treatment on nude mice bearing FE8 using the same conjugate, revealed a substantially increased time delay in tumour growth for the multiple dose PDT treatment.

The activated ester approach has been applied to produce conjugates of benzoporphyrin derivative conjugated to an anti-EGFR antibody (C225), which had been previously conjugated with a 10 kDa-branched polyethylene glycol (PEG) chain.[50] The benzoporphyrin derivative-NHS ester was prepared by the EDCI catalysed reaction between NHS and benzoporphyrin derivative in dimethylsulfoxide. The activated benzoporphyrin derivative-NHS ester was then added to the PEGylated C225 dissolved in a dimethylsulfoxide-aqueous solvent system. The dual solvent system was used to avoid photosensitiser aggregation and possible non-covalent interactions; additionally the conjugation medium did not exceed 50 % dimethylsulfoxide to prevent precipitation and denaturing of C225. The conjugation mixture was then centrifuged and passed through a Sephadex G-50 column to yield the purified conjugate. Depending on the stoichiometry of the benzoporphyrin derivative-NHS ester relative to the antibody, immunoconjugates with loading ratios ranging from 2-11 were prepared. The purity of

the conjugates was analysed using SDS-PAGE and it was found that there was approximately 5 % non-covalently bound photosensitiser for the conjugate with a loading ratio of 2, increasing to 10 % for the conjugate with a loading ratio of 11. The final yield of the conjugates was also influenced by the molar loading ratios, a yield of 75 % for the conjugate with a loading ratio of 2, decreasing to a yield of below 45 % for the conjugate with a loading ratio of 11. Phototoxicity experiments were performed by incubating benzoporphyrin derivative-C225-PEG with both A-431 (EGFR expressing) and NR6 (non-EGFR expressing) cell lines prior to light activation; the selectivity of the conjugate was realised as the A-431 showed a substantial reduction in cell viability (90 %), whereas no significant phototoxic effect was observed on the NR6 cells. Research concerning the benzoporphyrin derivative-C225-PEG conjugate was extended by conducting mechanistic studies.[51] It was found that the immunoconjugate was less phototoxic than benzoporphyrin derivative alone, on a molar basis. However, the conjugate did selectively target EGFR expressing cells, whereas no selectivity was observed for the free benzoporphyrin derivative. Savellano *et al.*[52] used a similar protocol for the conjugation of pyropheophorbide-a to the PEGylated HER50 and HER66 mAb targeting the anti-epidermal growth factor receptor HE2 expressed by ovarian and breast cancer. The activated photosensitiser was conjugated to the PEGylated antibody in PBS (pH 7.4); purification using a Sephadex G50 spin column afforded the immunoconjugates. SDS-PAGE revealed that the conjugates contained unbound pyropheophorbide-a ranging from 2.3-20.9 %, dependent on the preparation and antibody used. *In vitro* studies indicated that phototoxicity could be improved by increasing the photosensitiser loading ratio, and by using multiepitope targeting; namely the administration of a mixture of immunoconjugates in a single dose. Benzoporphyrin derivative and pyropheophorbide-a, have also being conjugated to an anti-HER2 scFv (C6.5).[53] The photosensitiser was activated using NHS in the presence of DCC, with pyropheophorbide-a dissolved in a mixture of anhydrous tetrahydrofuran-dichloromethane (9:1) and benzoporphyrin derivative in anhydrous tetrahydrofuran. The pyropheophorbide-a-NHS ester was isolated by removal of the dicyclohexylurea precipitate by filtration, then precipitation of the crude product using hexane over chloroform followed by column chromatography, whereas benzoporphyrin derivative-NHS ester was purified more simply by column chromatography. The photosensitiser dissolved in dimethylsulfoxide was added to C6.5 in PBS containing 6 % acetonitrile and the resulting conjugate was dialysed against PBS. On average, each C6.5 was loaded with 10 photosensitisers, of which up to 20 % were non-covalently bound.

Cellular uptake experiments, using HER-2 positive SKOV-3 cells and HER-2 negative KB cells demonstrated the selectivity of the pyropheophorbide-a-C6.5 conjugate. Additionally, enhanced retention with SKOV-3 cells was observed for the benzoporphyrin derivative-C6.5 in comparison to unconjugated benzoporphyrin derivative. Bhatti *et al.*[54] extended this research by synthesising a library of conjugates consisting of pyropheophorbide-a conjugated to C6.5, MFE-23, D1.3, F1, GP6 and HuBC-1 scFv's, as well as the benzoporphyrin derivative-C6.5 conjugate, illustrating the versatility of this conjugation methodology. The final pyropheophorbide-a conjugate concentrations were limited to approximately 0.25 mg/mL due to the hydrophobic nature of pyropheophorbide-a, resulting in aggregation, whereas the more hydrophilic sulfo-NHS-pyropheophorbide-a, produced conjugates with C6.5 at higher concentrations. The conjugates were more potent than the corresponding free photosensitiser when tested with an appropriate cell line, both *in vitro* and *in vivo*.

Carcenac *et al.*[55,56] have utilized the activated ester approach to synthesise immunoconjugates involving derivatised aluminium tetrasulfophthalocyanine ($AlPcS_4$). The sulfonic acid groups expressed by $AlPcS_4$ were converted into sulfonyl chloride functionalities by treatment with thionyl chloride, to which, aliquots of a solution of 6-aminohexanoic acid and sodium carbonate in suitable stoichiometry were added, yielding the monosulfonamide product ($AlPcS_4A_1$). The carboxylic acid thus introduced, was converted into the activated ester by treatment with sulfo-NHS and EDCI in sodium phosphate buffer (pH 5). Chromatography on reversed-phase C_{18} preparative plates using phosphate buffer/methanol as the eluent and subsequent lyophilisation purified the $AlPcS_4A$-NHS ester.[57] The first exploratory paper involved the coupling with a radioiodinated 35A7 mAb, which targets a carcinoembryonic antigen.[55] $AlPcS_4A_1$-NHS ester in phosphate buffer (pH 5) was added dropwise to the 35A7 mAb contained in sodium bicarbonate (pH 9). The resulting mixture was passed through a Sephadex G25 column using PBS (pH 7.4), which contained 0.01 % azide. The immunoreactivity and biodistribution of the conjugates, measured using the radiolabel, was comparable to the 35A7 mAb. This research was then extended to produce conjugates with 35A7 mAb, targeting the non-internalising carcinoembryonic antigen, FSP77 mAb, that has an affinity towards the internalising ErbB2 antigen, and an irrelevant PX mAb.[56] *In vitro* experiments were performed on a SKOv3-CEA-1B9 cell line which expressed similar levels of both ErbB2 and carcinoembryonic antigens. Following activation by light, the $AlPcS_4A_1$-35A7 conjugate reduced the cell lines growth by 68 % when incubated for 20 hours at 2.5 µg/mL; in comparison the

$AlPcS_4A_1$-FSP77 caused 96 % growth inhibition after been incubated for 8 hours at 1.25 µg/mL, thus demonstrating the enhanced potency of internalising conjugates.

An exploratory article by Halime *et al.*[58] has used 5-(2-*N*-triphenylmethylaminophenyl)-10,15,20-tri(2-aminophenyl)porphyrin (TrTAPP),[59] for conjugations with IgG and Fab. The hydrophilic succinyl groups were introduced to TrTAPP by treated with ethyl succinyl chloride in the presence of triethylamine. The trityl protecting group was removed by trifluoroacetic acid hydrolysis to afford an amino functionality, which upon treatment with succinic anhydride yielded a carboxyl group that was subsequently converted into the NHS activated ester. The derivatised porphyrin dissolved in dimethylsulfoxide was added to the antibody in a sodium phosphate dihydrate buffered solution (pH 6) and the purified conjugates were obtained using a Sephadex G25 column (Scheme 3). The same strategy was also applied to derivatising the antibody with an activated ester to facilitate coupling with an amino functionality present on the porphyrin moiety. Reduction of the disulfide bridges of an IgG antibody using 2-mercaptoethanolamine yielded thiol groups, which were reacted with the bi-functional crosslinker *N*-succinimidyl(4-iodoacetyl)aminobenzoate (SIAB) in a sodium tetraborate decadihydrate based buffer solution to introduce an activated ester. The coupling was also performed in a sodium tetraborate decahydrate based buffer solution and Sephadex G25 column chromatography was used for purification (Scheme 4).

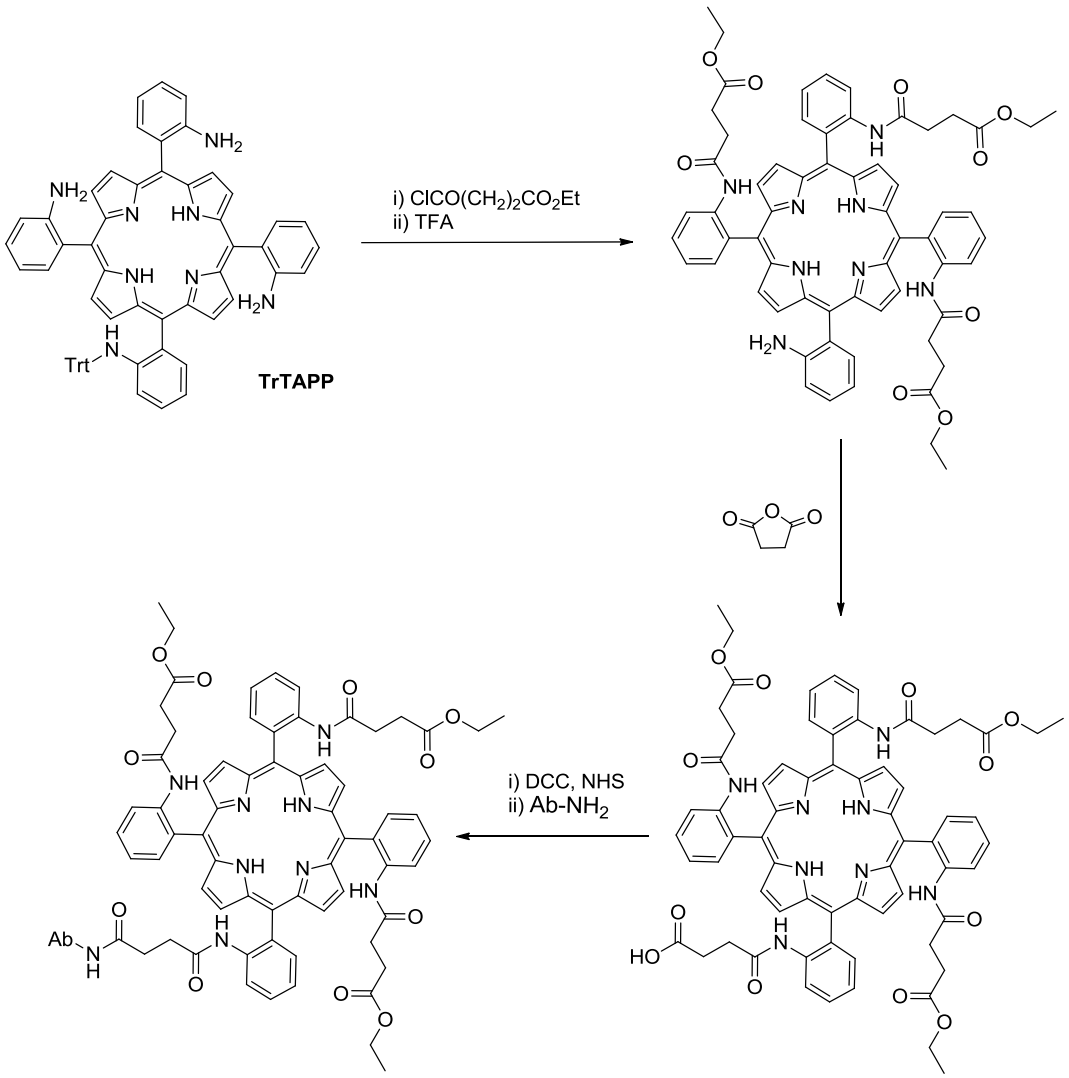

Scheme 3: TrTAPP conjugation to an antibody by the NHS-activated ester approach.[58]

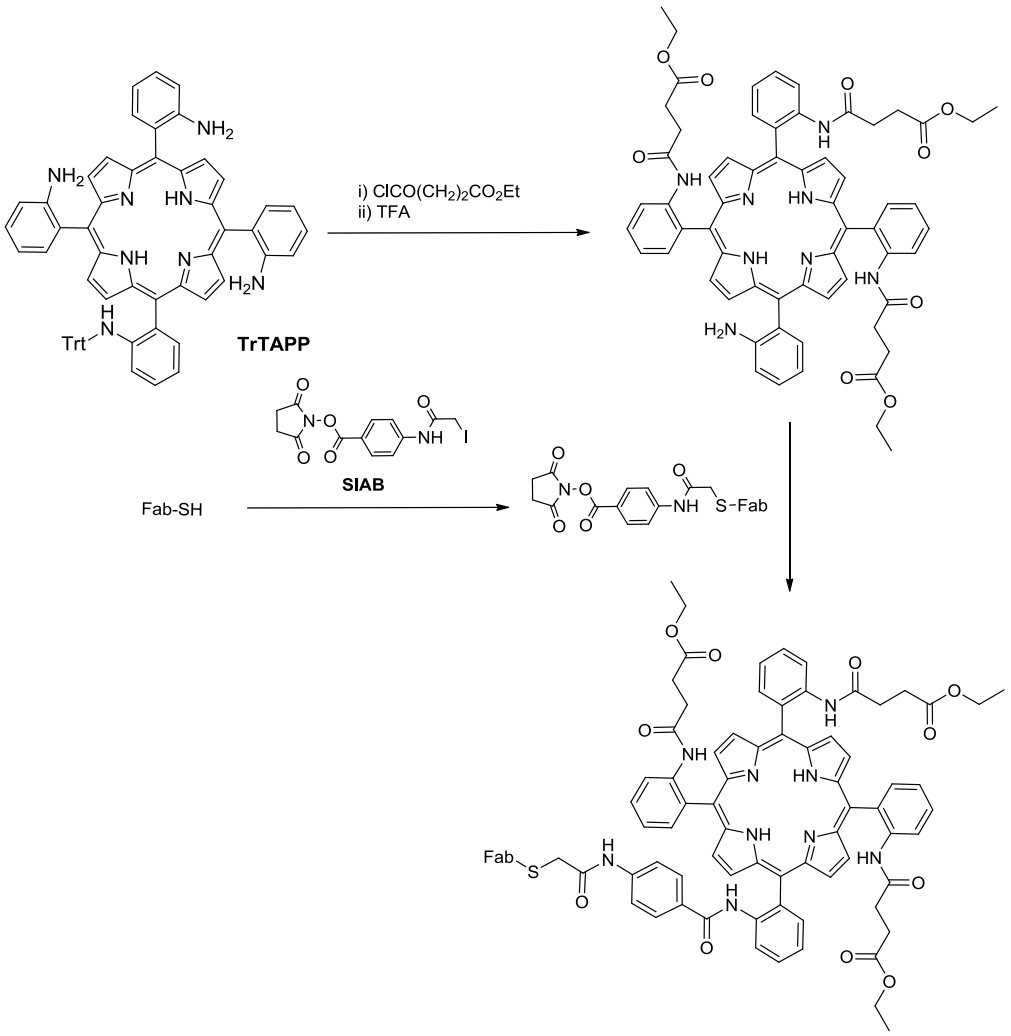

Scheme 4: TrTAPP conjugation to modified antibody.[58]

Vrouenraets *et al.*[38,60,61,62] have utilised an alternative activated ester method, based on tetrafluorophenol (TFP), for successfully producing immunoconjugates. A reaction between the commercially available photosensitiser 5,10,15,20-tetra(*m*-hydroxyphenyl)chlorin (Foscan®, Temoporfin®) and iodoacetic acid resulted in enhanced hydrophilicity via tetracarboxymethylation of the hydroxyl groups. The carboxylic acid groups formed were subsequently converted into activated esters by EDCI mediated coupling with TFP and the intermediate was purified by HPLC. Partial hydrolysis of the activated esters using stepwise additions of sodium carbonate in buffer solution produced a mixture of completely hydrolysed esters, mono-ester, and trace amounts of di-ester; the antibody in buffered saline (pH 9.5) was then added to the mixture. The conjugates were purified by gel permeation chromatography (Scheme 5).[38,61]

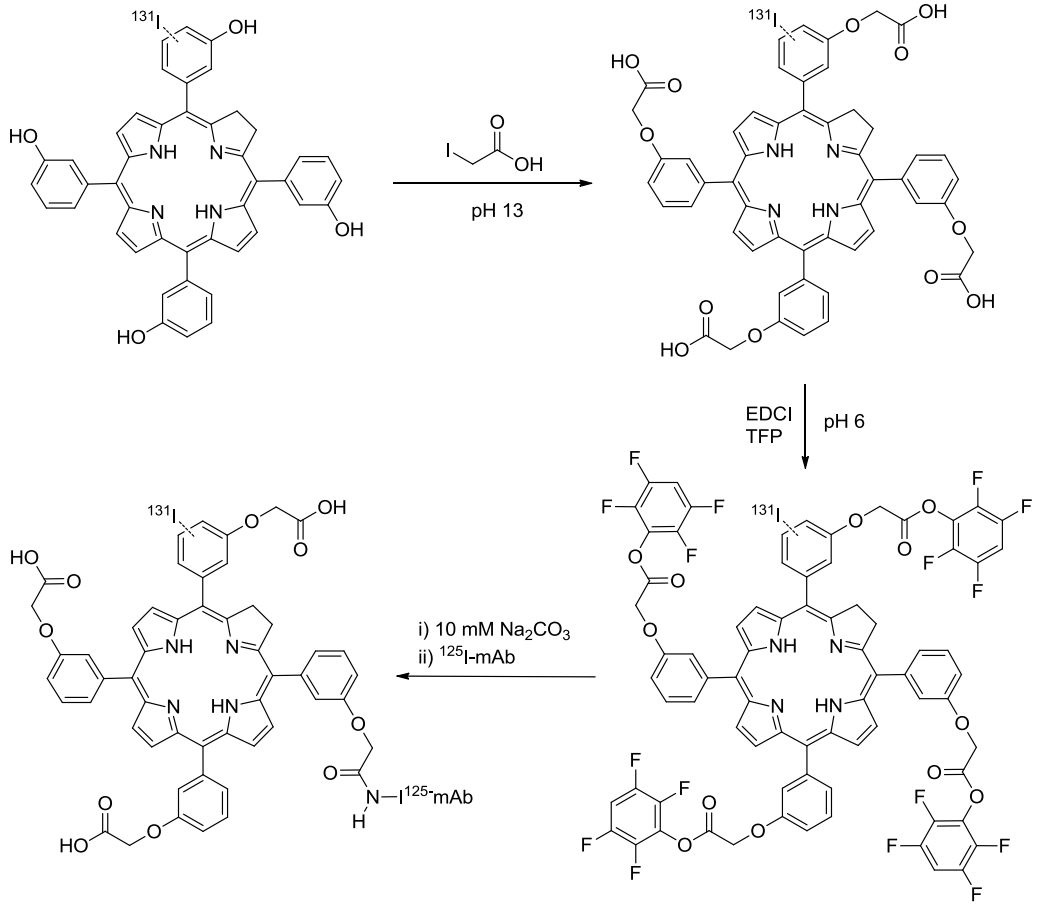

Scheme 5: Modification of Foscan® and conjugation to mAb using TFP activated ester strategy.[38,61]

This approach was used to form conjugates with the internalising 425 mmAb and the non-internalising cmAb U36 antibodies, which target antigens associated with squamous cell carcinomas. Conjugates with a molar ratio of up to 4 photosensitisers per mAb were prepared. SDS-PAGE revealed that the conjugates contained a minor higher molecular weight impurity, which was ascribed to oligomers formed by trace amounts of di-ester in the conjugation mixture. The Temoporfin®-U36 conjugate was radioiodinated to enable pharmacokinetic studies in mice bearing head and neck squamous cell carcinomas. The conjugate exhibited an enhanced selectivity towards the tumour, although this was not as prominent as expected based on the distribution of the unconjugated U36, furthermore the conjugates with a higher molar ratio of photosensitiser were cleared from the blood more rapidly. Both the Temoporfin®-U36 and carboxymethylated Temoporfin® showed significant accumulation in the liver, however skin photosensitisation was lower for the conjugate 48 hours after administration. *In vitro* studies were also performed comparing the internalising and non-internalising conjugates, with the internalising conjugates being more phototoxic.[38]

The research was further developed to enable conjugation with $AlPcS_4$. Thionyl chloride facilitated the conversion of the sulfonic acid groups into sulfonyl chloride functionalities, which in turn were reacted with glycine to produce carboxysulfonamides. These transformations were performed in dimethylformamide, however glycine is insoluble in dimethylformamide therefore *N,O*-bis(trimethylsilyl)acetamide was required to form a disilylated intermediate with glycine so the reaction in dimethylformamide could occur. The carboxyl groups were then treated with TFP in the presence of EDCI, leading to the formation of the activated esters. Partial hydrolysis of the activated ester was not required as the esters are sufficiently labile under aqueous conditions. The photosensitiser in acetonitrile was added to the antibody in buffer solution (pH 9.5) and the resulting conjugate was purified by gel permeation chromatography.[60,61] Conjugations with the mmAb E48 and 425 as well as the cmAb U36 were achieved using this methodology. *In vitro* experiments employing an A431 cell line demonstrated that the internalising $AlPc(S0_2N_{Gly})_4$-425 conjugate was 7500 times more toxic than the un-conjugated photosensitiser. The $AlPc(S0_2N_{Gly})_4$-425 conjugate was also more toxic than the unconjugated Temoporfin®.[60] Vrouenraets *et al.*[62] have coupled a novel photosensitiser, 5-[4-[5-(carboxyl)-1-butoxy]phenyl]-10,15,20-tris-(4-methylpyridiniumyl)porphyrin iodide,[63] to the mmAb E48 and 425 as well as cmAb U36 using the TFP activated strategy as previously described. The selectivity of the conjugates was illustrated and the *in vitro* studies revealed that internalising conjugates were phototoxic to A431 cells, but that the non-internalising conjugates were not at concentrations up to 1 µM.

1.2.2.3 Reductive amination

Reductive amination involves the reaction between formyl and amino groups leading to the generation of an imine, which is usually reduced *in situ* to form a stable amine linkage.

Yarmush and co-workers[64,65,66,67] have used a reductive amination approach for synthesising Sn(IV)chlorin e_6 monoethylenediamine photo-immunoconjugates with IgG,[64] PO37,[64] α-ICAM,[65] and PR2D3[66,67] mAb. The general procedure involves DCC coupling between a chlorin e_6 carboxylic acid group and ethylene diamine to yield a short chain extension terminating in an amino group. The core of chlorin e_6-monoethylenediamine was then derivatised by the insertion of tin using stannous chloride, affording Sn(IV)chlorin e_6 upon air oxidation. For the Sn(IV)chlorin e_6 monoethylenediamine precursor possessing axial ligands, excess triethanolamine was added to Sn(II)chlorin e_6, yielding bis(triethanolamine)Sn(IV)chlorin e_6 monoethylenediamine. Sodium periodate was added to the antibody solution causing oxidation of an oligosaccharide moiety present in the Fc domain, ethylene glycol was added to quench the oxidation process and the oxidised mAb solution was purified by gel permeation chromatography. The photosensitiser in PBS and modified antibody in phosphate buffer were then mixed, leading to the formation of an imine, which was reduced using sodium cyanoborohydride dissolved in water (Scheme 6).[64]

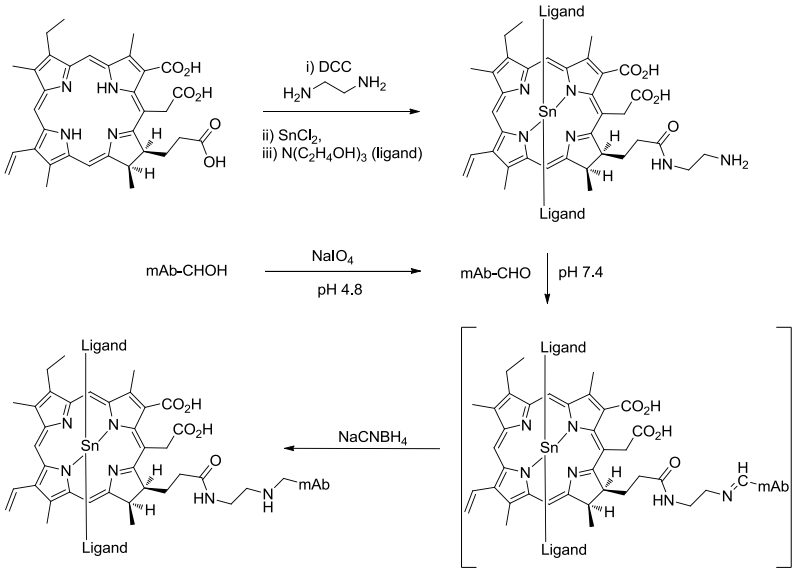

Scheme 6: Reductive amination reaction between derivatised chlorin e_6 and oxidised antibody.[64]

Radioiodated Sn(IV)chlorin e_6 monoethylenediamine-PO37, targeting *P. aeruginosa*, and Sn(IV)chlorin e_6 monoethylenediamine-IgG conjugates were prepared, both with and without the triethanolamine ligands. The photosensitiser to mAb ratios, which were determined spectroscopically, ranged from 1.6-10 and was dependent on the molar excess of photosensitiser used for coupling. Batch to batch preparations were considered to be relatively reproducible, although some preparations did contain immunoglobulin dimers and other aggregates, as determined by HPLC analysis. The singlet oxygen quantum yield of the conjugates had slightly diminished, in comparison to the Sn(IV)chlorin e_6 monoethylenediamine precursor, possibly due to structural changes in the photosensitiser and/or aggregation. *In vitro* assays confirmed that the phototoxicity of the conjugates increased concomitantly with photosensitiser loading. The immunoreactivity of the conjugate was retained, indicated by a competitive inhibition radioimmunoassay. *In vitro* biodistribution studies showed that bis(triethanolamine)Sn(IV)chlorin e_6 monoethylenediamine had a significant effect on retention of the conjugate; Sn(IV)chlorin e_6 monoethylenediamine conjugates were cleared promptly from the mice. The presence of triethanolamine ligands also considerably enhanced the stability of the conjugate in human plasma.[64] This strategy was then utilized to produce conjugates with the α-ICAM mAb specific to cell surface antigens present on melanoma cells. *In vitro* experiments on M21 cells consisting of administering bis(triethanolamine)Sn(IV)chlorin e_6 monoethylenediamine-α-ICAM at various concentrations, and using different light intensities, were conducted to investigate the mechanics of photo-induced cell membrane damage resulting from PDT. A fluorescent integrity probe and microscopy was used to monitor the reactions. A time lag was observed before a point rupture at the cell surface resulted in cell lysis and the time lag was inversely proportional to the reactive oxygen species which had diffused to the cell membrane.[65] This methodology was used for the production of a bis(triethanolamine)Sn(IV)chlorin e_6 monoethylenediamine conjugate with an anti-fibroblast antibody (PR2D3), for the treatment of hypertrophic scars.[66,67] In a preliminary article the bis(triethanolamine)Sn(IV)chlorin e_6 monoethylenediamine-PR2D3 conjugate was synthesised; the loading ratio was determined spectroscopically and found to be, on average, 1.3 photosensitisers per PR2D3. An *in vivo* experiment was performed using mice implanted with human hypertrophic scar tissue; the conjugate was administered to the mice and, after a 24 hour time interval, the photosensitiser was activated with light. Treatment employing the bis(triethanolamine)Sn(IV)chlorin e_6 monoethylenediamine-PR2D3 conjugate caused

considerable growth reduction in the implants in comparison to the un-treated controls. An irrelevant conjugate was also tested *in vivo*, but no noteworthy phototoxic effect was observed.[66] The research was extended to produce a range of bis(triethanolamine)Sn(IV)chlorin e_6 monoethylenediamine-PR2D3 conjugates with loading ratios of 0.5, 1.0 and 2.0 photosensitiser/mAb, with the purity of the conjugates being confirmed by HPLC. Phototoxicity experiments using a cell line consisting of fibroblasts cultured in a fibroblast-populated collagen lattice (FPLC) were performed; it has been postulated that wound contraction resulting in severe scarring is facilitated by fibroblasts and myofibroblasts. The phototoxicity of the bis(triethanolamine)Sn(IV)chlorin e_6 monoethylenediamine-PR2D3 conjugate was found to be dependent on the photosensitiser concentration and intensity of light used for activation. A correlation between increasing rate of lattice contraction and number of viable fibroblasts was observed.[67]

1.2.2.4 Isothiocyanate conjugation

The isothiocyanate functional group enables conjugation with lysine residues via an addition reaction, thus no by-products are produced that could potentially contaminate the conjugate. Additionally, no activating agents or reagents are required. Boyle and co-workers[68,69] have synthesised a range of porphyrins (Figure 5) bearing hydrophilic substituents, such as hydroxyl or quaternised pyridyl groups, and a single isothiocyanate group for bioconjugation; thus eliminating the possibility of antibody cross-linking during the coupling procedure.

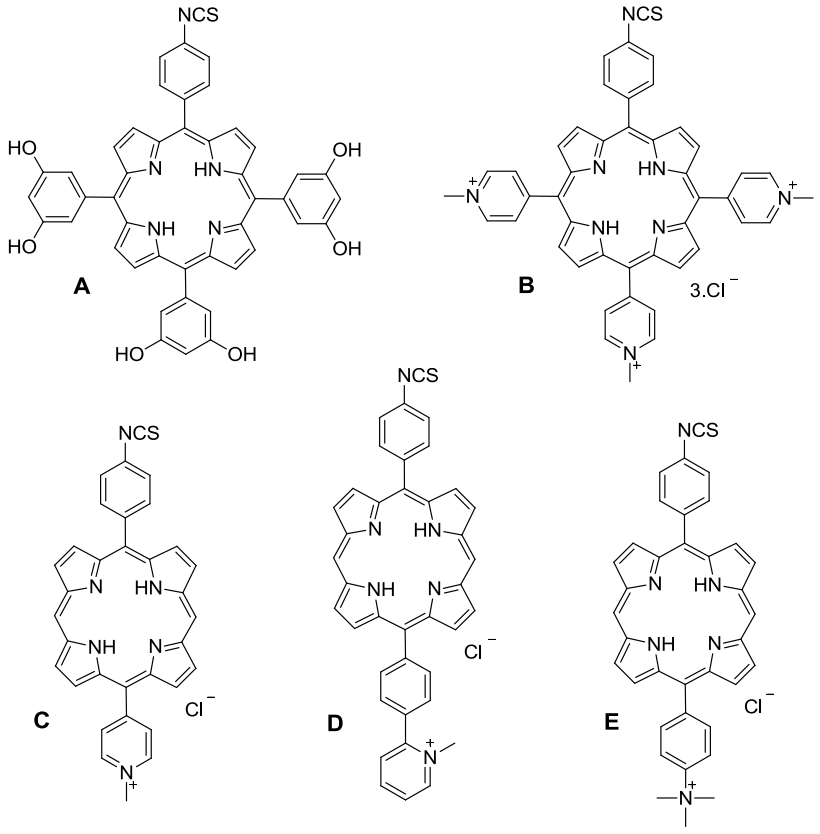

Figure 5: Hydrophilic photosensitiser bearing an isothiocyanate group.

The hexahydroxy porphyrin (**A**) was synthesised from a porphyrin precursor possessing one protected amino group and six methoxy groups. The methoxy functionalities were demethylated using boron tribromide and the single amino group, after deprotection, was transformed into the isothiocyanate functionality by reacting it with 1,1-thiocarbonyldi-2,2`-pyridone (TDP).[68] The cationic compounds (**B**-**E**) were derived from porphyrins bearing a protected amino group, and one or three pyridyl groups for **B**-**D**, or a dimethylamino group for **E**. TDP treatment yielded the isothiocyanate functionality and hydrophilicity was introduced via methylation of the dimethylamino

or pyridyl functionalities. The cationic compounds were treated with amberlite IRA resulting in chloride ion-exchange and enhanced water solubility.[68,69] In a study by Boyle *et al.*[70] the porphyrinic photosensitisers (**A** and **B**) were coupled to the internalising FSP 77 and 17.1A (IgG2a) mAb and the non-internalising 35A7; the antibodies were radioiodinated prior to conjugation to enable biodistribution studies. The conjugation procedure involved **A** in dimethylsulfoxide or **B** in water being added at various molar excesses (20, 40 or 60) to the antibody in sodium bicarbonate buffer (pH 9.2). The conjugates were passed through a Sephadex G25 column using PBS as the eluent, and the purified conjugate loading ratios were determined spectroscopically. The loading ratios calculated ranged from 1.4 to 2.5 and variations occurred between the different photosensitisers and antibodies used. Generally, the loading ratio increased when higher molar excesses of photosensitiser were used for couplings, except for conjugations between **A** and FSP77 mAb, where a decrease in photosensitiser loading was observed, possibly due to reduced solubility in PBS for the photosensitiser at higher concentrations. The behaviour of the conjugates was generally comparable to the corresponding unconjugated mAbs, as indicated by flow cytometry, *in vitro* binding and *in vivo* biodistribution. However a decrease in tumour uptake occurred for conjugates of **B** with higher loading ratios. The *in vivo* biodistribution also showed that tumour to peritumoural ratios were favourable; for example, for **A**-35A7 this was found to be 33.3:1. The SKOv3-CEA-1B9 cell line was used to compare the phototoxicity of the conjugates; an enhanced phototoxic effect occurred for the internalising **A**-FSP77 conjugate, but no phototoxicity was observed for the non-internalising **A**-35A7, whereas both **B**-FSP77 and **B**-35A7 increased in phototoxicity. The absence of phototoxic effect for **A**-35A7, but not for **B**-35A7 was thought to be caused, at least in part, by the greater inherent phototoxicity of **B**, as unconjugated **B** was up to 3 times more phototoxic than **A**. The internalising conjugates were more phototoxic than the non-internalising conjugates, which is in agreement with previous work by Carcenac *et al.*[56]. The research was extended to produce conjugates between **C**, **D** and **E** (Figure 5) and anti-EpCAM or anti-CD104 antibodies.[69] The loading ratios were in the range of 0.3-1.74 photosensitiser/mAb and the variations were dependent on the photosensitiser: **E**>**C**>**D**, as well as the mAb: anti-CD104>anti-EpCAM. Pharmacokinetic studies indicated that the binding efficiency of the conjugates was similar to the corresponding unconjugated antibody. The enhanced phototoxicity of the conjugates was also demonstrated using CORL23 and LoVo cell lines, both of which express the EpCAM and CD104 antigens, however the LoVo cell line expresses 10 times more EpCAM

antigens. The phototoxicity of the anti- EpCAM conjugates on the LoVo and CD104 cell lines was similar and did not seem to reflect differences in antigen expression between the cell lines, thus suggesting that the biology associated with the antibody and/or antigen influences the overall photodynamic effect. Boyle and co-workers[71] then utilized the isothiocyanate approach to produce conjugates with an irrelevant anti-NIP scFv, and LAG3 scFv which targets antigens associated with colorectal malignancies. Various molar excesses of **A** and **B** (Figure 5), ranging from (2.5-60), were added to the scFv in sodium hydrogen carbonate buffer (pH 9.2). The final loading ratios differed substantially for the different photosensitiser used: for **A** loading ratios varied from 4-20 while **B** only loaded between 0.67-1.2 molecules of photosensitiser per scFv. Flow cytometry assessment of the immunoreactivity of the conjugates showed that antigen affinity of the **A** conjugates had been severely compromised, possibly due to non-covalent binding and/or the photosensitiser coupling in the scFv antigen recognition region. The conjugates of **B** retained binding reactivity, with the binding efficiency diminishing with increasing molar loading ratios. *In vitro* cytotoxicity experiments illustrated that **B**-LAG3 scFv had a selective cytotoxic effect on Caco-2 cells, causing cell death primarily via an apoptotic pathway.

1.2.2.5 Maleimide conjugation

Milgrom and O'Neill [72] have synthesised a maleimide substituted porphyrin by a series of modifications to a synthetic, unsymmetrical porphyrin, 5,10,15-tris(4-methoxycarbonylphenyl)-20-(4-hydroxyphenyl)porphyrin, which was subsequently coupled to a thiolated B72.3 mAb (Scheme 7). The hydroxyl group was modified to present an amino group by treating the hydroxyl group with *N*-(2-bromoethyl)phthalimide in the presence of sodium carbonate, and secondly, converting the 2-phthalimidoethoxy group into an amine by treatment with an ethanolic solution of methylamine. A heterobifunctional crosslinking agent, *N*-succinimidyl-3-maleimidopropionate (SMP), in the presence *N*-methylmorpholine, was used to introduce the maleimide group onto the photosensitiser. An aqueous buffered solution of the antibody was treated with 2-iminothiolane hydrochloride (Traut's reagent), resulting in the lysine residues expressing thiol functionalities. A thiol assay using 4,4'-dithiodipyridine indicated that approximately 1.58 thiol groups had been introduced to each antibody. The photosensitiser dissolved in dimethylformamide was added to the thiolated antibody solution leading to the formation of a precipitate, thus indicating that this solvent system was not optimal for conjugation due to the hydrophobic nature of the photosensitiser. The conjugate was finally purified by gel permeation chromatography.

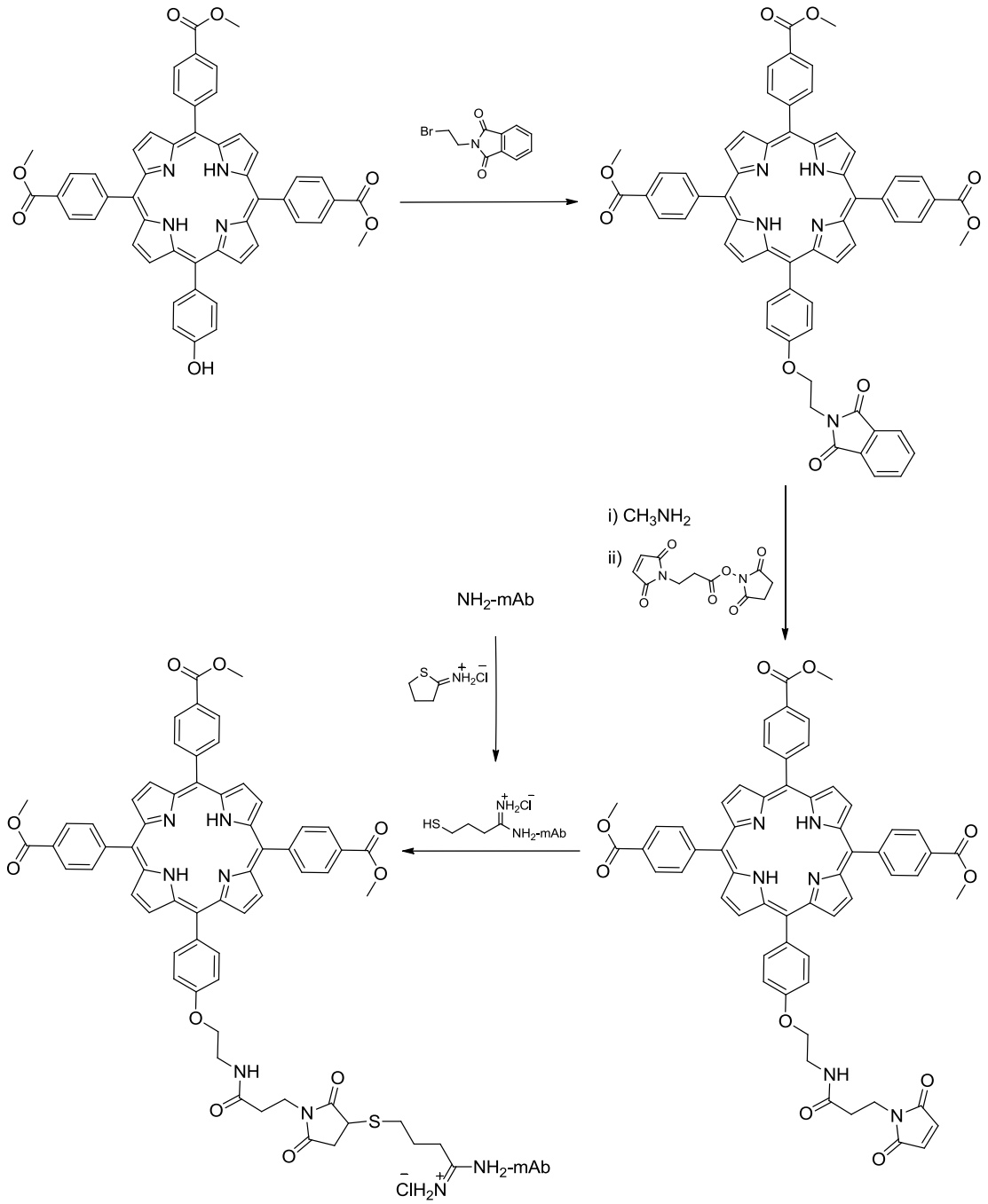

Scheme 7: Coupling of thiolated antibody to a maleimido porphyrin.[72]

1.2.2.6 Acryloyl conjugation

5,10,15-Tris(2-(3-(ethoxycarbonyl)propionamido)-phenyl))-20-(2-aminophenyl)porphyrin has been derivatised to present a thiol reactive acryloyl group.[58] The amino functionality was converted into the acryloyl bioconjugation handle via treatment with acryl chloride in the presence of triethylamine. The photosensitiser dissolved in dimethylsulfoxide was then added to the reduced IgG in sodium phosphate buffer (pH 6). Finally, Sephadex G25 gel permeation chromatography afforded the conjugate (Scheme 8).

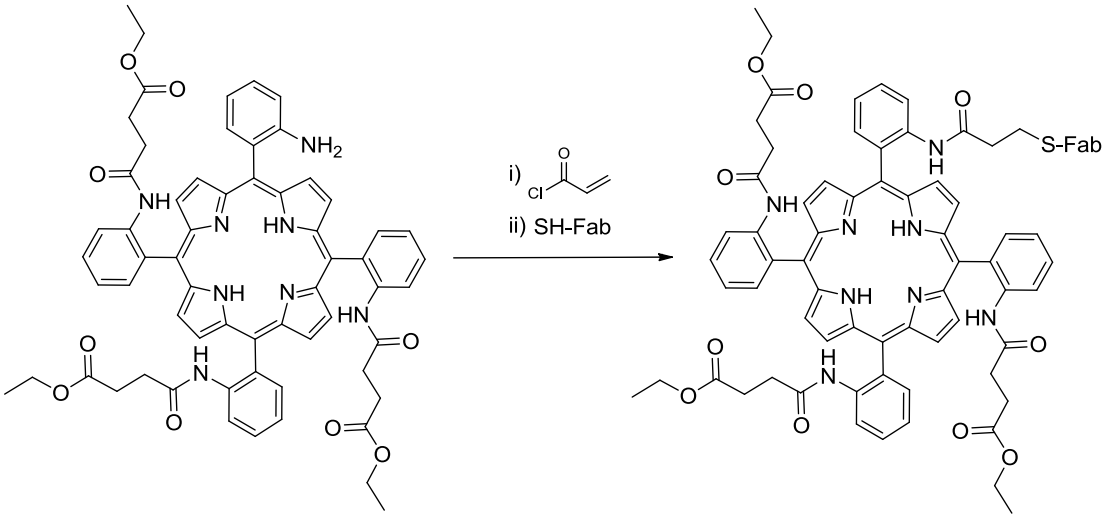

Scheme 8: Bioconjugation involving the acryloyl functionality.[58]

1.2.3 Conjugations using polymeric linkers

Polymeric linkers used for bioconjugation are generally water soluble molecules that posses multiple functionalities, which can be used for coupling with mAbs and photosensitisers. The possibility of loading multiple photosensitisers to the polymer before attachment to the mAb, and thus potentially enhancing photoactivity, is attractive, providing the targeting efficiency of the construct is maintained. Due to the availability of many conjugation sites, photosensitiser will load in a statistical manner. At higher loading ratios this can lead to conjugates bearing photosensitisers in close proximity to each other, and potentially result in quenching of excited states and loss of photoactivity. The relatively large size of the polymer can also present problems if conjugation occurs near the binding site, which can lead to loss of immunoreactivity. Polymeric linkers are generally a mixture of different lengths with average molecular weight, and conjugation will result in this property being transferred to the conjugate, producing conjugates that are ill defined structures.

1.2.3.1 Dextran

The glucose polymer, dextran, which contains multiple hydroxyl groups, is fully water soluble and non-toxic, and has been used to couple multiple photosensitiser units to a variety of antibodies; including anti-Leu-1,[73,74] anti-BSA mAb 9.1,[73,74] anti-melanoma 2.1,[75,76,77] and anti-lymphoma 2.130.[75,76] In preliminary studies, chlorin e_6 monoethylenediamine was prepared by converting one available carboxyl group in to an anhydride using a stoichiometric amount of ethyl chloroformate in the presence of triethylamine. Subsequent addition of ethylene diamine introduced the amino functionality required for reaction with dextran. Sodium periodate was then used to oxidise the dextran and a 5- molar excess of ethylene diamine was added, followed by addition of a 75-molar excess of chlorin e_6; the imines formed during this step were reduced with sodium borohydride. Finally, purified dextran-chlorin e_6 monoethylenediamine conjugate was reacted with the pre-oxidised antibody, and the resulting imine was reduced with sodium cyanoborohydride (Scheme 9). The conjugate was passed through a Sephacryl S-300 column, eluted with sodium phosphate.

The conjugate exhibited high loading ratios, up to 36 chlorin e_6 molecules for each antibody, as determined by UV-visible spectroscopy. The conjugate also retained

approximately 80 % antigen binding activity, as indicated by assays using appropriate antigen positive cell lines; furthermore increasing the photosensitiser loading ratio did not appear to influence the binding activity. Phototoxicity studies showed that photoactivity had been retained; the singlet oxygen quantum yield for the conjugate being identical to the unconjugated photosensitiser. *In vitro* assays determined that phototoxicity was dependent on light intensity, conjugate dose and was further enhanced in the presence of deuterated water, thus suggesting the involvement of singlet molecular oxygen. The conjugate also had a significant phototoxic effect on antigen expressing cell lines, whereas the unconjugated photosensitiser was ineffective at concentrations 100-fold greater than that of the conjugate.[73,74]

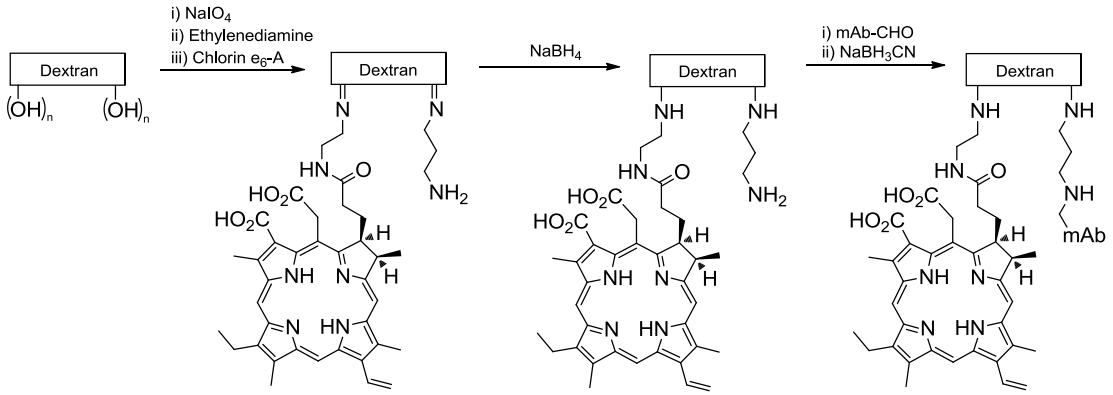

Scheme 9: Synthesis of dextran immunoconjugates.[73,74]

The synthesis of dextran photo-immunoconjugates was further developed so that the dextran carrier expressed a single bioconjugation handle at its terminus, enabling site specific conjugation between the dextran carrier and antibody.[75,76,77] The terminal glucose unit of dextran (35 kDa) was reduced with sodium cyanoborohydride enabling *in situ* reductive amination with adipic dihydrazide. The derivatised dextran, now bearing an amino group, was then reacted with a novel linker; bearing an activated ester and trityl protected hydrazide at opposite ends of a short alkyl chain. Treatment with ethyl chloroformate in the presence of triethylamine resulting in the formation of an activated ester located at the centre of the glucose moieties. Hydrazone was then added to the derivatised dextran, resulting in the formation of multiple amino groups, which were subsequently reacted with various concentrations of Sn(IV)chlorin e_6, pre-activated with EDCI / hydroxybenzothiazole (HOBt). Capping of the un-reacted amino groups was achieved via a reductive amination reaction with acetaldehyde and sodium cyanoborohydride. Acid hydrolysis of the trityl group yielded a single amino group which participated in bioconjugation with an oxidised antibody; to achieve this the

dextran carrier, dissolved in water, was added to the oxidised mAb in acetate buffer (pH 4.75) leading to the formation of a hydrazone linkage. The reduction of this hydrazone was performed, but did not influence the stability of the conjugate, therefore this step was not included for the optimized conditions. Once the reaction was complete, potassium phosphate was added to increase the basicity of the conjugation mixture (pH 7.5). The crude conjugate was then applied to a protein G-Sepharose column, to remove the unconjugated photosensitiser-dextran, and eluted with a glycine solution (pH 2.5). The conjugates had formed as postulated, which was indicated by SDS-PAGE, with HPLC analysis revealing a signal for the pure conjugate in molecular weight range 200-240 kDa, and also a minor signal (< 10 %) corresponding to 2 mAb coupled to a single dextran. The number of Sn(IV)chlorin e_6 molecules coupled to the dextran carrier was dependent on the concentration of Sn(IV)chlorin e_6-HOBt used; various loading ratios were prepared ranging from 1-10 Sn(IV)chlorin e_6 units per dextran. The number of photosensitisers present on the dextran slightly reduced the conjugation yield, but had no influence on the number of dextrans conjugating to each mAb; approximately 2 dextran carriers were conjugated to each mAb. Competitive inhibition assays using antigen positive cell lines, indicated that the binding activity of the conjugate was reduced, but still remained similar to the unconjugated antibody.[75] A series of Sn(IV)chlorin e_6-dextran-anti-melanoma 2.1 conjugates were then assessed *in vitro*[76,77] with the SK-MEL-2 cell line. The selectivity of the conjugate was shown by *in vitro* photolysis experiments; the Sn(IV)chlorin e_6-dextran-anti-melanoma 2.1 conjugates were considerably more phototoxic to SK-MEL-2 cells, in comparison to Sn(IV)chlorin e_6-dextran-anti-lymphoma 2.130. Additionally, phototoxicity was enhanced by increased photosensitiser loading with a higher dose of light.[76] A competitive inhibition assay confirmed that the immunoreactivity of the conjugate had slightly reduced, but the immunoreactivity was independent of photosensitiser loading. The singlet oxygen quantum yield was also calculated and showed the conjugate had a reduced singlet oxygen yield, attributed to a reduced triplet excited state, determined by time resolved absorbance spectroscopy.[77]

1.2.3.2 Polyvinyl alcohol

Polyvinyl alcohol (PVA), average molecular weight 10 kDa, was deemed a suitable polymeric linker due to the presence of multiple hydroxyl groups; giving PVA hydrophilic character as well as facilitating the introduction of multiple photosensitisers. This polymeric carrier has been used for couplings involving benzoporphyrin derivative and T48 mAb.[78] PVA was pre-activated with 2-fluoro-1-methyl pyridinium toluene-4-sulfonate (FMP) and subsequently reacted with 1,6-diaminohexane. An EDCI mediated reaction resulted in conjugation of benzoporphyrin derivative to the derivatised PVA, which now bore amino functionalities. The PVA carrier was modified further so it expressed thiol groups; this was achieved by EDCI coupling of 3-mercaptopropionic acid to available hydroxyl groups. The heterobifunctional crosslinker sulfo-*m*-maleimidobenzoyl-*N*-hydroxysuccinimide ester (SMBS) was then used to modify the antibody; the activated ester reacting with the mAb lysine amino groups resulting in introduction of the thiol reactive maleimide group. The reaction conditions were modified so that 2-3 SMBS were added to each antibody. The benzoporphyrin derivative-PVA and modified antibody were then reacted in acetate buffer (pH 5.5) and the reaction monitored by TLC (Scheme 10). The conjugation mixture was dialysed against PEG and then, in the presence of low molecular weight PVA, was applied to a Sepharose CL-4B column equilibrated with acetate buffer. After purification SDS-PAGE confirmed covalent attachment had occurred and revealed two peaks at 75 and 105 kDa, attributed to cross-linking between one heavy chain and the photosensitiser scaffold, and the PVA carrier cross-linked between the mAb heavy and light chains respectively. Jiang *et al.*[79] investigated these PVA conjugates further by coupling the benzoporphyrin derivative-PVA to a mAb targeting a glycoprotein on human squamous carcinomas of the lung, 5E8 mAb. The benzoporphyrin derivative-PVA carrier was synthesised with a loading ratio of 25:1 and the carrier was coupled to the mAb with a ratio of 1:1. Once conjugated, ELISA analysis determined that 80 % of the binding activity had been retained for benzoporphyrin derivative-PVA-5E8, and the benzoporphyrin derivative-PVA-T48 did show enhanced binding in comparison to benzoporphyrin derivative-PVA. A phototoxicity study employing the antigen positive A549 cells, demonstrated enhanced potency of the benzoporphyrin derivative-PVA-5E8, which was 10 fold more phototoxic than the irrelevant conjugate. Additionally, the phototoxicity increased in the presence of 10 % foetal calf serum. The irrelevant

conjugate was found to be more cytotoxic to A549 cells than the unconjugated photosensitiser, probably due to benzoporphyrin derivative associating with serum proteins; the association is less prominent once benzoporphyrin derivative is conjugated.

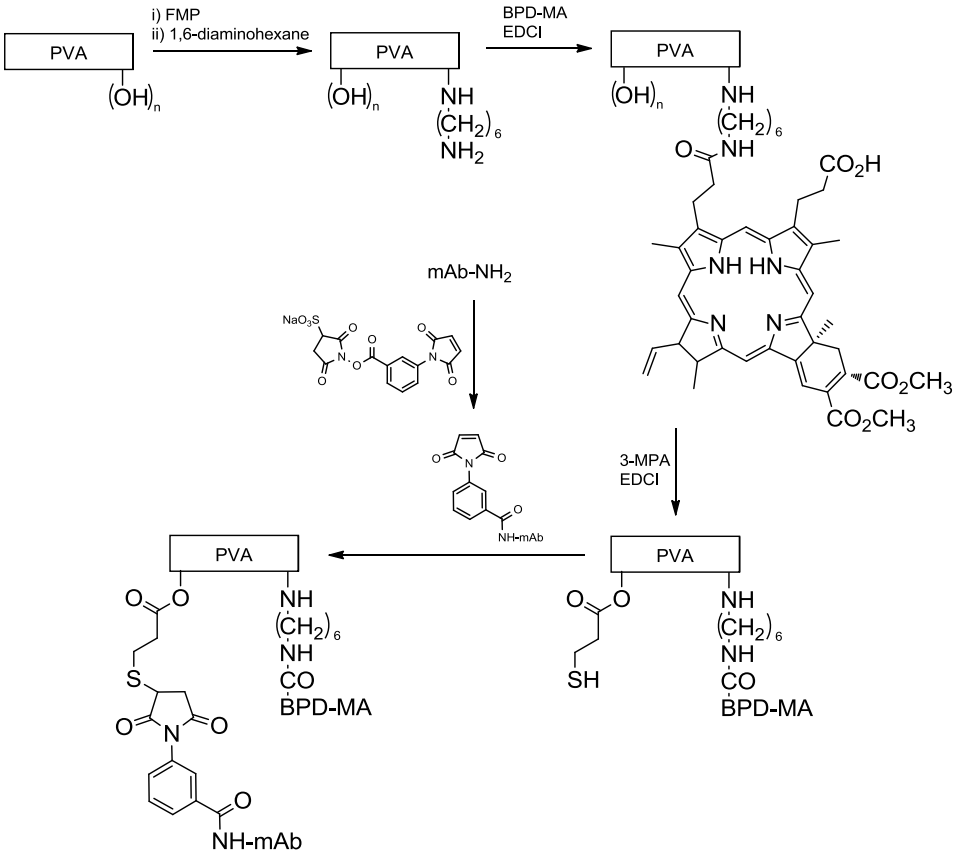

Scheme 10: Synthesis of immunoconjugate using polyvinyl alcohol as a polymeric linker.[78]

Further *in vitro* studies were conducted by comparing the phototoxic effect when the conjugate remained on the cell surface or was internalised; if the conjugate was internalised an increase in phototoxicity was observed.[80]

The biodistribution of the conjugates was then assessed *in vivo* with DBA/2 mice bearing M1 tumours and nude mice with A549 tumours. The photosensitiser was labelled with ^{13}C, and the conjugation was performed using 2 equivalents of benzoporphyrin derivative-PVA to 1 equivalent of mAb, the final photosensitiser:mAb loading ratios were 50-70:1 as indicated by UV-visible spectroscopy. The benzoporphyrin derivative biodistribution in the different mice was similar, except for the tumour (less benzoporphyrin derivative detected for nude mice) and lymph nodes

(more benzoporphyrin derivative detected in nude mice). The conjugates remained in the blood of the nude mice for a longer time period than the unconjugated photosensitiser and generally the conjugates were retained in all tissues to a greater extent, and for a longer period of time, than the unconjugated photosensitiser. The kidneys, liver, lungs and spleen contained the highest concentrations of photosensitiser. The free photosensitiser clearly had a completely different pharmacokinetic profile to the conjugates, thus the conjugates were assumed to be relatively stable *in vivo*.[81]

Hemming *et al.*[82] studied the potential of benzoporphyrin derivative-PVA conjugates by comparing the biodistribution with unconjugated benzoporphyrin derivative and cytotoxicity against the commercially available Photofrin II®. An anti-EGFR IgG1, which has an affinity for oral squamous cell carcinomas, and anti-CEA IgG1, were coupled to benzoporphyrin derivative-PVA by the method previously described.[78] A hamster contralateral cheek pouch model containing squamous cell carcinomas was employed. The tumour to peritumoural ratio for benzoporphyrin derivative (2:1) was considerably less favourable than the benzoporphyrin derivative-PVA-anti-EGFR IgG1 (26:1). The 1 month cancer free survival of the hamsters showed that the therapies with benzoporphyrin derivative were more effective than that with Photofrin II®; 67 % survival for benzoporphyrin derivative but only 27 % for Photofrin II®. However the benzoporphyrin derivative-PVA-anti-EGFR IgG1 conjugate was significantly more cytotoxic than the free photosensitiser; 80 % of the hamsters survived with a twentieth of the dose in comparison to the benzoporphyrin derivative treatment.

1.2.3.3 Polylysine

An alternative polyamino acid carrier, polylysine (average molecular weight 25 kDa), has been used for synthesising cationic and anionic bioconjugates with OC125 $F(ab')_2$;[83,84,85,86] targeting ovarian cancer antigens, 17.1A, mAb;[87,88,89] which bind to colorectal cancer associated antigen (EpCAM) and an irrelevant rabbit IgG.

The initial study investigated the effect of charge on the activity of the conjugates, as cationic character has been reported to enhance the rate of endocytosis. Firstly, the chlorin e_6 was converted to its activated ester form using a DCC mediated reaction with NHS, which was subsequently reacted with polylysine in the presence of *N*-ethylmorpholine. The heterobifunctional crosslinker pyridyldithiopropionic acid-NHS ester was then used to introduce a disulphide bioconjugation handle to the polymeric linker. The lysine required further functionalisation in order to produce the anionic immunoconjugate; the addition of a large excess of succinic anhydride resulted in amino groups being converted to amide groups bearing carboxyethyl groups. The cationic character was provided by protonation of the lysine amino groups, whereas deprotonation of the carboxylic acid groups resulted in anionic properties being expressed. The antibodies were treated with mercaptoethylamine in phosphate buffer containing ethylenediaminetetraacetate (EDTA), causing partial reduction of the cysteine residues in the hinge region. The reactive thiol expressed by the antibody could then participate in a disulphide exchange reaction with the disulphide bioconjugation handle, resulting in covalent coupling. Conjugations were performed by the reaction of a 3-fold excess of the derivatised lysine in dimethylsulfoxide with the reduced antibody in phosphate buffer (pH 7.5) (Scheme 11), a Sephadex G200 column was finally used for purification. SDS-PAGE confirmed the conjugation had occurred. The loading ratio was calculated using UV-visible spectroscopy, and was found to be 15-20 photosensitisers/antibody. The immunogenicity of the conjugates was maintained, relative to the unconjugated antibody, as shown by ELISA competition assays on an antigen positive OVCAR-5 cell line. Cellular uptake studies revealed a six-fold enhancement of cationic conjugate uptake, in comparison to the anionic conjugate, after a 6 hour incubation time, increasing to a 17-fold enhancement after a 24 hour incubation time. Furthermore, raising the temperature of the cellular uptake assays also improved uptake of the cationic conjugate, these findings indicated that an active uptake process was occurring. Phototoxicity studies confirmed the enhanced potency exhibited by the cationic conjugate.

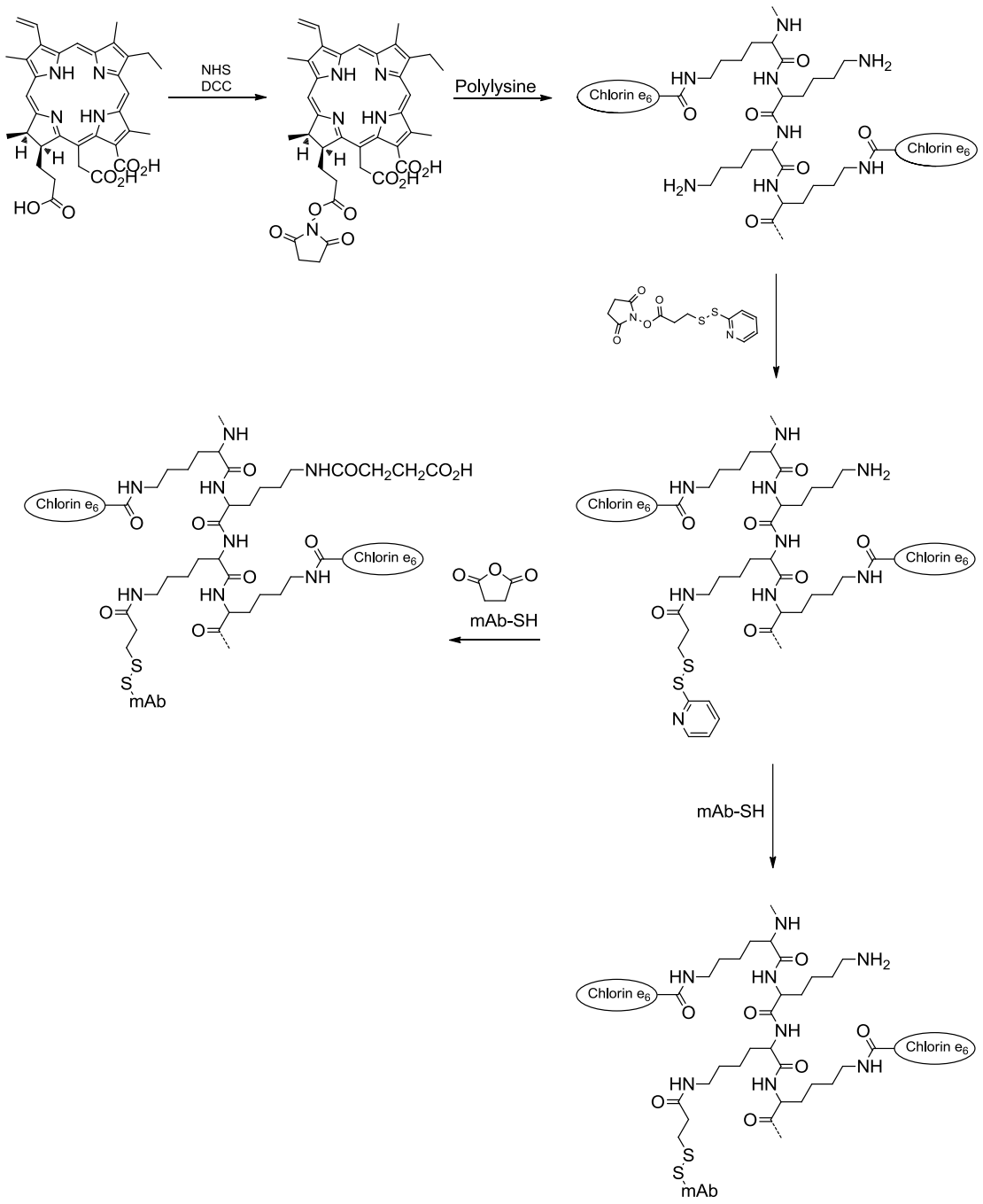

Scheme 11: Cationic and anionic lysine based immunoconjugates.[83]

These photo-immunoconjugates were then tested *in vivo*, using mice bearing ovarian tumours.[84] The biodistribution of the conjugates was analysed 3 hours and 24 hours post administration by harvesting the vital organs of the mice and calculating the tumour to peritumoural ratio. The cationic conjugates were significantly better at delivering photosensitiser to the target tissue in comparison to the anionic conjugates. After 3 hours the cationic chlorin e_6-polylysine-OC125 $F(ab')_2$ conjugate had caused less photosensitiser accumulation in the liver, kidneys, intestine and skin in comparison to the corresponding anionic analogue. However after 24 hours, the cationic conjugate showed a greater photosensitiser accumulation in the intestine and skin. Ovarian cancer can become resistant to cisplatin treatment, therefore a study was conducted to determine whether chlorin e_6-polylysine-OC125 $F(ab')_2$ could be used for a PDT pre-treatment to overcome the resistance.[85] *In vitro* assays were performed comparing cisplatin, PDT, and a combination of the two treatments with various cisplatin sensitive and resistant cell lines. The combination of the two treatments generally enhanced the overall cytotoxic effect, with the enhancement being less prominent for the cisplatin sensitive cells. The photodynamic effect caused by anionic and cationic chlorin e_6-polylysine-OC125 $F(ab')_2$ conjugates to mice with ovarian cancer xenografts was also investigated.[86] The experiments involved injection of the non-conjugated photosensitiser or conjugates, followed by a 3 hour interval before the application of light; this procedure was repeated 3 times for each treatment. All PDT treatments caused a reduction in tumour size compared to the control, with the mice treated with the cationic chlorin e_6-polylysine-OC125 $F(ab')_2$ surviving longer (44 days) than the mice receiving the other treatments (36 days).

The polylysine conjugation method was then utilised for the synthesis of conjugates using the 17.1A mAb which has an affinity towards colorectal cancer cells.[87,88,89] An ELISA binding assay showed that the anionic conjugate binding activity had been compromised, whereas the cationic conjugate exhibited an enhanced targeting efficiency compared to the unconjugated antibody. Furthermore, the cellular uptake for the cationic chlorin e_6-polylysine-17.1A mAb conjugate was 4 times greater than the anionic analogue, although both conjugates were more selective towards antigen positive cells than the irrelevant conjugates and the unbound photosensitiser. Photo-killing studies using an antigen positive cell line showed that the cationic conjugate was the most potent.[87] The biodistribution of the conjugate and precursors were then assessed *in vivo*. Mice were injected with HT29 cells, inducing the expression of tumours on the liver. Post 3 hours and 24 hours photosensitiser administration, the

biodistribution was determined by quantifying the fluorescence spectra for each of the tissues analysed. After 3 hours, the anionic conjugate had delivered five times more photosensitiser to the tumour compared to the cationic conjugate; which delivered approximately half the quantity of photosensitiser, compared to the unconjugated chlorin e_6. Accumulation in the bladder was noted for all the photosensitisers and a significant amount of photosensitiser was present in the lungs for the cationic conjugate. Additionally, the cationic conjugate was cleared from the blood more rapidly and was not significantly retained in the skin, in comparison to the anionic photosensitiser and chlorin e_6. The anionic conjugate also exhibited a slightly more favourable tumour to peritumoural (liver) ratio (2.52:1) in compared to the cationic conjugate (2.2:1), however the most favourable ratio was observed for the free chlorin e_6 (3.61:1). The free chlorin e_6 had accumulated substantially in the skin, with a tumour to peritumoural (skin) ratio (1.94:1) in comparison to the conjugates and precursor (38-81.4:1). After 24 hours, the quantity of photosensitiser present in the tumour had reduced, although a substantial quantity was still present in the target tissue for the anionic conjugates, furthermore the tumour to peritumoural ratios were less for the liver (1.54:1) compared with the skin (87.1:1). Mice treated with the cationic photosensitiser still had significant accumulation in the lungs, whereas the anionic conjugate caused substantial photosensitiser retention in the bladder.[88] Due to the promising biodistribution results obtained for the anionic conjugate, phototoxic *in vivo* assessments of the long and short term benefits and survival rates following PDT was made, employing mice with colorectal tumours of the liver. Short-term tumour response indicated that the conjugate reduced tumour growth substantially more than chlorin e_6 and the control. The median survival results correlated well with the enhanced phototoxicity observed during the short term experiments; the mice treated with the conjugate (102 days) survived longer than the treatments with the chlorin e_6 precursor (77 days) and the control (62.5 days). Increasing the light dose was also found to enhance the cytotoxic effect, with the laser-induced hyperthermia of the target cells being a contributing factor to the overall cytotoxic effect.[89]

1.2.3.4 *N*-(2-hydroxypropyl)methacrylamide

N-(2-hydroxypropyl)methacrylamide (HPMA) based polymers are both biocompatible and hydrophilic, and as such have been selected as a suitable polymeric linker for use in bioconjugation.[90]

Kopeček and co-workers,[91] have described the synthesis of HPMA copolymer-chlorin e_6 monoethylenediamine-immunoconjugates, using either OV-TL16 IgG or Fab' targeting antigens related with ovarian carcinoma. A radical precipitation copolymerisation procedure was used to produce two different co-polymers using HPMA, and either *N*-methacryloylglyclphenylalanylleucylglycine *p*-nitrophenylester (co-polymer 1) or *N*-methacyloylglycylglycine *p*-nitrophenyl ester (co-polymer 2). The first immunoconjugate bearing the unmodified OV-TL16 IgG was synthesised by reacting co-polymer 1 dissolved in dimethylsulfoxide, with chlorin e_6 monoethylenediamine, in the presence of triethylamine. The subsequent polymeric precursor in dimethylformamide was added to the OV-TL16 IgG in PBS, with the pH being maintained at 7.2 for 2 hours, which was then increased to pH 8.3 over a 3 hour period (Scheme 12). Purification of the immunoconjugate was performed by, firstly using a Sephadex G-25 column to remove the low molecular weight impurities, followed by a Superose 6 (HR16/60) column to collect the desired immunoconjugate fraction. The polymeric immunoconjugate was characterised using a combination of techniques, including UV-visible spectroscopy, refractive index detection and Lowry assay. The approximate molar ratio was calculated, and found to be: protein:polymer:photosensitiser 1:4:9.

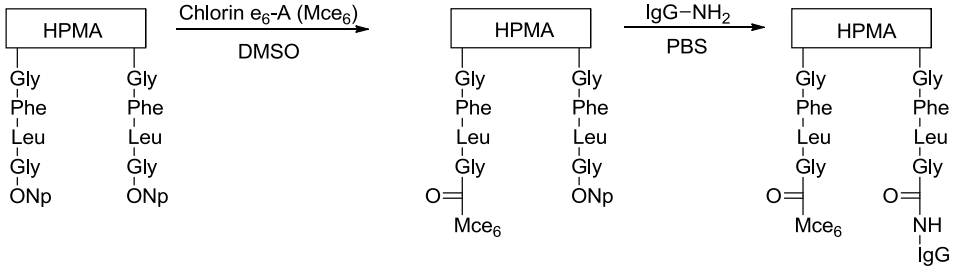

Scheme 12: Synthesis of chlorin e_6 monoethylenediamine-HPMA-co-polymer 1-IgG.[91]

The remaining two conjugates were prepared using the same polymeric precursor; co-polymer 2 was treated with chlorin e_6 monoethylenediamine, in dimethylsulfoxide, followed by the drop-wise addition of hydrazine hydrate in dimethylformamide. The polymeric precursor was dialysed against ethanol/water, dilute hydrochloric acid, followed by water, in order to remove un-reacted hydrazine. The immunoconjugate was prepared by oxidising OV-TL16 IgG, using sodium periodate, which was subsequently added to the polymeric precursor in acetate buffer, pH 5.2, leading to the formation of a stable imine linkage (Scheme 13). The crude mixture was applied to a Superose 6 (HR16/60) column and the relevant fractions collected. The approximate molar ratio was again calculated and found to be: protein:polymer:photosensitiser 1:2.5:4.

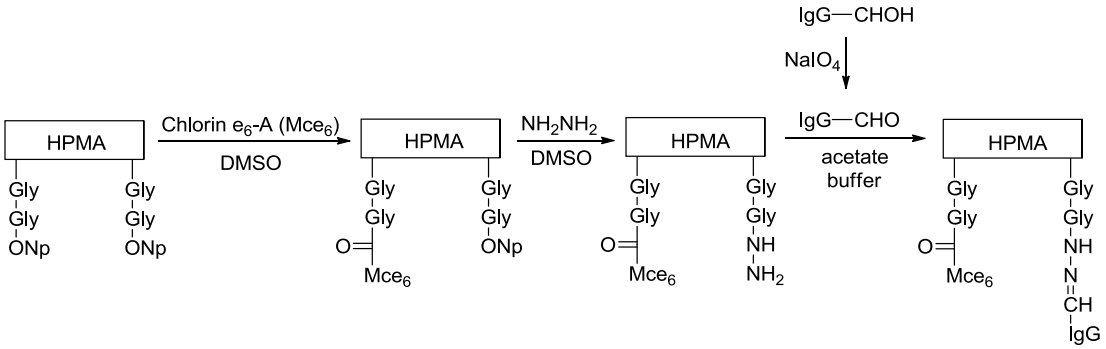

Scheme 13: Synthesis of chlorin e_6 monoethylenediamine-HPMA-co-polymer 2-IgG_{ox}.[91]

The remaining immunoconjugate used a OV-TL16 Fab'; OV-TL16 IgG was enzymatically cleaved using ficin, the $F(ab')_2$ fragment was isolated and subsequently treated with dithiothreitol affording the Fab' fragment. The polymeric precursor dissolved in anhydrous dimethylformamide was treated with the heterobifunctional linker 4-(*N*-maleimidomethyl)cyclohexanecarboxylic acid *N*-hydroxysuccinimide ester (SMCC) in the presence of triethylamine, furnishing a reactive maleimide group. The derivatised polymeric precursor in a sodium phosphate buffer (pH 7.4) containing EDTA was added to the OV-TL16 Fab' in the same buffer solution, resulting in the formation of a thioether bond (Scheme 14). Purification using a Superdex 200 (HR 16/50) size exclusion column afforded the immunoconjugate. The approximate molar ratio was calculated and found to be: protein:polymer:photosensitiser 1:1:1.5.

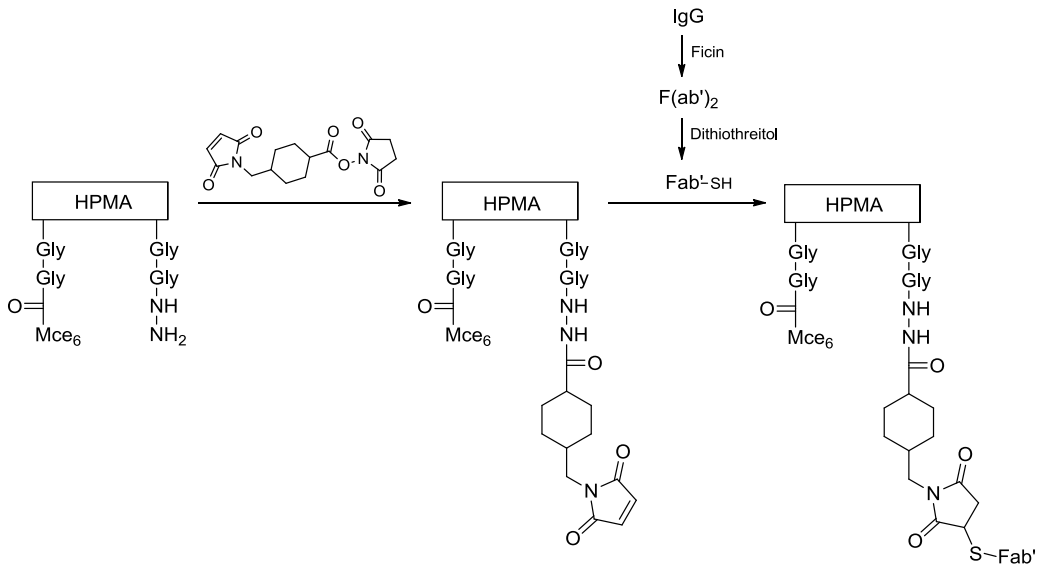

Scheme 14: Synthesis of chlorin e_6 monoethylenediamine-HPMA-co-polymer 2-Fab'.[91]

An immuno-assay was performed employing antigen positive OVCAR-3 cells, enabling a comparison between the native antibody and immunoconjugate affinity constants. The affinity constant of OV-TL16 IgG (8×10^{-8} M^{-1}) was compared to chlorin e_6 monoethylenediamine-HPMA-co-polymer 1-IgG (1×10^{-8} M^{-1}) and chlorin e_6 monoethylenediamine-HPMA-co-polymer 2-IgG_{ox} (3×10^{-8} M^{-1}); both conjugates exhibited a substantial decrease in binding efficiency, with chlorin e_6 monoethylenediamine-HPMA-co-polymer 1-IgG showing the lowest affinity constant, due to polymer attachment to the IgG around the antigen binding region. The chlorin e_6 monoethylenediamine-HPMA-co-polymer 2-Fab' (3×10^{-8} M^{-1}) also showed a decrease in antigen binding activity compared to the $F(ab')_2$ (6×10^{-8} M^{-1}).

The HPMA co-polymer 2 has also been used to facilitate the formation of an immunoconjugate bearing chlorin e_6 monoethylenediamine and OV-TL16 IgG, as shown in Scheme 15. HPMA co-polymer 2 was reacted with chlorin e_6 monoethylenediamine, leading to the formation of an amide linkage, and the resulting polymeric precursor was purified by chromatography. The OV-TL16 IgG in a phosphate buffer containing sodium chloride (pH 7.2), was added to the polymeric precursor in dimethylformamide, and after 2 hours, the pH was slowly increased to 8.3 over a 3 hour period. A competitive immuno-assay was performed, employing the OVCAR-3 cell line and immunoconjugate, in the presence, and absence of the native antibody; the presence of the native antibody significantly reduced cellular uptake of the conjugate, thus demonstrating the conjugates antigen targeting ability. *In vitro*

cytotoxicity studies were also conducted, evaluating the IC_{50} doses for the immunoconjugate (0.38 μM), HPMA- chlorin e_6 monoethylenediamine precursor (290 μM) and free photosensitiser (0.34 μM). The immunoconjugate exhibited an enhanced potency in comparison to the chlorin e_6 monoethylenediamine precursor, however the free photosensitiser was the most potent, an effect which was attributed to diffusion of the free photosensitiser into the cell being more efficient than the pinicytosis mechanism required for the HPMA derivatives.[92]

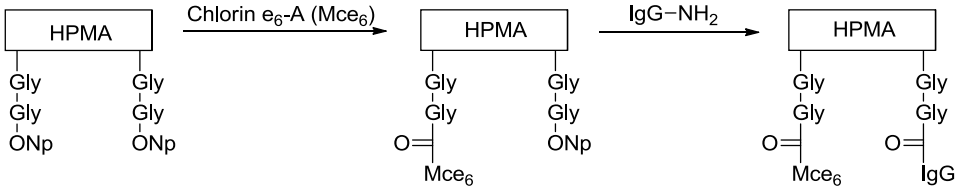

Scheme 15: Synthesis of chlorin e_6 monoethylenediamine-HPMA-co-polymer 2-IgG.[92]

In vivo studies have been performed using chlorin e_6 monoethylenediamine-HPMA-co-polymer 1-IgG and nude nice bearing OVCAR-3 xenografts. The immunoconjugate accumulated in the tumour considerably more than the precursors, and following activation of light, the chlorin e_6 monoethylenediamine-HPMA-co-polymer 1-IgG treatment caused a notable reduction of tumour volume, whereas the free photosensitiser had little effect. The article also described the synthesis of a doxorubicin immunoconjugate, and the benefit of combining targeted chemotherapy with PDT was demonstrated, relative to treatment with the individual conjugates.[93]

A biodistribution study comparing chlorin e_6 monoethylenediamine and chlorin e_6 monoethylenediamine-HPMA-co-polymer 1 showed that the HPMA conjugate exhibited a substantial accumulation of photosensitiser in the liver and spleen, both of which were greater than the same parameter for the tumour.[94]

HPMA has also been copolymerised with polymerisable Fab' and chlorin e_6 monoethylenediamine fragments, bearing methylacryloyl functionalities. The polymerisable Fab' was prepared by firstly derivatising methylacryloyl chloride, using a series of synthetic steps, leading to the introduction of a spacer terminating with an amino group. SMP was added to the derivatised polymerisable fragment, resulting in the introduction of a maleimide group, thus enabling the subsequent addition of the Fab' fragment. The polymerisable chlorin e_6 monoethylenediamine fragment was prepared using a methylacryloyl precursor, containing an enzyme cleavable tetra-peptide chain

terminating with a *p*-nitrophenoxy group; the activated ester was then used to form a stable amide bond between the polymerisable precursor and photosensitiser. The polymerisable antibody and photosensitiser fragments were copolymerised with HPMA, using an azo initiator (VA-044), leading to the formation of the immunoconjugate, as illustrated in Scheme 16. *In vitro* cytotoxicity studies revealed that treatment using the immunoconjugate led to an increase in internalised photosensitiser, which localised in the lysosomal compartment, and as such, was more potent than the native photosensitiser and a copolymer employing HPMA and the polymerisable photosensitiser fragment.[95]

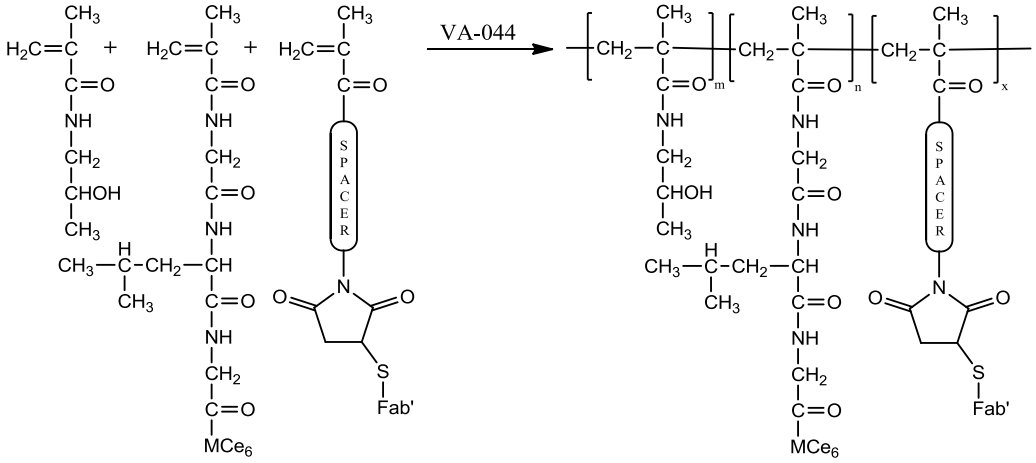

Scheme 16: Formation of HPMA co-polymer immunoconjugate.[95]

Lu *et al.*[96] utilised the same methodology to synthesise a polymerisable Fab' fragment, containing a PEG spacer. The presence of the PEG chain enhanced the solubility of the fragment, resulting in a higher polymerization activity in comparison to the previously reported polymerisable Fab' fragment.[95]

1.3 Cysteine reactive functionalities

The reduced SIP(L19) fragment selected for this research project expresses two thiol functionalities which are available for conjugating to the photosensitiser moiety, thus the photosensitiser must posses a complementary functionality to facilitate the conjugation. It has been reported that porphyrins bearing maleimide[72] and acroyloyl[58] functionalities have participated in conjugations with antibodies expressing thiol groups. Additionally, it has also been demonstrated that an antibody bearing a thiol group can be modified with SIAB to express an activated ester, which can subsequently conjugate to a porphyrin bearing an amino group.[58] A variety of other conjugation strategies involving the thiol group have been reported. A range of proteins have been modified to express either *N*-iodoacetyl or divinylsulfone functionalities, enabling selective conjugation to sulphydryl groups expressed by a peptide.[97] A similar approach has been used for the synthesis of a phospholipid-peptide conjugate, with the phospholipid modified to express an *N*-bromoacetyl functionality.[98] Disulphide exchange has also been utilised for conjugations involving thiol groups. The disulphide exchange reagent pyridyldithiopropionic acid-NHS ester has been used for synthesising a photosensitiser-lysine-antibody conjugate as previously described.[83] An oligonucleotide which posses an activated disulphide bond, has been treated with a thiol expressing peptide, leading to the generation of a disulphide linked oligonucleotide-peptide conjugate.[99] The literature suggested that the maleimide functionality was the most commonly used group for participating in conjugation reactions involving sulphydryl expressing antibodies, and was therefore selected for this research project.

1.3.1 Maleimide

During the research project, Endo *et al.*[100] reported the transformation of an amino functionality, expressed by a pre-formed porphyrin, into a maleimide group, as illustrated in Scheme 17. A solution of 5-(4-aminophenyl)-10,15,20-tri(4-sulfonatophenyl)porphyrin tris-tetrabutylammonium salt dissolved in anhydrous acetonitrile, was treated with maleic anhydride for 5 hours at reflux. The solvent was removed under reduced pressure and the intermediate was subsequently treated with acetic anhydride in the presence of sodium hydrogencarbonate, resulting in

cyclodehydration of the maleic acid and formation of the maleimide, with an overall yield of 90 %.

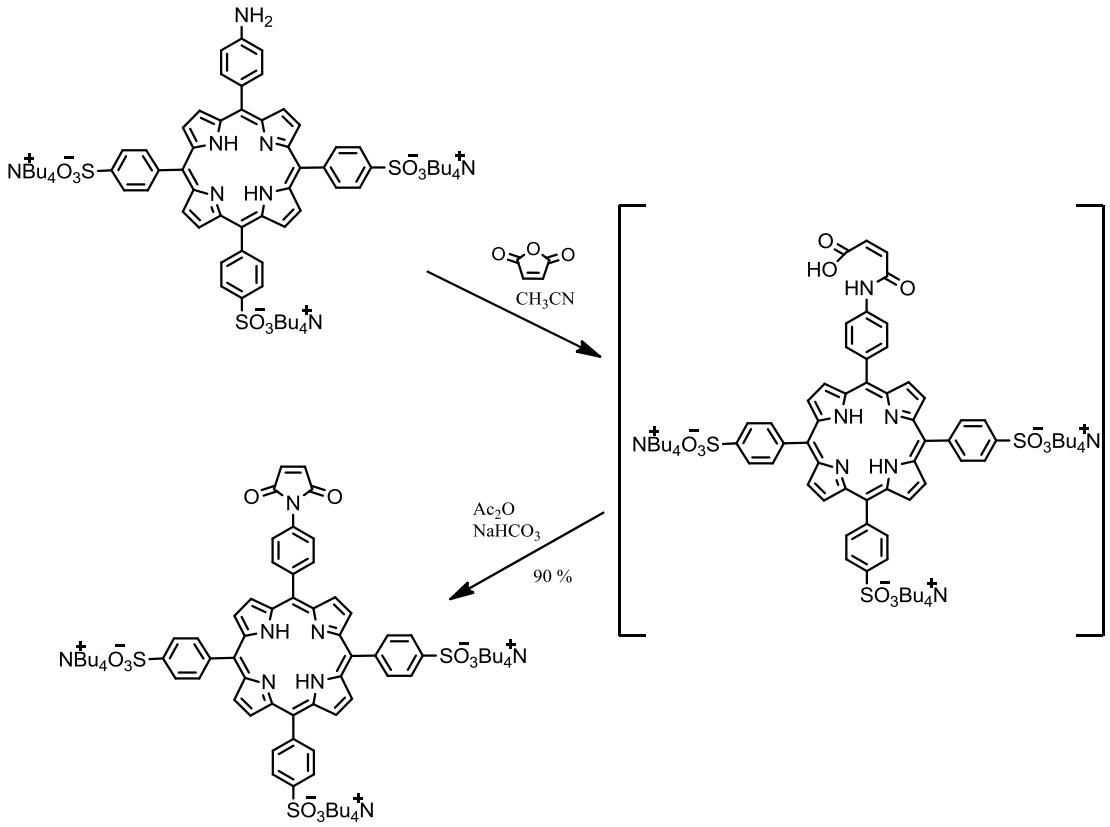

Scheme 17: Synthesis of 5,10,15-tris(4-methoxycarbonylphenyl)-20-(4-(2-(3-maleimido)propionamido)phenyl)porphyrin.[100]

A porphyrin bearing an amino functionality can be further modified to possess a maleimide group by using a hetero-bifunctional cross-linking reagent, such as SMP, as previously described.[72] In addition to SMP, SMCC is another hetero-bifunctional cross-linking reagent which has been used to incorporate a thiol expressing antibody into a HPMA immunoconjugate, as previously discussed.[91,95] The versatile SMCC has been utilised for production of an array of conjugates, including: glycogen phosphorylase b-thyroxine,[101] DNA-bisbenzimidazole,[102] ethidium homodimer-B72.3 mAb,[103] glucose oxidase-IgG,[104] and cholera toxin-liposome.[105] A variety of different reaction conditions have been reported for the addition of SMCC to an amino bearing compound, with the reaction being performed in dimethylformamide;[101] and in the presence of 4-dimethylaminopyridine (DMAP),[103] diisopropylethylamine (DIEA);[102] in chloroform/methanol (9:1) with the addition of triethanolamine[105] and in sodium phosphate buffer (pH 7).[104]

Although not applied to porphyrin chemistry, a Mitsunobu type reaction can be used to convert a hydroxyl group into maleimide functionality. A triphenylphosphine/ diethyl azodicarboxylate (DEAD) catalysed reaction between phenethyl alcohol and 1*H*-pyrrole-2,5-dione in tetrahydrofuran, afforded the maleimide derivative in 24-92 % yield. The reaction conditions were evaluated and it was observed that yields were improved when the reaction was performed at −78 ^{o}C, gradually increasing to ambient temperature; with a slight excess of the initial alcohol and in the presence of neo-pentyl alcohol.[106]

The maleimide functional group is susceptible to nucleophilic attack; therefore it would be feasible for conjugations to other amino acid residues, such as lysine, to occur. The nucleophilicity of the amino acid residues can be controlled using the environmental pH. When the pH of the surroundings is close to or above the amino acids pKa, deprotonation occurs, and the residue becomes more nucleophilic. If the conjugation is performed in a buffer solution of 6.5-7.5 pH, the maleimide reacts exclusively with thiol groups, as the pKa of cysteine (8.8-9.1) is slightly lower than lysine (9.3-9.5). Above the 6.5-7.5 pH range, the maleimide functional group would also react with lysine residues.[107,108]

Under basic conditions, the maleimide group can be hydrolysed, and once the maleimide ring has opened it renders it inactive towards thiol functionalities. The hydrolysis can also occur after thiol conjugation. The rate and degree of hydrolysis is dependent on the functionalities to which the maleimide is attached. Aromatic systems enhance maleimide hydrolysis, whereas unconjugated systems such as the cyclohexane ring of SMCC, increases stability. The steric hindrance provided by the cyclohexane ring could also be a contributing factor to the enhanced stability of SMCC.

As porphyrins are aromatic, and it has been reported that maleimides are more susceptible to hydrolysis when attached to a conjugated system, it seemed appropriate to employ an unconjugated linker in-between the porphyrin and maleimide functionality. SMCC was therefore selected to further modify the porphyrin moiety.

1.4 Synthetic overview

As part of a collaboration project with the research group of Professor Dario Neri at the Swiss Federal Institute (ETH), the aim of the project was to synthesise a photosensitiser-SIP(L19) conjugate for PDT. The photosensitiser/porphyrin moiety would be synthesised in Hull, which would then be sent to Zurich for subsequent conjugation to reduced SIP(L19) and biological studies.

The porphyrin moiety required dual functionality: a single maleimide bioconjugatable group, enabling conjugation to a cysteine residue, and functionalities which could be further modified to provide hydrophilicity, facilitating the conjugation to SIP(L19) under aqueous conditions. The strategies used for the introduction of dual functionality were functionalisation of a symmetrical porphyrin, and incorporation of the different functional groups during porphyrin formation via a mixed condensation. The hypothesised porphyrinic products are depicted in Figure 6.

Synthetically, the first major strategy decision was, at which point in the sequence of reactions leading to the target molecule was it most appropriate to switch the porphyrin from a hydrophobic to hydrophilic compound i.e. before or after addition of the maleimide. Due to difficulties in handling and purifying hydrophilic compounds, and the maleimide being susceptible to hydrolysis, it was hypothesised that the introduction of water solubility should be delayed as late into the synthetic sequence as possible. The quaternisation of pyridyl groups was selected as the method for inducing hydrophilicity, due to previous experience by members of the research group.

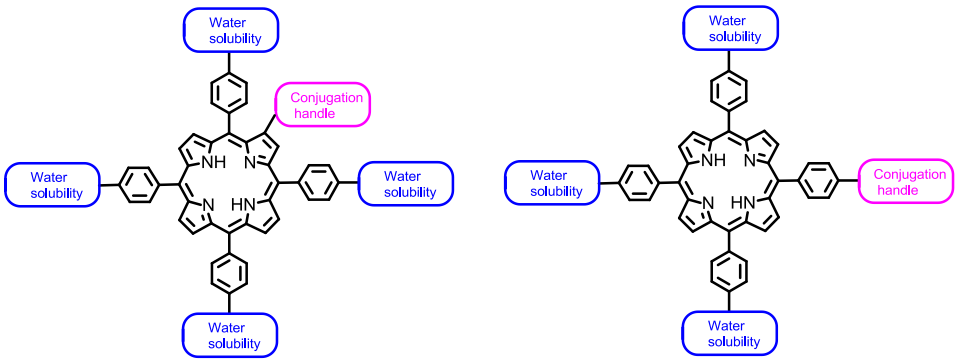

Functionalisation of a symmetrical porphyrin

Mixed condensation

Figure 6: Dual functional porphyrins.

Chapter 2: Functionalisation of symmetrical porphyrins

2.1 Introduction

In order to produce a dual functional porphyrin, two strategies can be adopted; functionalisation of a symmetrical porphyrin or incorporating the dual functionality during the formation of the porphyrin. The appeal of functionalising symmetrical porphyrins stems from the higher yields obtained, in relation to the 'mixed condensation' porphyrins, using the most common synthetic methods. The strategy described here involved the mono-functionalisation of a porphyrin in the *β*-position, providing a single reactive functional group, which upon further modification, could potentially lead to a group suitable for bioconjugation; the second set of functional groups, already incorporated during porphyrins synthesis, could then be modified to render the macrocycle water soluble.

2.2 Porphyrins

Porphyrin derivatives are aromatic tetrapyrrolic macrocycles, consisting of four pyrrolic subunits connected by methine bridges. Porphyrin derivatives are described using specific IUPAC nomenclature; a system devised by Professor R. Bonnett and collaborators, to supersede the previously used Fischer numeration (Figure 7). There are two different regions on the porphine core referred to as *β*-positions: the outermost pyrollic carbons and *meso*-positions: the methine bridges joining the pyrroles together, and these are often used as "shorthand" to denote the reactive positions e.g. *β*-substitution vs. *meso* substitution.[109]

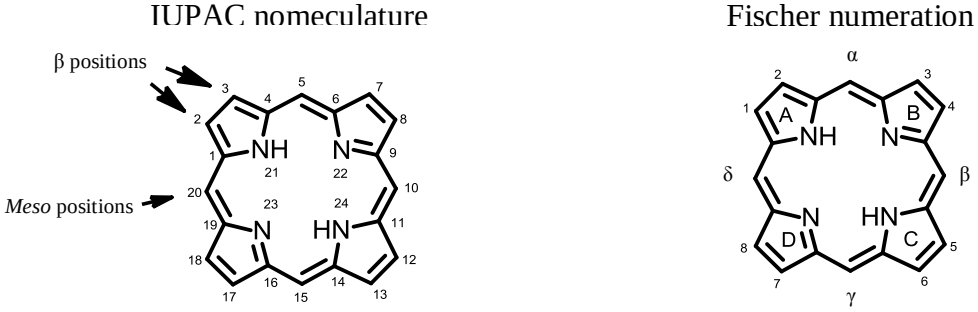

Figure 7: Porphyrin nomenclature.[109]

The porphyrin nucleus has a total of 22 π electrons, with 18 π electrons in a delocalised system, in compliance with Hückels rule of aromaticity. Generally, porphyrins participate in electrophilic and radical substitution reactions, due to the aromatic nature of the porphyrin core. The *meso* positions are the most electron dense and as such are the most reactive, however if the *meso* positions are occupied, the *β* positions can participate in electrophilic reactions.[110]

Free base porphyrins have a UV/visible spectrum consisting of one intense absorption band, referred to as the Soret band, at 380-430 nm, and four less intense signals, known as the Q bands at higher wavelengths. This phenomena can be explained using the Gouterman molecular orbital theory by considering the four frontier orbitals present on the porphyrin macrocycle; the two π-orbitals (a_{1u}/b_1) and (a_{2u}/b_2) and the degenerate pair of π*-orbitals (e_{gx}/c_1) and (e_{gy}/c_2). The two highest molecular orbitals have a similar energy, therefore it might be expected that there would be two coincident absorption bands due to the two different transitions of (a_{1u}/b_1) to (e_{gx}/c_1) and (a_{2u}/b_2) to (e_{gy}/c_2). However these two transitions combine, resulting in the formation of two different bands; constructive interference leads to the generation of the Soret band, whereas destructive interferences lead to the Q-bands. Free base porphyrins are unsymmetrical, hence there are different transitions in the x and y directions, thus there are 2 transitions, in the x and y directions, for the destructive combination transition, leading to a total of 4 bands being observed for the Q bands.[21] The exact position and intensity of these absorption peaks are dependent on both the concentration and the nature of the solvent. The optical properties of different porphyrin derivatives are dependent on the functional groups present in the *β* and *meso* positions.[22]

2.3 Porphyrin synthesis

From a retro-synthetic perspective, the porphyrin can be disconnected to four pyrrolic units and four bridging units (Figure 8). Correspondingly, porphyrins can be synthesised via a condensation reaction involving equimolar quantities of pyrrole and aldehyde.

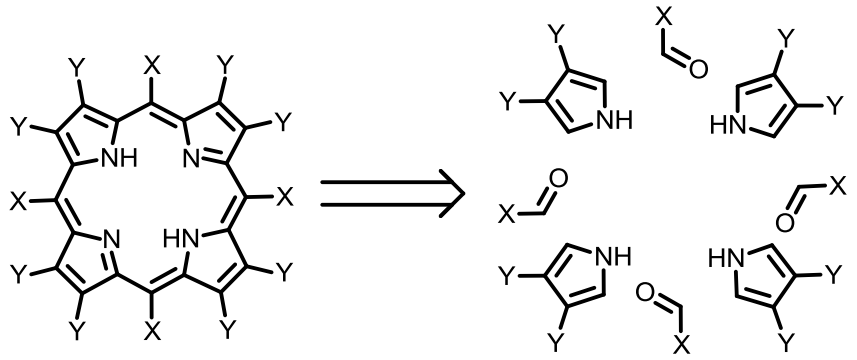

Figure 8: Retro-synthesis of porphyrin.

Rothemund[111] was the first to report the synthesis of a porphyrin using an aldehyde and pyrrole, by reacting benzaldehyde with pyrrole, in pyridine, in a sealed container, at 150 °C for 24 hours. The rationale for this reaction was that aromatic compounds are stable, porphyrins are aromatic; therefore reacting pyrrole and benzaldehyde at high temperatures will result in the formation of a stable porphyrin. Although the potential for synthesising porphyrins was demonstrated, the yields were low due to the harsh reaction conditions; for example tetra(4-chlorophenyl)porphyrin was synthesised with a 2.6 % yield,[112] and the zinc(II) complex of tetra(4-pyridyl)porphyrin was produced, with a yield of about 10 %.[113] Porphyrin research was therefore directed towards developing reaction conditions, enabling the production of a variety of *meso*-substituted porphyrins, with more reasonable reaction yields.

2.3.1 Adler-Longo porphyrin synthesis[114]

Adler and Longo[115] were the first to rigorously evaluate the reaction conditions, facilitating the production of *meso*-substituted porphyrins. The reaction model investigated was the synthesis of tetraphenylporphyrin (TPP), via the reaction between pyrrole and benzaldehyde. The reaction was performed using a Dean-Stark trap, thus demonstrating that porphyrin formation results from a dehydration reaction, with the

reaction stoichiometry suggesting an oxidation process was occurring. The reaction was also investigated at different temperatures, using various solvents; including acetic acid, acetic acid with a metal salt and benzene containing chloroacetic acid or trifluoroacetic acid. The reactions performed at elevated temperatures, employing acidic solvents produced higher reaction yields, in comparison to those performed at lower temperatures, in the presence of metal salts. These observations, coupled with further investigation of the reaction conditions, led to the use of propionic acid, in place of acetic acid.[114] It was observed that upon cooling, porphyrins synthesised in propionic acid can crystallise out of the reaction mixture, thus purification can be achieved simply by filtration and washing of the recovered crystals. Although the use of acetic acid produced TPP in higher yields, the additional chromatographic separation required was time consuming, and as such the reaction in propionic acid was considered to be more convenient. The optimised procedure, known as the Adler-Longo method[114], involved reacting equimolar quantities of pyrrole and an aldehyde in refluxing propionic acid for 30 min, in an open vessel. The Adler-Longo method produced TPP in a reproducible manner, with a yield of 20 %.

Further mechanistic studies were conducted to evaluate the postulated role of molecular oxygen in the formation of a porphyrin. Using the synthesis of TPP as the reaction model, experiments were performed under various pressures and concentrations of oxygen, and in the absence of oxygen; with the reactions being monitored by UV-visible spectroscopy. It was discovered that the oxidation processes was due to atmospheric oxygen, and therefore the overall reaction stoichiometry was determined, as shown in Figure 9, leading to a proposed mechanism shown in Scheme 18.[116]

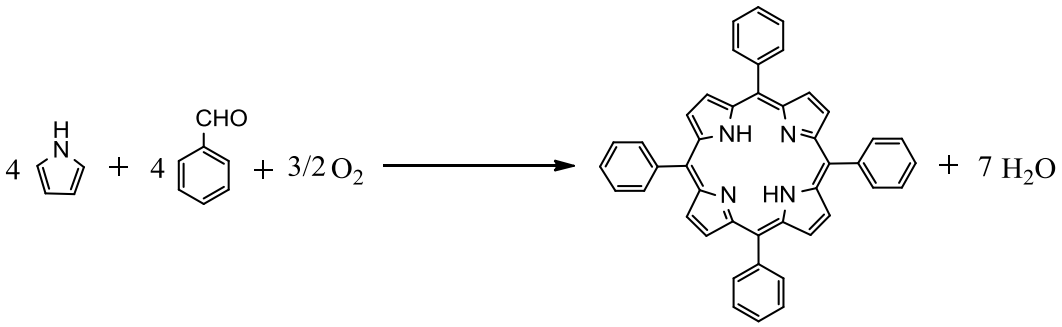

Figure 9: TPP reaction stoichiometry.[116]

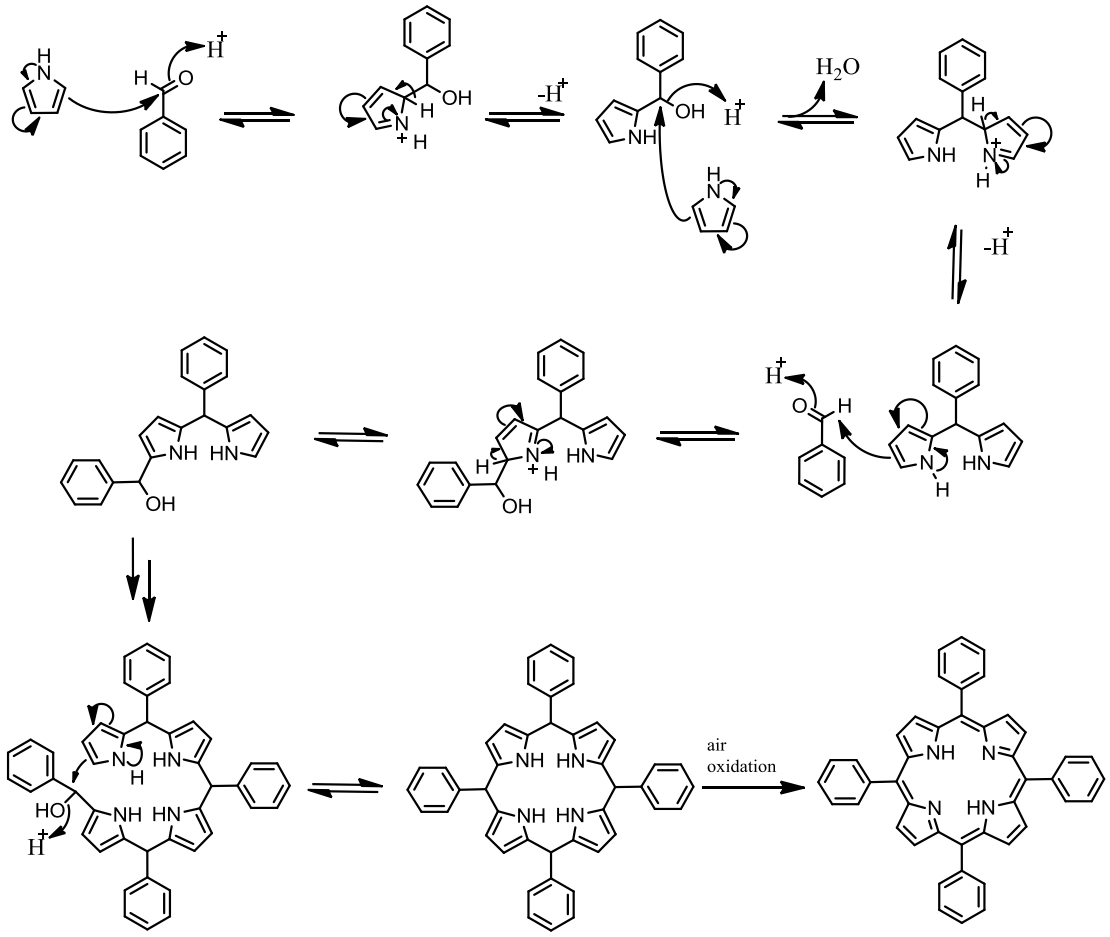

Scheme 18: Mechanism for the formation of a porphyrin using Adler-Longo conditions.[116]

The mechanism proposed by Adler and co-workers,[116] proceeded via a carbinol intermediate. To test the theory, Little[117] compared the reaction yields of porphyrins formed by either pyrryl carbinols, or corresponding aldehydes and pyrrole. The reaction yields were almost identical for the porphyrins evaluated, thus indicating that porphyrin formation occurs via a carbinol intermediate.

The Adler-Longo conditions,[114] for porphyrin synthesis can also lead to the presence of chlorin, resulting from the incomplete oxidation of the porphyrinogen. The chlorin impurities can be oxidised, forming the desired porphyrin, by treatment with 2,3-dichloro-5,6-dicyanobenzoquinone (DDQ); or can be removed be column chromatography.[118]

A wide variety of symmetrical porphyrins have been synthesised employing the Adler-Longo method,[114] including porphyrins synthesised by the addition of pyrrole to *p*-chlorobebenzaldehyde[114] or imidazole aldehydes,[119] as illustrated in Scheme 19.

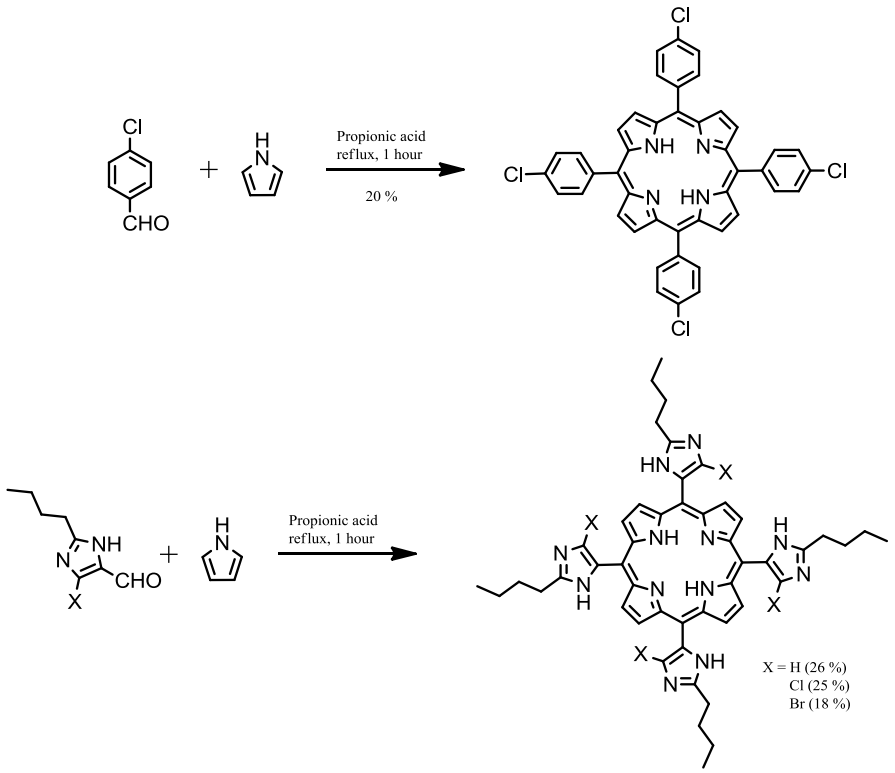

Scheme 19: Examples of symmetrical porphyrins synthesised under Adler-Longo condtions.[114,119]

The synthesis of porphyrins using aldehydes with ionisable groups, yields porphyrin acid salts, which are soluble in propionic acid, thus isolating the porphyrin can be problematic.[114] Research was therefore directed towards a more versatile porphyrin synthesis, to allow the incorporation of sensitive functional groups.

2.3.2 Lindsey porphyrin synthesis[120]

Lindsey *et al.*[120] postulated that during the condensation reaction between pyrrole and benzaldehyde with catalytic amounts of Bronstead or Lewis acids, the thermodynamically favoured product would be 5,10,15,20-tetraphenylporphyrinogen. Hence, if the reaction were performed under appropriate reaction conditions, there would be an equilibrium favouring the formation of the porphyrinogen derivative. Once the equilibrium was established the 5,10,15,20-tetraphenylporphyrinogen could then be oxidised, immediately by addition of a chemical oxidant, to yield TPP**.** Lindsey also proposed that high temperatures were not required, as the pyrrole and benzaldehyde were already highly reactive molecules. Furthermore, the milder reaction conditions could enable the use of aldehydes bearing more sensitive functional groups for

producing porphyrins, which could not at the time be obtained using the Adler-Longo[114] procedure.

The optimised Lindsey method for the production of TPP involved the addition of benzaldehyde, pyrrole and triethyl orthoacetate to anhydrous dichloromethane, under an inert atmosphere, at equimolar concentrations of 1×10^{-2} M. An aliquot of the acid catalyst: boron trifluoride etherate (1×10^{-3} M), was then added, and the reaction proceeded at room temperature for 1 hour. The acidic catalyst was neutralised by the addition of either potassium carbonate or triethylamine, followed by addition of the oxidant; either *p*-chloranil or DDQ. Once the reaction had been left at reflux for 1 hour, and cooled, the solvent was removed and flash chromatography afforded TPP, with a yield of 45-50 %. The reaction conditions were evaluated, and it was observed that the final porphyrin yield was influenced by the duration of the condensation period, the concentrations of the reagents, the presence of water in the solvent and the choice of acid catalyst and oxidant.

A wide range of porphyrins have now been produced under Lindsey conditions,[119] some of which are shown in Scheme 20.[121]

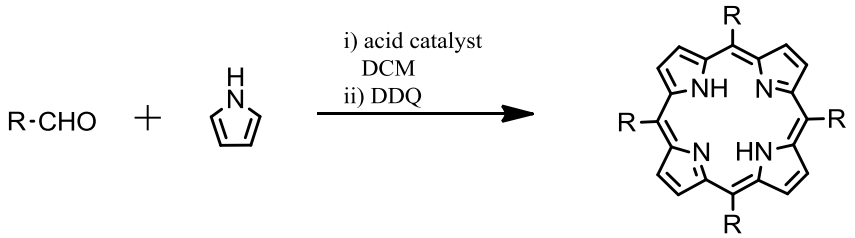

R Group	Acid Catalyst	Yield (%)
p-Tolyl	TFA	41
p-Tolyl	BF_3-etherate	17
C_6F_5	TFA	11
C_6F_5	BF_3-etherate	23
Hexyl	TFA	16
Hexyl	BF_3-etherate	12

Scheme 20: Porphyrins synthesised under Lindsey condtions.[121]

2.4 Functionalising the *β*-position of a symmetrically substituted porphyrin

2.4.1 Halogenation

Giraudeau and co-workers,[122] have reported the monochlorination of TPP at the *β*-position, via treatment with *N*-chlorosuccinimide in 1,2-dichloroethane, at reflux for 2 hours. Following chromatographic separation, the mono-substituted compound (TPP(Cl)) was isolated in 46 % yield, with the di-substituted compound (9 %) as the major impurity.

The bromination of TPP has also been demonstrated using *N*-bromosuccinimide; TPP was treated with 1.1 equivalents of *N*-bromosuccinimide in a mixture of dichloromethane and methanol, at reflux for 5 minutes. The mono-brominated porphyrin was obtained with a yield of 48 %.[123] Bromination using phenylselenyltribromide as the brominating agent has also been reported; 0.5 equivalents of phenylselenyltribromide was reacted with the nickel(II) complex of TPP, producing a mixture of the mono and di-substituted porphyrins in 40-60 % yield.[124]

2.4.2 Nitration

The introduction of a nitro group at the *β*-position, of copper(II) TPP, can be achieved via treatment with copper(II) nitrate hexahydrate, in the presence of acetic anhydride, at 35 °C, for 1 hour, as illustrated in Scheme 21.[122] A similar methodology for nitrating porphyrins has been reported by Hombrecher *el al.*[125]; TPP was treated with copper(II) nitrate trihydrate and acetic anhydride, at room temperature for 48 hours. The reaction relied on the *in situ* insertion of copper into the porphyrin core, and subsequent nitration, affording the copper complex of the nitrated porphyrin with a yield of 86 %.

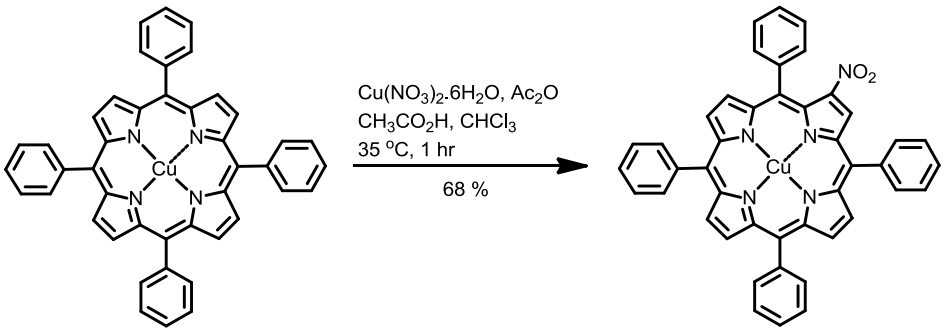

Scheme 21: Nitration of the copper(II) complex of TPP.[122]

Treating certain metalloporphyrins with nitrogen dioxide gas, suspended in a suitable solvent can also result in mono-nitration at the β-position.[126] It was observed that the choice of co-ordinated metal influenced the extent and position of the nitration. The copper(II), nickel(II) and palladium(II) chelates exclusively nitrate in the β-pyrrolic position, whereas, more electropositive metal complexes; including magnesium(II) and zinc(II) chelates, resulted in nitrations at the *meso*-positions, eventually leading to ring opening and the formation of non-porphyrinic products. The reaction conditions were refined, employing the dropwise addition of a dinitrogen tetroxide saturated solution of ether, to the copper(II) complex of TPP, with a reported yield of 88 %.[127] Interestingly, it has been reported that a range of tetraheteroarylporphyrins have been nitrated using nitrogen dioxide, including tetra(4-pyridyl)porphyrin, as shown in Scheme 22.[128]

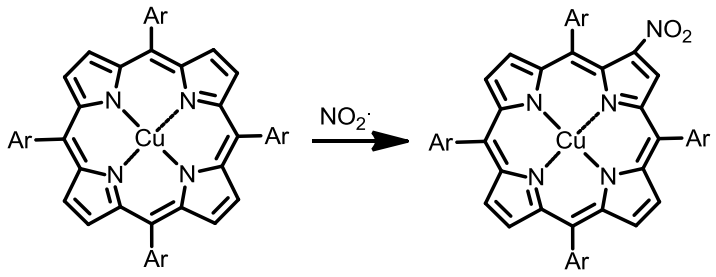

Ar	**Yield**
4-quinolinyl	quantitative
6-quinolinyl	quantitative
3-pyridyl	70 %
4-pyridyl	60 %

Scheme 22: Nitration of tetraheteroarylporphyrins.[128]

Catalano *et al.*[129] demonstrated that 2-nitro-copper(II)TPP is susceptible to nucleophilic attack, via a reaction with sodium methoxide. A solution of the copper(II) complex of 2-nitroTPP dissolved in anhydrous dimethylformamide, was treated with sodium methoxide for 18 hours at 0-25 ^{o}C, and after the reaction was quenched with water, the 2,2-dimethoxy-3-nitro-2,3-dihyrdoporphyrin intermediate was isolated in 91 % yield. Denitration of the intermediate using Bu_3SnH-AIBN in refluxing benzene, and subsequent elimination of methanol using aqueous oxalic acid, affords the copper(II)

complex of 2-methoxy-TPP in 90 % yield. It has also been illustrated that Grignard reagents react in a similar manner to oxygen nucleophiles, via a chlorin intermediate.[127] It has been reported that a nitro group on porphyrins can be reduced to an amino functionality, using various reductive treatments, including Sn/HCl, $NaBH_4$/LiCl in tetrahydrofuran, and NH_4O_2CH-Pd/C or $NaBH_4$/Pd/C in methanol. The amino functionality can then be converted into a diazonium salt, using sodium nitrite and sulphuric acid, which can subsequently react with an alcohol, producing the *β*-substituted alkoxy-porphyrin.[125]

2.4.3 Formylation

The Vilsmeier complex, formed by the interaction between phosphorus oxychloride and dimethylformamide at 0 °C, has been used for the introduction of an aldehyde functionality, to the *β*-position of the copper (II) complex of TPP. The metal centre was required to prevent protonation of the inner nitrogens, and to direct the electrophilic attack of the chloromethyleneiminium salt towards the *β*-pyrrolic position.[130] Once the intermediate iminium salt was hydrolysed, the formylated copper(II) complex of TPP was obtained in high yields (< 95 %). Demetallation of copper(II) complex of TPP was attempted using sulphuric acid, however the expected free base porphyrin was not produced, and the TLC of the reaction mixture revealed a mixture of porphyrinic fractions, and it was postulated that sulfonation and/or a secondary reaction of the formyl group had occurred.[131] Further investigations led to the discovery that acidic treatment caused an intramolecular cyclisation reaction between the carbonyl group, and the *ortho*-postion of the adjacent phenyl ring.[132] Bonfantini *et al.*[130] overcame the intramolecular cyclisation problem by demonstrating that the intermediate iminium salt was stable to acidic demetallating conditions, therefore, by performing the demetallation *in situ*, prior to the hydrolysis of the iminium salt, it was possible to synthesise the free base formylated TPP (2-formyl TPP) in high yield (95 %), as depicted in Scheme 23.

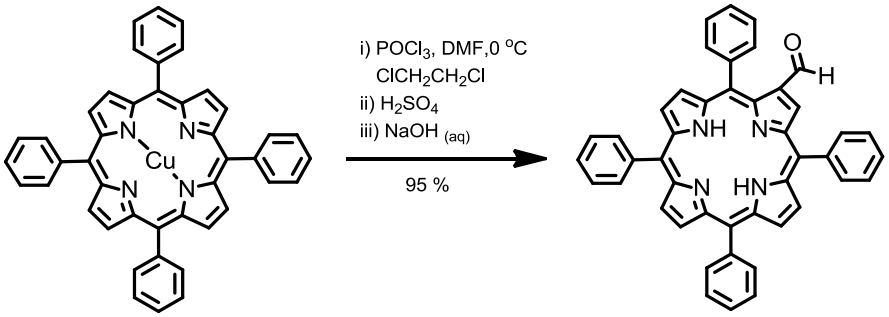

Scheme 23: Optimised formylation reaction conditions.[130]

The conversion of the formyl group into a Wittig type reagent has been demonstrated by a series of high yielding synthetic steps. Reduction of the aldehyde group, using sodium borohydride, yields the reactive 1^{o} alcohol functionality (95 %), which upon further treatment with a mixture of pyridine/thionyl chloride, transforms the alcohol into a chloromethyl derivative (84 %). The final synthetic step involved formation of the phosphonium chloride salt (90 %), which was achieved via treatment with triphenylphosphine.[130]

It has also been established that 2-formyl TPP, and the zinc analogue, can participate in a Horner-Wadsworth-Emmons reaction with a fullerene adduct, bearing an appropriate phosphonate group, as illustrated in Scheme 24. The yields for the porphyrin-C_{60} dyads were low to moderate, for reactions performed involving 2-formyl TPP (18 %) and the zinc derivative (41 %).[133]

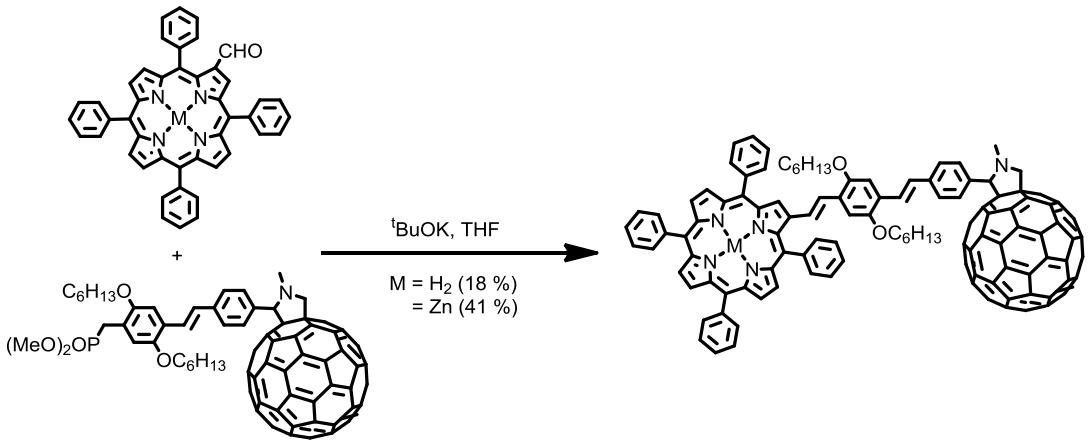

Scheme 24: Formation of porphyrin-fullerene dyad.[133]

Stephenson *et al.*[134] also performed a modified Horner-Wadsworth-Emmons reaction, using the zinc(II) complex of 2-formyl TPP and a variety of halophosphonates, leading to the formation of porphyrins bearing acetylene linked substituents at the *β*-position, as illustrated in Scheme 25. Generally, the Horner-Wadsworth-Emmons reaction requires

2 molar equivalents of base, however, when applied to this particular reaction, the major product formed was the halovinyl intermediate. In order to form the acetylene linkage, 80 molar equivalents of base were required. The reaction yields varied considerably, and were dependent on the initial halophosphonate used.

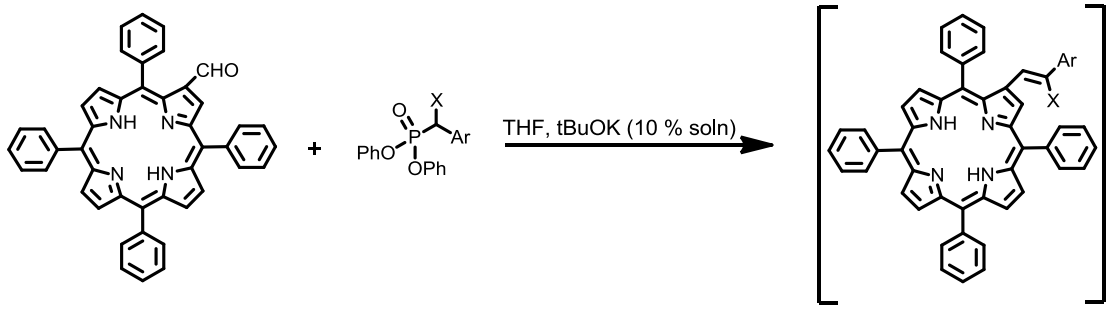

Ar	X	Yield (%)
Phenyl	Cl	54
4-Methoxyphenyl	Cl	84
4-Benzonitrile	Br	26
5,5-Dimethyl-2phenyl-[1,3]dioxane	Br	88
4-Pyridyl	Cl	70
4-Benzamide	-	36

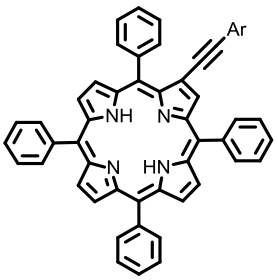

Scheme 25: Modified Horner-Wadsworth-Emmons reactions of 2-formyl TPP.[134]

It has been reported that under appropriate conditions, metallated 2-formyl TPP can react with a 2^{o} amine, generating an azomethine ylide, which can participate in Diels-Alder reactions. The nickel(II) complex of 2-formyl TPP was treated with *N*-methylglycine in refluxing toluene, under an inert atmosphere. The resulting ylide, formed *in situ*, was reacted with a variety of dipolarophiles, including *N*-phenylmaleimide, *trans-β*-nitrostyrene and dimethyl formate Due to the nature of the reaction, diastereoisomers were generated, and as such, chromatographic separation was required.[135]

The nickel(II) complex of 2-formylTPP has also been shown to react with glycine methyl ester hydrochloride, using lanthanum(III) triflate as the catalyst, in the presence of a base; to deprotonate the 1^{o} amine. The crude imine, formed via the interaction between the amine and formyl groups, can be reduced leading to the formation of the stable 2^{o} amine linkage. The combined synthesis gave a reasonable yield, as illustrated

in Scheme 26. Demetallation can be achieved using sulphuric acid, producing the free base porphyrin in quantitative yield.[136]

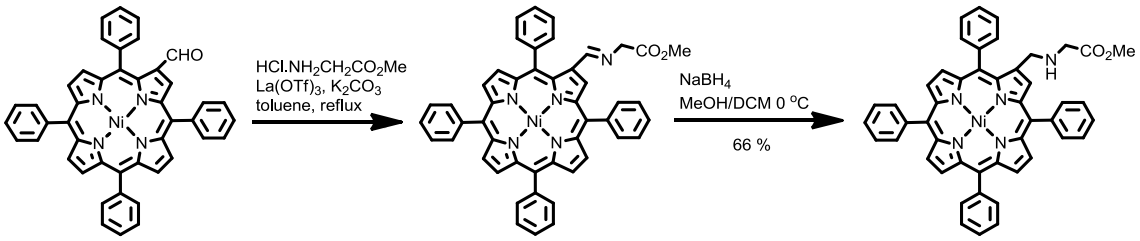

Scheme 26: Reductive amination of the nickel(II) complex of 2-formyl TPP.[136]

The reductive amination type reaction, catalysed by acetic acid, has also been applied to form adducts between free base 2-formyl TPP and a variety of 1^{o} amines, including aniline. Two distinct reaction procedures were described, with the reactions performed in either tetrahydrofuran or toluene, and addition of sodium cyanoborohydride, prior and post imine formation. The reactions performed in toluene used a Dean-Stark trap to remove water, driving the reaction towards formation of the imine intermediate. The reactions were then cooled, and sodium cyanoborohydride was used to reduce the imine, as shown in Scheme 27. The other procedure used tetrahydrofuran as the solvent; therefore a Dean-Stark trap could not be used as water and tetrahydrofuran are miscible. In this case all the reagents were added together in a one-pot synthesis, therefore as the imine formed, it was immediately reduced, driving the reaction towards formation of the product.[137]

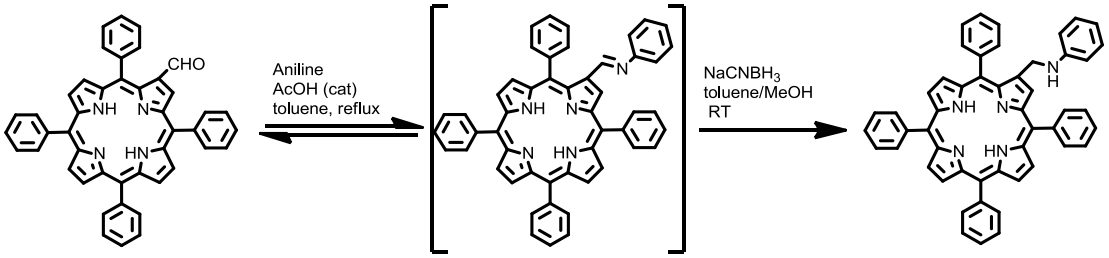

Scheme 27: Reductive amination of 2-formyl TPP.[137]

The reaction yields ranged from 20-77 % and were mainly dependent on the 1^{o} amine used. The lower reaction yields were obtained for the cyclen adducts (20 and 52 %), whereas the less sterically hindered amines produced more reasonable yields (61-77 %), as shown in Figure 10. The article also described reactions involving the 2^{o} amino linkage and halogen electrophiles, under basic conditions. A range of unique

compounds were synthesised, including a cyclen-porphyrin dimer; in spite of the steric hindrance involved.[137]

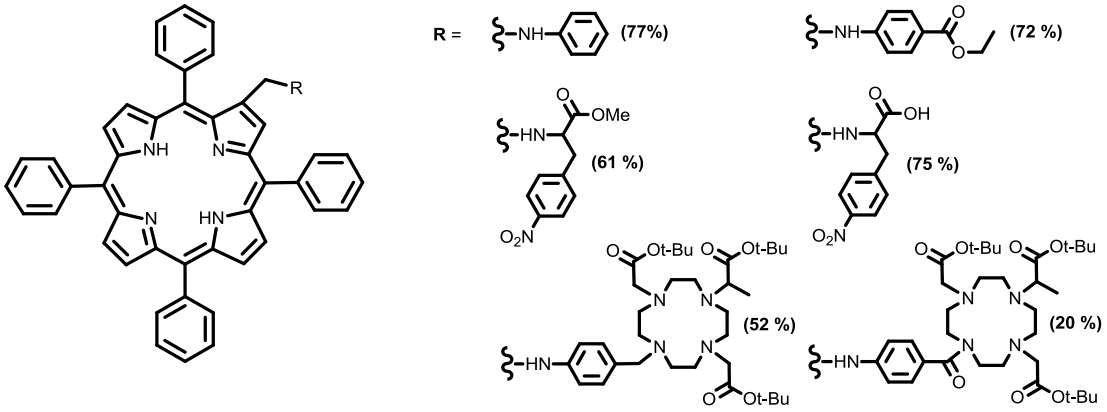

Figure 10: Range of adducts produced via reductive amination of 2-formyl TPP.[137]

2.5 Synthetic strategy

Based on previous experience in our laboratory, the Adler-Longo[114] method for synthesising porphyrins was selected for initial investigations. The literature suggested that the formylation and nitration reactions produced the highest yield of mono-functionalised porphyrin, and as such, the formylation method was selected for this project. It was decided that a synthetic strategy using TPP should firstly be developed, due to the extensive literature describing reactions using 2-formyl TPP. Synthetic methodology could then be extended to formylation of porphyrins bearing water solubilising groups in the *meso*-positions.

There did not appear to be any preferential, high yielding reaction involving 2-formyl TPP, with the Wittig and reductive amination type reactions producing similar yields. Due to the extra synthetic step required for the Wittig reaction, and the availability of chemical procedures recently developed by members of our research group; the reductive amination reaction was selected as the best route to further modify the porphyrin. As it was desirable for the porphyrin to ultimately have an amino functionality, which upon treatment with SMCC, would provided the maleimide bioconjugation handle; *N*-Boc-1,12-diaminododecane and *N*-Boc-1,3-diaminopropane hydrochloride were initially selected to react with 2-formyl TPP, as illustrated in Scheme 28. The Boc group is stable to the sodium cyanoborohydride reducing conditions,[138] therefore no compatibility issues were anticipated.

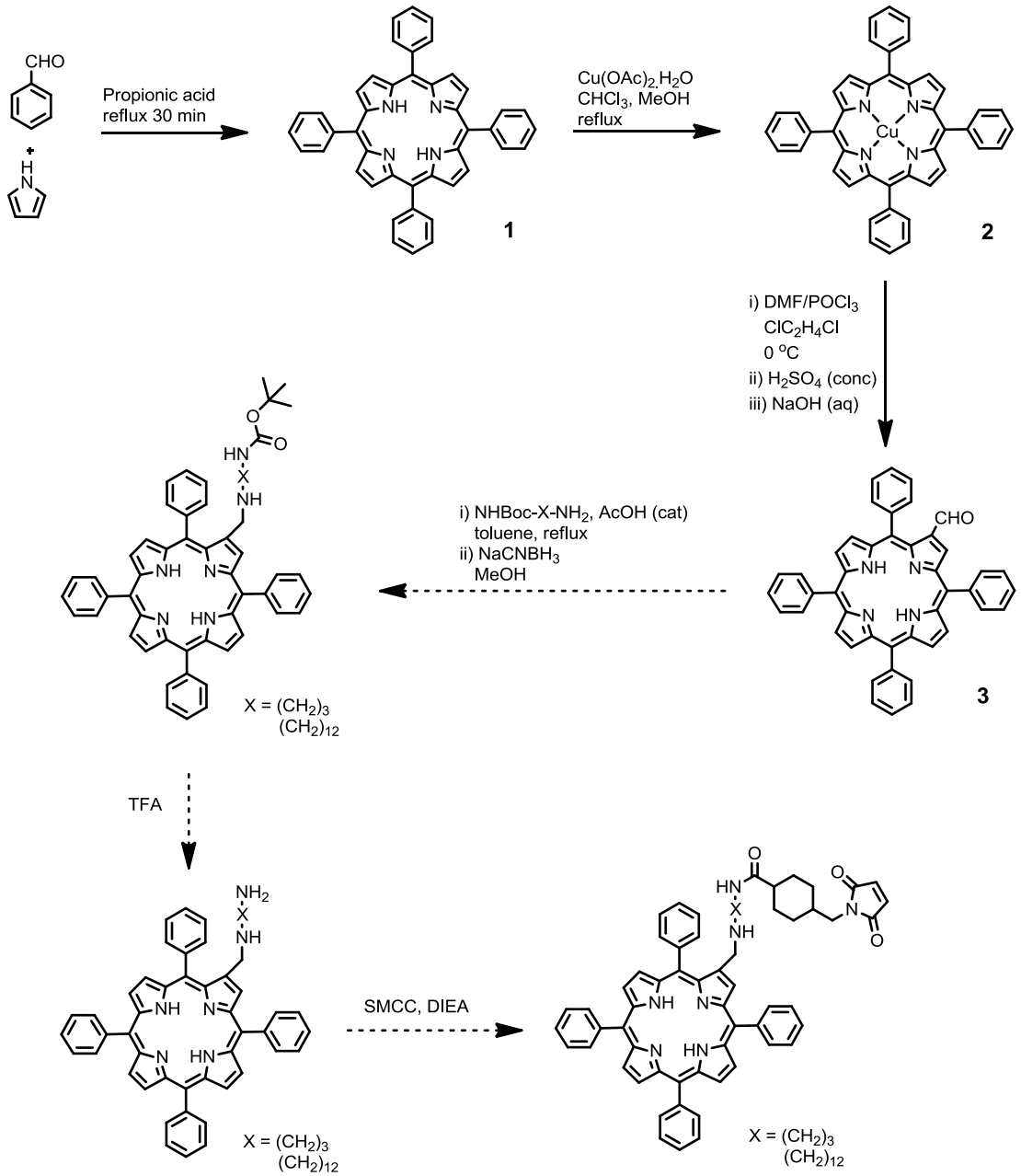

Scheme 28: Reductive amination synthetic strategy for mono functionalisation of porphyrins.

2.5.1 2-Formyl-5,10,15,20-tetraphenylporphyrin (3)

Following the synthetic strategy outlined in Scheme 28; TPP (**1**) was synthesised using the Adler-Longo method,[114]. Following a reported method,[130] **1** was then treated with a methanol/water solution of copper(II) acetate monohydrate, under reflux conditions. The hot solution was poured on to a silica pad, where the excess copper(II) acetate monohydrate was retained on top of the silica, while the product was recovered from the eluent. The copper(II) complex of TPP (**2**) was isolated in reasonable yield, 89 %, after precipitation from chloroform by the addition of methanol. Evidence that the reaction had proceeded as expected was provided by UV-visible spectroscopy and mass spectrometry. The UV-visible spectrum showed the typical transformation; 5 peaks for TPP, reducing to 3 peaks for the copper(II) complex, additionally, mass spectrometry revealed the expected mass signal of 678 *m/z* corresponding to the $(M)^+$ ion, with a copper isotope distribution pattern being observed. Compound **2** was converted into 2-formyl TPP (**3**), using the Vilsmeier-Haack formylation conditions, as previously reported by Bonfantini *et al.*[130]

The ^{1}H NMR spectrum of **3** was also in agreement with the previously reported data,[130] and exhibited the expected signal transformations from TPP; with the formation of 2 singlet peaks at 9.41 ppm and 9.22 ppm, corresponding to the formyl and neighbouring *β*-pyrrolic protons.

2.6 Reductive Amination

The versatile reductive amination reaction involves the interaction between either a ketone or aldehyde; with ammonia, or a 1^o or 2^o amine; leading to the formation of a carbinol amine intermediate. In the presence of a proton source, dehydration of the hydroxylamine occurs, and the resulting imine can be reduced, furnishing the alkylated amino product (Scheme 29).[139]

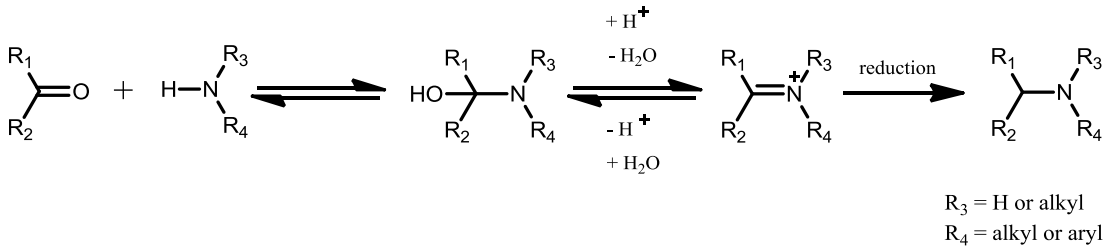

Scheme 29: Illustration of the reductive amination reaction.[139]

Formation of the imine can be enhanced by using an acid catalyst, usually acetic acid and/or removal of water. The removal of water would shift the equilibrium of the reaction towards the formation of the imine; with the acid catalyst protonating the carbonyl group making it more susceptible to nucleophilic attack from the amine, as well as favouring dehydration of the hydroxylamine intermediate. However, it would be possible for the amine to become protonated under high concentrations of acid, therefore only a catalytic amount of acid should be used. Reduction of the imine can be performed *in situ*; or after the imine has been isolated. Sodium cyanoborohydride is a suitable reducing agent for *in situ* reductions as its stable to acidic conditions and it is soluble in hydroxylic solvents, furthermore, the rate at which sodium cyanoborohydride reduces the aldehyde or ketone starting material, is relatively slow, and at pH 6-8, the imine is protonated preferentially over the carbonyl functionality, facilitating the reductive process.[139] Sodium borohydride can also be used for reducing imines, and is preferable to sodium cyanoborohydride due to a lower toxicity. However 2-formyl TPP can also be reduced using sodium borohydride, hence it can not be used for *in situ* reductions.

2.6.1 Reductive amination synthetic strategy

The literature suggests that there are two distinct methodologies for performing reductive aminations employing formylated porphyrins. The first, one pot strategy, involves the acid catalysed reaction between the free base formyl porphyrin and amine; with the sodium cyanoborohydride reducing agent being added post or prior imine formation.[137] The other procedure uses lanthanum(III) triflate to catalyse the reaction between the formylated porphyrin metal complex and amine, with isolation of the imine intermediate and subsequent reduction with sodium borohydride.

The presence of water shifts the reaction equilibrium back towards the initial starting materials or the hydroxylamine intermediate, therefore removal of water using activated molecular sieves, or a Dean-Stark trap would result in shifting the reaction equilibrium towards product formation. Additionally, the reactions should be performed under an inert atmosphere to avoid exposure to moisture.

2.6.2 Attempted reductive aminations involving alkyl diamines

The first reductive amination attempts are shown in Scheme 28. Compound **3** and 1.2 equivalents of either *N*-Boc-1,3-diaminopropane hydrochloride or *N*-Boc-1,12-diaminododecane were dissolved in anhydrous toluene, a catalytic amount of acetic acid was added and the mixtures were heated at reflux, under an inert atmosphere (N_2), while using a Dean-Stark trap to remove water. The reactions were monitored via TLC, over a 16 hour period; the reaction employing *N*-Boc-1,12-diaminododecane showed no change, whereas a trace amount of a polar UV-active spot evolved during the reaction using *N*-Boc-1,3-diaminopropane hydrochloride, but nearly all the starting material remained unconsumed. Mechanistically, the formation of an imine is an equilibrium process, therefore excess sodium cyanoborohydride in methanol was added to the mixtures to observe whether there was a shift in the equilibrium, favouring product formation. After 14 hours (overnight) the TLC of the reaction mixture using *N*-Boc-1,12-diaminododecane showed the presence of multiple UV-active fractions, including a significant amount of **3**, therefore the reaction was discarded. The TLC of the reaction involving *N*-Boc-1,3-diaminopropane hydrochloride showed that the previous trace fraction (suspected imine) was present, with the development of another major UV-active fraction (suspected product), and trace amounts of **3**. The reaction employing *N*-

Boc-1,3-diaminopropane hydrochloride was worked-up and applied to a preparative TLC plate, however decomposition was observed, hence the reaction was discarded.

The reactions were repeated in a similar manner using 10 equivalents of the alkyl diamines; to maximise the probability of interactions with the formylated porphyrin, and activated molecular sieves; to ensure removal of any water. The modified reaction conditions did not seem to enhance imine formation. Once excess reducing agent was added, the formation of the suspected product was more prominent, indicating an excess of amine favoured imine formation. The reaction using *N*-Boc-1,12-diaminododecane again produced a complex mixture of UV-active fractions, including a significant quantity of starting material; due to the high yielding criteria of the strategy, reductive aminations employing *N*-Boc-1,12-diaminododecane were deemed unsuitable for this particular reaction.

The reaction was performed again using 5 equivalents of *N*-Boc-1,3-diaminopropane hydrochloride, with sodium cyanoborohydride being added with the starting reagents, prior to imine formation. The TLC of the reaction showed the development of a polar, UV-active fraction, with trace amounts of starting material being detected, however the reaction did appear to be cleaner than the previous attempts. The reaction was worked-up, and the crude mixture was re-dissolved in dichloromethane and applied to a preparative TLC plate, then eluted with 5 % methanol/ dichloromethane. The relevant fraction was collected and the product was precipitated from dichloromethane by the addition of hexane. Once dried, acquisition of a ^{1}H NMR spectrum was attempted, but it was apparent that the sample had decomposed; a hypothesis confirmed by comparing the TLC's of the sample over a period of time and by conducting a 2D TLC experiment.

To determine whether the reaction had proceeded as postulated, ^{1}H NMR analysis was conducted just after the suspected product was isolated via preparative TLC, and an attempt to assign the signals of the ^{1}H NMR spectrum is shown in Figure 11. The ^{1}H NMR spectrum possessed a signal at 1.41 ppm which could be attributed to the *tert*-butyl region of the Boc group, and was used as the reference integral. Although the porphyrinic signals seemed to integrate correctly, in the expected positions; not all of the signals corresponding to the propyl protons were observed, potentially due to signals being beneath the solvent signals. The multiplet signal at 1.53-1.61 ppm had a quintet type appearance, corresponding to the middle CH_2 of the propyl chain, however the peak was too poorly resolved to be assigned as a quintet. One of the CH_2 units of the propyl chain was also observed as a quartet at 3.0 ppm. To ensure the proposed signal assignments were correct, 2D COSY and HMBC experiments were conducted, however

the solvent peaks were too prominent to obtain spectrum of suitable quality, and attempts to dry the sample led to decomposition; therefore there was no conclusive evidence that the ^{1}H NMR signal assignment was correct and the reaction had proceeded as postulated. The broad singlet at 3.89 ppm, which appears to integrate to approximately 2, could potentially be an amino signal, as the assigned singlet at 4.11 ppm does not have the typically broad appearance which would usually be observed. As the sample was not dried and decomposition was observed, all the signals in the alkyl region could potentially be solvent signals or other impurities, thus there was not any conclusive evidence for the proposed, newly formed 2^{o} amine, nor the methyl group which would be attached to the β-position of the porphyrin; although the sample did seem to posses signals for both the porphyrinic and diamine moieties. As the crude ^{1}H NMR was inconclusive and the product was unstable, it was hypothesised that the suspected product could have been the iminium ion intermediate, therefore the sample was dissolved in anhydrous dichloromethane and treated with a methanolic solution of sodium borohydride at 0 °C, for 15 minutes; once acetic acid was added to neutralise the excess sodium borohydride and the porphyrin was worked-up and isolated, the suspected product remained unchanged as indicated by TLC.

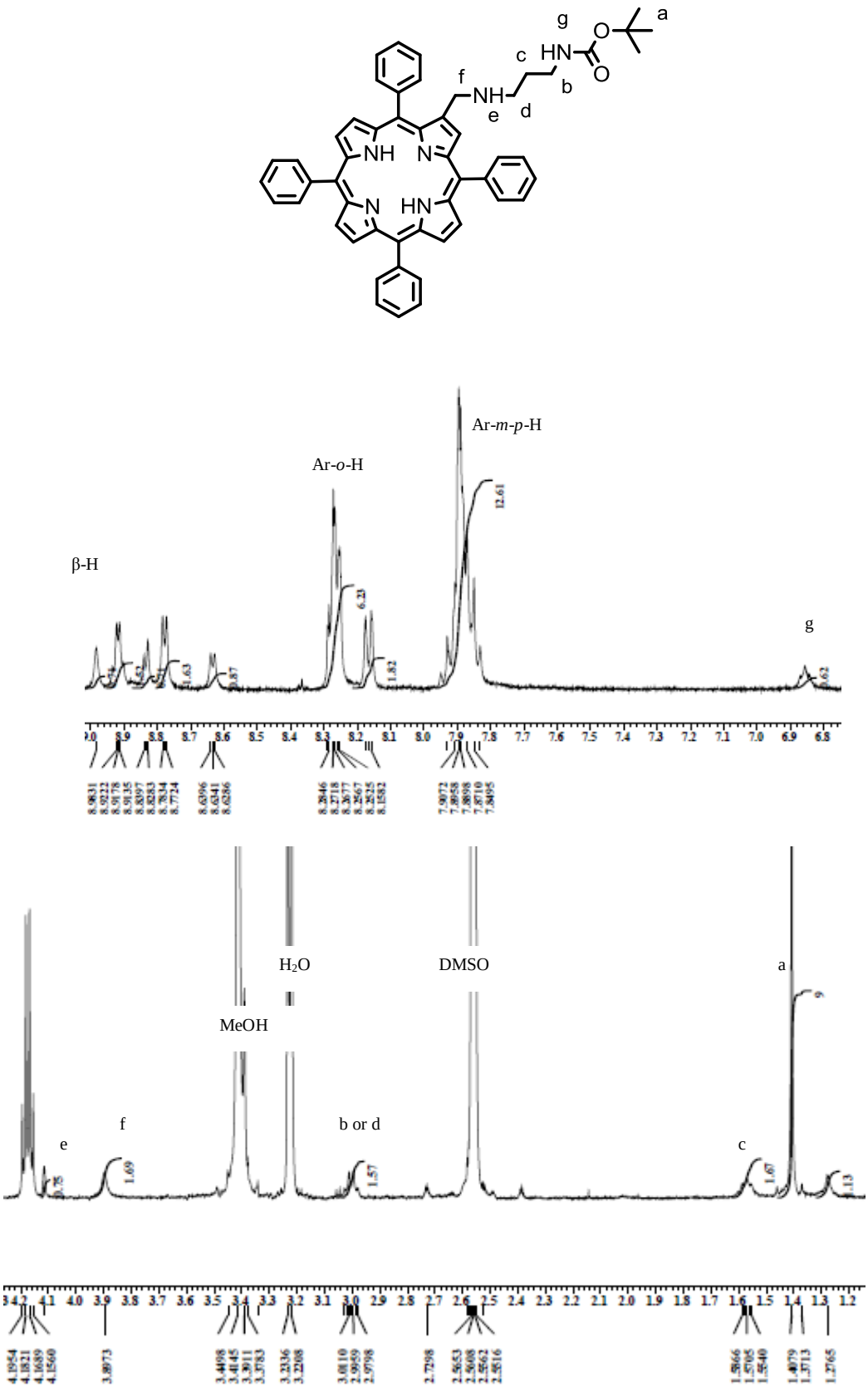

Figure 11: Crude ^{1}H NMR of suspected *tert*-butyl(3-((5,10,15,20-tetraphenylporphyrin-2-ylmethyl)amino)propyl)carbamate.

Further reductive amination attempts were conducted, as outlined in Scheme 30. The toluene solvent was replaced with tetrahydrofuran, to ascertain whether a change in solvent stabilised the suspected product. A lanthanum(III) triflate catalysed reaction was also attempted, to establish whether the different reaction conditions enabled imine formation.

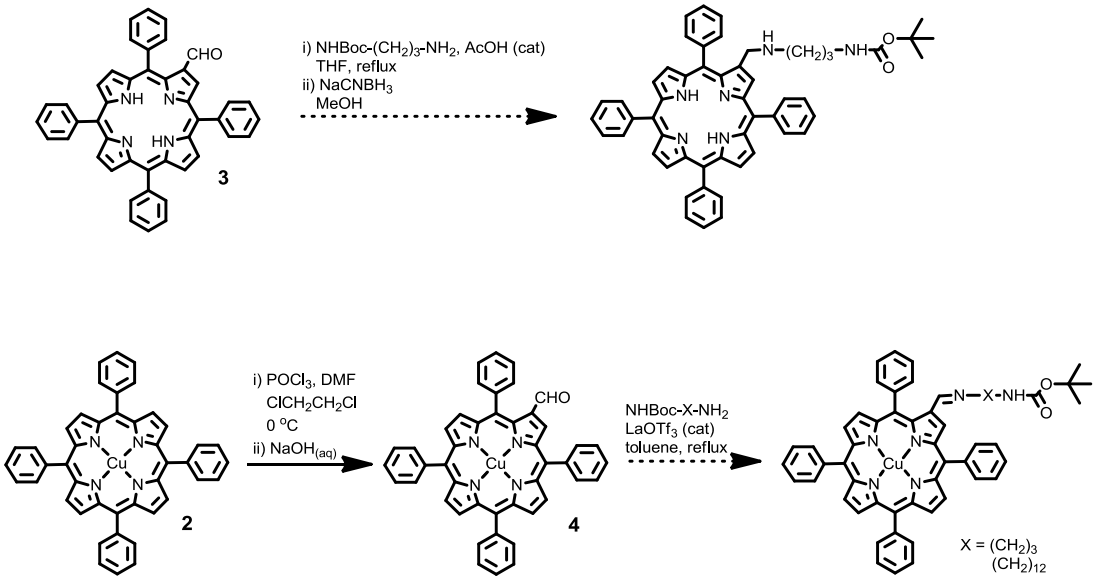

Scheme 30: Attempted reductive amination employing alkyl diamines.

Acid catalysed reductive amination attempts were conducted as previously reported.[137] Experiments were performed under an inert atmosphere, in tetrahydrofuran containing activated molecular sieves. The experiments proceeded in exactly the same manner as those performed in toluene, therefore the acid catalysed synthetic strategy was deemed unsuitable.

The other reductive amination methodology, reported by Silva *et al.*,[136] used lanthanum(III) triflate to catalyse the formation of an imine between the nickel(II) complex of 2-formyl TPP and amine. Due to the low yield of **3** previously obtained, the formylation reaction was performed without the intermediate demetallation step, with the aim of producing the copper(II) complex of 2-formyl TPP in higher yield. The isolated yield of the copper(II) complex of 2-formyl TPP (**4**) was 74 %, which represented a slight improvement in yield in comparison to the 67 % obtained for **3**. The lanthanum(III) triflate catalysed reactions between **4** and either *N*-Boc-1,12-diaminododecane or *N*-Boc-1,3-diaminopropane hydrochloride were monitored over a 3 day period, with no apparent reaction occurring as indicated by TLC, with only porphyrin starting material being recovered.

2.6.3 Reductive amination reaction involving aniline

Due to the somewhat negative results concerning alkyl amines, it was prudent to perform a known reductive amination reaction using aniline, as shown in Scheme 31.

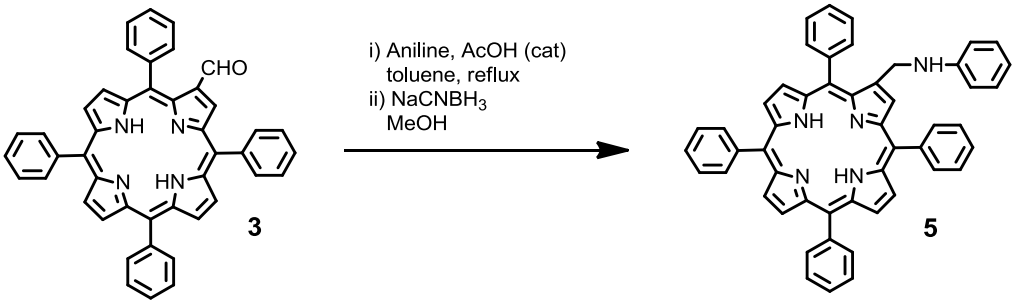

Scheme 31: Reductive amination of **3** with aniline.

The reaction was performed as formerly reported.[137] The reaction was monitored after 2 hours, with the TLC revealing the presence of two UV-active fractions corresponding to the starting material and a polar product, which was suspected to be the imine. After 24 hours, the TLC of the reaction mixture showed that nearly all of **3** had been converted into the imine; therefore sodium cyanoborohydride dissolved in methanol was added. After 2 hours at reflux, the reaction mixture was cooled, and following aqueous work-up, the mixture was chromatographically separated and, following precipitation, **5** was obtained with a yield of 67 %. The characterisation studies were in agreement with the literature determinations.[137] Although lower than the literature yield of 77 %, the reported reductive amination reaction was successful, and indicated that a large excess of amine should not be required, as only 1.7 equivalents of aniline was used; imine formation also should be evident after only a few hours.

2.6.4 Reductive aminations involving aryl amine derivatives

Due to the unsuccessful reductive amination attempts using alkyl amines, the synthetic strategy was modified to incorporate a phenyl moiety, directly attached to the amine, which would form an imine with the formylated porphyrin. The aryl amino derivative also possessed a protected amine, which could be transformed into the bioconjugation group, as previously postulated. Both the acetic acid and lanthanum(III) triflate catalysed reactions were attempted, as shown in Scheme 32.

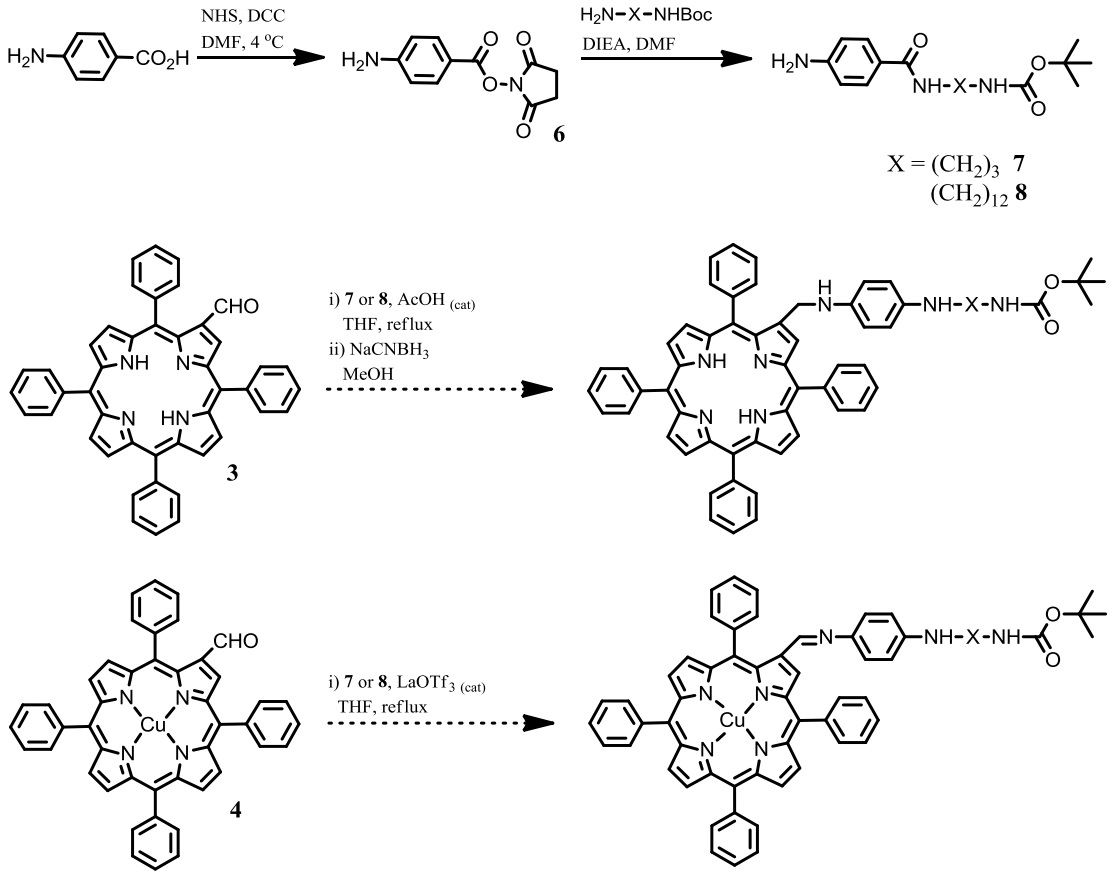

Scheme 32: Attempted reductive aminations using **3** and **4** with aryl linkers.

The synthesis of succinimdyl-4-aminobenzoate (**6**) was achieved using a modified procedure reported by Franek *et al*.[140] Compound **6** contains an activated ester and amino group, therefore if the reaction were performed for extended time periods, under thermodynamically favourable conditions, the molecule would react with itself, leading to the production of oligomers. The succinimidyl group and activated ester are moisture sensitive; therefore the reaction was performed in anhydrous dimethylformamide, under an inert atmosphere. Equimolar equivalents of 4-aminobenzoic acid, NHS and DCC were dissolved in anhydrous dimethylformamide, under an inert atmosphere (N_2). The mixture was stirred at 4 °C, for 16 hours (overnight) until all the 4-aminobenzoic acid starting material had been consumed, as indicated by TLC. The reaction mixture was filtered to remove the dicyclohexylurea by-product and dimethylformamide was removed by evaporation under reduced pressure, the crude mixture was re-dissolved in 40 % dichloromethane/ethyl acetate, washed with water to remove residual dimethylformamide, and dried over anhydrous sodium sulphate. The crude product was isolated using column chromatography and precipitation, affording **6** as white crystalline needles, with a yield of 58 %. It was reported that **6** was synthesised *in situ*, prior to coupling with BSA, thus there was no published characterisation studies concerning **6**.[140] The ^{1}H NMR and ^{13}C NMR spectra for compound **6** are shown in Figure 12.

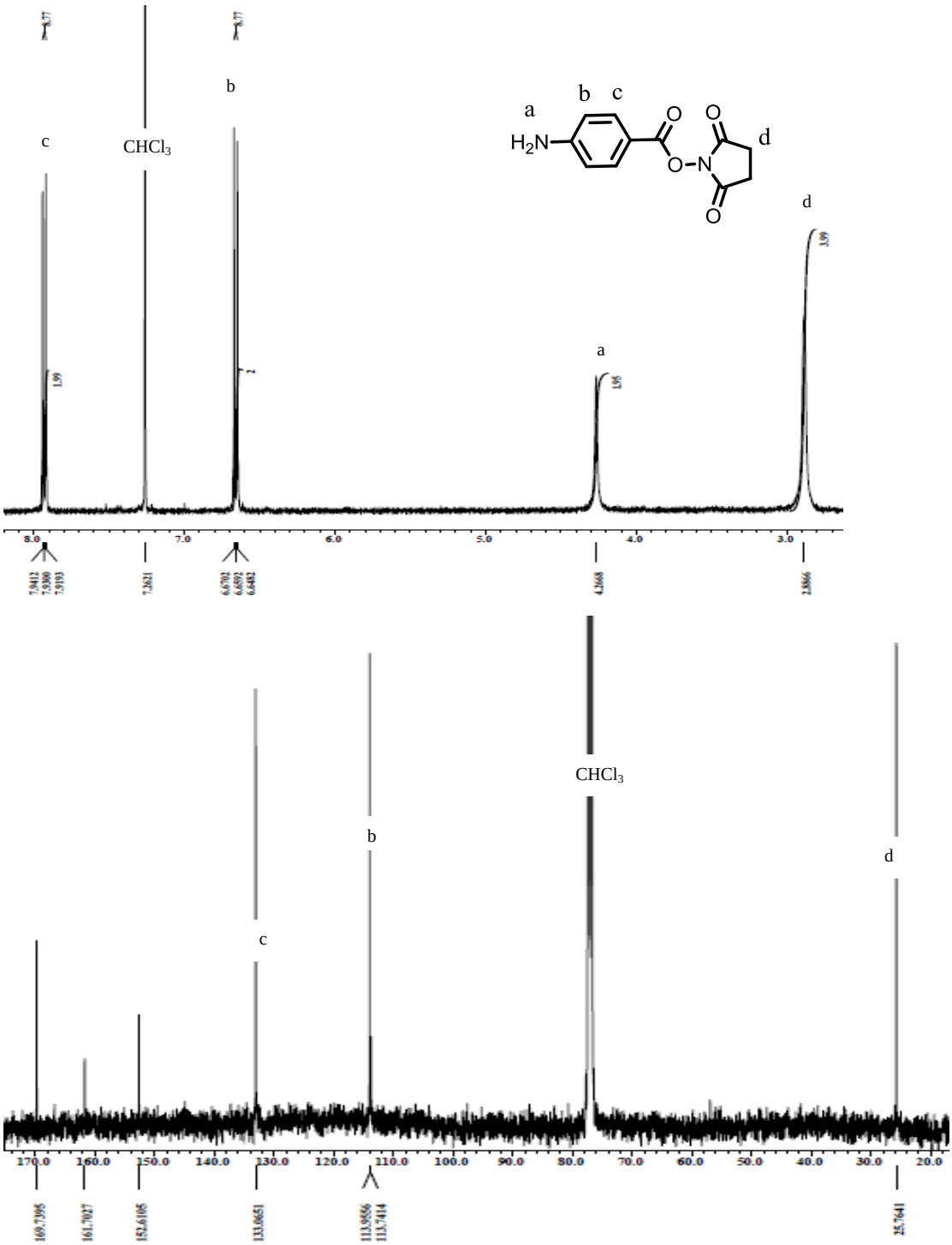

Figure 12: ^{1}H NMR and ^{13}C NMR spectrum's of compound **6**.

The NMR studies suggested the reaction had proceeded as expected; the ^{1}H NMR exhibiting a distorted set of doublets (**c**) and (**b**), which had a 'roof-top' (AB) appearance due to the phenyls 1,4 substitution pattern, a broad singlet (**a**) for the amino protons and a singlet (**d**) corresponding to the succinimidyl protons; the ^{13}C NMR spectrum exhibited the expected number of signals, corresponding to each of the carbon environments. The mass spectrum gave the expected *m/z* signal, however the sample did

appear to be impure, with a major signal corresponding to a dimeric intermediate, thus demonstrating the instability of the molecule.

The initial attempt at synthesising compound **7** employed equimolar equivalents of **6** and *N*-Boc-1,3-diaminopropane hydrochloride dissolved in dimethylformamide, in the presence of 2 mole equivalents of *N*,*N*-diisopropylethylamine; the base was required to neutralise the hydrochloric acid, ensuring the amine was available to react with the activated ester. It was hypothesised that the difference in reactivity between the different amines, i.e. the less reactive aromatic amine of **6,** and the more reactive primary amine of *N*-Boc-1,3-diaminopropane hydrochloride, should favour the production of the target compound **7**.

The TLC of the reaction mixture showed the presence of **6**, the formation of a major fraction corresponding to **7** and another more polar fraction located at the base line; which could be attributed to oligomers of **6.** The solvent was removed *in vacuo,* the crude product was re-dissolved in ethyl acetate and washed with water to remove residual dimethylformamide and *N*-Boc-1,3-diaminopropane hydrochloride. Chromatographic separation and precipitation led to **7** being isolated with a yield of 35 %. Isolation of compound **7** was problematic due to the presence **6** and other polar impurities, which accounts for the low yield. To suppress the production of oligomers, a 2 mole equivalent of *N*-Boc-1,3-diaminopropane hydrochloride was employed, which resulted in complete consumption of **6** and trace polar impurities being observed by TLC. The solvent was again removed by evaporation *in vacuo,* re-dissolved in ethyl acetate and washed with water to remove residual dimethylformamide and *N*-Boc-1,3-diaminopropane hydrochloride. Compound **7** was isolated as a yellow powder with a yield of 66 %, after chromatographic separation and precipitation. The ^{1}H NMR spectrum gave the expected signals, which integrated correctly, however the sample exhibited the presence of methanol, as shown in Figure 13. Compound **8** was synthesised with yields of 56 % and 76 %, by applying the same reaction conditions used for the production of **7**, using a slightly larger volume of dimethylformamide due to the solubility of *N*-Boc-1,12-diaminododecane. The ^{1}H NMR spectrum for **8** had a similar appearance to that of **7**, with a methanol peak being prominent, with the exception of the multiplet signal at 1.16-1.25 ppm, attributed to the middle section of the dodecyl alkyl chain.

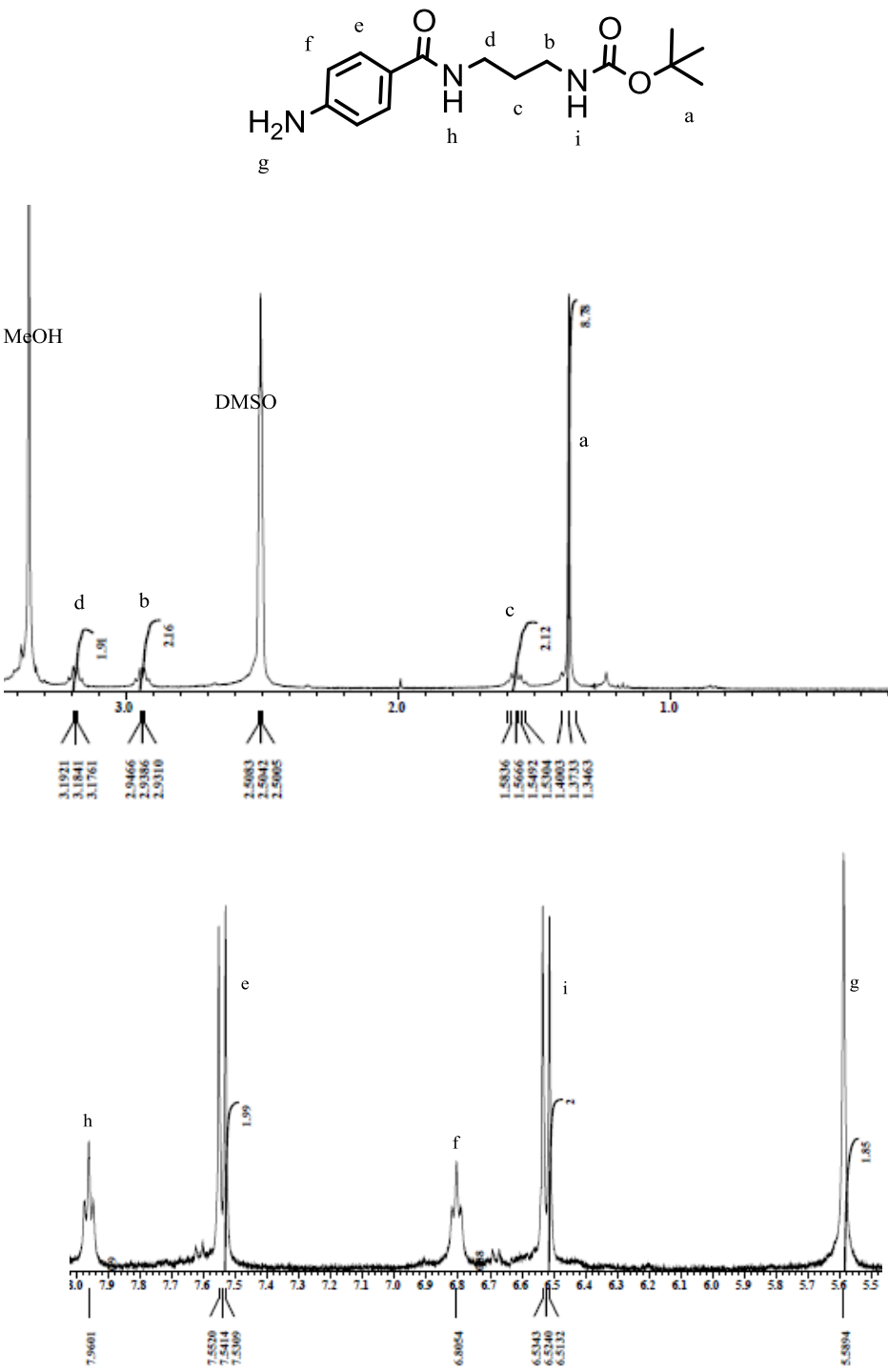

Figure 13: ^{1}H NMR spectrum of compound **7**.

The preliminary reductive amination attempts involving aryl linkers **7** and **8**, followed the published acid catalysed strategy.[137] Compounds **7** and **8** were poorly soluble in toluene, therefore anhydrous tetrahydrofuran was selected and the reactions were conducted under an inert atmosphere, in the presence of activated 3Å molecular sieves. The initial reaction was performed using 1.2 equivalents of **7**, relative to **3**, in the presence of the acetic acid catalyst. The reaction was monitored by TLC, with the development of a trace polar fraction located at the base line being observed after 12

hours, with almost complete recovery of **3**. A methanolic solution of sodium cyanoborohydride was added and, after 24 hours, TLC analysis indicated the presence of trace amounts of a newly formed porphyrinic fraction, the previous base line polar fraction and a significant amount of **3**. The reaction may have failed due to too much acid catalyst being added, protonating the amine rendering it inactive; although literature suggests that 1-2 equivalents of acetic acid can be used to catalyse the reaction.[139] As the formation of the imine was not evident, the reaction was repeated using 2 molar equivalents of **7**, adding the sodium cyanoborohydride reducing reagent at the start of the reaction. The reaction was monitored by TLC, and after 24 hours, almost complete consumption of **3** had occurred. The solvent was removed, re-dissolved in dichloromethane, washed with water and chromatographically separated. After drying, the suspected product had decomposed in a similar manner to the reaction involving *N*-Boc-1,3-diaminopropane. The reaction was repeated in exactly the same manner, and to ensure reduction of any imine had occurred, additional sodium cyanoborohydride dissolved in methanol was added after the 24 hour period. After a further 4 hours, TLC analysis showed the reaction mixture remained unchanged, and following work-up and isolation the suspected product had decomposed in exactly the same manner. The initial reductive amination attempt concerning compound **8** was performed without the addition of the sodium cyanoborohydride in the first step; after 24 hours TLC analysis revealed a trace, polar UV-active fraction, with almost all of **3** remaining. Sodium cyanoborohydride dissolved in methanol was added and after 24 hours the development of a variety of fractions including a major polar UV-active fraction with **3** also being detected. An additional methanolic solution of sodium cyanoborohydride was added and after 24 hours no additional change to the reaction mixture was observed by TLC. Once worked-up and chromatographically separated, the product exhibited decomposition. The reaction was repeated, adding the sodium cyanoborohydride dissolved in methanol at the beginning of the reaction. Following 24 hours at reflux, no further consumption of **3** was observed, with the development of two other UV-active fractions. Sodium cyanoborohydride was again added and after 13 hours, the composition of the reaction mixture remained unchanged. The reaction mixture was worked-up and the suspected product isolated via preparative TLC chromatography. Once dried the suspected product had decomposed, therefore the preparative TLC chromatography procedure was repeated and a crude ^{1}H NMR analysis was conducted before suspected decomposition. The ^{1}H NMR spectrum possessed a sharp singlet at 1.42 ppm, which could correspond to the *tert*-butyl group, a pair of

doublets at 6.42 and 7.42 ppm which might correspond to the phenyl group adjacent to the dodecyl chain, and a range of signals located in the aromatic and alkyl regions; none of which integrated correctly. Partial assignment of the ^{1}H NMR spectrum was not attempted as the spectrum was not resolved well enough, although there were signals which could potentially be due to porphyrin and aryl linker components. Due to the instability of the suspected product, the acid catalysed strategy for the aryl linkers was abandoned.

The lanthanum(III) triflate methodology was also attempted employing either compounds **7** and **8** with the copper(II) complex of the formylated porphyrin **4.** The reactions were performed in tetrahydrofuran in the presence of activated 3Å molecular sieves and under an inert atmosphere (N_2). Both sets of reactions were monitored over a 3 day period with no apparent change to **4** being detected by TLC.

2.6.5 Reductive amination using methyl 4-aminobenzoate

As the reductive aminations using the novel aryl compounds **7** and **8** had failed, and the reaction using aniline was successful, it was decided that a different aniline derivative should be used, which possessed a different functionality, and upon further modification could be transformed into the reactive maleimide bioconjugation group. It has been reported that 2-formyl-TPP can participate in reductive aminations with ethyl-4-aminobenzoate, producing ethyl-4-((5,10,15,20-tetraphenylporphyrin-2-ylmethyl)amino)benzoate with a good yield of 72 %.[137] By performing a reaction using methyl 4-aminobenzoate, and hydrolysing the ester, this would provide a carboxyl group that could then be transformed in a similar manner to that of compound **6** (Scheme 32), eventually terminating in an amino group which could be transformed into the maleimide functionality. The synthetic strategy involving methyl 4-aminobenzoate is outlined in Scheme 33.

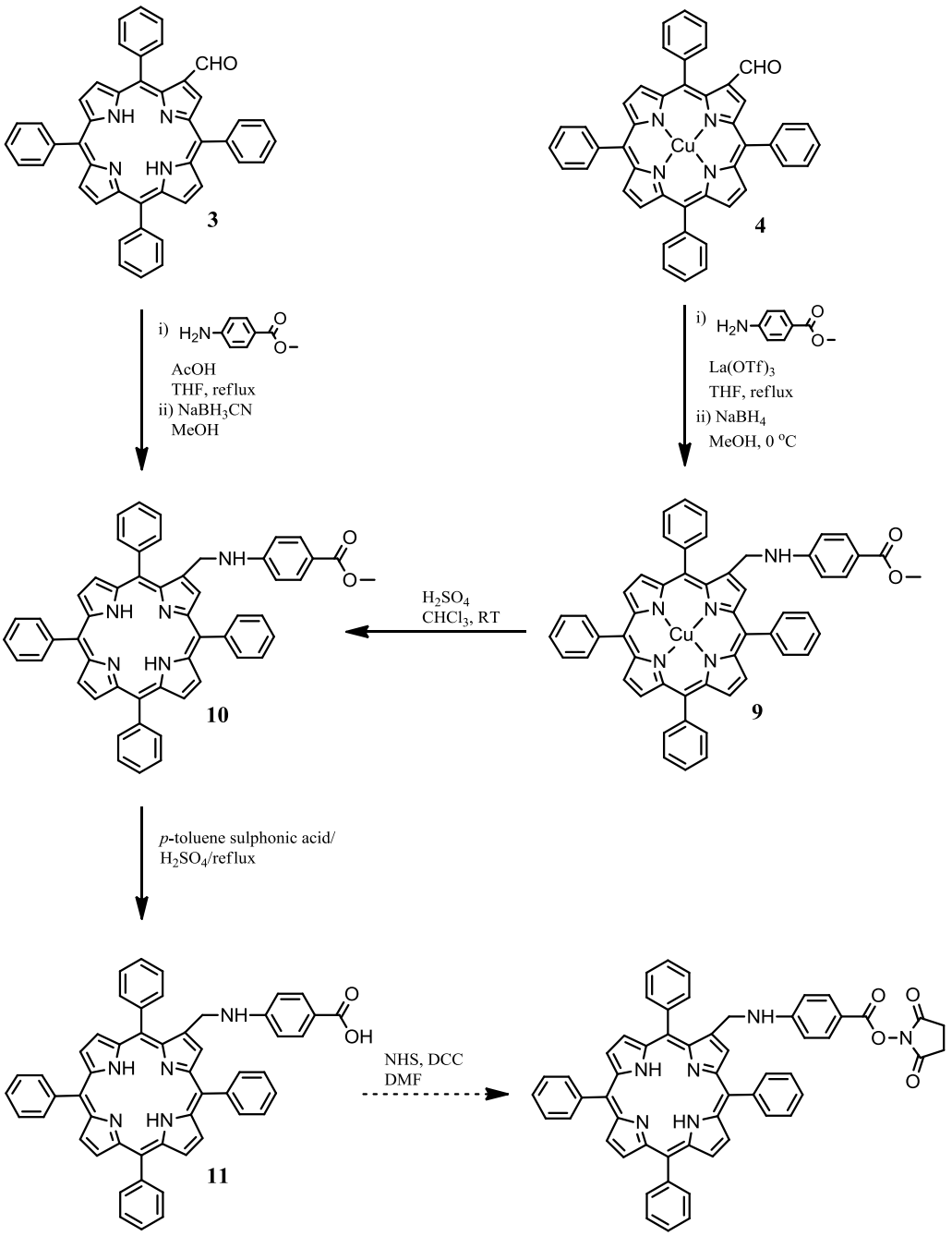

Scheme 33: Synthetic strategy involving methyl 4-aminobenzoate.

As compounds **3** and **4** were both available, two different routes for synthesising compound **10** were explored. Methyl 4-aminobenzoate appeared to be more soluble in tetrahydrofuran in comparison to toluene, although heating was required; therefore tetrahydrofuran was used for the reactions. By following a known procedure,[136] compound **4,** methyl 4-aminobenzoate and lanthanum(III) triflate were added to tetrahydrofuran. The reaction was heated to reflux, under an inert atmosphere (N_2) protected against light and in the presence of activated 3Å molecular sieves. After 44 hours, TLC analysis of the reaction mixture showed no further change, with the

presence of a major, more polar UV-active fraction and compound **4**. Once the solvent was removed by evaporation *in vacuo*, the mixture was re-dissolved in dichloromethane, filtered to remove the lanthanum(III) triflate catalyst and washed with water to remove excess methyl 4-aminobenzoate and tetrahydrofuran. The solution was dried over anhydrous sodium sulphate, the solvent was removed under reduced pressure and the crude mixture was dried under vacuum, to avoid the presence of water, which could react with sodium borohydride liberating flammable hydrogen gas. The crude mixture was dissolved in anhydrous dichloromethane and the imine reduced with a methanolic solution of sodium borohydride under an inert atmosphere. Acetic acid was added to neutralise the excess sodium borohydride. Once aqueous work-up had been performed the TLC of the reaction showed two major porphyrinic fractions, corresponding to **4** and **9**. Compound **9** was isolated as a red powder, with a yield of 65 %, after column chromatography and precipitation from dichloromethane by the addition of pentane. The initial mass spectrum showed a major 837 *m/z* peak $(M+H)^+$, implying that the imine had been produced, therefore the reduction procedure using a methanolic solution of sodium borohydride was repeated. The high resolution mass spectrum provided the expected 861.2134 *m/z* signal, corresponding to the $(M+Na)^+$ ion; although fragmentation was prominent, as shown in Figure 13.

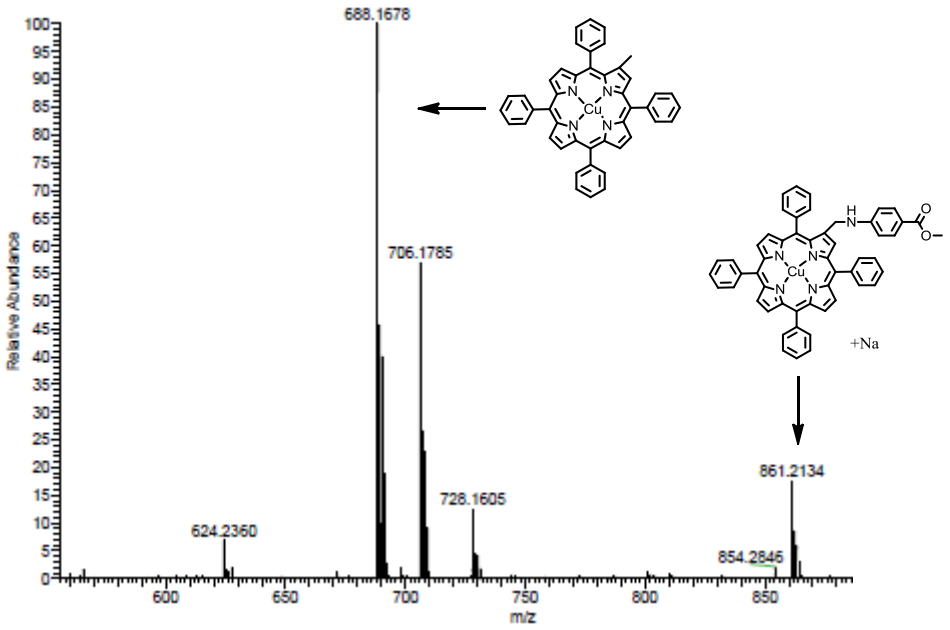

Figure 13: Mass spectrum of **9**.

The demetallation of **9** was initially attempted using relatively mild acidic conditions, as previously reported.[141] Dissolution of **9** in anhydrous dichloromethane was followed by

treatment with a 2 % sulphuric acid/trifluoroacetic acid solution, the mixture was stirred vigorously for 2 minutes, and once extracted and purified, the reaction only showed the presence of **9** as indicated by TLC. The reaction was repeated using 15 % sulphuric acid/trifluoroacetic acid, 50 % sulphuric acid/trifluoroacetic acid and 25 % trifluoroacetic acid/sulphuric acid, and by extending the reaction time to 5 minutes. The expected colour change to green; due to the protonation of the inner nitrogens, was not being observed. The procedure reported by Bonfantini *et al.*[130] was therefore employed, with **9** dissolved in chloroform being treated with sulphuric acid for 5 minutes. The protonation of the porphyrin was observed, and basic work-up resulting in a colour change from green to purple in the organic layer. After work-up, chromatographic separation and precipitation in methanol over dichloromethane, **10** was afforded as a purple powder, with a yield of 62 %.

Compound **10** was also synthesised via a published procedure.[137] A solution of **3** dissolved in anhydrous tetrahydrofuran was treated with 1.5 equivalents of methyl 4-aminobenzoate in the presence of a catalytic amount of acetic acid. After 6 hours at reflux, TLC analysis detected the development of a minor polar fraction, as well as a substantial quantity of **3**. A methanolic solution of sodium cyanoborohydride was added and the reaction was monitored by TLC. After 40 hours the reaction was not developing further, with porphyrinic fractions corresponding to **3** and **10** being detected. Following work-up and column chromatography, **10** was isolated with a yield of 26 %. The yield for **10** using the acetic acid catalysed reductive amination was significantly less than the combined yield for the lanthanum(III) triflate catalysed reaction, coupled with the copper demetallation, an overall yield of 40 %, thus the lanthanum(III) triflate approach was considered to be the preferred strategy. The ^{1}H NMR spectrum of **10** is shown in Figure 14. The assignment of the signals was achieved using a combination of ^{13}C NMR 2D COSY and CH-correlation experiments. The assignment of the signals in the alkyl region was quite straight-forward, with a singlet corresponding to the methyl group of the ester (**a**) at 3.78 ppm and the methyl group (**e**) neighbouring the porphyrin core giving the expected doublet signal, which had the same coupling constant, J = 5 Hz, as the neighbouring triplet (**d**), corresponding to the amino group. The 2D COSY experiment showed that the doublet at 6.38 ppm coupled to the doublet at 7.74 ppm with the signals having a similar coupling constant, which gave an averaged value of J = 8.9 Hz, thus these signals were assigned to the phenyl ring directly attached to the amino group. The other signals were assigned by using a combination of the integrals

and considering the shielding effect of the porphyrin core. The mass spectrum gave the expected 778.3171 *m/z* signal, due to the $(M+H)^+$ ion.

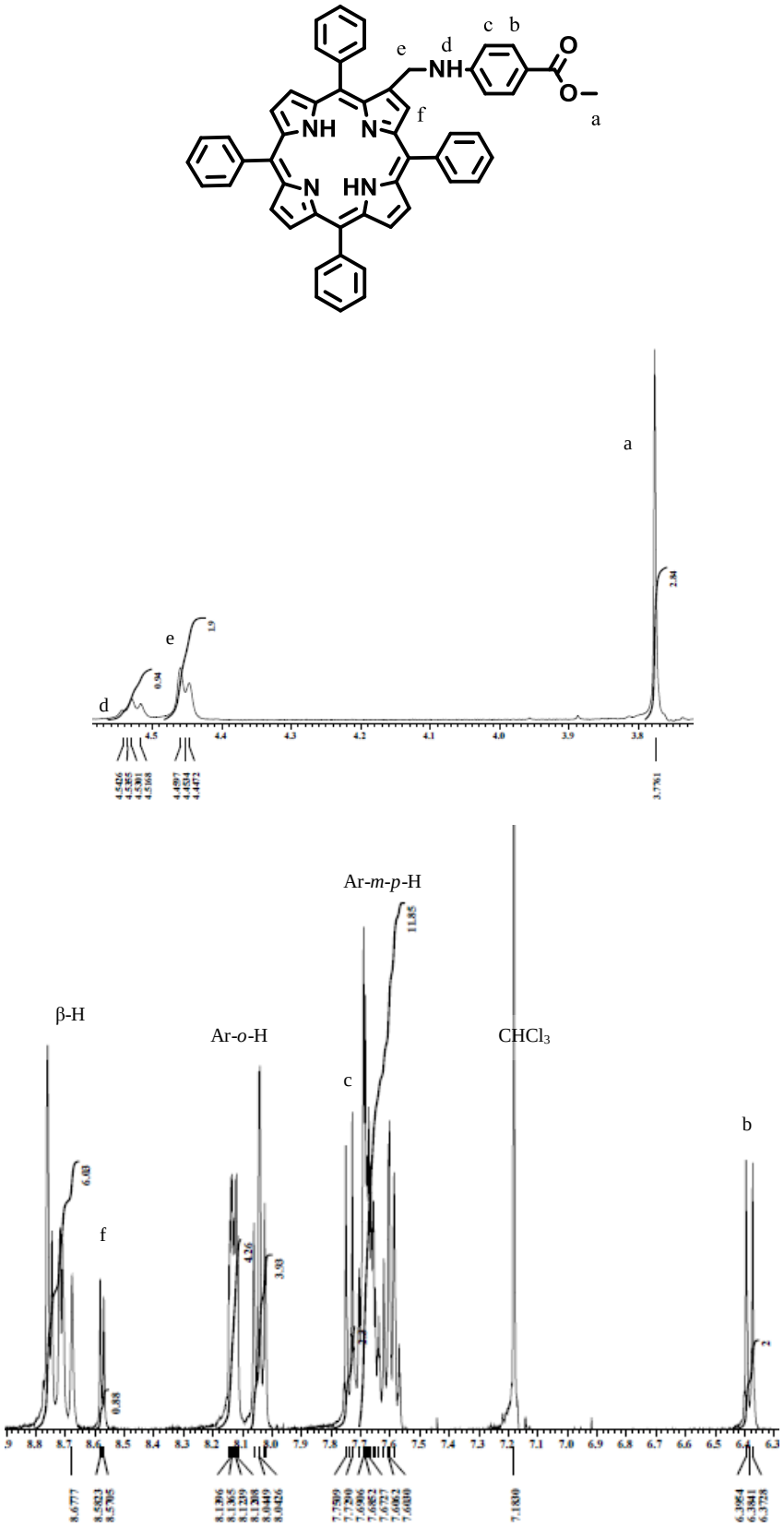

Figure 14: ^{1}H NMR spectrum of **10**.

The hydrolysis of **10** was attempted using a modified known procedure.[142] A solution of **10** dissolved in a 50 % ethanol/dichloromethane solution was treated with a 2 M potassium hydroxide solution, at reflux, while avoiding exposure to light. The reaction was monitored over a 3 day period, with no change to **10**, as shown by TLC. The basic hydrolysis of the ester was also attempted using a method developed by Silva *et al*.,[136] a 1 M sodium hydroxide solution was added to **10** dissolved in tetrahydrofuran, and the resulting mixture was stirred at 50 ^{o}C. The reaction was monitored via TLC, with only **10** being detected after 4 days. The reaction was repeated in a similar manner, using a 4 M sodium hydroxide solution. After 16 hours, (overnight), TLC analysis showed full consumption of **10**, the development of a trace polar UV-active fraction and another major porphyrinic fraction. Following work-up and chromatographic separation, ^{1}H NMR analysis of the newly formed porphyrinic fraction showed that **3** had re-formed. Since the base hydrolysis of **10** had caused the reformation of **3**, it suggested that the starting material could have been the iminium ion intermediate, although ^{1}H NMR analysis of the starting material **10** showed the presence of the amino proton at 4.53 ppm and the neighbouring methyl protons at 4.45 ppm. Two postulated mechanisms for the basic cleavage of methyl 4-aminobenzoate from **10** are illustrated in Scheme 34. Another basic hydrolysis of the ester was also attempted following a procedure devised by Stephenson *et al.*[134] A solution of **10** dissolved in tetrahydrofuran, was treated with a 20 molar excess potassium hydroxide in water and methanol (10:1), and the resulting mixture was heated to reflux under an inert atmosphere. After 46 hours, the TLC of the reaction mixture showed that all of **10** had been consumed, with the development of trace polar fractions and a significant quantity of **3**. Following work-up and chromatographic separation, the ^{1}H NMR confirmed the newly formed porphyrinic fraction was **3**, thus the ester base hydrolysis strategy was abandoned.

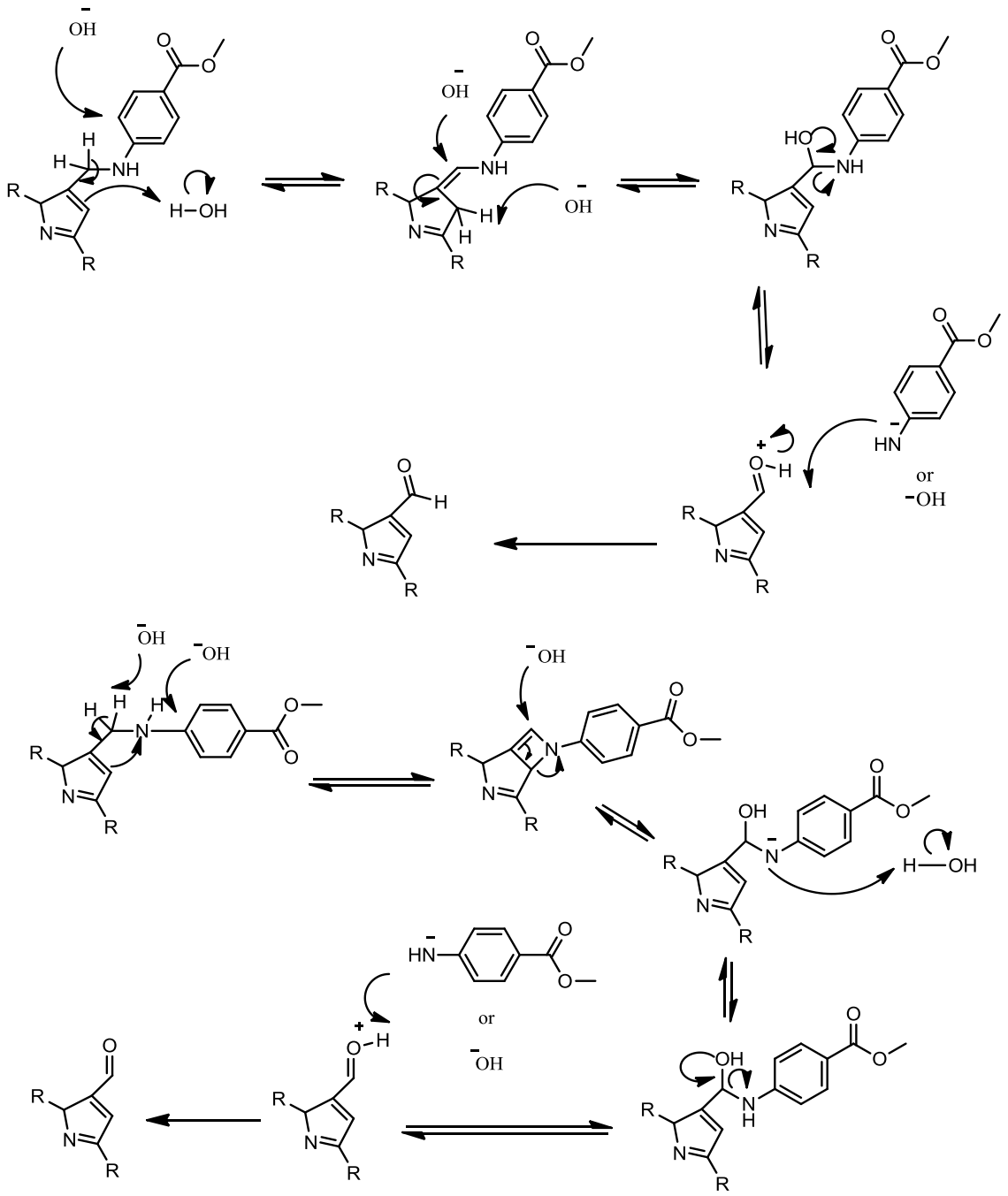

Scheme 34: Hypothetical mechanisms for base cleavage of **10** leading to the formation of **3**.

The carboxyl group can be deprotected using acidic hydrolysis conditions, as reported by Walter and co-workers.[143] The article described the hydrolysis of a variety of *meso*-carbomethoxyphenyl substituted porphyrins using a mixture of organosulfonic acid dissolved in 4 M sulphuric acid, under reflux conditions. Compound **10** dissolved in 4 M sulphuric acid was treated with 4 molar equivalents of *p*-toluenesulfonic acid monohydrate and the mixture was heated under reflux conditions. After 20 hours, TLC analysis of the reaction mixture revealed complete consumption of **10** with a newly formed, polar fraction was detected. An ice cooled 1 M sodium hydroxide solution was added to the vigorously stirred reaction mixture, until a colour change from green to red/yellow was observed, indicating that the acid had been sufficiently neutralised. The crude product was extracted into dichloromethane, and washed with a saturated sodium hydrogen carbonate solution to remove any residual acid, and water to remove residual base. Once chromatography and precipitation procedures had been performed, **11** was furnished as a purple powder in a 73 % yield. The ^{1}H NMR spectrum for **11**, shown in Figure 15, exhibited a singlet at 12.02 ppm, due to the newly formed carboxyl proton and in comparison to the ^{1}H NMR spectrum for **10**, no signal for the methyl group of the ester was observed, providing evidence that hydrolysis of the ester had occurred. The signal for the amino proton adjacent to the porphyrin exhibited a shift from 4.53 ppm to 7.27 ppm, although this was probably due to the different solvent systems used for the analysis. The doublet at 6.51 ppm had the same coupling constant, J = 8.8 Hz, as the doublet at 7.63 ppm, therefore these signals were assigned the phenyl group attached to the β-position of the porphyrin. The other signals were assigned by considering the shielding effect of the porphyrin and the signal integrals. The HRMS gave the expected 764.3013 *m/z* peak due to the $(M+H)^{+}$ ion. Therefore there was enough evidence to suggest that the reaction had proceeded as expected.

The sequential yield of compound **11**, from the initial aldehyde and pyrrole starting materials was 3.8 %, which is lower than what would be expected for a mixed condensation synthesis of an unsymmetrically substituted porphyrin. Therefore the synthetic route was abandoned as there was no obvious advantage relative to the porphyrin synthesis using a statistical mixture of aldehydes.

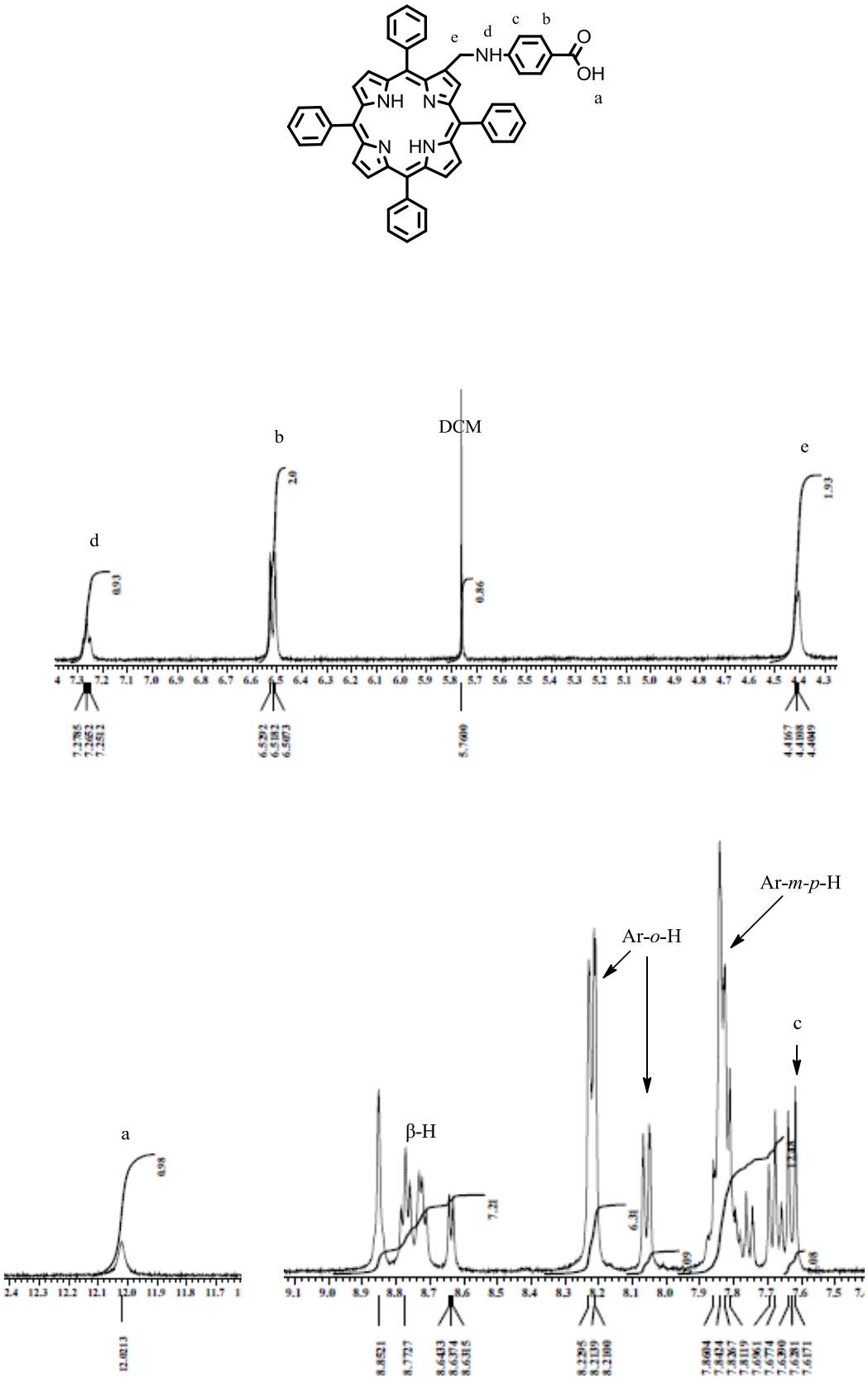

Figure 15: ^{1}H NMR spectrum of compound **11**.

2.7 Formylation of porphyrins bearing water solubilising functionalities in the *meso*-positions

Although the optimisation of conditions required for introducing a maleimide to TPP was unsuccessful, it was still interesting to ascertain whether the Vilsmeier formylation conditions could be applied to porphyrins bearing functionalities in the *meso*-positions, which could be further modified to induce water solubility. The porphyrins; tetra(4-pyridyl)porphyrin (**12**) and tetra(3,5-dimethoxyphenyl)porphyrin (**14**) contain functional groups which can modified to render the porphyrins fully water-soluble. Compound **12** possess pyridyl groups which can be methylated by treatment with methyl iodide, and the pyridinium ions provide hydrophilicity, whereas compound **14** has methoxy groups which can be de-methylated using boron tribromide, with the hydroxyl groups enabling water-solubility.[68] Formylating these porphyrins, and performing a series of modifications to the formyl group, eventually leading to the expression of a bioconjugation "handle", fits the overall strategy outlined in the introduction. The formylation attempts are shown in Scheme 35.

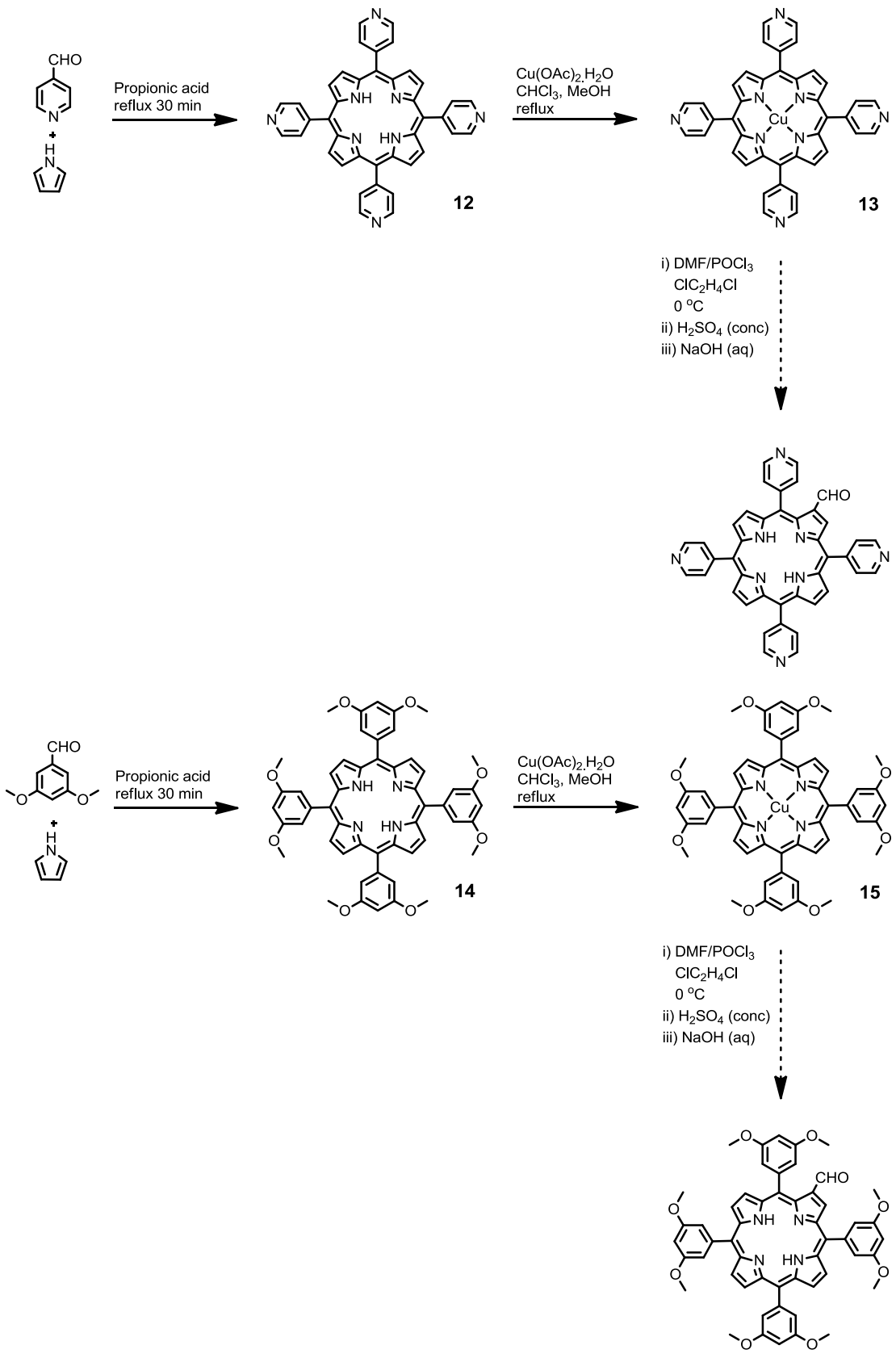

Scheme 35: Attempted formylation reactions involving porphyrins with water solubilising groups in the *meso*-positions.

2.7.1 Attempted formylation of tetra(4-pyridyl)porphyrin (12)

Tetra(4-pyridyl)porphyrin (**12**) was synthesised as a purple crystalline solid with a yield of 11 % by following the Adler-Longo method.[114] The yield of the porphyrin was quite low, with a significant quantity of the porphyrin being retained in the propionic acid, possibly due to ionization of the pyridyl groups under the acidic conditions which would lead to the formation of a porphyrin acid salt.[114] The ^{1}H NMR spectrum for **12** gave the expected signals, which integrated correctly. The signal for the aromatic *ortho*-protons, has a higher ppm value compared to the β and aromatic *meta*-protons, due to the inductive effect exerted by the nitrogen. The mass spectrum showed the 619 *m/z* peak due to $(M+H)^{+}$, therefore there was sufficient evidence that **12** had been produced. Compound **12** was then treated with a methanol/water solution of copper(II) acetate monohydrate, under reflux conditions.[130] During the purification of **13**, a silica column was initially used which resulted in the entire product being retained on the silica, thus when the experiment was repeated a neutral alumina column was used, allowing efficient purification. This suggested that even the mild acidity of silica gel was sufficient to cause protonation of the pyridyl groups. Following work up compound **13** was isolated as a red powder, with a yield of 93 % .The mass spectrum of **13** gave the expected 679 *m/z* peak and the typical copper isotope pattern. The UV-visible spectrum of **13** gave 3 signals, whereas the spectrum of **12** gave 5 signals. This was due to **13** being more symmetrical. Compound **13** was treated with the Vilsmeier complex as previously reported.[130] Following work-up, only compound **12** was detected by TLC**.** The reaction could have failed due to the electron deficient nature of the pyridyl groups drawing electron density more towards the *meso*-positions of the porphyrin, resulting in the β-position not being sufficiently nucleophilic towards the Vilsmeier reagent.

2.7.2 Attempted formylation of tetra(3,5-dimethoxyphenyl)porphyrin (14)

The Adler-Longo method,[114] was used for the production of tetra(3,5-dimethoxyphenyl)porphyrin (**14)**, which was furnished as a purple solid with a yield of 15 %. The ^{1}H NMR analysis, coupled with the mass spectrum, confirmed that **14** had been successfully synthesised, in a reasonable yield.

Following a reported procedure[130] **14**, dissolved in chloroform, was treated with a slurry of copper(II) acetate monohydrate in methanol-water, at reflux for 5 hours. After work-up, **15** was isolated a red/purple solid with a yield of 95 %. The evidence provided by the different UV-visible spectra of **14** and **15**, as well as the mass spectrum for **15,** indicated that the metallation had occurred as postulated.

Compound **15** was treated under Vilsmeier formylation conditions, as previously reported.[130] Following work-up, TLC analysis indicated that the reaction mixture contained no UV-active fraction, with the product having a yellow/brown viscous appearance.

2.8 Summary / further work

The development of a high yielding synthetic pathway, involving the mono-functionalisation of a symmetrical porphyrin and further modification into a group suitable for bioconjugation was unsuccessful, mainly due to the instability, and yields of products from the reductive amination reactions. Time permitting, it should be possible to react the carboxyl group possessed by **11** with a Boc protected diamine, which could deprotected and react with SMCC.

The formylations of the copper(II) complexes tetra(4-pyridyl)porphyrin (**13**) and tetra(3,5-dimethoxyphenyl)porphyrin (**15**) were also unsuccessful. The formylation of **15** should be further explored, but without the *in-situ* demetallation and conducting reductive aminations on the formylated copper(II) complex.

Chapter 3: Synthesis of immunoconjugate bearing a linker between photosensitiser and targeting moiety.

3.1 Introduction

Due to the problems associated with functionalising a symmetrical porphyrin, an alternative strategy was adopted involving incorporation of the required functionally during formation of the porphyrin. The types of reaction associated with forming porphyrins with multiple functional groups, including mixed condensations, are generally lower yielding than those for symmetrical porphyrins, however, developing the chemistry associated with forming water soluble maleimido porphyrins, performing successful conjugation to SIP(L19), and evaluating the characteristics of the subsequent immunoconjugates, validates the overall strategy.

Members of our group, had previously coupled the lysine reactive, 5-[4-(succinimidyl-*N*-oxycarbonyl)phenyl]-10,15,20-tri-(4-*N*-methyl-pyridiniumyl)porphyrin triiodide (**PS3**) to SIP(L19). Alonso *et al*.[144] had also conjugated the SIP(L19), to a cationic porphyrin bearing a maleimide group directly attached to the porphyrin core; 5-(4-maleimidophenyl)-10,15,20-tri-(4-*N*-methyl-pyridiniumyl)porphyrin triiodide (**PS4**).

Therefore, by conjugating the same antibody fragment (SIP(L19)), to a similar porphyrin, which possessed a linker between the porphyrin and the maleimide group, it would be possible to assess the influence the linker had on the conjugates immunogenic and photophysical properties. Additionally, it would also be possible to further evaluate the effect on the immunoconjugates characteristics, of having the photosensitiser coupled to either the lysine or cysteine residues.

3.2 Synthesis of unsymmetrical porphyrins

3.2.1 Mixed condensation porphyrin synthesis

The mixed condensation approach involves reaction between at least two different aldehydes, and pyrrole, and as such the approach can be applied to synthesising porphyrins under either Adler-Longo[114] or Lindsey[120] reaction conditions. In terms of producing a dual functional porphyrin, suitable for forming bioconjugates, two different aldehydes would be used; one bearing a functional group which can be transformed into the bioconjugatable group, and another which facilitates water solubility. From a statistical perspective, this can produce six different porphyrins (Figure 16); therefore exhaustive chromatographic separation is required. The yield of the porphyrin can be enhanced by using appropriate stoichiometry, while also considering the reactivates of the different aldehydes.

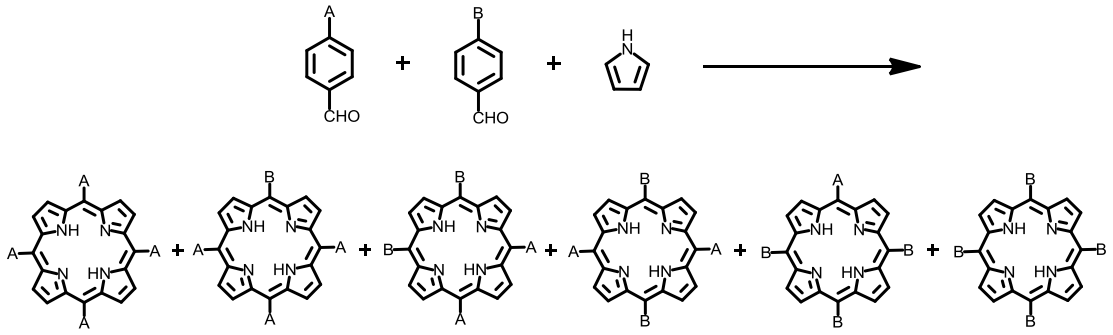

Figure 16: Representation of porphyrins produced during a mixed condensation porphyrin synthesis.

When performing a mixed condensation, using Adler-Longo conditions,[114] a major by-product is poly-pyrrole, therefore the crude material is usually first passed through a plug of silica to isolate the porphyrins from the tarry mixture. Although limited by the stability of the aldehyde to propionic acid, a wide variety of unsymmetrical porphyrins have been synthesised using this methodology, as shown in Scheme 36. Interestingly, it has been reported that boronic acids withstand the harsh acidic conditions.[145]

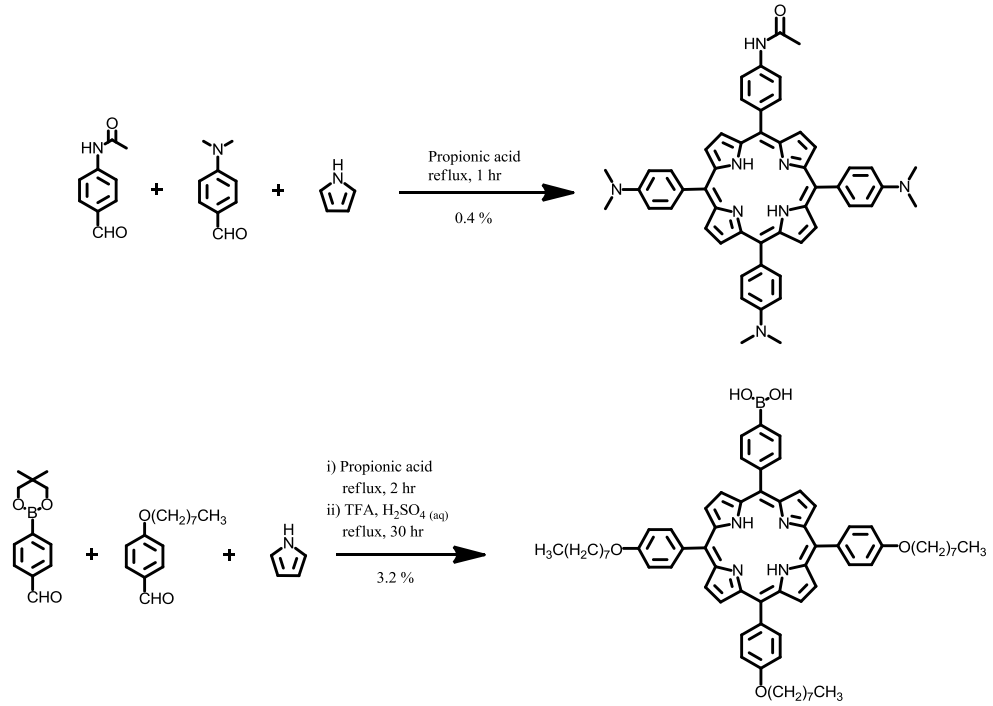

Scheme 36: Examples of unsymmetrical porphyrins synthesised using Adler-Longo conditions.[145,146]

The yields of unsymmetrical porphyrins synthesised under Adler-Longo conditions[114] are usually lower than those synthesised via the Lindsey method,[120] thus it would be appropriate to use Lindsey conditions,[120] if the reagents and corresponding porphyrinogen intermediate are soluble in chlorinated solvents. In addition to producing porphyrins in higher yields, as demonstrated by the yields of TPP obtained during preliminary studies, Lindsey conditions[120] are also more tolerant of acid sensitive functional groups. Würthner *et al.*[147] reported the synthesis of an anthryl-bithienyl porphyrin using the Lindsey procedure (Scheme 37); in this case using Lindsey reaction conditions were advantageous, as it was unlikely that the thienyl functionality would withstand boiling acidic conditions. Furthermore, the Adler-Longo method,[114] only produces low yields of *meso*-alkyl porphyrins, e.g. *meso*-tetrapropylporphyrin in 2.8 % yield.[148] Lindsey conditions[120] have also being used for the synthesis of 5,10,15-tris(4-[2,3,4,6-tetraacetyl-*β*-D-glucosyl]phenyl)-20-mono(2,3,4,5,6-pentafluorophenyl)porphyrin (Scheme 37).[149] Equimolar equivalents of the aldehydes were used for the synthesis; however the major porphyrinic product was the symmetrical glycosylated porphyrin (9.5 %), thus demonstrating the importance of considering the reactivates of the aldehydes, in order to obtain the optimum yield of the desired porphyrin.

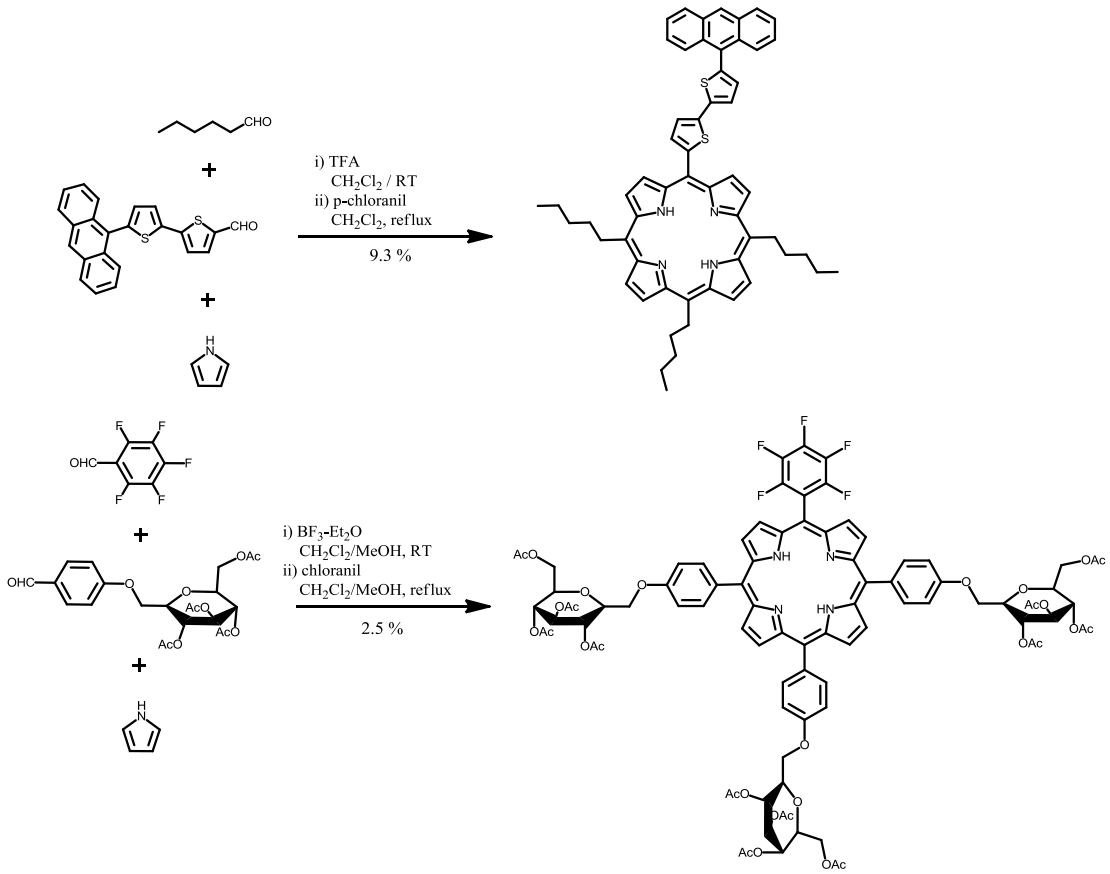

Scheme 37: Unsymmetrical porphyrins synthesised using Lindsey conditions.[148,149]

3.2.2 MacDonald porphyrin synthesis.[150]

The 2+2 porphyrin synthesis is often used referring to reactions pioneered by MacDonald and co-workers,[150] as an alternative method for producing multi-functionalised porphyrins. The procedure involved the acid catalysed reaction between two dipyrromethanes; one of which possesses formyl groups on the carbons neighbouring the pyrrolic nitrogens, leading to the formation of a porphyrinogen, which was oxidised by air to afford porphyrin, as depicted in Scheme 38.

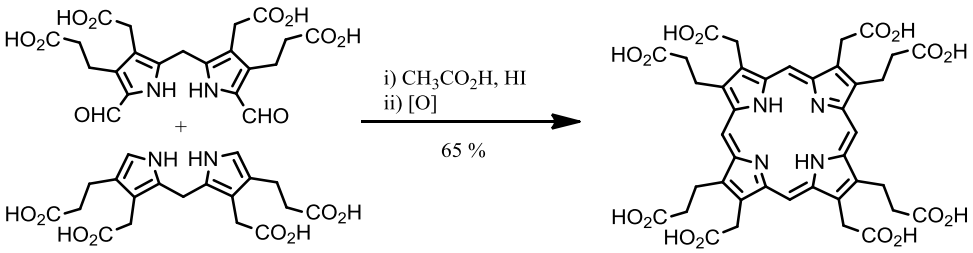

Scheme 38: Example of MacDonald porphyrin synthesis.[150]

A similar 2+2 methodology has also been applied to dipyrromethane-carbinols, enabling the expression of multiple substituents in the *meso*-positions, as shown in Scheme 39. The production of the dipyrromethane-carbinol is achieved by initial acylation of the dipyrromethane, via treatment with ethylmagnesium bromide; producing the dipyrromethane anion, which is nucleophilic towards the subsequent substituent bearing a carbonyl attached to a good leaving group e.g. chloride or thiolated pyridyl group. Generally, acylations using the pyridyl thiolate derivatives produce higher yields, in comparison to acid chlorides, using polar solvents. Additionally, mono and di-acylation can be controlled by using appropriate stoichiometry. Reduction of the carbonyls using sodium borohydride affords the carbinol, which can be condensed with a dipyrromethane in the presence of acid, to furnish the porphyrinogen, which is oxidised by DDQ to afford the porphyrinic product.[151]

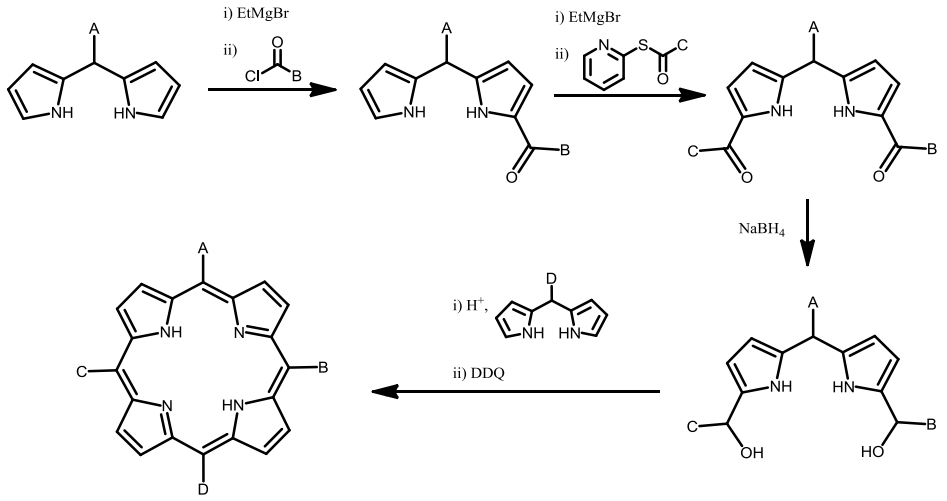

Scheme 39: Theoretical synthesis of multifunctional porphyrin using 2+2 carbinol strategy.

There has been a wide variety of porphyrins synthesised using the carbinol intermediate, with a few examples illustrated in Scheme 40.

The scope of the 2+2 carbinol strategy is restricted mainly by the acylation procedure, due to incompatibility between the basic Grignard reagent or sodium borohydride, with the substituent which is to be appended to the dipyrromethane; for example, acylations using an acetamido substituted thioester were unsuccessful due to the acidity of the NH group.[152] The synthesis of a mono-functionalised pyridyl porphyrin has been reported, as illustrated in Scheme 40; however the yield was significantly lower than previously reported porphyrins which were synthesised in a similar manner.[153]

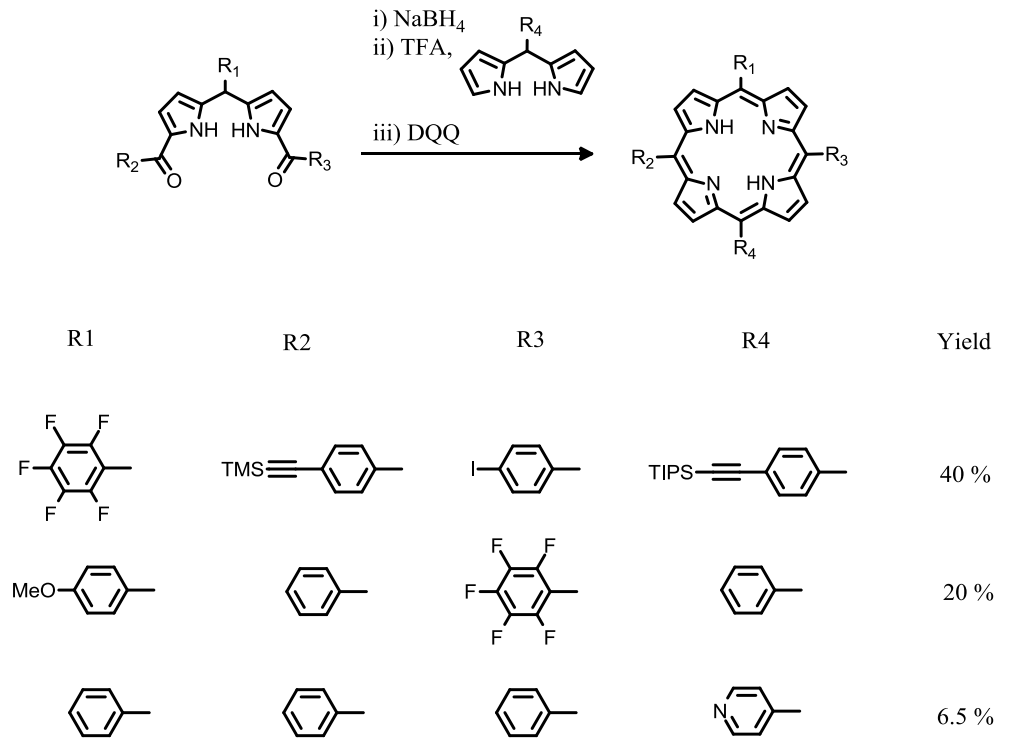

Scheme 40: Porphyrins synthesised using the carbinol intermediate.[151,153]

3.2.3 Polymer supported synthesis of mono-functionalised porphyrin

A polymer support can also be employed for the synthesis of mono-functionalised porphyrins, as demonstrated by Borhan and co-workers.[154] The procedure involved the anchoring of 4-carboxybenzaldehyde to a functionalised solid support bearing a reactive alkyl halide, resulting in the carboxylic group forming an ester with the solid support. The derivatised solid support was then reacted with benzaldehyde and pyrrole, under Adler-Longo[114] conditions, leading to formation of the mono-functionalised porphyrin attached to the solid support, and TPP in solution. The solid support was isolated by filtration, washed, and base hydrolysis of the ester afforded the mono-functionalised porphyrin in a reasonable yield of 6 %, as shown in Scheme 41. A similar methodology was then applied to a derivatised polymer bearing an alkyl halide. The polymer in ethyl acetate, was treated with 4-carboxybenzaldehyde in the presence of triethylamine, in a sealed tube at 90 ^{o}C; which resulted in anchoring of the aldehyde to the polymer via an ester bond. The derivatised polymer was reacted with pyrrole and benzaldehyde, under Lindsey conditions.[120] The polymer was collected, washed with methanol, and the ester was cleaved using sodium hydroxide. The 5-(4-carboxyphenyl)10,15,20-tri(phenyl)porphyrin was isolated in an excellent yield of 30 %. Considering only the

reaction yields, the porphyrin synthesised under Adler-Longo conditions[114] didn't exhibit an advantage over the mixed condensation approach, whereas the Lindsey conditions[120] produced a substantially higher yield. The main advantage of using the solid support strategy is the absence of the undesirable di, tri or tetra substituted porphyrins, therefore reducing the amount of chromatographic separation required and making isolation of the product more efficient.

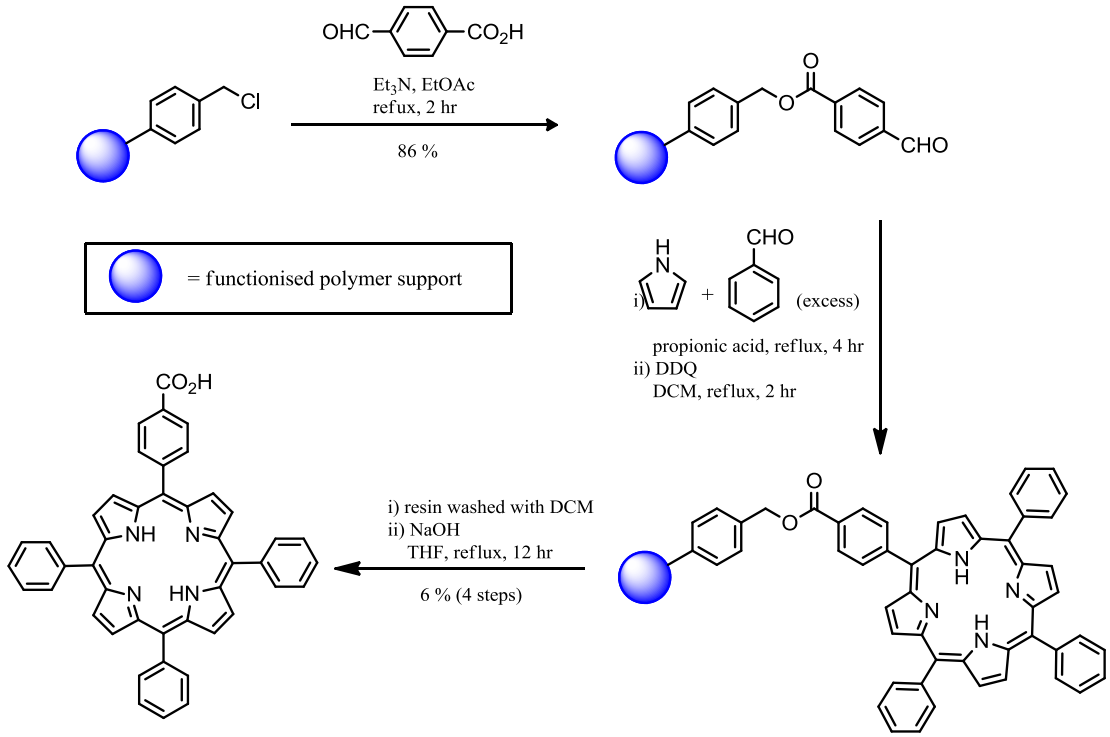

Scheme 41: Polymer supported synthesis of mono-functionalised porphyrin.[154]

3.3 Porphyrins bearing amino functionalities.

The amino group is a nucleophilic species. Therefore if the amino group is to be integrated into the porphyrin structure during porphyrin formation it must be protected to avoid condensation with the aldehyde. During porphyrin formation, amino groups are generally introduced as acetamido, [68,155,156] or phthalimide groups,[157] or as a nitro precursor.[157,158,159] The acetamido functionality can be hydrolysed by either base or acid treatment, yielding the amino group. The hydrolysis of 5-(4-acetamidophenyl)-10,15,20-tri-(4-methoxyphenyl)porphyrin has been demonstrated by Fungo *et al.*,[155] via basic treatment with potassium hydroxide, yielding the amino derivative with a yield of 75 %; whereas Boyle and co-workers,[68] deprotected the same porphyrin under acidic conditions, employing aqueous hydrochloric acid, affording the amino porphyrin in 93 % yield (Scheme 42). The nitro group can be reduced to the amino functionality, as shown by Liu *et al.*[158]; 5-(4-nitrophenyl)-10,15,20-tri(4-*tert*-butylphenyl)porphyrin was treated with a mixture of tin(II) chloride and hydrochloric acid, furnishing the amino derivative in 84 % yield, as illustrated in Scheme 42. The phthalimide functionality can be cleaved using hydrazine monohydrate, via nucleophilic attack at the phthalimide carbonyls, leading to the production of a stable cyclic by-product; for example, the amino analogue of 5-(4-phthalimidophenyl)-10,15,20-tri(4-trifluoromethylphenyl)porphyrin was produced in a 85 % yield,[157] as depicted in Scheme 42.

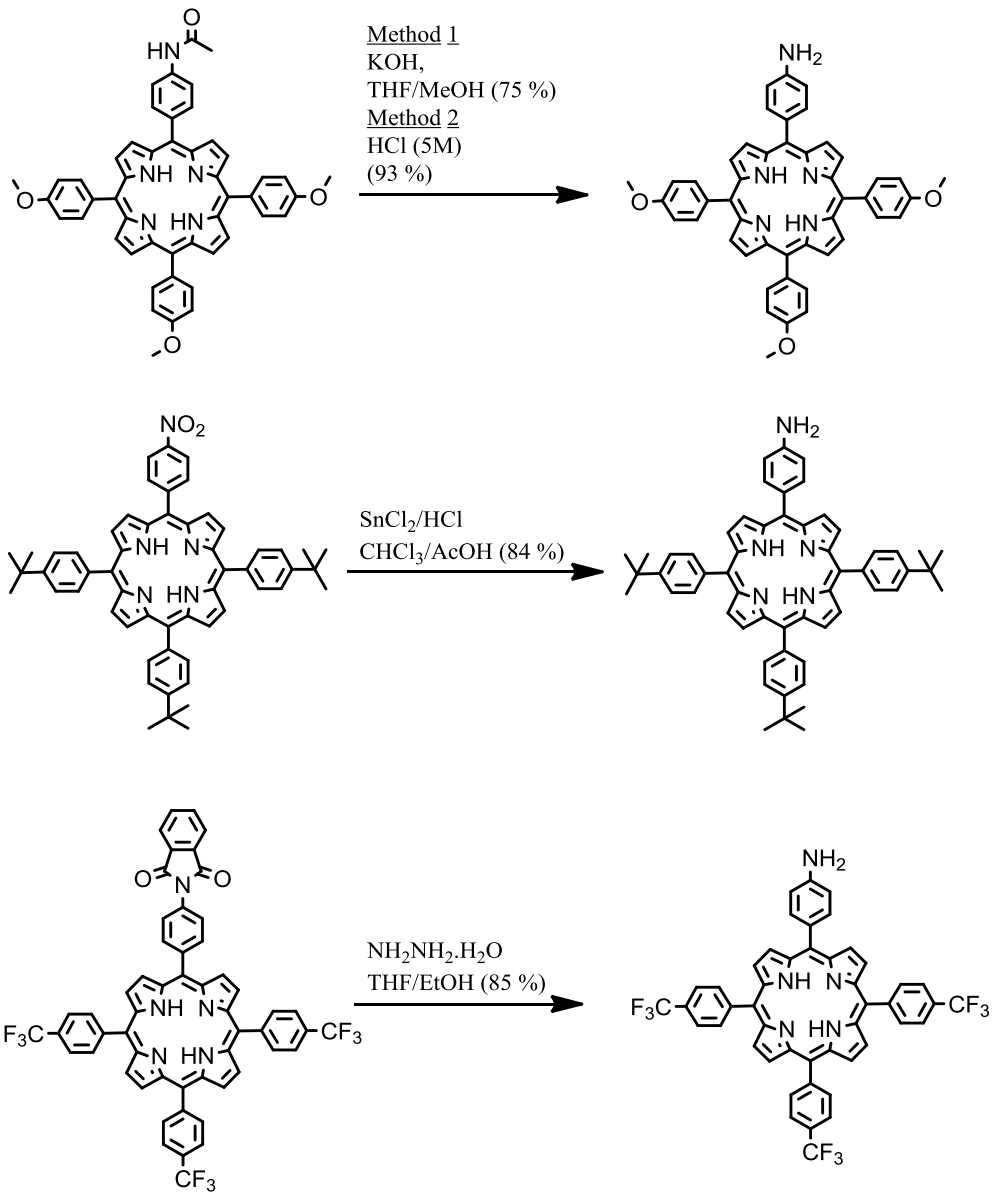

Scheme 42: Amino porphyrins from acetamido,[68,155] nitro,[158] and phthalimide[157] analogues.

It has been demonstrated that amino porphyrins can participate in DCC mediated couplings and a variety of nucleophilic substitution reactions. An article by Wang *et al.*[157] has described the DCC mediated coupling between tetra(4-aminophenyl)porphyrin with Boc protected valine. The reaction was performed in dichloromethane in the presence of 4-dimethylaminopyridine for 72 hours at 6 ^{o}C, furnishing the product in 38 % yield. Feng and Senge,[160] have performed a DCC catalysed reaction involving (−)-2,3:4,6-di-*O*-isopropylidene-*L-gulo*-hex-2-ulofuranosonic acid and 5-(4-aminophenyl)-15-butyl-10,20-diphenylporphyrin in dichloromethane, for 3 hours at ambient temperature, affording the desired porphyrin in 70 % yield. Interestingly, it has been

reported that DCC couplings involving 5-(4-aminophenyl)-10,15,20-tri-(4-pyridyl)porphyrin and Boc protected glutamic acid were unsuccessful; attributed to the amino group having a low nucleophilicity, due to the nitrogen's lone pair of electrons delocalising into the phenyl ring. However, the coupling was achieved by pre-activating the glutamic acid's carboxyl group with ethyl chloroformate, and the resulting anhydride was reacted with the amino porphyrin *in situ*, producing the adduct in 80 % yield.[161]

5-(4-Aminophenyl)-15-butyl-10,20-diphenylporphyrin has also been shown to react with maleic anhydride, to furnish the maleic acid analogue. The porphyrin, dissolved in anhydrous tetrahydrofuran, was treated with aliquots of maleic anhydride, and the resulting mixture was stirred at ambient temperature for 30 minutes. The excess maleic anhydride was neutralised with an aqueous solution of sodium hydroxide, and the maleic acid derivative was isolated in 92 % yield, after aqueous washings and chromatographic separation.[160]

Flamigni *et al.*[159] have shown that 5-(4-aminophenyl)-10,15,20-tri-(4-trifluoromethylphenyl)porphyrin can react with a corrole bearing an acid chloride, as shown in Scheme 43. The corrole, bearing a carbomethoxy group, was treated with trifluoroacetic acid, acetic acid and sulphuric acid under an argon atmosphere, for 24 hours at 100 °C. The carboxyl functionality was then converted into the acid chloride by dissolving the corrole in anhydrous tetrahydrofuran, and treatment with oxalyl chloride at 60 °C for 30 minutes. The solvent was removed, and the intermediate acid chloride was re-dissolved in a mixture of dry tetrahydrofuran and triethylamine. The amino porphyrin was subsequently added and the reaction was stirred at 50 °C over night; following work-up, the dyad was isolated in 48 % yield.

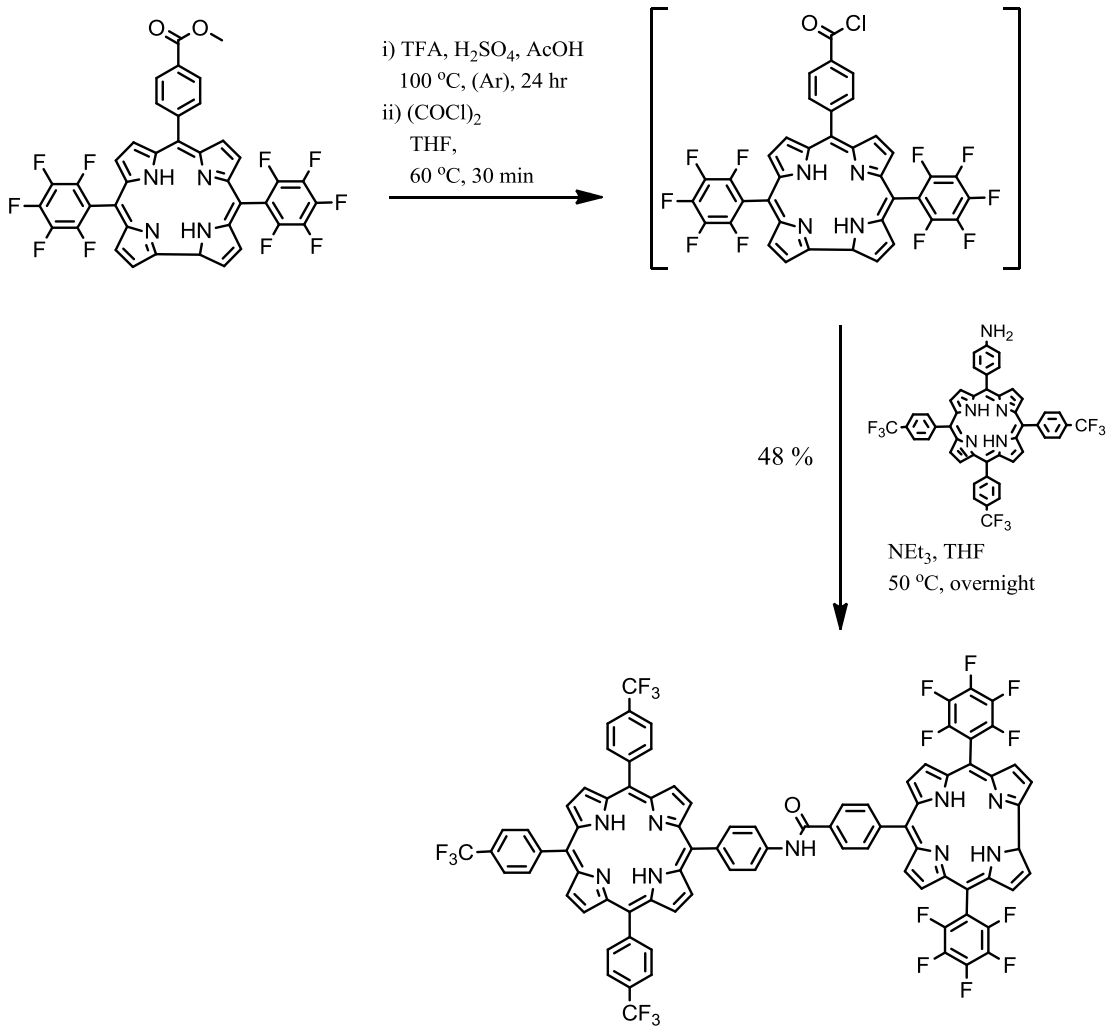

Scheme 43: Synthesis of porphyrin-corrole adduct.[159]

5-(4-Aminophenyl)-10,15,20-tri-(2,4,6-trimethoxyphenyl)porphyrin has been shown to participate in a nucleophilic substitution reaction with 1-chloro-2,6-dinitro-4-trifluorometilbenzene. The reagents were dissolved in chloroform, and the reaction proceeded after potassium hydroxide was added to activate the amino group, and in the presence of the phase transfer catalyst tetrabutylammonium bromide, affording the product in 90 % yield.[156]

3.4 Porphyrins bearing carboxyl functionalities

The carboxyl group doesn't require protection prior to porphyrin formation, however Yamaguchi *et al.*[142] and Ishikawa *et al.*[162] synthesised 5-(4-carboxyphenyl)-10,15,20-tri-(4-pyridyl)porphyrin via the base hydrolysis of the methyl ester analogue. The reasons for this strategy are unknown, as the reaction yields of 1.4 %[142] and 5 %,[162] are not favourable, and there is no significant difference in cost between methyl 4-formybenzoic acid and 4-carboxybenzaldehyde.[163]

It has been reported that porphyrins bearing carboxyl groups can be utilised for reactions that require coupling reagents. An EDCI mediated reaction between 5-(4-carboxyphenyl)-10,15,20-tri-(3,5-di-*tert*-butylphenyl)porphyrin and a fullerene which possessed a polyethylene glycol chain terminating in a hydroxyl group has been reported. The coupling proceeded in anhydrous dichloromethane and in the presence of 4-dimethylaminopyridine. The mixture was stirred for 18 hours, and following work-up and isolation, the adduct was furnished in 51 % yield.[164] It has also been shown that EDC and 4-dimethylaminopyridine can catalyse a coupling involving 5-(4-carboxyphenyl)-10,15,20-tri-(2-pyridyl)porphyrin and an oligonucleotide possessing an amino functionality. The reaction was performed at room temperature, overnight, in dry dichloromethane, with the conjugate isolated in 73 % yield. [165] Habdas *et al.*[166] have reported the DCC/4-dimethylaminopyridine coupling of aminophosphonates with 5-(4-carboxyphenyl)-10,15,20-tri-(4-pyridyl)porphyrin. The amino phosphonate, 4-dimethylaminopyridine and triethylamine were dissolved in anhydrous dichloromethane, which was subsequently added to a solution of the porphyrin and DCC, dissolved in dry dichloromethane. The mixture was stirred at 0 °C for 2 hours, and then at room temperature for a further 24 hours, with the porphyrin-phosphonate derivatives produced in 65 % and 70 % yields, as illustrated in Scheme 44.

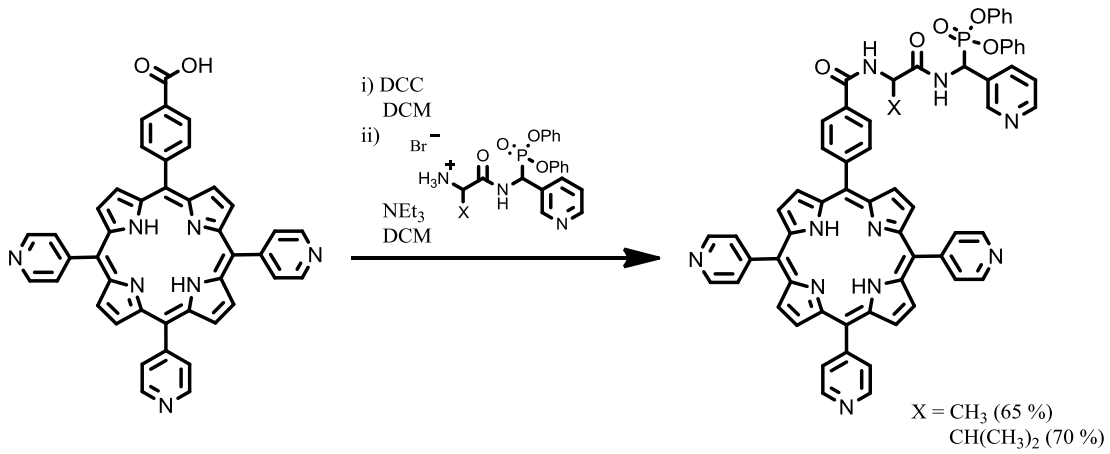

Scheme 44: DCC coupling of porphyrin and phosphonate derivatives.[166]

Acridines bearing an alkyl chain, of varying lengths, terminating in an amino group, have been used for synthesising a library of porphyrin-acridine conjugates, via the carbonyldiimidazole catalysed coupling with 5-(4-carboxyphenyl)-10,15,20-tri-(4-pyridyl)porphyrin. The porphyrin was pre-activated with carbonyldiimidazole, dissolved in a mixture of dimethylformamide and dimethylsulfoxide at 0 °C. The acridine, dissolved in the same solvent system was added, and the resulting solutions were stirred at 0 °C for 20-47 hours, affording the porphyrin-acridine conjugates in 22-46 % yields.[162]

Carboxyl groups can be transformed into an activated form, e.g. activated esters or acid chlorides, making them susceptible to nucleophilic attack. Frochot and co-workers,[167] converted 5-(4-carboxyphenyl)-10,15,20-tri-(phenyl)porphyrin into an activated ester via a DCC mediated reaction with *N*-hydroxysuccinimide in dry 1,4-dioxane, at room temperature for 4 hours, affording the *N*-hydroxysuccinimide activated porphyrin in 91 % yield. The activated ester dissolved in anhydrous tetrahydrofuran was reacted with a PEG chain terminating in amino groups, one of which was Boc protected. The reaction mixture was stirred at room temperature for 18 hours, yielding the porphyrinic product in 75 % yield, as depicted in Scheme 45. The *N*-hydroxysuccinimide activated porphyrin was also treated with a folic acid derivative which possessed an amino functionality. The reaction was performed in a mixture of anhydrous dimethylsulfoxide and pyridine, for 24 hours at ambient temperature, giving the porphyrin-folic acid conjugate in 34 % yield.

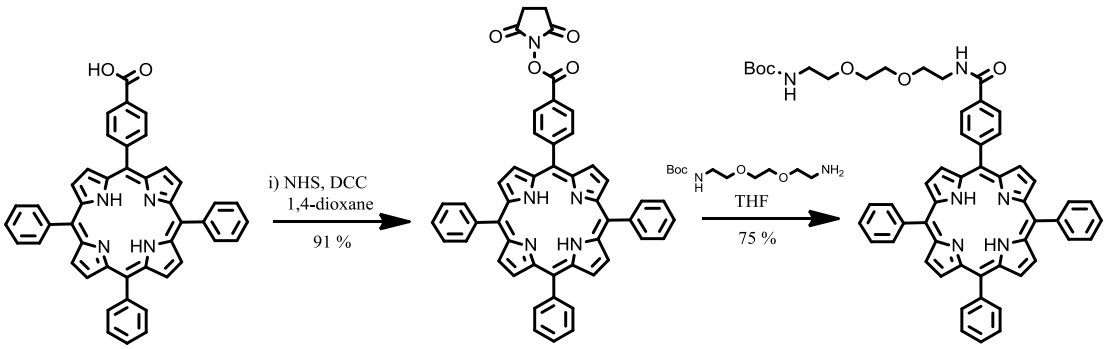

Scheme 45: Reaction between *N*-hydroxysuccinimide activated porphyrin and PEG derivative.[167]

5-(4-Carboxyphenyl)-10,15,20-tri-(4-pyridyl)porphyrin has also been converted into the *N*-hydroxysuccinimide activated ester derivative, as demonstrated by Tomé *et al.*[168] A solution of the carboxyl porphyrin dissolved in dry pyridine was treated with thionyl chloride, and the mixture was stirred for 30 minutes at 50 °C. *N*-hydroxysuccinimide was subsequently added to the mixture, and the reaction was continued for a further 3 hours. Once worked-up, 5-[4-(succinimide-*N*-oxycarbonyl)phenyl]-10,15,20-tri-(4-pyridyl)porphyrin was isolated in 91 % yield. The porphyrin bearing the activated ester was then used to synthesise a porphyrin-polylysine conjugate.

3.5 Synthetic strategy involving addition of SMCC to 5-(4-aminophenyl)-10,15,20-tri-(4-pyridyl)porphyrin (17)

Previous experimental experience led to selection of the Adler-Longo method,[114] for porphyrin synthesis. The overall aim was to produce a porphyrin bearing two different functional groups in the *meso*-positions; one functional group facilitating the addition of a linker; eventually terminating in a maleimide group, with the remaining *meso*-positions occupied by functionalities, which upon further modification, could provide the hydrophilic character. It was decided that pyridyl groups, which upon methylation would provide hydrophilicity, with an amino group present in the remaining *meso*-position, which could be further modified with SMCC, leading to the introduction of a short linker, terminating with a maleimide bioconjugatable group. The amino group had to be protected during porphyrin formation, and literature suggested that the highest yielding deprotection was the acid hydrolysis of the acetamido group. Therefore, the target porphyrin became the product of the mixed condensation between 4-acetamido-benzaldehyde and 4-pyridinecarboxaldehyde, with pyrrole. The overall synthetic strategy is illustrated in Scheme 46.

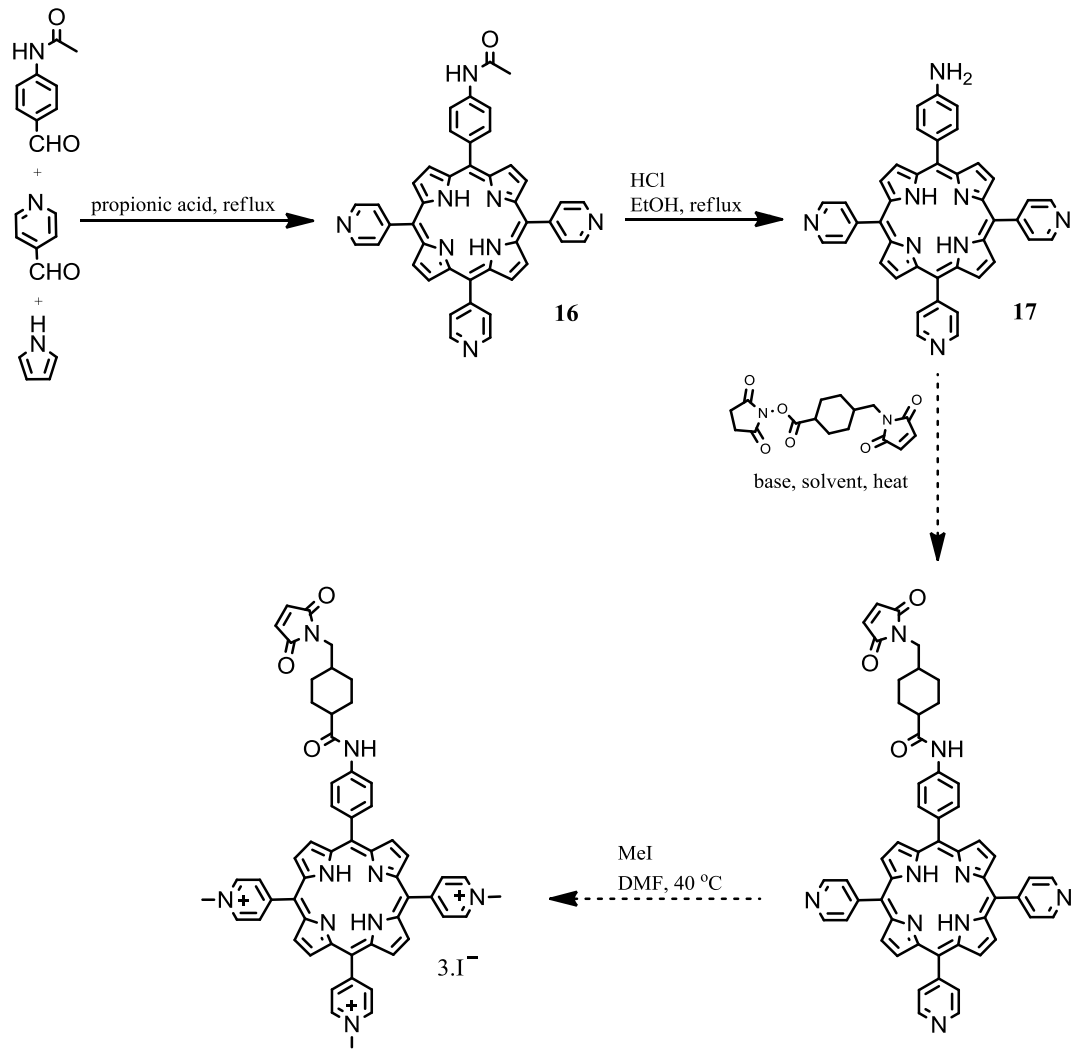

Scheme 46: Synthetic strategy involving addition of SMCC to 5-(4-aminophenyl)-10,15,20-tri-(4-pyridyl)porphyrin.

3.5.1 Attempted addition of SMCC to 5-(4-aminophenyl)-10,15,20-tri-(4-pyridyl)porphyrin (17)

Following a known procedure,[68] 5-(4-acetamidophenyl)-10,15,20-tri-(4-pyridyl)porphyrin (**16**) was synthesised with a yield of 5 %. Characterisation studies were in agreement with the reported data, although the ^{13}C NMR spectrum for **16** had 16 signals when theoretically 23 signals should be observed.

The acidic hydrolysis of the acetamido group was firstly performed by treating **16** with a 5 M hydrochloric acid solution, at reflux for 3 hours, as previously described.[68] Following removal of hydrochloric acid, the crude product was dissolved in a solution of triethylamine in dichloromethane, to neutralise the residual hydrochloric acid and deprotonate the porphyrins inner nitrogens. Following chromatographic separation and precipitation from chloroform by the addition of methanol, **17** was isolated with a yield of 82 %. The yield was lower than the published yield of 90 %, thus the hydrolysis was performed using a slightly modified procedure,[169] with **16** being dissolved in ethanol prior to the acidic treatment, affording **17** with a yield of 91 %. The ^{1}H NMR spectrum of **17** exhibited no singlet at 2.35 ppm corresponding to the methyl protons, however no signal for the newly formed amino protons was observed, possibly due to proton-deuterium exchange. The mass spectrum gave the expected 633 *m/z* $(M+H)^+$ peak, therefore there was sufficient evidence that the reaction had occurred as postulated.

The addition of SMCC to **17** was then attempted by dissolving the two reagents in anhydrous dichloromethane, and the resulting solution was stirred at 30 ^{o}C for 2 hours. TLC analysis (silica, eluent: 10 % methanol/dichloromethane) of the reaction mixture showed only the presence of **17**, therefore a drop of diisopropylethylamine was added to ensure the amine was not protonated. After 16 hours, the TLC of the reaction mixture showed that **17** remained unchanged, therefore the reaction mixture was discarded. The reaction was repeated, employing dry chloroform, and with the addition of portions of diisopropylamine successively after the SMCC. The reaction mixture was monitored over a 6 day period with no apparent change to **17**. The reaction was also attempted in anhydrous pyridine, with no base being required, due to the basicity of the solvent. The reaction was monitored over a 4 day period by TLC, with only **17** being detected.

It was hypothesised that the reactions had failed because the amino groups lone pair of electrons had delocalised into the phenyl ring, impairing nucleophilicity.

3.6 Synthetic strategy involving synthesis of porphyrin bearing an alkyl chain terminating with a maleimide bioconjugatable group.

Since the addition of SMCC to the amino porphyrin **17** was unsuccessful, the synthetic strategy required modification, with the aim of producing a porphyrin bearing a more nucleophilic aliphatic amino functionality, enabling the reaction with the activated ester of SMCC. Due to the low reactivity of the aromatic amino group of **17**, it was postulated that if the porphyrin bore a different functionality, which facilitated a reaction with a aliphatic linker, terminating with an amino group, the reaction with SMCC could then occur. A porphyrin bearing a carboxyl and pyridyl groups, was selected for further modification, hence the target porphyrin was a product of the mixed condensation between 4-carboxybenzaldehyde, 4-pyridinecarboxaldehyde, with pyrrole. The literature suggested that coupling reagents such as DCC,[166] EDC,[165] and carbonyldiimidazole[162] can be employed for coupling carboxyl porphyrins bearing pyridyl groups to derivatives bearing amino groups, with some reasonable yields being reported. The other predominant type of reaction concerning carboxyl porphyrins involved converting the carboxyl group into an activated *N*-hydroxysuccinimide ester, facilitating reactions with nucleophilic species, such as amino groups.[167,168] There wasn't a preferential reaction involving carboxyl porphyrins, but since the synthesis of 5-[4-(succinimidyl-*N*-oxycarbonyl)phenyl]-10,15,20-tri-(4-pyridyl)porphyrin, has been reported,[168] and a reaction between a diamine and the activated ester had also being established,[167] the activated ester strategy was selected. The next requisite was for the porphyrin to posses a terminal 1^{o} amino group, therefore *N*-Boc-1,6-diaminohexane hydrochloride was chosen to react with the activated ester. One of the amino groups was Boc protected, to prevent the porphyrin reacting at both ends of the alkyl linker, leading to the formation of a porphyrin dimer. Once the Boc group had been cleaved under acidic conditions, a subsequent reaction with SMCC resulted in introduction of the maleimide functionality. The final step of the reaction sequence involved quatenisation of the pyridyl groups to induce water-solubility, as illustrated in Scheme 47.

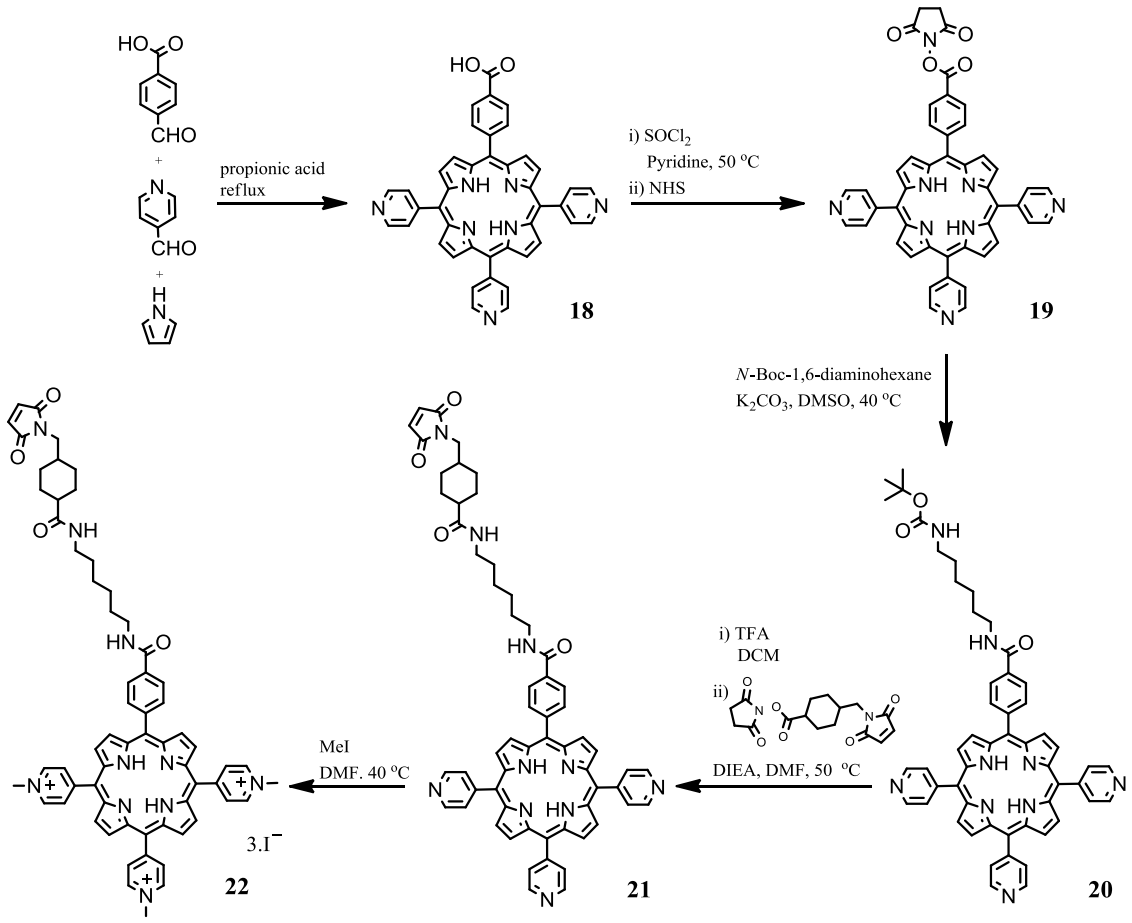

Scheme 47: Synthesis of hydrophilic porphyrin bearing an alkyl chain terminating with a maleimide group.

3.6.1 Synthesis of 5-(4-((6-*tert*-butylcarbamate)hexyl-1-amino-*N*-carbonyl)phenyl)10,15,20-tri-(4-pyridyl)porphyrin (20)

Following a literature procedure,[170] **18** was isolated in 6 % yield. The ^{1}H NMR of **18** was similar to the reported data, except the signal for the β and 10,15,20-*meta*-aromatic protons had merged into a multiplet at 8.74-9.09 ppm, which integrated to 14, and the signal corresponding to the carboxyl proton was not observed.

Using a reported method,[168] **19** was synthesised in a 90 % yield. The ^{1}H NMR spectrum of **19** was more resolved than the literature data, with the signal for the 10,15,20-aromatic protons appearing as double doublets at 8.17 ppm and 9.06 ppm, and the signal for the β protons splitting into 2 signals; one doublet corresponding to 2 β-protons at 8.85 ppm, with the remaining 6 β-protons appearing as a multiplet at 8.86-8.90 ppm.

Both **19** and *N*-Boc-1,6-diaminohexane hydrochloride were soluble in dimethylsulfoxide, therefore it was deemed a suitable solvent for the synthesis of **20**.

Furthermore, the dimethylsulfoxide solvent had to be dry, to avoid hydrolysis of the porphyrin's activated ester. The *N*-Boc-1,6-diaminohexane hydrochloride available amino group was in a protonated form with a chloride counter ion, thus to ensure the amino group was sufficiently nucleophilic towards the activated ester, the reaction was performed in the presence of base. Potassium carbonate was soluble in dimethylsulfoxide and was therefore selected for the reaction. Using a modified method,[167] compound **20** was synthesised multiple times, using slightly different reaction conditions, as illustrated in Table 1. The synthesis of **20** was initially achieved by dissolving **19**, *N*-Boc-1,6-diaminohexane hydrochloride (2.5 equivalents) and potassium carbonate (4.9 equivalents) in anhydrous dimethylsulfoxide (10 mL), and stirring the reaction mixture at 40 °C, while protected against light and moisture. The reaction was monitored by TLC (silica, eluent: 10 % methanol/dichloromethane), and after 40 minutes complete consumption of **19** was observed, with the development of a more polar UV-active fraction corresponding to **20**. The product was extracted into dichloromethane and washed with copious amounts of water to remove the excess *N*-Boc-1,6-diaminohexane hydrochloride, potassium carbonate, the 1-hydroxypyrrolidine-2,5-dione by-product and dimethylsulfoxide. Anhydrous sodium sulphate was added to the organic layer, to remove residual water, and the filtrate was collected. The solvent was removed *in vacuo*, and the crude product was chromatographically separated (silica, eluent: 6 % methanol/dichloromethane) with **20** isolated in 57 % yield after precipitation from dichloromethane by the addition of hexane. The yield of 57 % seemed reasonable, therefore the reaction was repeated in the same manner, however a lower yield was obtained (49 %) and when the reaction was scaled up, using 98 mg of **19,** the yield diminished further, with **20** being produced in 40 % yield. The lower yield obtained for the scaled-up reaction meant that subsequent reactions were done using approximately 50 mg of **19**. The reaction was repeated using a lower volume of dimethylsulfoxide, thus the concentration of **19** was increased to 6.8 mg/mL, from 5.9 mg/mL for the initial reactions.

As a large excess of base was used for the initial reactions, the reaction was performed using a lower amount of potassium carbonate (4.1 equivalents), which resulted in **20** being produced in 46 % yield. Reducing the base, reduced the yield of **20**, therefore the reaction was repeated using a higher amount of both potassium carbonate (6.9 equivalents) and *N*-Boc-1,6-diaminohexane hydrochloride (2.8 equivalents), furnishing **20** in 84 % yield. For the conditions evaluated, the quantity of base present in the reaction mixture seemed to have the most dramatic effect on the yield of **20**. The

reaction was repeated in a similar manner, using a slightly lower amount of *N*-Boc-1,6-diaminohexane hydrochloride (2.5 equivalents) and potassium carbonate (6.3 equivalents), affording **20** in 82 % yield.

19	**DMSO**	***N*-Boc-1,6-diaminohexane hydrochloride**	**Potassium carbonate**	**20**
59 mg, 78 µmol	10 mL	50 mg, 197 µmol, 2.5 equiv.	53 mg, 383 µmol, 4.9 equiv.	38 mg, 57 %
59 mg, 78 µmol	10 m	50 mg, 197 µmol, 2.5 equiv.	53 mg, 383 µmol, 4.9 equiv.	33 mg, 49 %
98 mg, 129 µmol	18 mL	82 mg, 324 µmol, 2.5 equiv.	89 mg, 644 µmol, 5 equiv.	45 mg, 40 %
68 mg, 90 µmol	10 mL	57 mg, 225 µmol, 2.5 equiv.	62 mg, 449 µmol, 5 equiv.	39 mg, 50 %
68 mg, 90 µmol	10 mL	57 mg, 225 µmol, 2.5 equiv.	62 mg, 449 µmol, 5 equiv.	47 mg, 61 %
58 mg, 76 µmol	10 mL	50 mg, 197 µmol, 2.5 equiv.	43 mg, 311 µmol, 4.1 equiv.	30 mg, 46 %
47 mg, 61 µmol	8 mL	43 mg, 170 µmol, 2.8 equiv.	58 mg, 420 µmol, 6.9 equiv.	Combined with below reaction
47 mg, 61 µmol	8 mL	43 mg, 170 µmol, 2.8 equiv.	58 mg, 420 µmol, 6.9 equiv.	88 mg, 84 %
51 mg, 67 µmol	9 mL	43 mg, 170 µmol, 2.5 equiv.	58 mg, 420 µmol, 6.3 equiv.	47 mg, 82 %

Table 1: Reaction conditions used for the synthesis of **20**.

The relevant sections of the ^{1}H NMR spectrum for **20,** is shown in Figure 17. The assignment of the signals was achieved using a combination of ^{13}C NMR, 2D COSY and CH-correlation experiments. The assignment of the signals in the alkyl region was achieved by evaluating the 2D COSY experiment, depicted in Figure 18.

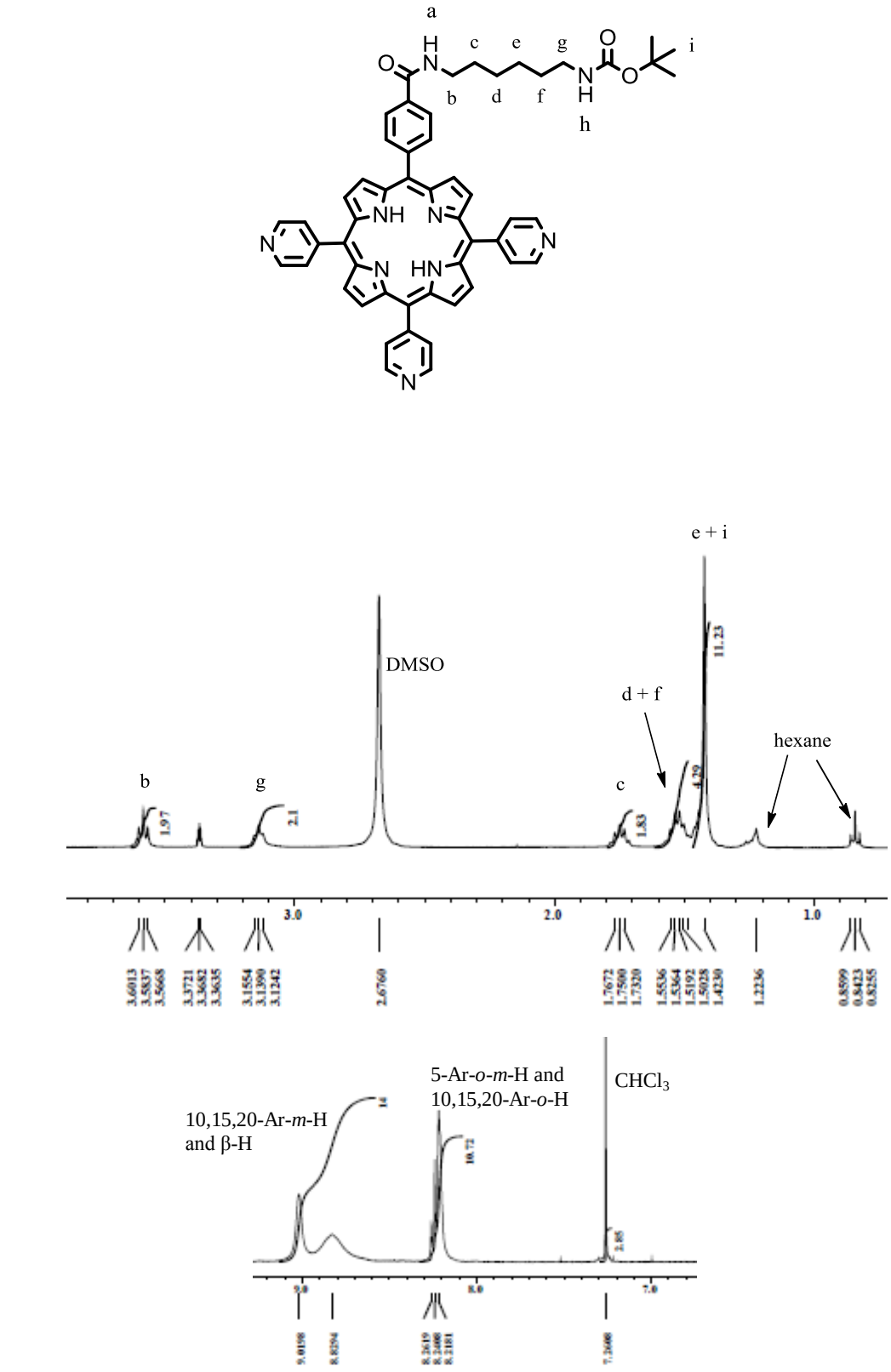

Figure 17: ^{1}H NMR spectrum of **20**.

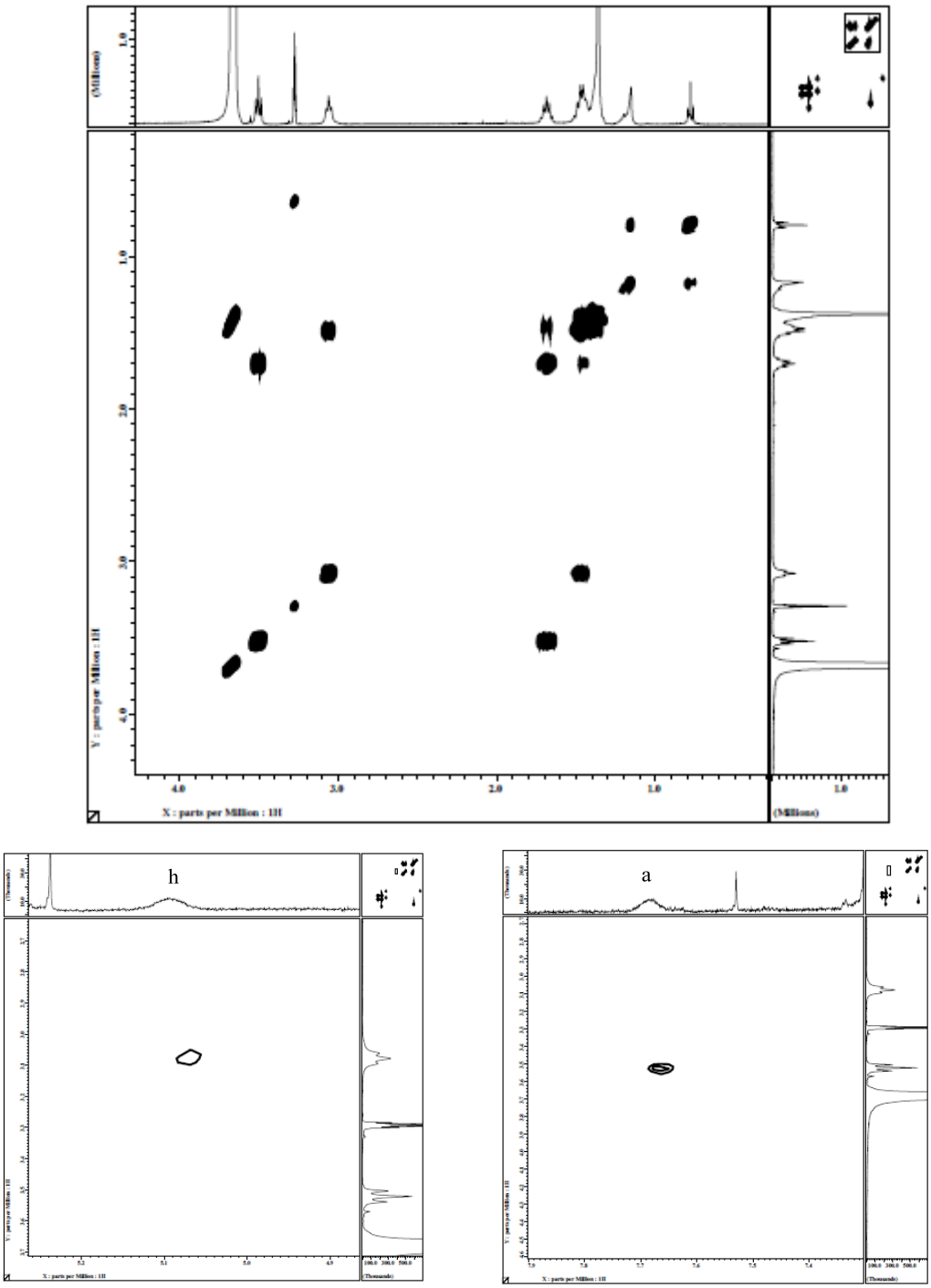

Figure 18: ^{1}H NMR COSY of **20**.

The signal at 1.37-1.47 ppm which integrates to 11, is in the region which would be expected for the *tert*-butyl protons of the Boc group, however the 2D COSY shows coupling with a signal at 1.48-1.58 ppm, and theoretically the Boc protons should not couple with any other proton environment. Therefore the peak at 1.37-1.47 ppm corresponds to the 9 protons of the *tert*-butyl region of the Boc group (**i**), and 2 protons of a CH_2, neighbouring a proton environment which produces the signal at 1.48-1.58

ppm. The multiplet signal at 1.48-1.58 ppm appears to couple with 3 other signals; the multiplet at 1.37-1.47 ppm, the quintet at 1.75 ppm and the multiplet at 3,06-3.18 ppm, therefore that peak must be from 2 different proton environments. As the multiplet at 1.48-1.58 ppm integrates to 4, and couples to 3 other signals, and the multiplet at 1.37-1.47 ppm only couples to 1 signal, the CH_2 from the multiplet at 1.37-1.47 ppm must be in-between 2 CH_2 environments from the signal at 1.48-1.58 ppm. The signal at 1.75 ppm integrates to 2, and appears as a quintet, thus it must be from a CH_2 located in the middle of the hexyl chain. The 2D COSY analysis showed that the quintet at 1.75 ppm couples with the triplet at 3.58 ppm, and as none of the amino protons were observed for that particular ^{1}H NMR analysis, the peak at 3.58 ppm was assigned proton environment (**b**). Once (**b**) was determined, the other signals were subsequently assigned; the quintet at 1.75 ppm (**c**), the multiplet at 1.48-1.58 ppm (**d**) and (**f**), and the multiplet at 1.37-1.47 ppm (**i**) and (**e**). The remaining multiplet signal in the alkyl region at 3.06-3.18 ppm, integrated to 2, and coupled with proton environment (**f**), therefore it was assigned (**g**). The ^{1}H NMR and 2D COSY experiments were repeated, to obtain amino proton signals, with the 2D COSY shown in Figure 18. The signal for proton environment (**b**) couples to a broad singlet at 7.68 ppm, which was assigned amino (**a**), and peak (**g**) couples with a broad singlet at 5.09 ppm, which was attributed to amino group (**h**). Although not well defined, the signals in the aromatic region integrated correctly and were subsequently assigned; a multiplet at 8.11-8.29 ppm corresponding to the 5-aromatic and 10,15,20-*ortho*-aromatic protons and another multiplet at 8.63-9.08 attributed to the β and10,15,20-*meta*-aromatic protons. The mass spectrum gave the expected 860.4029 *m/z* peak due to the $(M+H)^+$ ion, so there was sufficient evidence that **20** had been produced.

3.6.2 Synthesis of 5-(4-(6-(4-(*N*-maleimidomethyl)cyclohexane-1-amido)hexyl-1-amino-*N*-carbonyl)phenyl)-10,15,20-tri-(4-pyridyl)porphyrin (21)

The acid hydrolysis of the Boc protecting group of **20** was attempted using a modified published procedure.[157] A solution of **20** dissolved in anhydrous dichloromethane was treated with trifluoroacetic acid for 50 minutes at room temperature, until complete consumption of **20** had occurred as indicated by TLC (silica, eluent: 10 % methanol/chloroform). The resulting mixture was poured onto an ice cooled aqueous solution of sodium hydrogen carbonate, to neutralise the trifluoroacetic acid; a colour change from green to red was observed in the organic layer, due to deprotonation of the porphyrin inner nitrogens. The product was extracted into dichloromethane, and the organic layer was washed with water to remove residual sodium hydrogen carbonate and dried over anhydrous sodium sulphate to remove residual water. Initial chromatographic separation was attempted (silica, eluent: 10 % methanol/dichloromethane), which resulted in the porphyrinic product being retained on top of the silica; a result of the extra polarity provided by the amino functionality, and subsequent ionic interactions with the polar hydroxyl groups from the silica gel. Therefore flash chromatography was attempted using neutral alumina and 10 % methanol/dichloromethane eluent. Once the relevant fraction had been collected, the TLC of the product revealed that decomposition had occurred, and the ^{1}H NMR of the suspected deprotected **20** was inconclusive. Isolation of the amino porphyrin was also attempted using alumina coated preparative TLC plates, but decomposition of the product was again observed. Because isolation of deprotected **20** was problematic and the TLC of the reaction mixture indicated that complete amino deprotection had been achieved, the reaction was repeated, without the amino porphyrin been isolated and the crude intermediate was used in the next synthetic step.

Reaction of SMCC with the crude amino porphyrin was achieved following a modified published procedure.[102] A solution of the crude amino-porphyrin dissolved in anhydrous dimethylformamide was treated with SMCC (1.2 equivalents relative to **20**) in the presence of diisopropylethylamine (2.2 equivalents relative to SMCC). The resulting mixture was stirred for 50 minutes at ambient temperature, while protected against moisture and light until the composition of the mixture exhibited no further change, as shown by TLC (silica, eluent: 10 % methanol/dichloromethane) with the presence of both the amino porphyrin intermediate and **21** being detected. An ice cooled solution of diethyl ether and hexane was added to the reaction mixture to initiate precipitation of

the crude product, which was subsequently chromatographically separated (silica, eluent: 5 % methanol/chloroform). The relevant fraction was collected, with **21** isolated in 36 %, after precipitation from hexane over dichloromethane. The reaction yield was quite low, with the TLC of the reaction mixture indicating that not all of the amino-porphyrin had reacted with the SMCC. Therefore it was postulated that a proportion of the amino groups were in a protonated form, hence were not nucleophilic towards the activated ester of SMCC. Therefore the reaction was repeated using 5 equivalents of diisopropylethylamine, to ensure complete deprotonation of the ammonium groups. After the reaction mixture had been stirred at room temperature for 50 minutes, the TLC of the reaction mixture showed almost complete consumption of the amino porphyrin intermediate, and following work-up, **21** was isolated in 85 %.

The important regions of the ^{1}H NMR spectrum for **21**, are shown in Figure 19. Despite multiple attempts, ^{1}H NMR spectrum where all the protons in the alkyl region were accounted for was not achieved. As the solvent peaks were prominent, it was possible that signals for proton environments corresponding to the hexyl chain and/or the cyclohexane ring, were beneath solvent signals, however drying the sample led to decomposition. A 2D COSY experiment was performed, however only partial assignment of the signals could be made due the complex nature of the spectrum and the presence of solvent peaks, and not all of the protons in the alkyl region were accounted for. Importantly, the alkyl region of the ^{1}H NMR spectrum for **21** does not show the presence of the *tert*-butyl protons which were detected for **20** at 1.37-1.47 ppm. The aromatic region of the spectra provided conclusive evidence that **21** had been synthesised as envisaged, with the detection of a singlet at 6.62 ppm due to the maleimide protons. All the other peaks in the aromatic region were accounted for and assigned. The HRMS gave the expected 979 *m/z* peak due to the $(M + H)^{+}$ ion, therefore it was concluded that **21** had been synthesised.

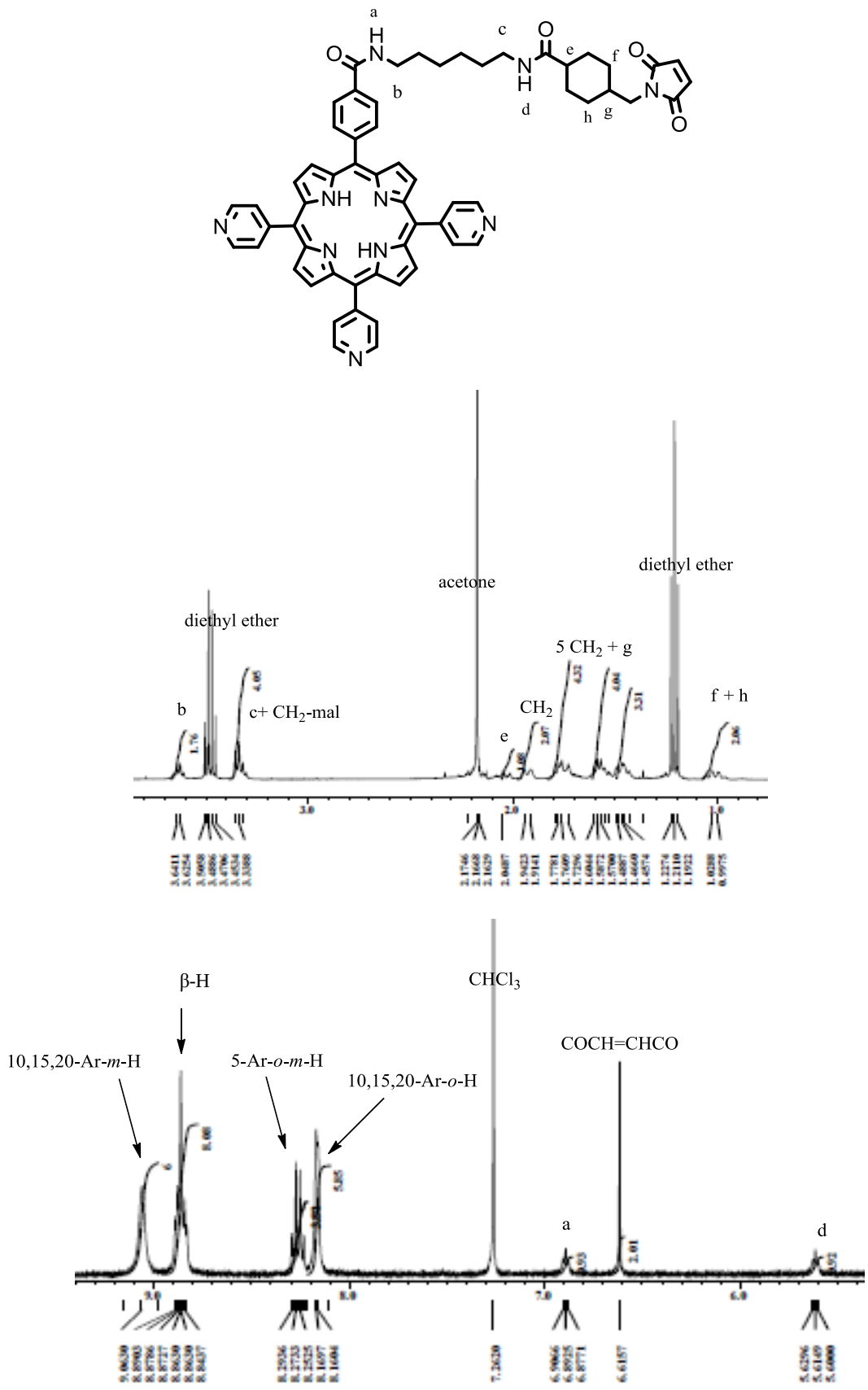

Figure 19: ^{1}H NMR spectrum of **21**.

3.6.3 Synthesis of 5-(4-(6-(4-(*N*-maleimidomethyl)cyclohexane-1-amido)hexyl-1-amino-*N*-carbonyl)phenyl)-10,15,20-tri-(4-*N*-methyl-pyridyniumyl)porphyrin triiodide (22)

Following a published method,[68] **21** was quaternised via treatment with methyl iodide. Due to the volatile and harmful nature of methyl iodide, the reaction was performed in a vessel fitted with a reflux condenser which had tubing feeding into a triethylamine solution, in order to destroy any methyl iodide which could evaporate from the reaction mixture at 40 °C. A solution of **21** dissolved in anhydrous dimethylformamide was treated with a large excess of methyl iodide and the resulting mixture was stirred for 4 hours at 40 °C. The reaction mixture was then cooled to ambient temperature over ice, with the addition of an ice cooled mixture of diethyl ether and hexane initiating precipitation of the product. The precipitate was collected, and the crude product was washed with warm diethyl ether to remove any residual dimethylformamide and methyl iodide, furnishing **22** in 80 % yield.

The relevant regions of the ^{1}H NMR spectrum for **22,** is shown in Figure 20. A combination of 2D COSY, C-H correlation and HMBC experiments were used for assignment of the aliphatic signals. The two singlets at 4.72 ppm and 4.73 ppm, which gave a combined integral of 9, indicated that methylation of the pyridyl groups had occurred. The maleimide group, which produces a singlet at 6.97 ppm, was present, indicating that the maleimide bioconjugatable group had remained unaffected under the methylation conditions.

The mass spectrum of **22**, produced a 341 *m/z* signal which corresponded to the $(M)^{3+}$ ion. Therefore there was sufficient evidence that **21** had been successfully quaternised, affording the target photosensitiser (**22**).

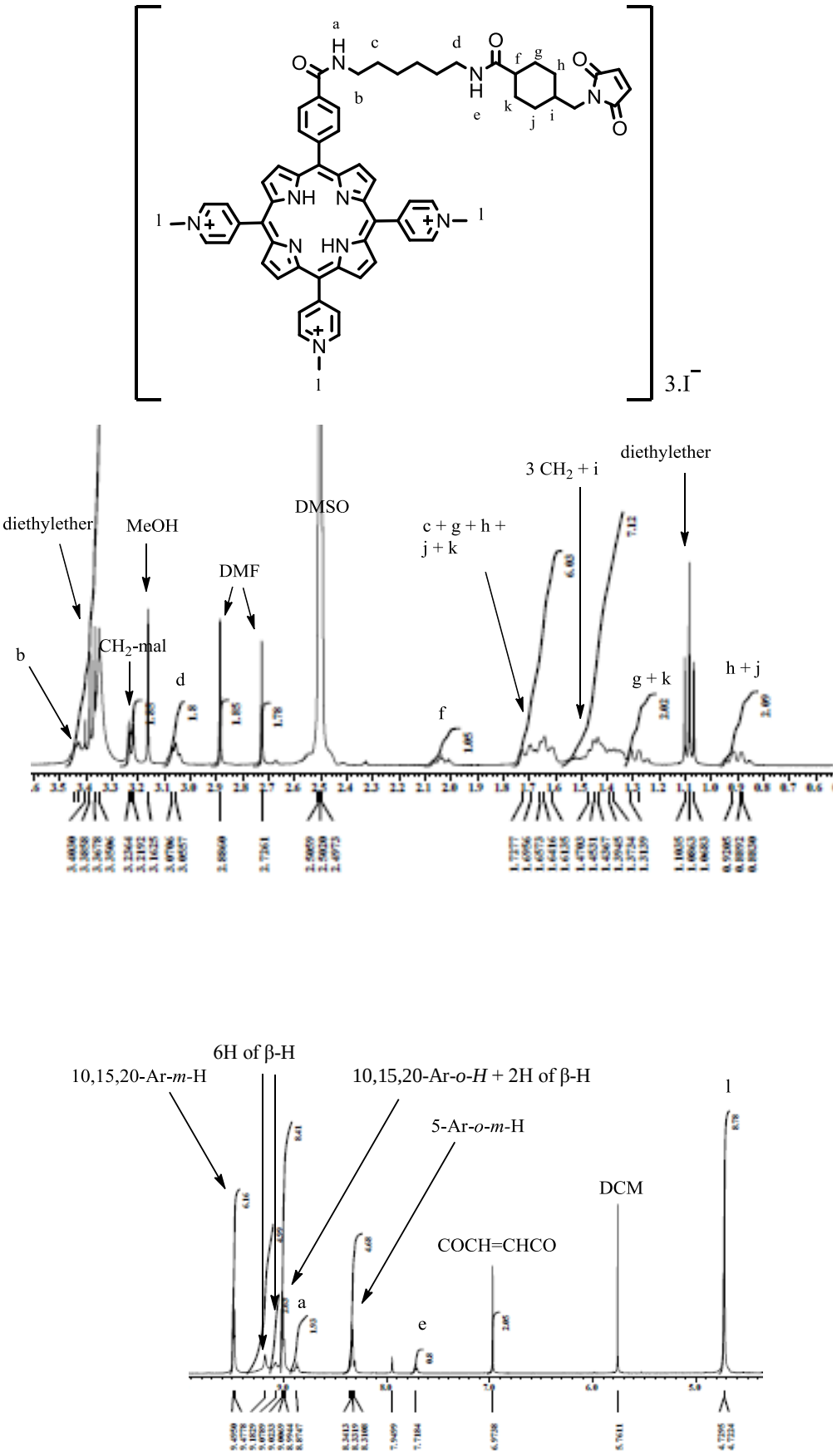

Figure 20: ^{1}H NMR spectrum of **22**.

3.7 Synthesis of photosensitisers PS3 and PS4

Photosensitiser **PS3** was synthesised by a literature method.[168] During this research project, Alonso *et al*.,[144] synthesised **PS4**, as depicted in Scheme 48. A solution of 5-4-amino)-10,15,20-tri-(4-pyridyl)porphyrin in nitrobenzene, was treated with maleic anhydride, and the subsequent cyclodehydration of the maleic acid intermediate resulted in the formation of the single maleimide bioconjugatable group. Quaternisation of the pyridyl groups rendered the porphyrin fully water soluble, facilitating the conjugation to the antibody in aqueous media.

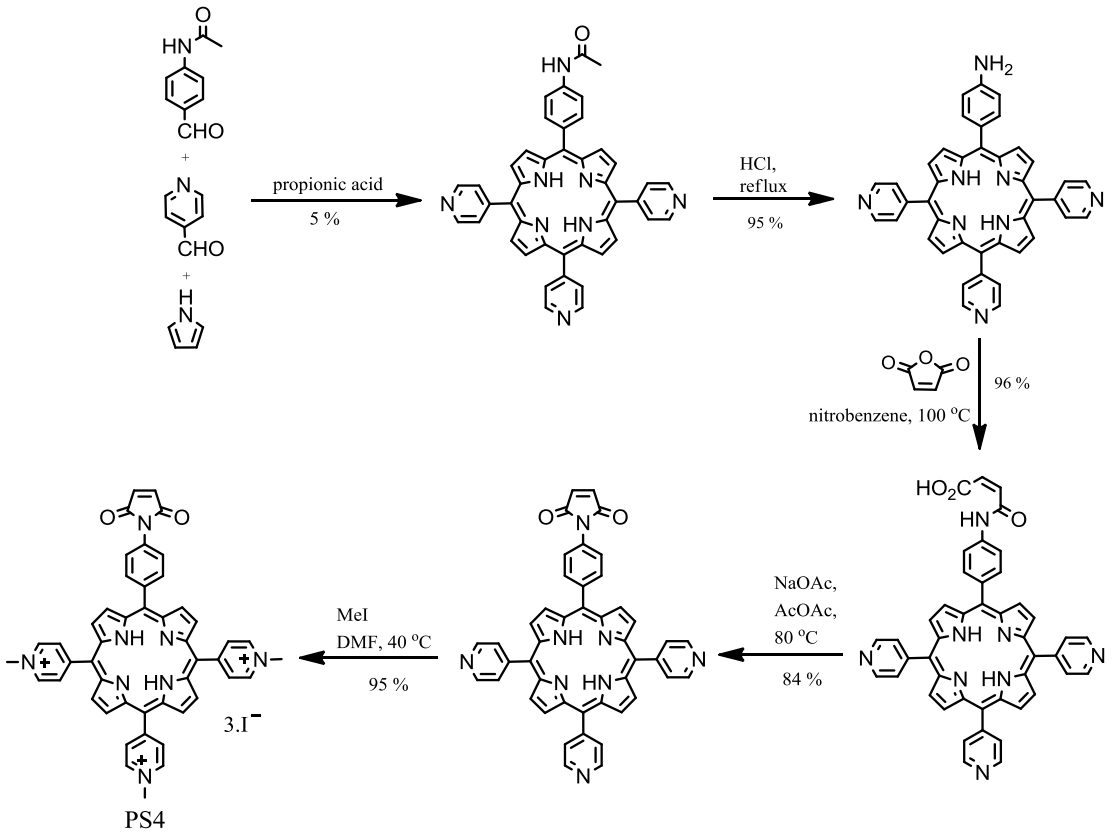

Scheme 48: Synthesis of 5-(4-maleimidophenyl)-10,15,20-tri-(4-*N*-methyl-pyridiniumyl)porphyrin triiodide (**PS4**).[144]

3.8 Photoimmunoconjugates

3.8.1 Photoimmunoconjugate preparation

The water-soluble porphyrins bearing either *N*-hydroxysuccinimide (**PS3**) or maleimide (**PS4** and **22**) bioconjugatable groups (Figure 21) , were investigated as components for the formation of photoimmunoconjugates of SIP(L19) in collaboration with the research group of Professor Dario Neri at the Swiss Federal Institute (ETH) based in Zurich. The synthesis of the immunoconjugates and subsequent biological studies were conducted by Alessandro Palumbo and Corinne Hutter, under the supervision of Professor Dario Neri.

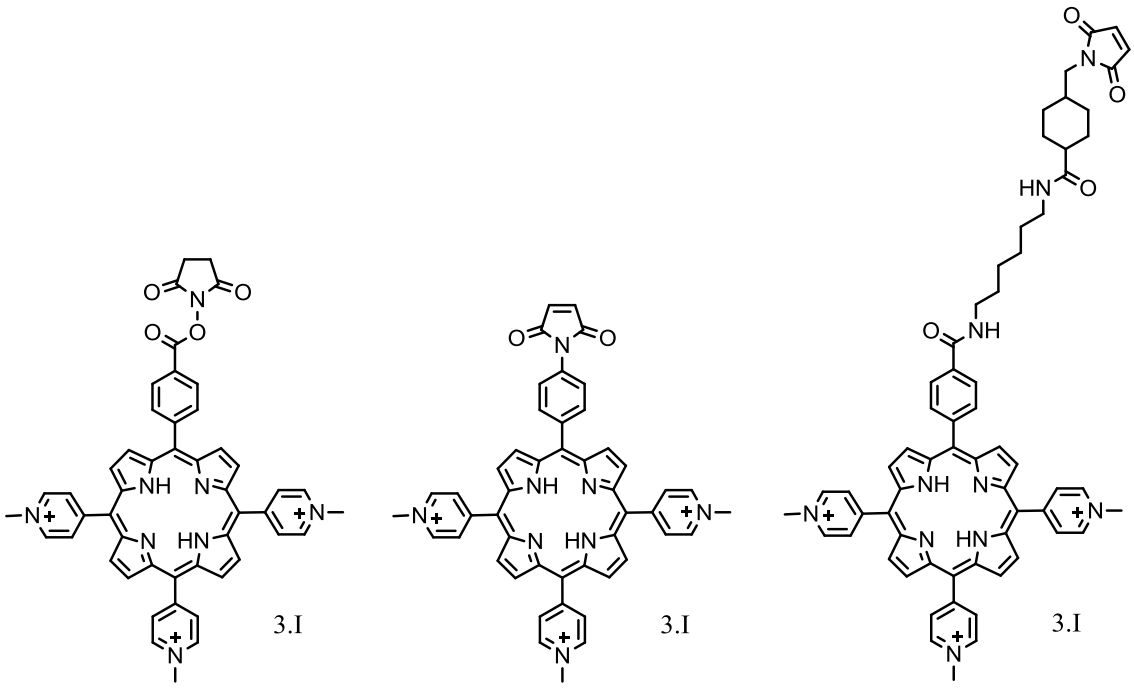

PS3 **PS4** **22**

Figure 21: Hydrophilic porphyrins **PS3**, **PS4** and **22**.

3.8.1 Conjugation to SIP(L19)

A solution of SIP(L19) in PBS (pH 7.4) was treated with a 30-fold excess of the mild reducing agent: TCEP to reduce the cysteine residues in the c-terminal region while leaving the intra-domain disulphide bridges intact; thus enabling site specific coupling. The resulting mixture was incubated for 12 hours at 4 °C. A 40 molar excess of the photosensitiser (**PS3**, **PS4** or **22**) dissolved in dimethylsulfoxide was added to the reduced SIP(L19), and the resulting mixture was incubated for 3 hours, at ambient temperature, with gentle shaking. The photoimmunoconjugate was purified by passing the crude mixture through a PD-10 gel permeation column, and then the relevant fraction was dialysed against PBS (pH 7.4) at 4 °C.

3.8.2 Photoimmunoconjugate characterisation

To ensure that covalent coupling between the photosensitiser and antibody had occurred, the photoimmunoconjugate was analysed by SDS-PAGE.

SDS-PAGE is an electrophoresis separation technique where molecules, within a sodium dodecyl-sulphate (SDS) solution, migrate on a polyacrylamide gel solid support, with the rate of migration dependent on the size of the molecule and the electronic field strength applied. SDS is an anionic detergent which binds to proteins, causing them to denature, so when a protein solution is charged on to the polyacrylamide gel and the electric field is applied, different proteins separate based on molecular mass.[171] The SDS-PAGE of photoimmunoconjugates **PS4**-SIP(L19) and **22**-SIP(L19) is shown in Figure 22. Visualisation of the antibody component on the polyacrylamide gel was achieved via staining with coomassie blue. The comassie blue dye binds to proteins mainly via electrostatic interactions between the dyes sulphonate groups, and the proteins protonated amino groups; with hydrophobic interactions, hydrogen bonding, van der Waals forces and electrostatic interactions also contributing to the dye-protein interaction.[172] The photosensitiser moiety was detected more simply by fluorescence imaging.

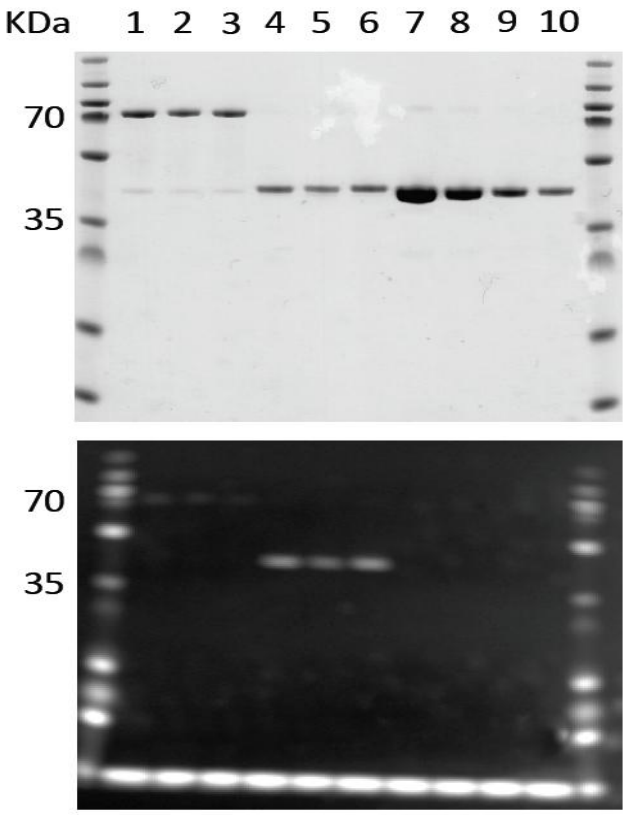

Lanes 1 and 2: control reactions involving **PS4** and **22** with SIP(L19) which has not been reduced. Lanes 4 and 5: **PS4** and **22** coupling with reduced SIP(L19). Lanes 7-10: SIP(L19) reference standards (0.8 mgL^{-1}, 0.4 mgL^{-1}, 0.2 mgL^{-1} and 0.1 mgL^{-1}).
A: Stained with coomassie blue. B: Fluorescence imaging using a Cy5 filter lamp
Figure 22: SDS-PAGE of SIP(L19), **PS4**-SIP(L19) and **22**- SIP(L19).

The purpose of the control reactions was to evaluate whether the photosensitisers coupled to the SIP(L19), when the cysteine residues were unavailable. Lanes 1 and 2 did not produce a fluorescent signal, therefore the photosensitiser had not coupled to the non-reduced SIP(L19). Furthermore, when stained with coomassie blue, lanes 1 and 2 both showed that the SIP(L19) homodimer, had a molecular weight of ≈ 80 KDa. Lanes 4 and 5, which were stained with coomassie blue, shows that SDS-PAGE analysis detects the reduced SIP(L19) in the monomeric form, and that complete reduction of SIP(L19) had been achieved. The fluorescent signals produced by lanes 4 and 5, indicated that the photosensitisers had covalently coupled with the reduced antibody. The fluorescent signal at the base line of the polyacrylamide gel plate was due to the presence of bromophenol blue within the SDS loading buffer.

The SDS-PAGE analysis of **PS3**-SIP(L19) (data not shown), indicated that the photosensitiser covalently coupled to the antibody under both reducing and non-reducing conditions, indicating that coupling had occurred through lysine residues.

Under optimal conditions exactly two photosensitisers should couple to each intact SIP(L19), corresponding to the two available thiol reactive sites. To test the hypothesis, the photosensitiser: antibody loading ratio was calculated using both UV-visible spectroscopy and MALDI-TOF/TOF techniques. For the **22**-SIP(L19) immunoconjugate: the UV-visible spectroscopy method for estimating the loading ratio involved producing a conjugate sample, which gave an absorbance of 1.4 units at 280 nm, as it is known that the SIP is at a 1 mg/mL concentration at that reading. The conjugates absorbance was then measured at 424 nm. The porphyrin's extinction coefficient at 424 nm and the recorded absorbance were then used to calculate the concentration of the porphyrin in the conjugate sample using Beer-Lamberts law. The concentration of the porphyrin moiety was divided by the concentration of the antibody moiety, to give a photosensitiser:antibody loading ratio of 0.9. The theoretical photosensitiser:antibody loading ratio should be 2, because the reduced SIP(L19) has two thiol groups available for conjugations, therefore a MALDI-TOF/TOF technique was used to confirm the estimated loading ratio, shown in Figure 23.

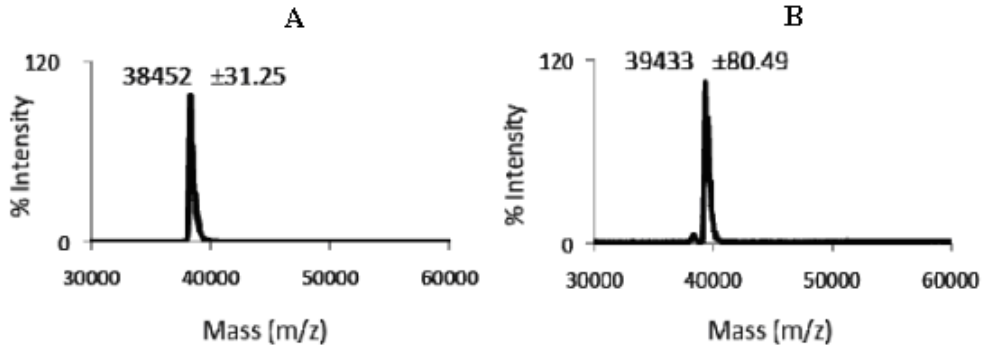

Figure 23: MALDI-TOF/TOF spectra for (A) SIP(L19), (B) **22**-SIP(L19).

The intact SIP(L19) is a homodimer which is covalently linked through a disulfide bond and has a molecular weight of approximately 80 KDa. The MALDI-TOF/TOF spectrum for the SIP(L19), prior to reduction, shows a signal of 38452 ± 31.25 *m/z*, which is equivalent to a molecular weight of 38 KDa, therefore the MALDI-TOF/TOF analysis detects the SIP(L19) as the $(M)^{2+}$ ion or as two monomer fragments. The MALDI-TOF/TOF of **22**-SIP(L19) shows a signal of 39433 ± 80.49 *m/z*. If the mass signal of the

antibody is subtracted from the mass signal for the conjugate, the mass contribution from the photosensitiser is calculated:

$$\begin{aligned}\text{Photosensitiser mass} &= \text{Conjugate's mass} - \text{Antibody's mass} \\ &= 39433 \pm 80.49\ m/z - 38452 \pm 31.25\ m/z \\ &= 981 \pm 111.74\ m/z\end{aligned}$$

Compound **22** has a molecular weight of 1404 $gmol^{-1}$, however mass spectrometry does not detect the iodide counter ions, giving **22** an observed molecular weight of 1023 $gmol^{-1}$. The calculated photosensitiser mass, with the experimental error, showed that a single photosensitiser had coupled to the monomeric SIP(L19), thus the photosensitiser:antibody loading ratio was 2:1 for the SIP(L19) in the dimeric form.

The loading ratios were calculated in a similar manner for **PS3**-SIP(L19) and **PS4**-SIP(L19). UV-visible spectroscopy was used to estimate the loading ratios for the other immunoconjugates, 1.75 for **PS3**-SIP(L19) and 0.76 for **PS4**-SIP(L19), however the MALDI-TOF/TOF analysis indicated that a loading ratio of approximately 2 was obtained for both immunoconjugates.

The conjugate was then analysed by size exclusion chromatography to assess whether once conjugated, the dimeric nature of SIP(L19) was retained under an aqueous environment, despite the absence of the disulfide linkage. The size exclusion chromatographic profiles of SIP(L19) and **22**-SIP(L19), illustrated in Figure 24, were very similar, indicating that the conjugates antibody moiety was in a dimeric form.

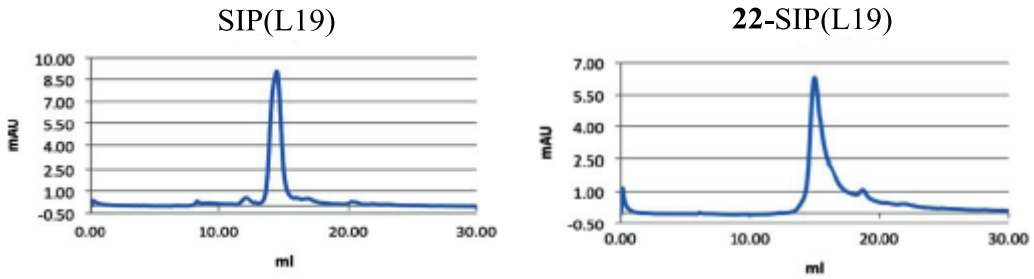

Figure 24: Size exclusion chromatography profile of SIP(L19) and **22**-SIP(L19).

Similar size exclusion chromatography profiles were observed for **PS3**-SIP(L19) and **PS4**-SIP(L19).

3.8.3 Photoimmunoconjugate Immunoreactivity

BIAcore analysis uses surface plasmon resonance (SPR) biosensitisers to evaluate, in real time, interactions of binding biomolecules. The biosensor chip possesses one of the biomolecules immobilised on its surface, with a solution of the other biomolecule being passed over the chip. The SPR detector can monitor the amount of complex formed between the two biomolecules by measuring the change of refractive index of the solvent near the sensors surface, caused by the association and dissociation of the complex.[173,174]

The experiment involved passing the immunoconjugates or SIP(L19); in a reduced or non-reduced state; at a concentration of 0.3 μM in PBS, over a biosensor chip which possessed immobilised EDB of fibronectin. Once the association equilibrium had been reached, the chip was washed with a constant stream of PBS, resulting in the exponential decay of the sensogram signal, due to dissociation of the immunoconjugate/SIP(L19)-EDB fibronectin complex. The dissociation BIAcore sensogram for the immunoconjugates and SIP(L19) is shown in Figure 25. The BIAcore analysis showed that the reduction of the SIP(L19) marginally improved the binding efficiency of the antibody fragment. The immunoconjugates which are produced via the cysteine residues, exhibited a similar sensogram profile in comparison to the unconjugated SIP(L19), indicating that the binding efficiency of the antibody moiety had been retained for those conjugates. The sensogram for **PS3**-SIP(L19) showed a decrease in immunoreactivity when compared to the other conjugates. Thus, conjugating the photosensitiser to the antibody fragment through a lysine residue, could result in the photosensitiser being attached to the binding region of the antibody, resulting in diminished binding efficiency for the antibody moiety.

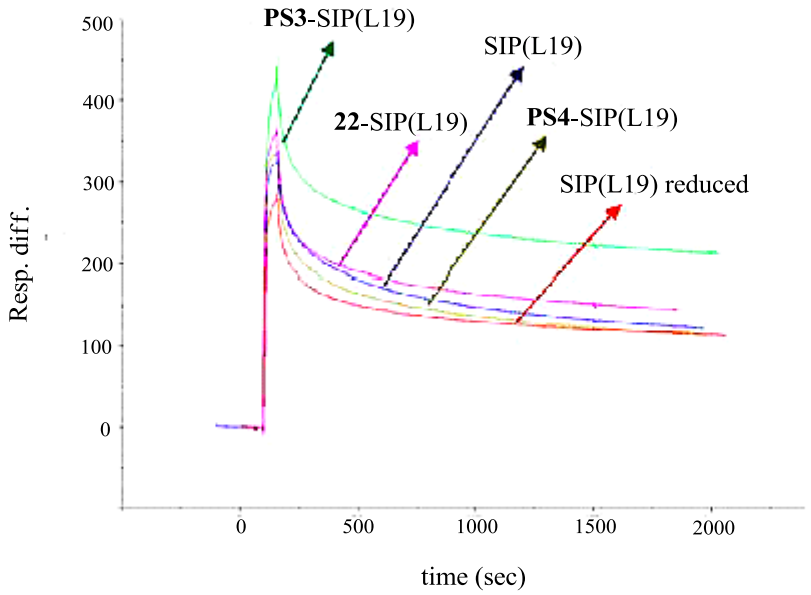

Figure 25: BIAcore analysis of photoimmunoconjugates and SIP(L19).

3.8.4 Photoimmunoconjugate photoactivity

An *in vitro* photocytotoxicity assay was used to assess the photoactivity of the immunoconjugates. 96 Well plates, expressing antigen positive LM fibroblasts, were incubated with 50 µL of the immunoconjugate being evaluated, or the SIP(L19) control, dissolved in PBS at either a 35 or 3.8 µg/mL concentration, for 1 hour at 37 ^{o}C. The plates were washed with PBS, to remove any unbound immunoconjugate or antibody, and then each of the wells was covered with 50 µL of PBS. A KL 1500 electronic tungsten halogen light fitted with a 620/20 filter was used to irradiate the plates with a light dose of 60 J/cm^2. Following the administration of light, the PBS was removed and 100 µL of growth medium was added, the cells were subsequently incubated overnight, at 37 ^{o}C under a 5 % carbon dioxide atmosphere. In order to evaluate the photoactivity of the immunoconjugates, control experiments were also performed including the immunoconjugates in the absence of light, SIP(L19) only and light, and PBS only and light. The cell viability was then measured using a Cell Titer 96 Aqueous One Solution Cell Proliferation Assay. The cell death percentage was calculated from the cells detected for the treated experiment (cells treated with immunoconjugate plus light) divided by the cells detected from the control experiment (cells treated with immunoconjugate without light). The *in vitro* photocytotoxicity for **22**-SIP(L19), **PS3**-SIP(L19) and **PS4**-SIP(L19) is illustrated in Figure 26.

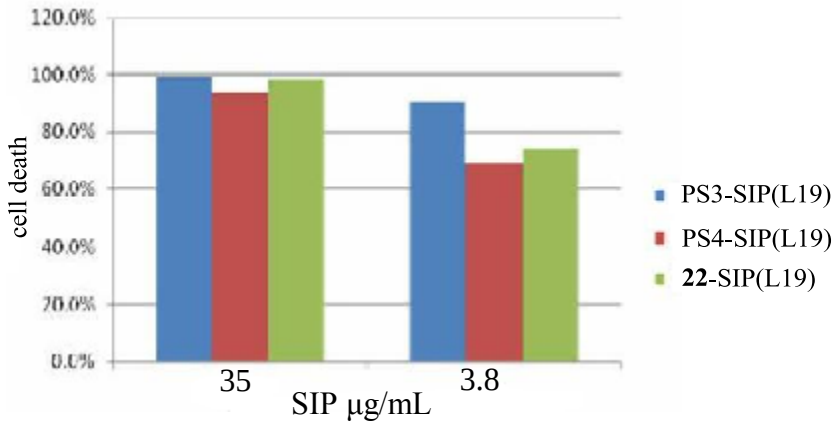

Figure 26: *In vitro* photocytotoxicity assay of photoimmunoconjugates on LM fibroblasts.

The **PS3**-SIP(L19) conjugate, which contains porphyrins bound to the antibody fragment through lysine residues, had a lower immunoreactivity compared to **PS4**-SIP(L19) and **22**-SIP(L19), therefore it would be expected that the **PS3**-SIP(L19) would exhibit the lowest photocytotoxicity considering the photosensitiser moieties, and loading ratios for each of the immunoconjugates analysed were almost identical.

However it was found that **PS3**-SIP(L19) had the highest photocytotoxicity, with 90.7 % cell inhibition when administered at a concentration of 3.8 µg/mL, whereas **22**-SIP(L19) (73.7 %) and **PS4**-SIP(L19) (69.1 %) caused lower cell inhibition when tested under the same reaction conditions. As each of the conjugates possessed the same number of porphyrin moieties, and the immunoreactivity of **22**-SIP(L19) and **PS4**-SIP(L19) was higher than **PS3**-SIP(L19); it was postulated that the **22**-SIP(L19) and **PS4**-SIP(L19) photosensitisers in the excited triplet state must be losing energy, leading to less energy being available for producing reactive oxygen species. When reduced, the SIP(L19) expresses two thiol reactive sites which are in close proximity, thus when the photosensitiser coupled to these thiol groups, they would also be next to each other. It is known that porphyrin aggregation influences the photophysical properties of the porphyrin, hence the production of reactive oxygen species.[175] Therefore the close proximity of the porphyrin moieties on the SIP(L19) could lead to a quenching of the excited state energy, leading to diminished production of reactive oxygen species. Evidence that the quenching phenomena is occurring is provided by the photoactivity of **22**-SIP(L19) being greater than **PS4**-SIP(L19), as the porphyrin moieties are further apart, due to the presence of the alkyl chain, as shown in Figure 27. The quenching effect also explains why the loading ratios calculated for **22**-SIP(L19) and **PS4**-

SIP(L19) by UV-visible spectroscopy, were considerably lower than the MALDI TOF/TOF determination, and hypothetical model.

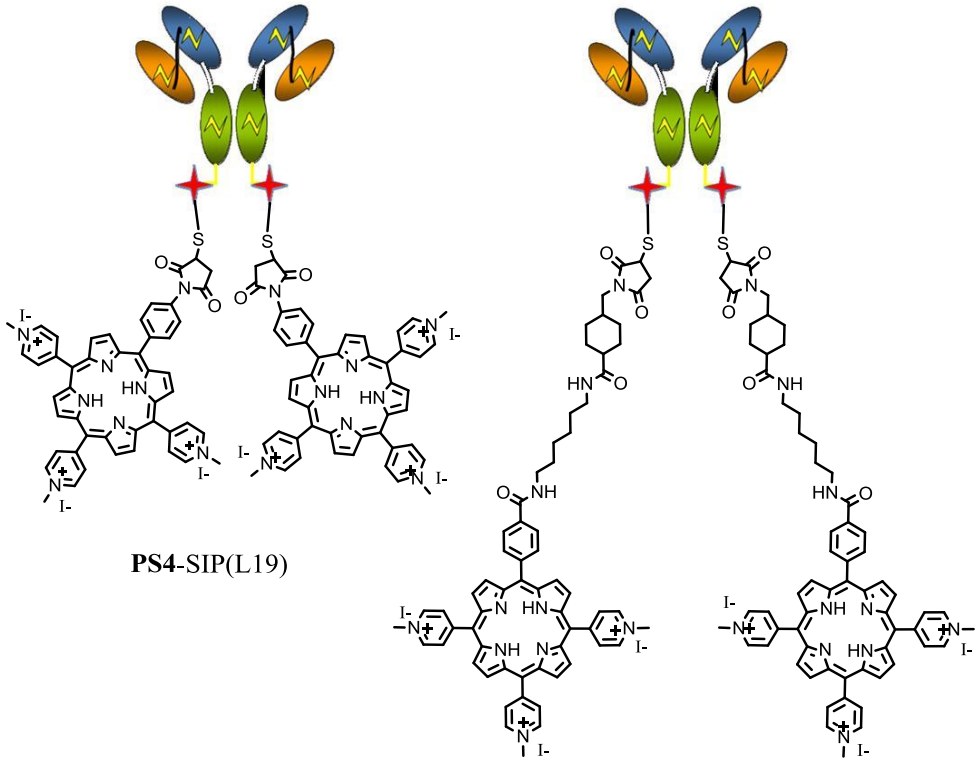

PS4-SIP(L19)

22-SIP(L19)

Figure 27: Illustrations of the **PS4**-SIP(L19) and **22**-SIP(L19).

3.9 Summary / further work

The synthesis of a hydrophilic porphyrin bearing a maleimide bioconjugatable group (**22**) has been demonstrated, with the photosensitiser being successfully conjugated to cysteine residues expressed by SIP(L19), in a quick, reproducible manner. The well characterised immunoconjugate (**22**-SIP(L19)) possessed no non-covalently bound photosensitiser and retained the targeting efficiency of the antibody moiety. The photoactivity of **22**-SIP(L19) was lower than expected in comparison to **PS3**-SIP(L19), possibly due to quenching of the excited state.

Time permitting, a library of photosensitiser analogues could be synthesised bearing alkyl chains of varying length. The effect of chain length on the immunoconjugates characteristics could then be evaluated.

Chapter 4: Preparation of immunoconjugate bearing a PEG linker.

4.1 Introduction

Although the presence of the alkyl chain reduced the quenching of the excited state for **22**-SIP(L19) in comparison to **PS4**-SIP(L19), the quenching effect was not completely abolished, as the phototoxicity of **PS3**-SIP(L19) was greater than that of **23**-SIP(L19), as discussed in chapter 3. Therefore it was postulated that if the photosensitiser possessed a hydrophilic PEG chain connecting to the maleimide group, it could abrogate the quenching phenomena. In contrast to the hydrophobic alkyl chain, the hydrophilic polyethylene glycol chains would be less likely to interact with each other, or with hydrophobic regions of the antibody, thus decreasing the proximity of the porphyrin moieties, and reducing or preventing the quenching of the photosensitisers excited state.

4.2 Polyethylene glycol (PEG)

PEG is a linear or branched polyether, which is commonly synthesised by the polymerisation of ethylene oxide, initiated by the nucleophilic attack by either a hydroxide or alkoxide ion on the ethylene oxide methylene group. Termination of the propagating species can be achieved using an electrophile, e.g. proton, as shown in Figure 28.[176,177] Polyethylene glycol oligomers possessing repeating ether units are relatively inert, therefore for derivatisation of PEG to take place, additional reactive terminal or pendent functionalities are required.[177]

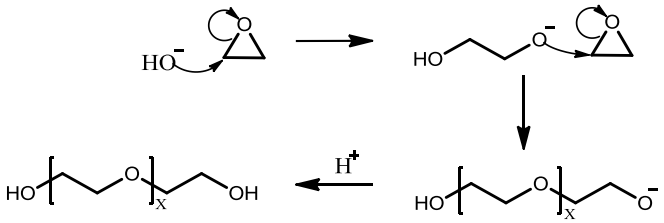

Figure 28: Hydroxide initiated anionic ring-opening polymerisation of ethylene oxide.[177]

4.3 Properties of PEGs

In terms of biocompatibility, PEGs exhibit some favourable characteristics, such as low toxicity and low immunogenicity. Additionally PEG is non-reactive towards many chemical agents, stable against hydrolysis, and soluble in many organic and aqueous environments. Therefore PEG is deemed suitable for modifying biological macromolecules.[176-178] Under aqueous conditions, PEG can bind to 2-3 water molecules per ethylene oxide unit, which effectively makes the PEG molecule behave as if it were 10 times larger than a hydrophilic protein of a similar size. Hence, conjugating PEG to a biological molecule influences its pharmacological properties by increasing its apparent size, thereby altering its biodistribution, and reducing renal filtration. PEG has the ability to shield the antigenic and immunogenic epitopes expressed by proteins, as well as receptor-mediated uptake and clearance by the reticuloendothelial system; thus reducing the immunogenicity of the macromolecule and increasing its circulation time. Furthermore, PEG prevents recognition by proteolytic enzymes and inhibits subsequent degradation.[176]

Savellano and Hasan,[50] have demonstrated that the PEGylation of the C225 mAb, prior to conjugation with the *N*-hydroxysuccinimide ester analogue of benzoporphyrin derivative, significantly affects the solubility of the resulting immunoconjugate. The benzoporphyrin derivative-C225 PEGylated and non-PEGylated immunoconjugates were stored in a dimethylsulfoxide/ aqueous (1:1) solutions and, over extended periods of time, the non-PEGylated immunoconjugate exhibited aggregation, whereas the PEGylated immunoconjugate remained in solution. Furthermore, aggregation was also observed when a concentrated sample of the non-PEGylated immunoconjugate, in the same solvent mixture, was further diluted with water. Preliminary cellular uptake studies were performed comparing the PEGylated and non-PEGylated immunoconjugates by employing A-431 cells (epidermal growth factor receptor positive cells), NR6 cells (antigen negative) and J774 macrophage cells. The PEGylated immunoconjugate exhibited a 2-3 fold decrease in non-specific J774 macrophage uptake, attributed to the reduced aggregation. For experiments using A-431 cells, the PEGylated immunoconjugate showed slight lower uptake, however the presence of non-covalently bound photosensitiser could have influenced the analysis.

Hamblin *et al.*[179] have incorporated PEG moieties into a chlorin $_{e6}$-polylysine conjugate, and assessed the effect the PEGylation had on photoactivity and biodistribution of the conjugate. An *in vitro* photoactivity assay, using an ovarian cancer cell line (OVCAR-5)

and a macrophage cell line (J774) showed that PEGylation caused a nine-fold increase in phototoxicity towards the OVCAR-5 cells, while a four-fold reduction in photoactivity towards J774 cells was observed. The conjugates differing photo-activities towards the OVCAR-5 and J774 cell lines was attributed to localisation of the conjugates within the different cells, and/or the presence of antioxidant enzymes in the macrophage cell line. The conjugates photodynamically induced oxygen consumption was then evaluated, by activating the conjugates in an oxygenated medium. The PEGylated conjugate consumed substantially less molecular oxygen in comparison to the non-PEGylated conjugate, indicating that the PEGylated conjugate produced reactive oxygen species via a type I mechanism. The biodistribution of the conjugates was then analysed, *in vivo*, by injecting the conjugates into nude mice bearing OVCAR-5 tumours. The PEGylated conjugate showed a 2-fold increase in accumulation in the tumour and exhibited considerably more favourable tumour to peritumoural ratios, for all organs harvested.

TPP has been functionalised with 1 to 4 low weight PEG chains, each containing 6 repeating ether units, as illustrated in Figure 29, and the effect the presence the PEG chains had on cellular uptake and phototoxicity was evaluated. Solubility and aggregation of the PEGylated porphyrins was assessed by comparing the fluorescence emission spectra from experiments conducted in either dimethylsulfoxide or HEPES buffer solution. Emission spectra for the porphyrin derivatives bearing 1 or 2 PEG chains were identical for both solvents. However, when the porphyrin was conjugated to 3 or 4 PEG chains, the fluorescence emission was greater in dimethylsulfoxide compared to the buffer; therefore it was postulated that porphyrin aggregation was occurring in the buffer solution. The time dependent cellular uptake of the PEGylated porphyrins into HEp2 cells was then investigated over a 24 hour period. During the first 2 hours, cellular uptake of the porphyrins was consistent. However after 2 hours, the uptake of the porphyrins bearing 3 or 4 PEG chains reached a plateau, while porphyrins functionalised with 1 or 2 PEG chains continued to accumulate in the cells. When the experiment was terminated, the porphyrins with 1 or 2 PEG chains showed a 12-fold increase in cellular accumulation in comparison to the porphyrins with 3 or 4 PEG chains, with the porphyrin bearing 2 PEG chains exhibiting the highest accumulation in the HEp2 cell line. The photocytotoxicity investigation involved exposing HEp2 cells to varying concentrations of the PEGylated porphyrins, and exposing them to a low light dose (1 J/cm^2). The porphyrins with 3 or 4 PEG chains showed no toxicity, up to a concentration of 10 μM, whereas the porphyrins bearing 1 PEG chain (IC_{50} = 2 μM) and

2 PEG chains (IC_{50} = 1.8 μM) were phototoxic. Fluorescence microscopy studies indicated that the TPP functionalised with 1 or 2 PEG chains accumulated in the mitochondria and endoplasmic reticulum, while the porphyrin derivatives possessing 3 or 4 PEG chains targeted the liposomal compartment.[180]

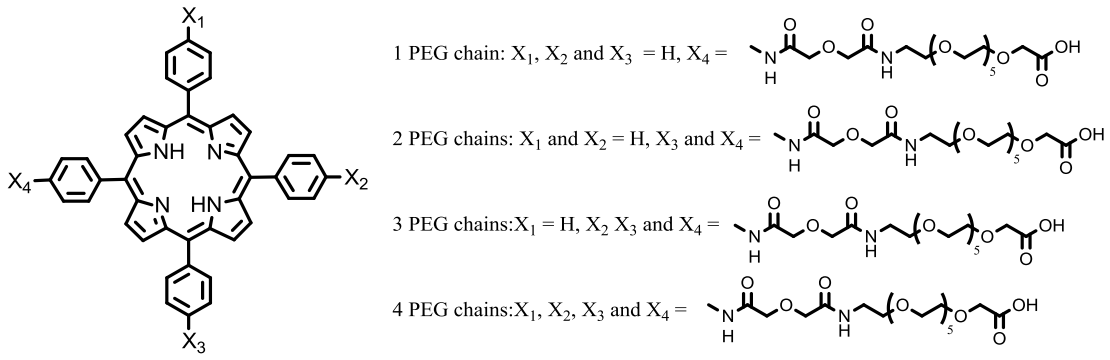

Figure 29: PEGylated TPP derivatives.[180]

4.4 Porphyrins functionalised with PEG moieties

The addition of a PEG chain bearing an amino functionality to a porphyrin which possessed an *N*-hydroxysuccinimide ester has been reported by Frochot and co-workers,[167] and was summarised in chapter 3. The PEGylated porphyrin was synthesised in 75 % yield.

An EDC mediated coupling between a fullerene derivative bearing a PEG chain terminating in a hydroxyl group and a porphyrin possessing a carboxyl group has been achieved, as discussed in chapter 3. The porphyrin-fullerene adduct was produced in 51 % yield.[164]

A TBTU coupling approach has been utilised for the synthesis of porphyrin-peptide conjugates, which contain a PEG chain between the photosensitiser and targeting moieties. 5-(4-Aminophenyl)-10,15,20-tri-(phenyl)porphyrin was treated with diglycolic anhydride, in dimethylformamide, for 24 hours. The functionalised porphyrin bearing a carboxyl group was produced quantitatively and was subsequently coupled to a PEG derivative; which had an amino group, and a carboxyl group protected as the *tert*-butyl ester, located at the termini; via a TBTU/ HOBt/ diisopropylamine mediated reaction. Once the mixture had been stirred for 48 hours at ambient temperature, the porphyrinic product was isolated in a 64 % yield, and the *tert*-butyl ester was cleaved, quantitatively, using trifluoroacetic acid. Finally, a TBTU catalysed reaction, in the presence of HOBt and diisopropylamine, led to the formation of an amide linkage

between the peptide and porphyrin derivative, and the conjugates were synthesised in 46-52 % yield, as shown in Scheme 49.[181]

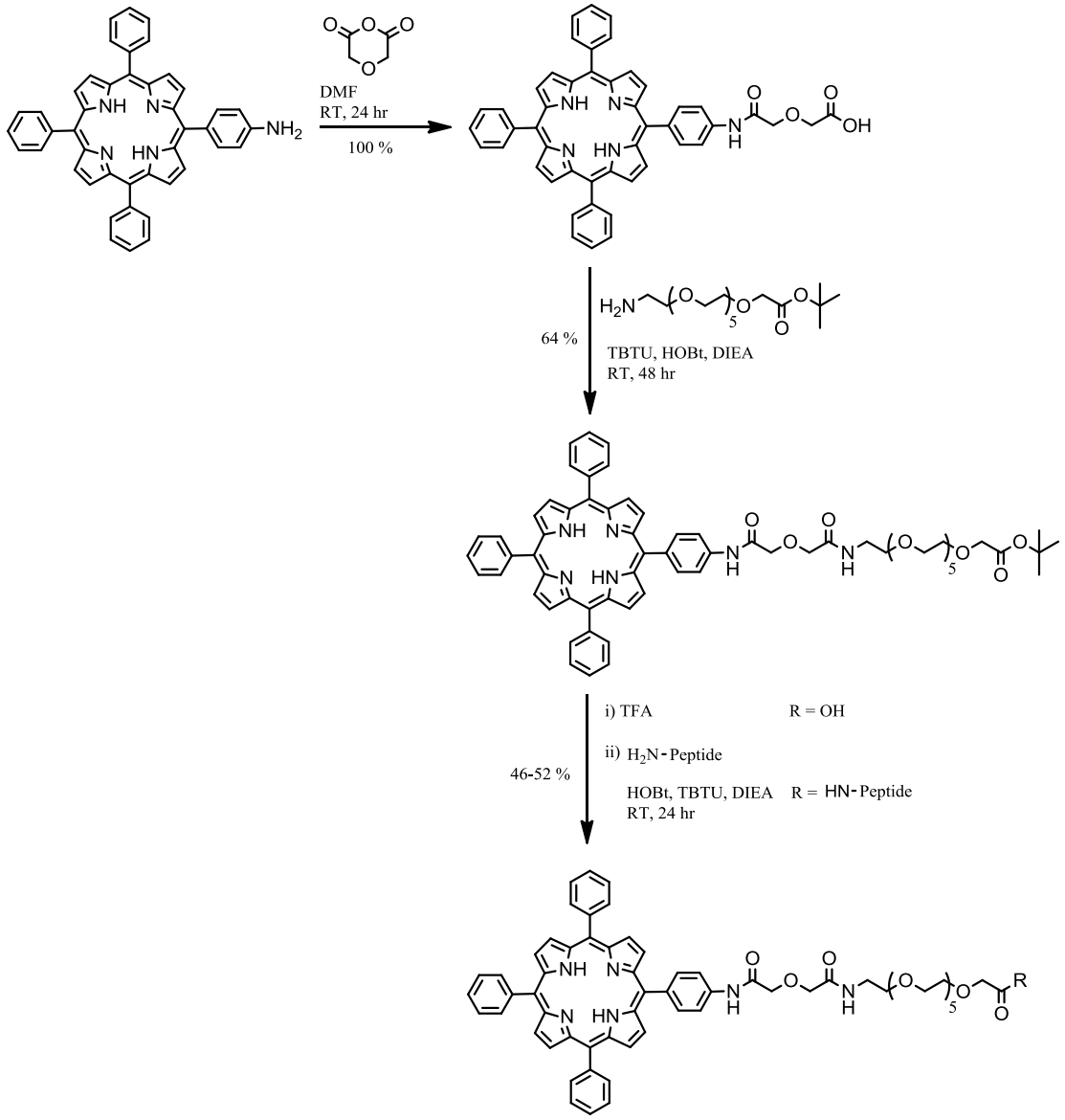

Scheme 49: Porphyrin-peptide conjugates.[181]

The synthetic strategy developed for the synthesis of the porphyrin-peptide conjugates was then transferred to the production of porphyrin-retinamide conjugates. A PEG derivative bearing amino groups located at either end, one of which was Boc protected, was used as a linker, with the coupling again mediated by TBTU/ HOBt/ diisopropylamine, giving the PEGylated porphyrin in 83 % yield. Trifluoroacetic acid was used to cleave the Boc protecting group quantitatively, and the same coupling conditions were used to form the porphyrin-retinamide conjugates, in 49-78 % yields.[182] Nawalany *et al.*[183] have reported the covalent attachment of a modified single PEG chain of various molecular weights (350, 2000 or 5000) to 5,10,15,20-tetra(4-

hydroxyphenyl)porphyrin, as illustrated in Scheme 50. For PEG(350), the methoxy-PEG chains were activated by insertion of a mesyl group, via treatment with mesyl chloride in the presence of triethylamine, for 24 hours at room temperature, producing the activated PEG chain in 86 % yield. PEGylation was achieved by mixing the activated PEG chains, porphyrin and caesium carbonate in dimethylformamide, for 24 hours at 100 °C. The reaction yields varied considerably: porphyrin-PEG(350) (40 %), porphyrin-PEG(2000) (87 %) and porphyrin-PEG(5000) (46 %).

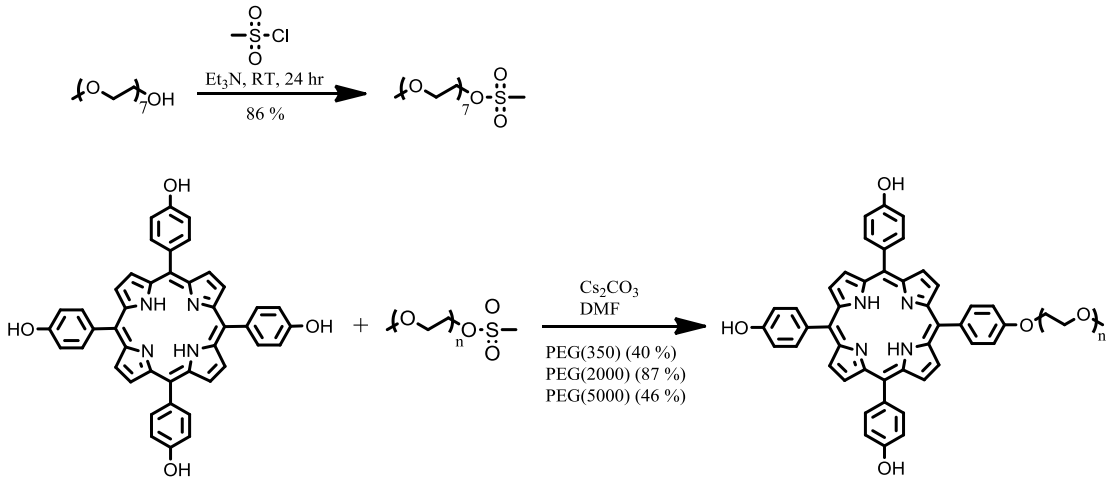

Scheme 50: PEGylated 5,10,15,20-tetra(4-hydroxyphenyl)porphyrin.[183]

A carbonylruthenium(II)porphyrin bearing pentafluorophenyl substituents in the *meso*-positions has been functionalised with a PEG chain, which possessed terminal hydroxyl functionality, via a nucleophilic substitution reaction at the *para*-position of one of the pentafluorophenyl moieties. The PEGylation proceeded by mixing the porphyrin derivative, methoxy-PEG and sodium hydride in dimethylformamide, affording the PEG functionalised porphyrin in 70 % yield.[184]

The PEGylation of 5,10,15,20-tetra(2,3,4,5,6-pentafluorophenyl)porphyrin derivatives, with PEG chains of different molecular masses (164, 550 and 750) has also been reported by Mewis *et al.*[185]. Firstly, the monomethoxy PEG chains hydroxyl groups were converted into mono-halides. PEG(164) hydroxyl group was substituted with a chloride, via treatment with thionyl chloride, in pyridine, for 3 hours under reflux conditions and an inert atmosphere, furnishing the chlorinated PEG chain in 89 % yield. The longer PEG chains were brominated via treatment with phosphorous tribromide, in dichloromethane at 0 °C for 1.5 hours, affording the brominiated PEG chains, BrPEG550 (40 %) and BrPEG(750) (76 %). 5,10,15,20-Tetra(2,3,4,5,6-pentafluorophenyl)porphyrin derivatives were PEGylated by adding the corresponding

halogenated PEG chain, sodium sulphide in dimethylformamide, and stirring the resulting mixture at ambient temperature, for 72 hours. The reaction yields were good to excellent, and depended on the PEG chain and porphyrin complex used, as illustrated in Scheme 51.

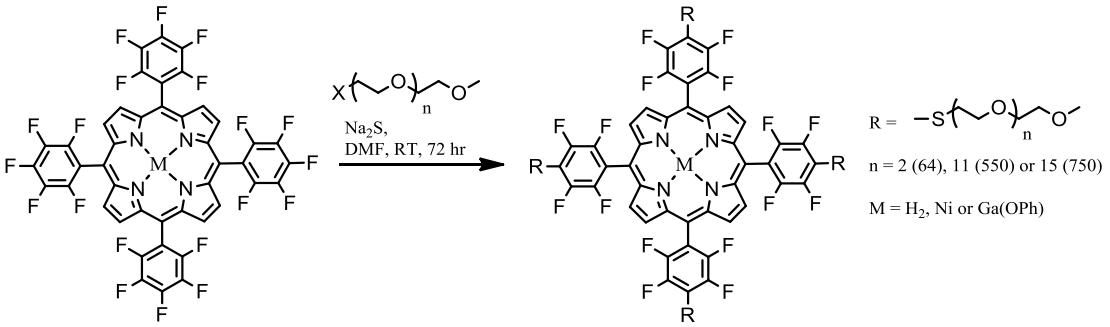

X	n	M	Yield (%)
Cl	2	H_2	75
Br	11	H_2	100
Br	15	H_2	87
Cl	2	Ni(II)	62
Br	11	Ni(II)	79
Br	15	Ni(II)	95
Cl	2	Ga(III)OPh	83
Br	11	Ga(III)OPh	94
Br	15	Ga(III)OPh	93

Scheme 51: PEGylation of 5,10,15,20-tetra(2,3,4,5,6-pentafluorophenyl)porphyrin derivatives.[185]

The PEGylation of 5-(4-pyridyl)-10,15,20-tri(4-methoxyphenyl)porphyrin has been reported, using di-halogenated PEG chains of various molecular weights (8000, 20000, and 35000). The reaction proceeded via quaternisation of the pyridyl group, using PEG chains that have chlorides located at the termini. The exact experimental conditions, and reaction yields were not discussed.[186,187]

Kim *et al.*[188] have synthesised a porphyrin dimer, with the porphyrin moieties connected through a short PEG chain. 5-(4-(Ethylcarbonyl)oxy)phenyl)-10,15,20-tri(4-pyridyl)porphyrin dissolved in dimethylformamide was treated with triethylene glycol ditosylate in the presence of sodium hydroxide, furnishing the PEGylated porphyrin in 34 % yield. The PEGylated porphyrin was added to a solution of 5-(4-

(ethylcarbonyl)oxy)phenyl)-10,15,20-tri(4-pyridyl)porphyrin in dimethylformamide, and potassium hydroxide was added to initiate the conjugation. The mixture was stirred for several hours and the dimeric intermediate was isolated after re-crystallisation. The porphyrin dimer dissolved in dimethylformamide was methylated by the addition of a large excess of methyl iodide, affording the hydrophilic dimer in 35 % yield, as depicted in Scheme 52.

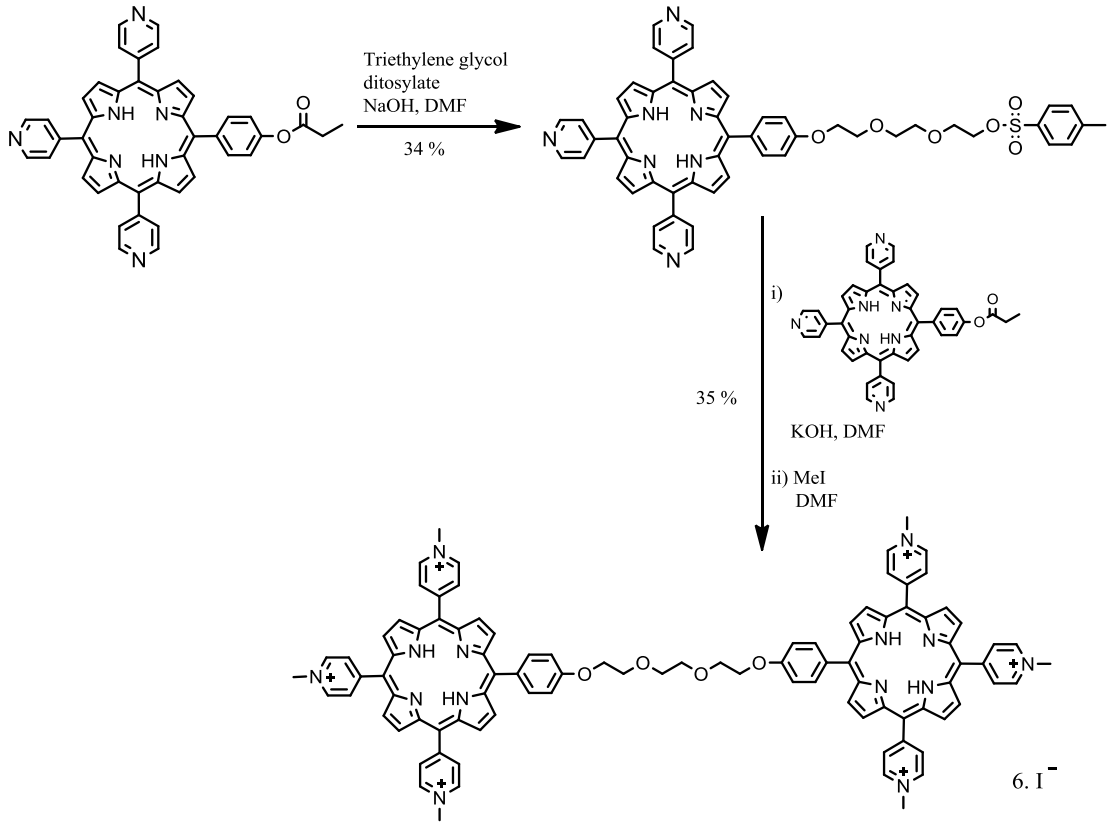

Scheme 52: Synthesis of porphyrin dimer with PEG connection.[188]

4.5 Synthetic strategy: synthesis of a hydrophilic porphyrin bearing a PEG chain terminating in a maleimide group

The aim was to produce a hydrophilic porphyrin bearing a PEG chain terminating with a maleimide group. In relation to the literature describing PEGylation of porphyrins, coupling strategies using EDC[164] or TBTU[181,182], and mesityl[183] or tosyl[188] PEG derivatives, produced the lowest yields. There does not appear to be any preference for the other PEGylation approaches, with the reactions using the porphyrin with an activated ester or pentafluorophenyl substituent's giving the highest PEGylation yields, 62-100 %.[167,184,185]

As the PEGylation strategy utilising the *N*-hydroxysuccinimide ester gave a high yield (75 %),[167] the availability of **19** and the experimental experience gained from the synthesis of **22**, it was deemed appropriate to use a similar approach for the synthesis of the target porphyrin. Therefore the PEG linker selected bore amino groups located at both termini, one of which was Boc protected; *O*-(2-Aminoethyl)-*O*'-[2-(Boc-amino)ethyl]-hexaethylene glycol. PEG derivatives have been shown to be to stable and inert in the presence of *N*-hydroxysuccinimide esters,[177,189] trifluoroacetic acid,[189] diisopropylethylamine[189], maleimide groups[177] and methyl iodide;[188] therefore no incompatibility issues were envisaged. The synthetic approach used for the synthesis of the target porphyrin **25**, is shown in Scheme 53.

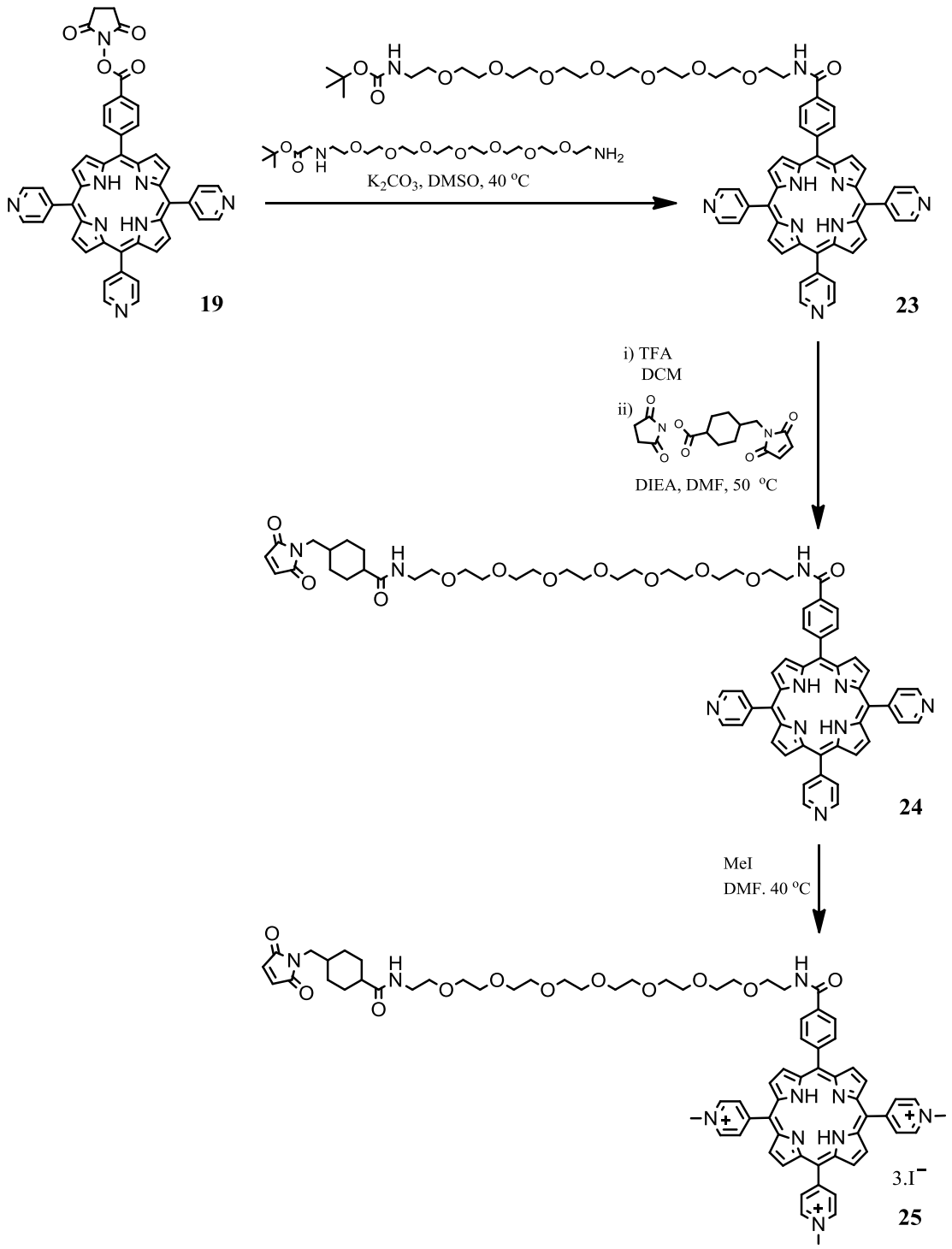

Scheme 53: Synthesis of the hydrophilic porphyrin bearing a PEG chain terminating with a maleimide group.

4.5.1 Synthesis of 5-(4-(23-(*tert*-butylcarbamate)-3,6,9,12,15,16,21-heptaoxadocosyl-1-amino-*N*-cabonyl)phenyl)-10,15,20-tri(4-pyridyl)porphyrin (23)

The *O*-(2-aminoethyl)-*O*'-[2-(Boc-amino)ethyl]-hexaethylene glycol linker and **19** were both soluble in dimethylsulfoxide, hence it was selected as the initial solvent for the synthesis of **23**. The free amino group of the PEG linker was not in a protonated form, thus, theoretically, the presence of base should not have been a requisite for the reaction to occur. However, to guarantee that the amino group was not protonated during the course of the reaction, base was added to the reaction mixture. Adapting a published procedure,[164] the porphyrinic intermediate **23** was synthesised multiple times to optimise the method, as shown in Table 2.

19	**Solvent**	***O*-(2-Aminoethyl)-*O*'-[2-(Boc-amino)ethyl]-hexaethylene glycol**	**Base**	**23**
45 mg, 59 µmol	DMSO, 5 mL	78 mg, 166 µmol, 2.8 equiv.	K_2CO_3, 38 mg, 275 µmol, 4.7 equiv.	21 mg, 32 %
68 mg, 90 µmol	DMSO, 7 mL	110 mg, 235 µmol, 1.2 equiv.	K_2CO_3, 50 mg, 362 µmol, 4 equiv.	54 mg, 53 %
56 mg, 74 µmol	DMF, 6 mL	85 mg, 181 µmol, 2.4 equiv.	DIEA, 63 µL, 360 µmol, 4.9 equiv. (× 2)	34 mg, 41 %
47 mg, 62 µmol	DMSO, 5 mL	71 mg, 152 µmol, 2.5 equiv.	K_2CO_3, 70 mg, 508 µmol, 8.2 equiv.	36 mg, 52 %

Table 2: Reaction conditions used for the synthesis of **23**.

The initial synthesis of **23** was achieved by treating a solution of **19** in anhydrous dimethylsulfoxide with *O*-(2-aminoethyl)-*O*'-[2-(Boc-amino)ethyl]-hexaethylene glycol (2.8 equivalents) in the presence of dry potassium carbonate (4.7 equivalents). The reaction mixture was protected from light and atmospheric moisture and was stirred at 40 °C, for 5 days, until complete consumption of **19** was observed as shown by TLC (silica, eluent: 10 % methanol/dichloromethane). The reaction mixture was partitioned between dichloromethane and water, the organic layer was collected and washed with water to remove the excess *O*-(2-aminoethyl)-*O*'-[2-(Boc-amino)ethyl]-hexaethylene glycol, residual dimethylsulfoxide, potassium carbonate and the 1-hydroxypyrrolidine-2,5-dione by-product. The dichloromethane was removed under

reduced pressure, and the crude product was chromatographically separated (silica, eluent: 8 % methanol/dichloromethane). Compound **23** was isolated as a purple solid in 32 % yield, after precipitation from dichloromethane by the addition of ethyl acetate and hexane. The initial yield of **23** was low, despite using a 2.8 fold excess of *O*-(2-aminoethyl)-*O*'-[2-(Boc-amino)ethyl]-hexaethylene glycol, and a 1.7 equivalents of base in relation to the PEG linker. Therefore the reaction was repeated using a lower proportion of *O*-(2-aminoethyl)-*O*'-[2-(Boc-amino)ethyl]-hexaethylene glycol, and a 3.3 equivalence of base in relation to the PEG chain, to ensure the amino group was deprotonated. Under the modified conditions, **23** was isolated in 53 % yield. The increase in yield resulting from the extra base added in relation to the PEG derivative, indicated that under the experimental conditions, a proportion of the PEG chains amino groups were in an inactive, protonated form, thus base was required to facilitate PEGylation. TLC of the reaction mixtures suggested that all of **19** had been converted into **23**, in a relatively clean reaction, hence the low yields obtained could be due to problems associated with isolating **23** from the dimethylsulfoxide solvent. Hence, the synthesis of **23** was attempted using dimethylformamide as an alternative solvent and diisopropylethylamine (2 equivalents relative to the PEG derivative) as the base. The reaction was monitored over a 3 day period by TLC, until the composition of the reaction mixture exhibiting no further change, however at this point both **19** and **23** could still be detected. As the reaction had not reached completion, additional diisopropylethylamine (2 equivalents relative to the PEG derivative) were added. The reaction was monitored for a further 3 days by TLC, but the extra addition of base did not influence the progression of the reaction. Following work-up and chromatographic separation, **23** was produced in 41 % yield. The change in solvent did not improve the yield of **23**, hence to further optimise the reaction conditions, a higher proportion of *O*-(2-aminoethyl)-*O*'-[2-(Boc-amino)ethyl]-hexaethylene glycol was used to increase the availability of amino functionalities. After work-up and isolation, **23** was synthesised in 52 % yield.

The important sections of the ^{1}H NMR spectrum for **23,** is depicted in Figure 30.

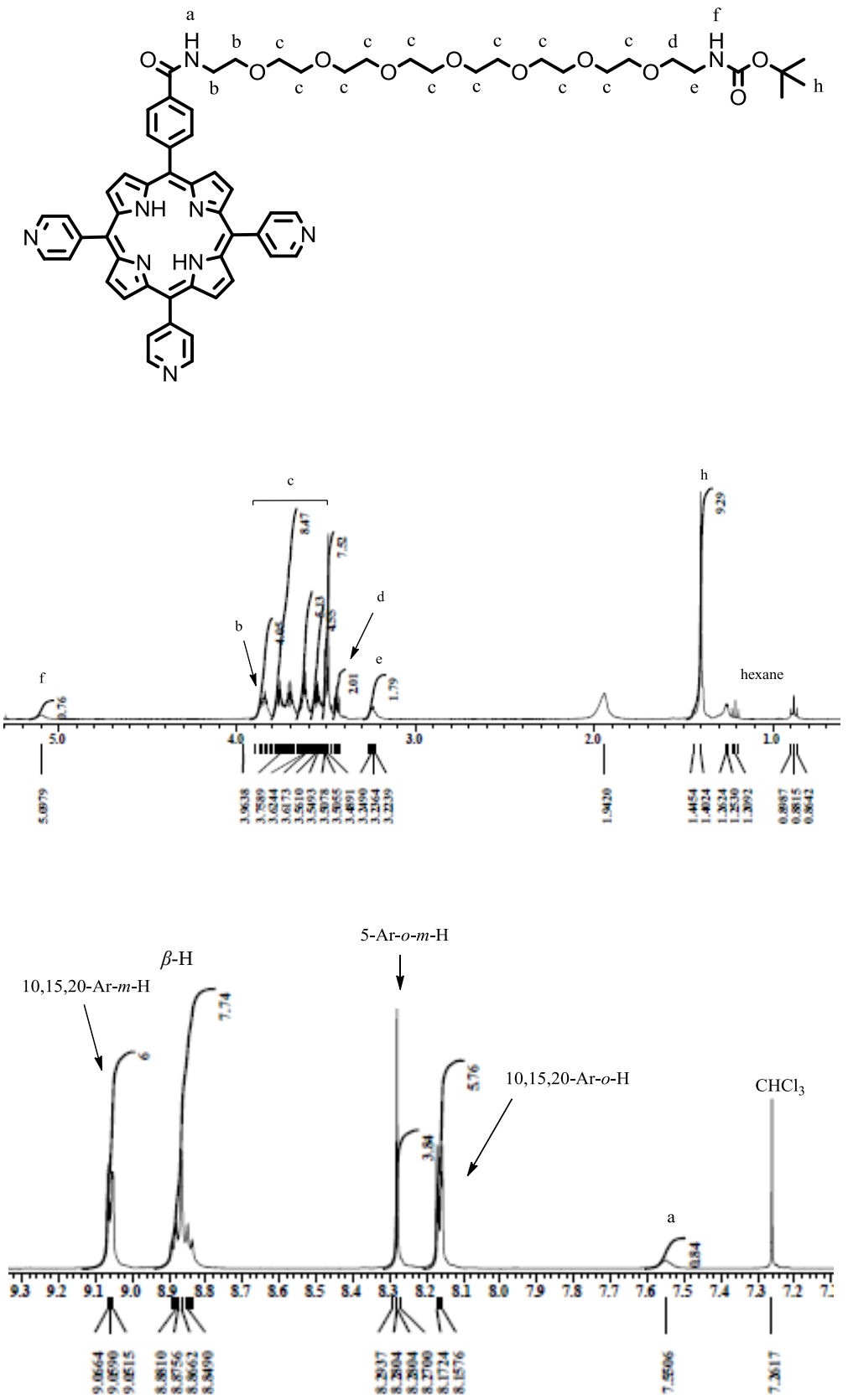

Figure 30: ^{1}H NMR spectrum of **23**.

Assignment of the signals was achieved using a combination of 2D COSY and C-H correlation experiments. For the alkyl region, the signal at 1.40 ppm which integrated to 9, did not couple with another signal, as indicated by the 2D COSY analysis, therefore it was assigned to the *tert*-butyl protons (**h**). Two broad singlets, with integrals of 1, were observed at 5.10 ppm and 7.55 ppm, with the 2D COSY showing that each peak coupled to one other signal in the alkyl region. By considering the shielding effect exerted by the porphyrin, these signals were assigned as the amino proton (**a**) at 7.55 ppm, and (**f**) at 5.10 ppm; although theoretically these signals should appear as triplets. The amino proton (**a**) coupled to a multiplet at 3.81-3.90 ppm, which integrated to 4, therefore that multiplet was assigned proton environment (**b**). The 2D COSY experiment revealed that amino proton (**f**) coupled to a quartet at 3.24 ppm, which integrated to 2, and was subsequently assigned as (**e**). The triplet at 3.44 ppm was assigned as proton environment (**d**), as it integrated to 2, it coupled with (**e**) and both signals had the same coupling constant; J = 5 Hz. The remaining 5 multiplets at 3.47-5.51 ppm, 3.52-3.58 ppm, 3.59-3.66 ppm, 3.67-3.73 ppm and 3.74-3.80 ppm, gave a total integral of 24, which corresponded to the remaining protons present in the PEG chain, and were assigned as proton environment (**c**). The assignment of the signals in the aromatic region was more straightforward. The doublet at 8.17 ppm integrated to 6 and coupled to the doublet at 9.06 ppm, which also had an integral of 6, both signals had the same coupling constant, J = 5.9 Hz, and by considering the inductive effect exerted by the pyridyl group, these signals were assigned as the pyridyl-*meta*-protons at 9.06 ppm and the pyridyl-*ortho*-protons at 8.17 ppm. The multiplet at 8.27-8.29 ppm had an integral of 4 and showed no coupling with any other signal, therefore it was assigned as the 5-aromatic-protons. The remaining signals; 2 doublets at 8.84 ppm and 8.89 ppm, and a multiplet at 8.86-8.88 ppm, gave a combined integral of 8 and was therefore assigned as the β protons. The UV-spectrum for **23** was typical for a free-base porphyrin. The mass spectrum of **23** gave the expected 1112 *m/z* peak due to the $(M + H)^+$ ion, therefore it was concluded that **23** had been successfully synthesised.

4.5.2 Synthesis of 5-(4-(23-(4-(*N*-maleimidomethyl)cyclohexane-1-amido)-3,6,9,12,15,18,21-heptaoxadocosyl-1-amino-*N*-cabonyl)phenyl)-10,15,20-tri(4-pyridyl)porphyrin (24)

Adapting a published procedure,[157] compound **23** dissolved in anhydrous dichloromethane, was treated with trifluoroacetic acid, while protected against moisture and light. The mixture was stirred for 50 minutes, at ambient temperature until complete cleavage of the Boc protecting group was observed, as shown by TLC (silica, eluent: 10 % methanol/dichloromethane). The excess trifluoroacetic acid was neutralised by pouring the reaction mixture on to an ice cooled saturated sodium hydrogen carbonate solution; a colour change in the organic layer was observed from green to red, due to deprotonation of the porphyrin's inner nitrogens. The crude intermediate was extracted into dichloromethane, washed with water to remove residual sodium hydrogen carbonate, and dried over anhydrous sodium sulphate to remove residual water. As it was not possible to isolate the amino intermediate derived from **20**, as discussed in chapter 3, isolation of the deprotected **23** was not attempted.

The crude amino porphyrin was treated with SMCC, using the modified optimised conditions determined for the production of **21**.[102] SMCC (1.2 equivalents relative to **23**) and diisopropylethylamine (4.1 equivalents relative to SMCC) were added to a solution of the amino derivative of **23** dissolved in dry dimethylformamide. The resulting mixture was stirred at room temperature for 14 hours (overnight), until the composition of the reaction mixture exhibited no further change, as indicated by TLC (silica, eluent: 10 % methanol/dichloromethane).The crude porphyrinic product was precipitated by the addition of diethyl ether and hexane, and column chromatography was used to isolate **24**. Precipitation was attempted by dissolving **24** in dichloromethane, and adding either methanol or hexane; in both cases **24** seemed to have an affinity towards the glass vessel, and could not be collected. Precipitation of the product was achieved in ethyl acetate/hexane (10:1) over dichloromethane, furnishing **24** in 32 % yield. The yield of **24** was lower than expected, thus the reaction was repeated using a higher quantity of diisopropylethylamine (5.3 equivalents relative to SMCC). Following work-up and isolation, **24** was afforded in 55 % yield. The relevant sections of the ^{1}H NMR spectrum of **24,** is shown in Figure 31.

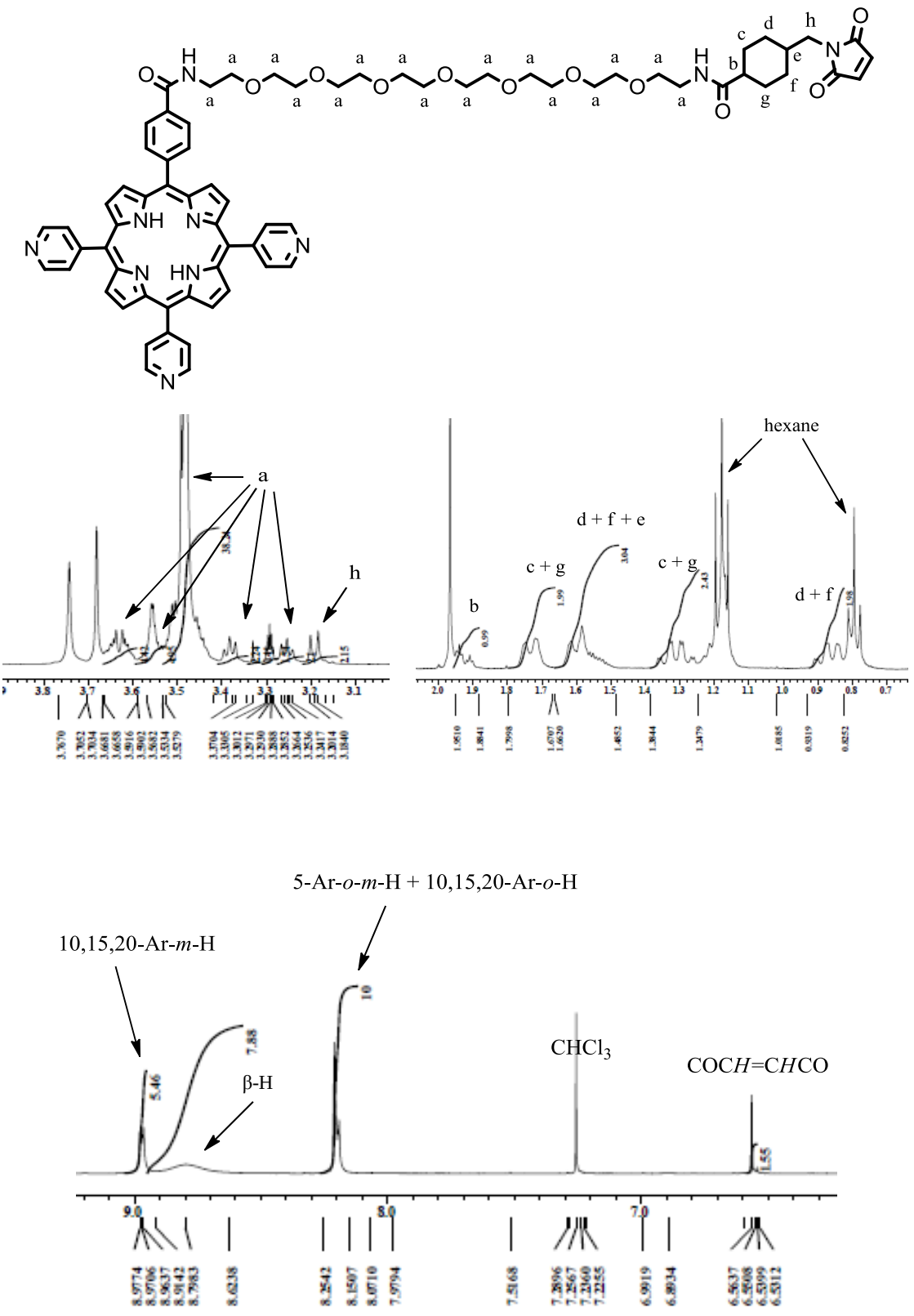

Figure 31: ^{1}H NMR spectrum of **24**.

The assignment of the peaks in the aliphatic region of the ^{1}H NMR spectrum for **24** corresponding to the cyclohexane ring substituent was achieved using a combination of 2D COSY, C-H correlation and HMBC experiments. The 2D COSY analysis of the region containing the signals for the cyclohexane substituent for **24**, is shown in Figure 32, with the yellow crosses depicting solvent couplings.

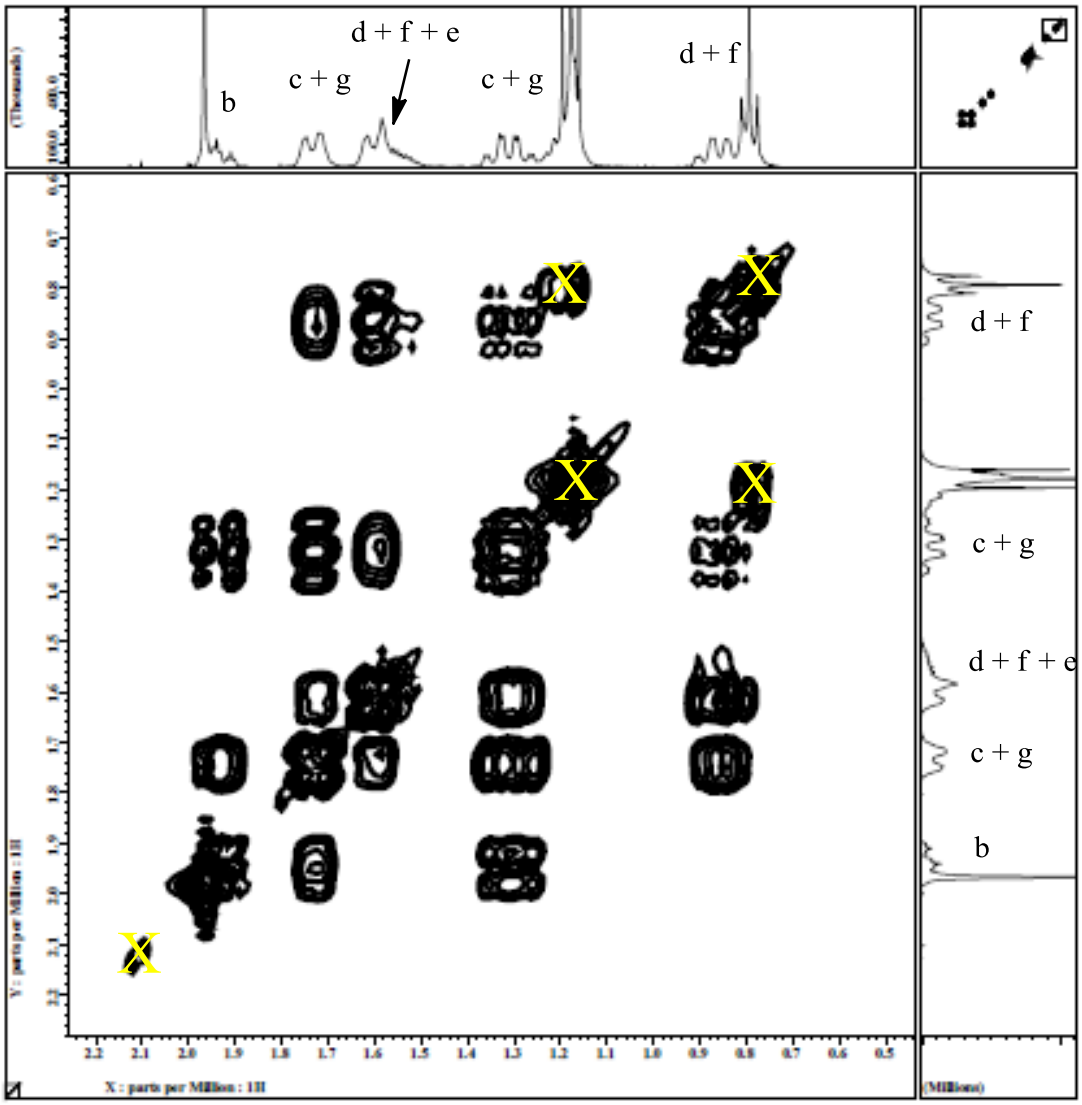

Figure 32: Aliphatic section of the 2D COSY of **24**.

The signal at 1.88-1.95 ppm, had an integral of 1, and coupled with multiplets at 1.67-1.80 ppm and 1.25-1.38 ppm, therefore it was a CH environment connecting to either the carbonyl or CH_2-maleimide. The peak at 1.49-1.66 ppm, coupled with 3 other signals which had integrals of 2; 0.83-0.94 ppm, 1.25-1.38 ppm and 1.67-1.80 ppm; thus it was a signal from protons which were on opposite sides of the cyclohexane ring. However, the signal at 1.49-1.66 ppm had an integral of 3, thus a section of that signal must be due to a CH environment. By considering the shielding effect exerted by the porphyrin, the multiplet at 1.88-1.95 ppm was assigned (**b**) and a part of the multiplet at 1.49-1.66 ppm was assigned (**e**). Signal (**b**) coupled with multiplets at 1.67-1.80 ppm and 1.25-1.38 ppm, which had a combined integral of 4, hence those signals were attributed to proton environments (**c**) and (**g**). The multiplet at 0.83-0.94 ppm and a proportion of the signal at 1.49-1.66 ppm were subsequently attributed to (**d**) and (**f**). The signal at 1.49-1.66 ppm exhibited coupling with the doublet at 3.19 ppm, thus the doublet at 3.19 ppm was assigned the CH_2 environment neighbouring the maleimide group (**h**). A combination of HMBC and C-H correlation experiments confirmed the signal assignments. Despite multiple attempts, a clean spectrum where all the peaks for the PEG protons were well defined, was not obtained. It appeared that a proportion of the signals corresponding to the PEG protons were beneath the methanol solvent peak. Importantly, the signal for the *tert*-butyl protons from the Boc group, which was observed at 1.40 ppm for the ^{1}H NMR spectrum for **23**, is not present in the ^{1}H NMR spectrum for **24**, thus confirming that the Boc group had been removed. The aromatic region of the spectrum exhibited a singlet at 6.80 nm, which corresponded to the maleimide protons, indicating the presence of the maleimide group. Although not well defined, the peaks corresponding to the protons from the porphyrin core were observed.

The UV-visible spectrum for **24** was typical for a free-base porphyrin.

The HRMS spectrum gave the expected 1231 *m/z* signal due to the $(M + H)^+$ ion.

The characterisation studies indicated that the reaction had proceeded as postulated

4.5.3 Synthesis of 5-(4-(23-(4-(*N*-maleimidomethyl)cyclohexane-1-amido)-3,6,9,12,15,18,21-heptaoxadocosyl-1-amino-*N*-cabonyl)phenyl)-10,15,20-tri(4-*N*-methyl-pyridyniumyl)porphyrin triiodide (25)

Following Scheme 53, and using a modified literature method,[68] a solution of **24** in anhydrous dimethylformamide was treated with a large excess of methyl iodide, at 40 °C for 4 hours. Once the reaction had reached ambient temperature, the reaction mixture was cooled over ice and an ice cooled solution of diethyl ether and hexane (50:1) was added to promote precipitation of the porphyrinic product. The product was collected by filtration, with the filtrate, containing residual methyl iodide, being neutralised with a solution of triethylamine. The precipitate was rapidly washed with ice cooled diethyl ether, to remove the residual methyl iodide and dimethylformamide. The precipitate was collected and dried under vacuum, furnishing **25** in 75 % yield.

The relevant sections of the ^{1}H NMR of **25** is shown in Figure 33, with the assignment of the peaks achieved using a combination of 2D COSY and C-H correlation experiments. The pair of singlet's at 4.73 ppm and 4.74 ppm, which have a combined integral of 9, corresponded to the 3 methyl groups from quaternised pyridyl groups. All the signals due to the other proton environments were accounted for, a further indication that the methylation had proceeded as expected, and the structure of the porphyrin withstood the quaternisation conditions.

The UV-visible spectrum for **25** was typical for a free-base porphyrin.

The MALDI mass spectrum of **25** provided the expected 1276 *m/z* peak which was due to the $[M+H]^{+}$ -3I ion. It was concluded that the methylation of **24** had been achieved.

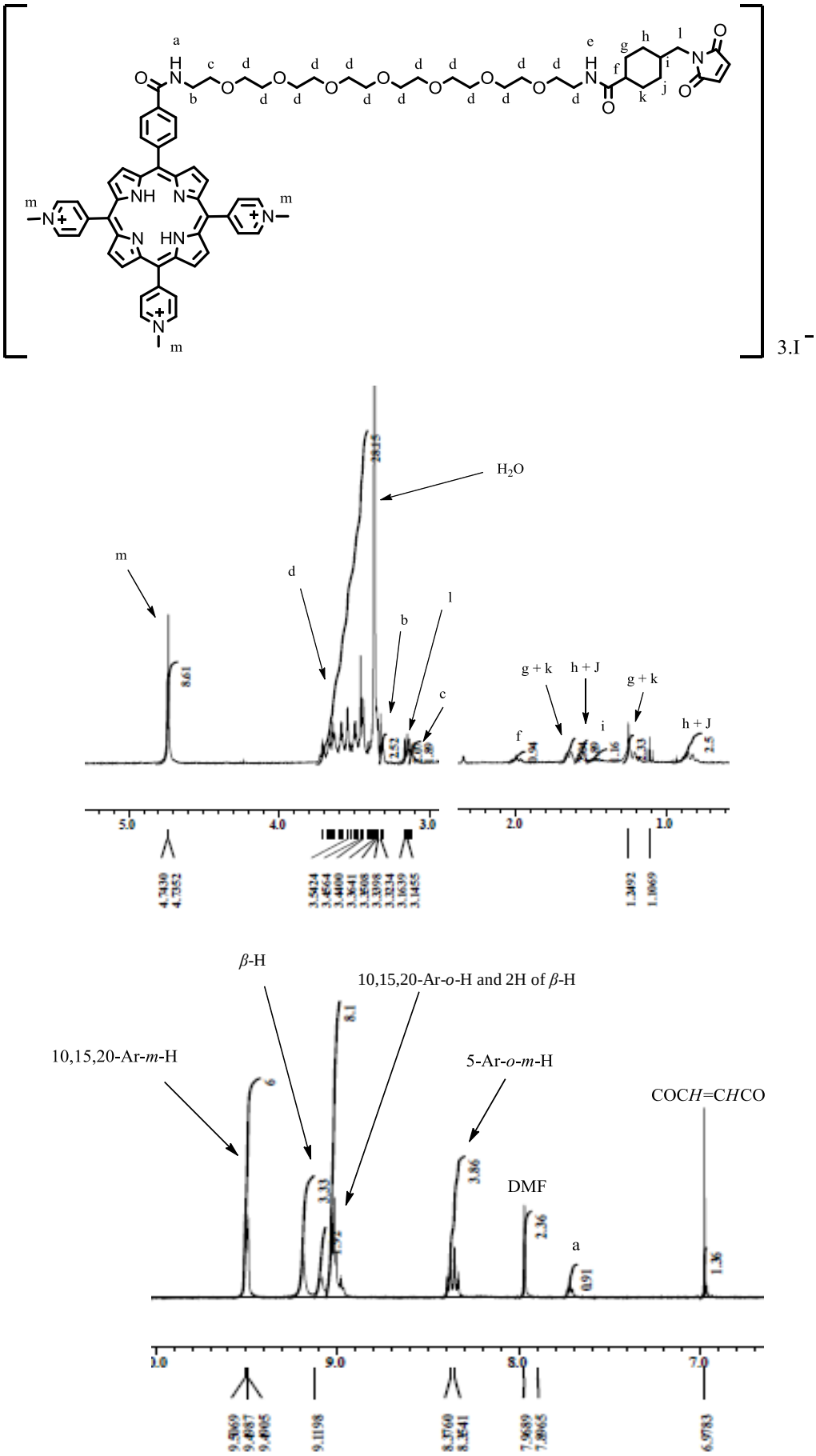

Figure 33: ^{1}H NMR spectrum of **25**.

4.6 Photoimmunoconjugates

The conjugation of **PS3**, **22** or **25** (Figure 34) to SIP(L19) was achieved using the same conjugation method as described in Chapter 3. The synthesis of the immunoconjugates and subsequent biological studies were performed by Alessandro Palumbo and Corinne Hutter, under the supervision of Professor Dario Neri.

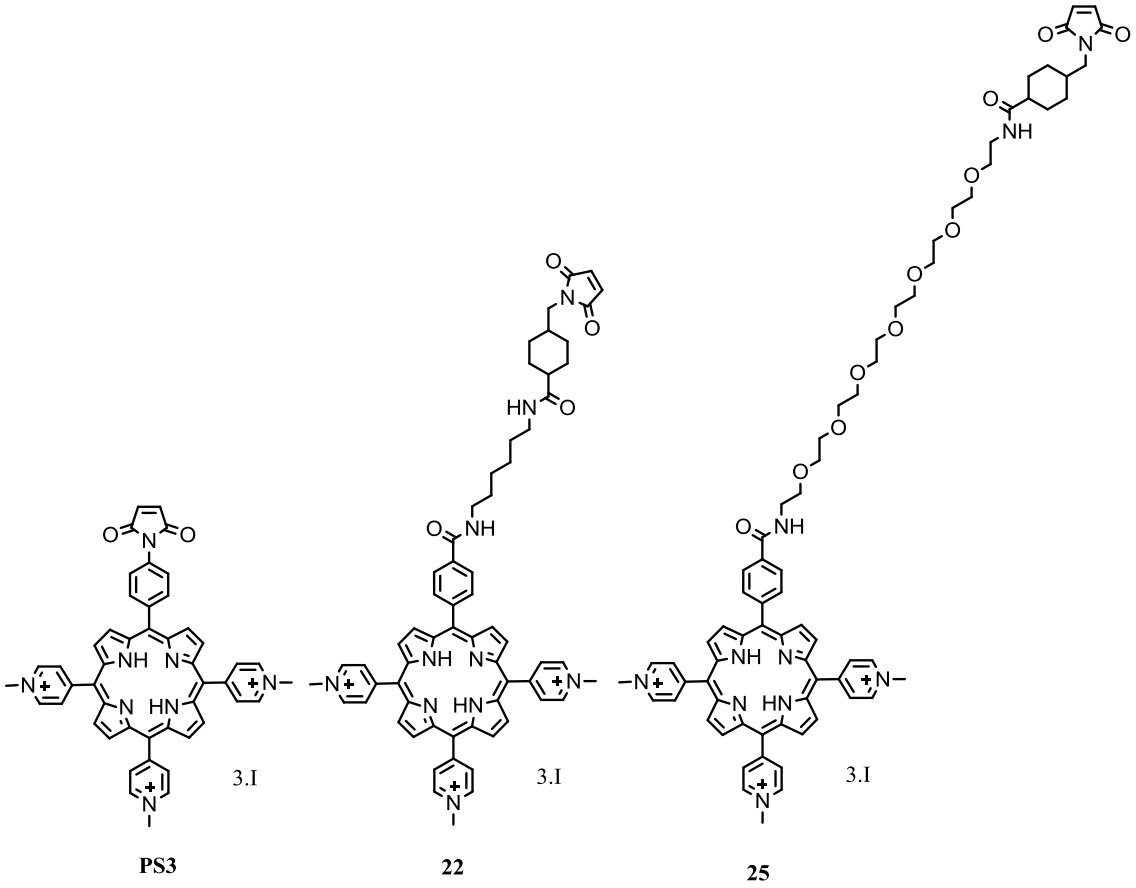

PS3 **22** **25**

Figure 34: Hydrophilic photosensitisers **PS3**, **22** and **25**.

4.6.1 Photoimmunoconjugate characterisation

The purity of **25**-SIP(L19) was assessed by SDS-PAGE analysis, with the SDS-PAGE profile of **25**-SIP(L19) being equivalent to **22**-SIP(L19). It was concluded that the SIP(L19) was fully reduced, covalent attachment of **25** to cysteine residues expressed by the reduced SIP(L19) was achieved, and non-covalently bound photosensitiser could not be detected.

The photosensitiser loading ratio was then determined by both UV-visible spectroscopy and MALDI TOF/TOF, in the same manner as described in Chapter 3 for **22**-SIP(L19). For the UV-visible estimation, the conjugate sample was prepared and gave an absorbance of 1.4 absorbance units at 280 nm, corresponding to 1 mg/mL of SIP(L19) within the sample. The absorbance of the same solution was then measured at 425 nm, and the extinction coefficient of **25** (188,489 M^{-1} cm^{-1}), was used to calculate the concentration of the photosensitiser in the sample. The concentration of the photosensitiser was divided by the concentration of SIP(L19) to give an estimated photosensitiser:antibody ratio of 1.75.

The loading ratio was then confirmed using MALDI-TOF/TOF as shown in Figure 35.

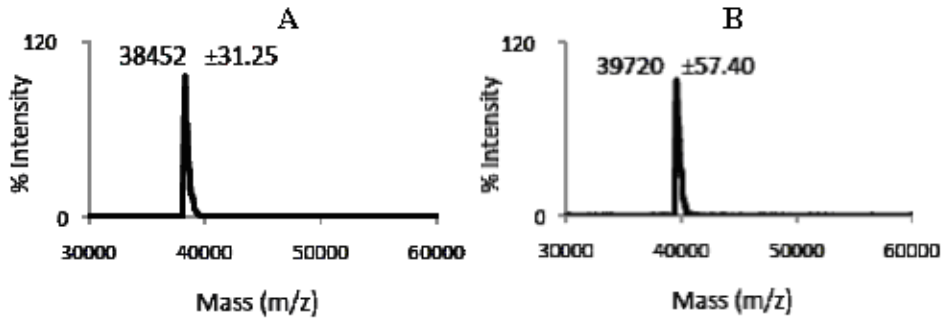

Figure 35: MALDI-TOF/TOF spectra for (A) SIP(L19), (B) **25**-SIP(L19).

The mass of the antibody in the monomeric form was subtracted from the **25**-SIP(L19) in the monomeric form, to give the mass contribution of the photosensitiser from half of the complete immunoconjugate.

Photosensitiser mass = Conjugate's mass − Antibody's mass

= 39720 ± 57.40 *m/z* − 38452 ± 31.25 *m/z*

= 1268 ± 88.65 *m/z*

Compound **25** had a molecular weight of 1656 $gmol^{-1}$, however mass spectrometry does not detect the iodide counter ions, therefore, **25** had an observed molecular weight of 1276 $gmol^{-1}$. The calculated photosensitiser mass, with the experimental error, showed that one photosensitiser had coupled to the monomeric SIP(L19), thus 2 photosensitisers had coupled to the intact SIP(L19). The **25**-SIP(L19) loading ratio calculated by UV-visible spectroscopy, was similar to the loading ratio calculated by MALDI-TOF/TOF and the hypothetical model. The similarity of the loading ratios calculated for **25**-SIP(L19) by the 2 methods, suggests that the quenching effect was less prominent, when compared to the previous **PS3**-SIP(L19) and **22**-SIP(L19) conjugates.

The size exclusion chromatography profile of **25**-SIP(L19) was then compared to the size exclusion profile of the non-reduced SIP(L19), to ascertain whether the dimeric nature of the immunoconjugate was retained after the reduction and subsequent coupling to **25**, under aqueous conditions. The similar size exclusion profiles of non-reduced SIP(L19) and **25**-SIP(L19) is shown in Figure 36, which indicates that dimeric nature of the antibody was maintained, when subjected to an aqueous environment.

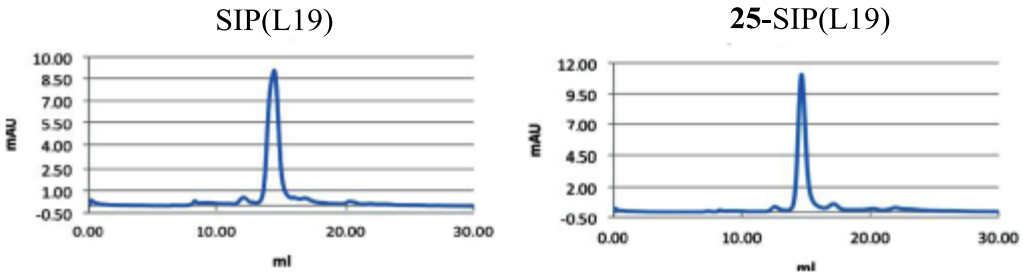

Figure 36: Size exclusion chromatography profile of SIP(L19) and **25**-SIP(L19).

4.6.2 Photoimmunoconjugate characterisation

The immunogenicity of **25**-SIP(L19) was evaluated by BIAcore analysis, which showed that the binding of the conjugate was similar to the native SIP(L19), suggesting that the targeting efficiency of the conjugates SIP(L19) moiety had been retained.

A photocytotoxicity assay was performed employing antigen positive (LM fibroblasts) and antigen negative (CHO-S and HEK293T) cell lines, to evaluate the selectivity of the immunoconjugates. Each of the cell lines were grown in DMEM media enriched with 10 % FCS and antibiotics, at 37 ^{o}C with 5 % CO_2. The supernatant was removed and the cells were washed with PBS and incubated with a trypsin-EDTA solution. The cell suspension was collected and diluted with growth medium. The cell lines were then incubated at 37 °C for 20 minutes, before being stored. Each cell line (50 μl cells, 3×10^4 cells) was added to wells of a 96 well plate, and was subsequently incubated at 37 ^{o}C, under a 5 % CO_2 atmosphere, overnight. The growth medium was removed and the cells were incubated with either 20 mg/mL of SIP(L19), or the immunoconjugates at a concentration of 50 μM with respect to the photosensitiser moiety, with DMEM medium, at 37 °C, under a 5 % CO_2 atmosphere, for 1 hour. The unbound SIP(L19) or immunoconjugate was removed via PBS buffer washings, and the cells were covered with 50 μL of PBS and irradiated using a KL 1500 electronic tungsten halogen light fitted with a 620/20 filter. Control experiments were also performed involving the cells treated with the immunoconjugate or SIP(L19), without light activation. The PBS buffer was removed and the 100 μL of fresh growth medium was added, before the cells were incubated at 37 ^{o}C, under a 5 % CO_2 atmosphere, overnight. The cell viability was then measured using a Cell Titer 96 Aqueous One Solution Cell Proliferation Assay. The cell death percentage was calculated from the cells detected for the treated experiment (cells treated with immunoconjugate plus light) divided by the cells detected from the control experiment (cells treated with immunoconjugate without light). The *in vitro* photocytotoxicity assay results, involving the administration of SIP(L19), **PS3**-SIP(L19), **22**-SIP(L19) or **25**-SIP(L19) to LM fibroblast, CHO-S or HEK293T cell lines, are shown in Figure 37. The results illustrate the selectivity of the immunoconjugates, as significant phototoxicity was observed on the antigen positive LM fibroblast cell line, whereas the antigen negative cell lines were relatively unaffected by the PDT treatments; although **25**-SIP(L19) did exhibit a low photoactivity against the antigen negative cell lines. The photoactivity assay performed on the LM fibroblasts showed the importance of the linker between the photosensitiser and

antibody moieties. The **PS3**-SIP(L19) caused ≈ 65 % cell death, which increased to ≈ 83 % cell death for **22**-SIP(L19), by the incorporation of a alkyl linker between the maleimide bioconjugatable handle and photosensitiser. The potency was further improved by using a longer, hydrophilic chain, as the photoactivity of **25**-SIP(L19), which caused ≈ 98 % cell death, was substantially greater than that of **22**-SIP(L19). Furthermore, the results also demonstrated that the un-conjugated SIP(L19) was not phototoxic towards the cell lines investigated.

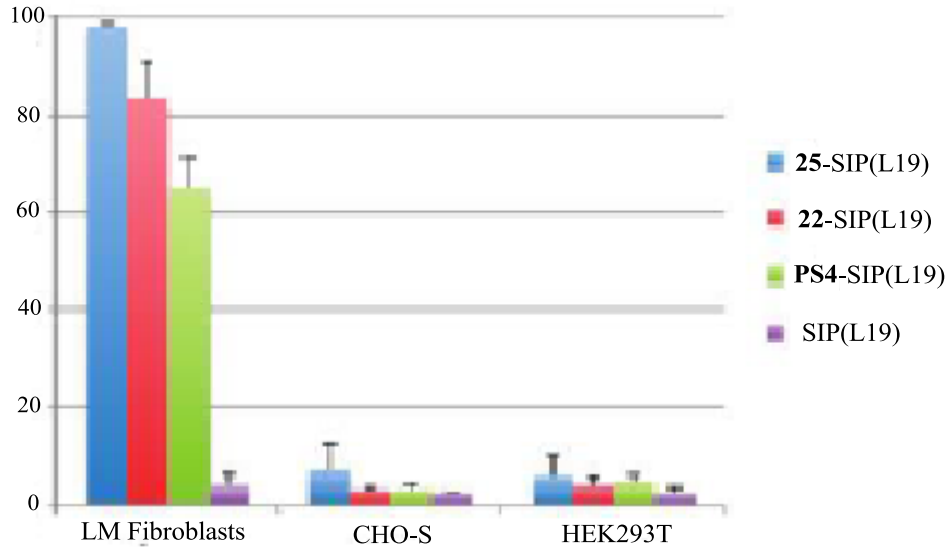

Figure 37: Phototoxicity of photoimmunoconjugates and SIP(L19) on antigen-positive (LM fibroblasts) and antigen-negative (CHO-S, HEK293T) cell lines.

Another *in vitro* phototoxicity assay, employing LM fibroblasts, was used to evaluate the photoactivity of the immunoconjugates at different concentrations, as shown in Figure 38, enabling the determination of the half maximal inhibitory concentrations (IC_{50}). The **25**-SIP(L19) (IC_{50} = 7-8 × 10^{-7} M) immunoconjugate was considerable more potent than the **22**-(SIP)L19 (IC_{50} = 7-8 × 10^{-6} M) which was more photoactive than **PS3**-SIP(L19) (IC_{50} = 5-6 × 10^{-6} M). These results are consistent with the quenching effect hypothesis, as increasing the chain length and hydrophilicity of the chain, would enable the conjugated porphyrins to have a greater freedom of movement, which would reduce the probability of the porphyrins quenching each other.

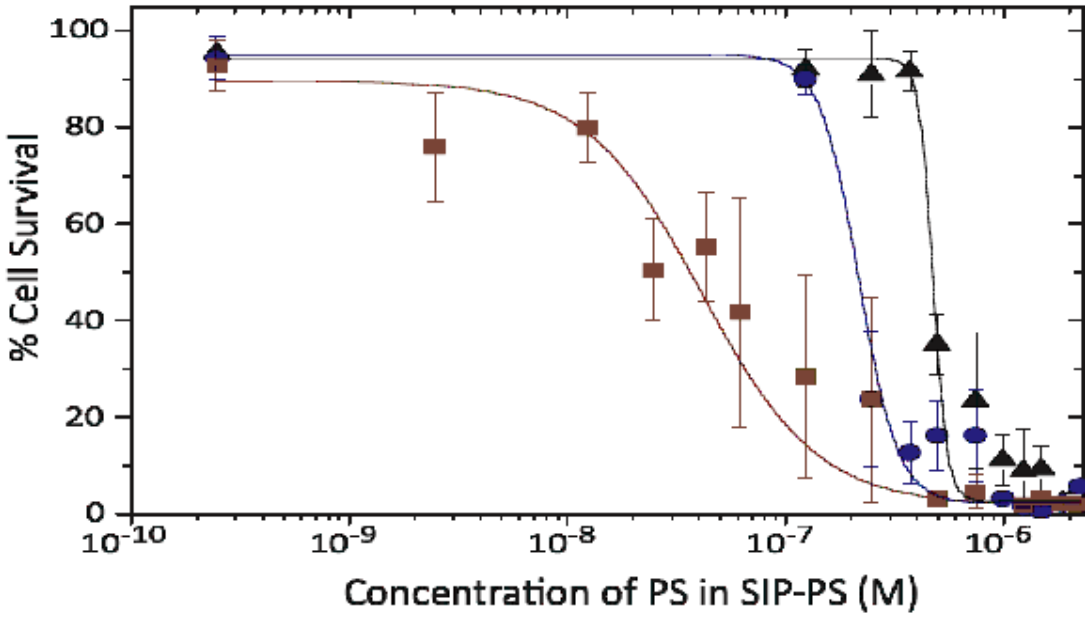

Figure 38: *In vitro* phototoxicity assay of **PS4**-SIP(L19) (black ▲), **22**-SIP(L19) (red ■) carried out on LM fibroblasts using MTS assay.

4.7 Summary / further work

The synthesis of a hydrophilic porphyrin bearing a maleimide group (**25**) has been demonstrated. The photosensitiser was conjugated to cysteine residues expressed by SIP(L19). The well characterised immunoconjugate (**25**-SIP(L19)) possessed no detectable non-covalently bound photosensitiser and retained the targeting efficiency of the antibody moiety. The photoactivity of **25**-SIP(L19) was substantially greater than **PS3**-SIP(L19) and **22**-SIP(L19), due to the presence of a hydrophilic linker in-between the antibody and photosensitiser moieties. It was postulated that the longer hydrophilic chain, provides the conjugated porphyrins with a greater freedom of movement, reducing the probability of the porphyrins coming together and quenching each others excited state, therefore improving the overall photoactivity.

Time permitting, a library of photosensitiser analogues could be synthesised bearing hydrophilic chains of varying lengths. The influence of chain length and/or hydrophilicity of the chain, on the immunoconjugates characteristics could then be evaluated.

Chapter 5: Towards a bioconjugatable porphyrin dimer

5.1 Introduction

Enhancing the photoactivity of a photoimmunoconjugate can be achieved by increasing photosensitiser loading. Since the reduced SIP(L19) only has two cysteine residues available for bioconjugation, the only strategy available for increasing porphyrin loading would be to increase the number of photosensitisers connected to each thiol group. It was postulated that the production of porphyrin dimers, bearing a single maleimide functionality, could effectively double the photosensitiser to antibody loading, and thus increase the overall photoactivity of the immunoconjugate.

5.2 Porphyrin dimers

5.2.1 Porphyrin dimer synthetic aims

From a retro-synthetic perspective, the target porphyrin dimer could be a product from the coupling of two different porphyrins, as illustrated in Figure 39. The proposed porphyrin would possess three functional groups in the *meso*-positions, which could be converted into hydrophilic moieties (**X**), with the remaining *meso*-position is occupied by a functional group (**A**) which could facilitate covalent attachment to another porphyrin. The second porphyrin would therefore have the complementary functionality (**B**), enabling attachment to the initial porphyrin via a reaction with functional group **A**. The second porphyrin would also possess a protected functional group (**Y**) that could be transformed into the bioconjugatable group, with the remaining *meso*-positions occupied by additional water solubilising groups (**X**). Thus in order to produce the porphyrin dimer, the initial porphyrin synthesised could be the product of a mixed condensation between aldehydes bearing groups **A** and **X**, and pyrrole. The *trans*-porphyrin would be synthesised from the condensation of a dipyrromethane bearing functionality **X**, and aldehydes bearing groups **B** and **Y**.

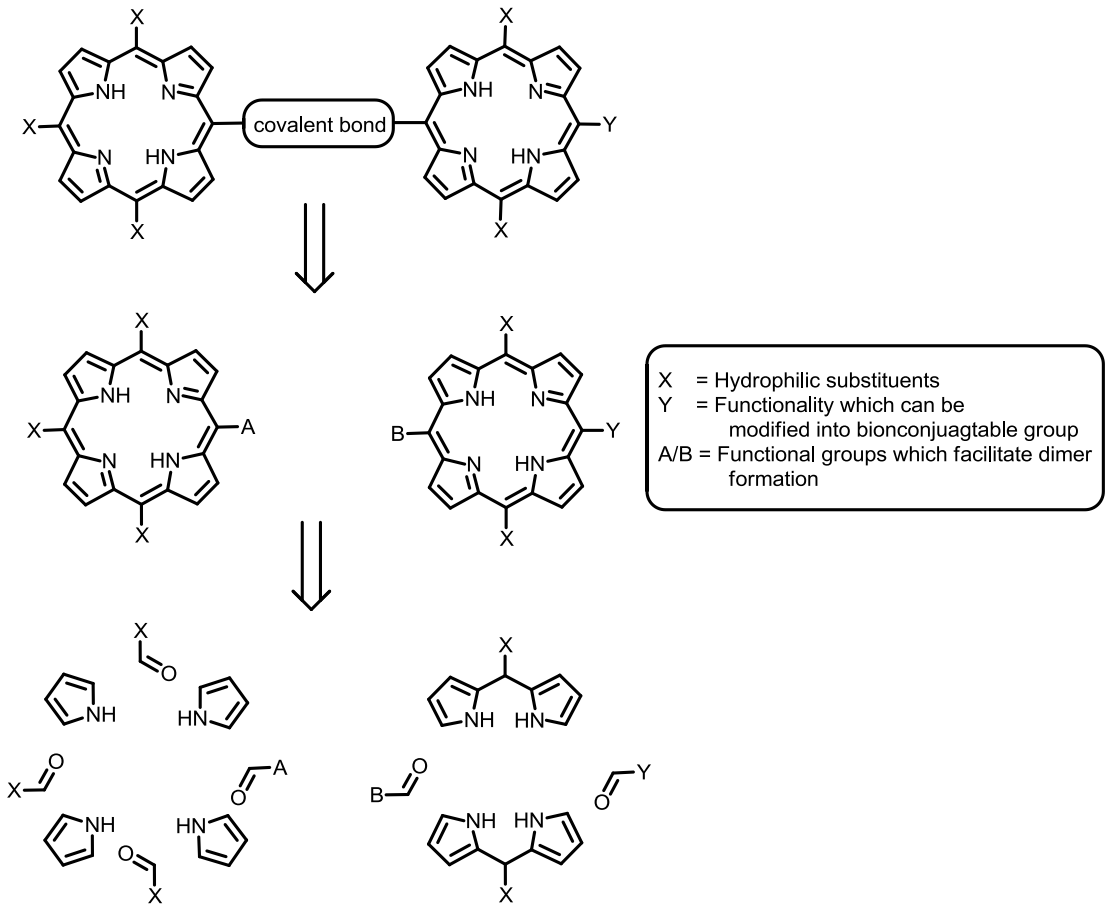

Figure 39: Retro-synthesis of bioconjugatable porphyrin dimer.

The literature describes a wide variety of approaches for coupling porphyrins together, including: reductive aminations;[136] amide formation, resulting form the reaction between an acid chloride and amino groups;[190,191] a nucleophilic substitution reaction, using an alkyl chain terminating in a halogen, and porphyrin bearing a hydroxyl group;[192] Grubb's catalysis,[193] imine formation,[194] and Sonogashira coupling.[194] Each of these techniques could be reviewed in there own right, however these approaches were not deemed appropriate for the purpose of synthesising the target porphyrin dimer required here, and will not be discussed further.

5.2.2 Suzuki coupling

The Suzuki reaction refers to the palladium catalysed cross-coupling between organic halides or triflates with organoboron compounds, in the presence of an inorganic base, resulting in the formation of a carbon-carbon bond. The reaction proceeds regio- and stereo-selectively, under relatively mild conditions, tolerating a variety of sensitive functional groups.[195] The organo-boron compound is generally stable under aqueous conditions, and an evaluation of the reaction, under both aqueous and anhydrous conditions, suggested that the presence of water did not influence the reaction yields.[196] The Suzuki catalytic cycle, depicted in Figure 40, initially involves the oxidative addition of the aryl halide to the palladium catalyst. The base then exhibits dual functions in the cycle; displacement of the halide by metastasis, and coordination with the boron atom, inducing nucleophilicity, so that the subsequent transmetallation with the palladium(II) complex can occur. Finally, reductive elimination yields the coupled product with re-generation of the palladium catalyst.[195,197] The catalytic cycle involves the reduction and oxidation of the palladium catalyst, thus the reaction is generally performed in de-oxygenated solvents.

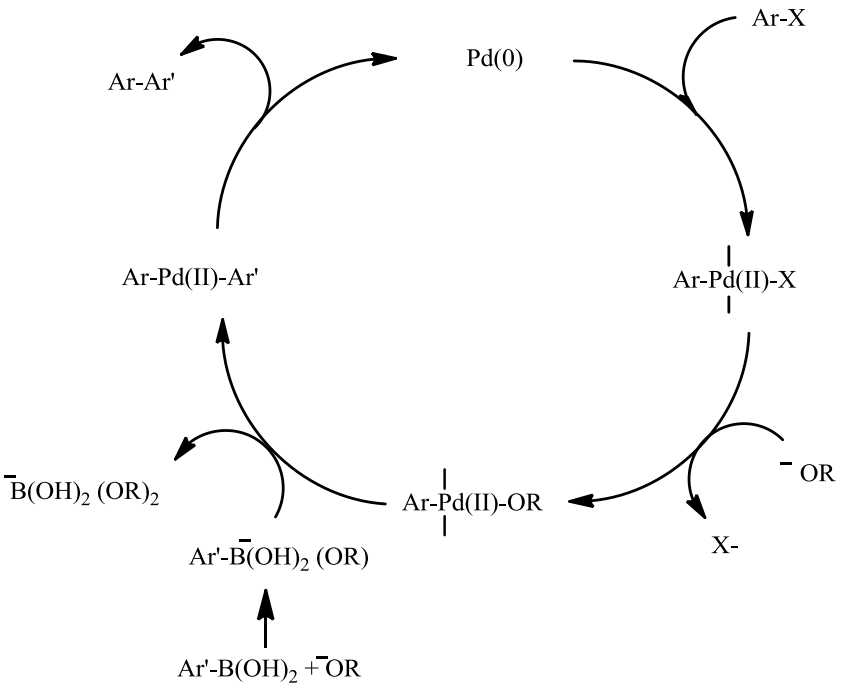

Figure 40: Suzuki catalytic cycle.[195]

Zhou *et al.*[198] have described the synthesis of a porphyrin dimer using Suzuki coupling conditions. The boronic ester porphyrin: 5-(4-boronatophenyl)-10,15,20-tetraphenyl porphyrin, was synthesised via the dehydration of benzaldehyde and 4-formylphenyl boronate with pyrrole, under Lindsey conditions,[120] furnishing the porphyrin in 33 % yield. The porphyrin boronate, 2-bromo-TPP, tetra(triphenylphosphine)palladium(0) and anhydrous potassium carbonate were dissolved in degassed toluene, and the resulting solution was heated at 90-100 ^{o}C, for 48 hours, under an inert atmosphere. Following work-up and chromatographic separation the dimer was isolated with a yield of 88 %.

A similar approach has been utilised for the production of a dimer between 5,15-bis(3,5-di-*tert*-butylphenyl)-10-mesityl-20-(4-(4,4,5,5-tetramethyl-1,3,2-dioxaborolan-2-yl)phenyl)porphyrin and 5,15-bis(3,5-di-*tert*-butylphenyl)-10-iodo-20-mesitylporphyrin, as illustrated in Scheme 54. The boronic ester porphyrin was synthesised from the acid catalysed condensation of a carbinol, and dipyrromethane bearing the boronic ester, with the porphyrin isolated in 16 % yield. The boronic ester porphyrin, iodo-porphyrin, tetra(triphenylphosphine)palladium(0) and anhydrous potassium carbonate were dissolved in a mixture of toluene and dimethylformamide, and the mixture was purged with argon. The mixture was heated at 75 ^{o}C for 3 hours, at which time, additional catalyst was added. The resulting mixture was heated at 90 ^{o}C for a further 15 hours, and following chromatographic separation, the dimer was afforded in 70 % yield.[199]

The incorporation of the boronic ester moiety during porphyrin formation has also been achieved under Adler conditions,[114] via a mixed condensation reaction, although only a low yield (3 %) of the target porphyrin was obtained.[145]

The zinc complex of 5-(3-iodophenyl)-10,15,20-tris(3,5-di-*tert*-butylphenyl)porphyrin has been used for the synthesis of a porphyrin trimer, using a tri(2,4,6-(4,4,5,5-tetramethyl-1,3,2-dioxaborolan-2-yl)phenyl linker. The boronic ester linker, iodo-porphyrin and sodium carbonate were dissolved in a mixture of toluene, ethanol and water, and the resulting solution was degassed. Tetra(triphenylphosphine)palladium(0) was added, and the reaction was heated at 80 ^{o}C, for 4 days, under an inert atmosphere. Following work-up and preparative TLC, the zinc porphyrin trimer was isolated in 80 % yield.[200]

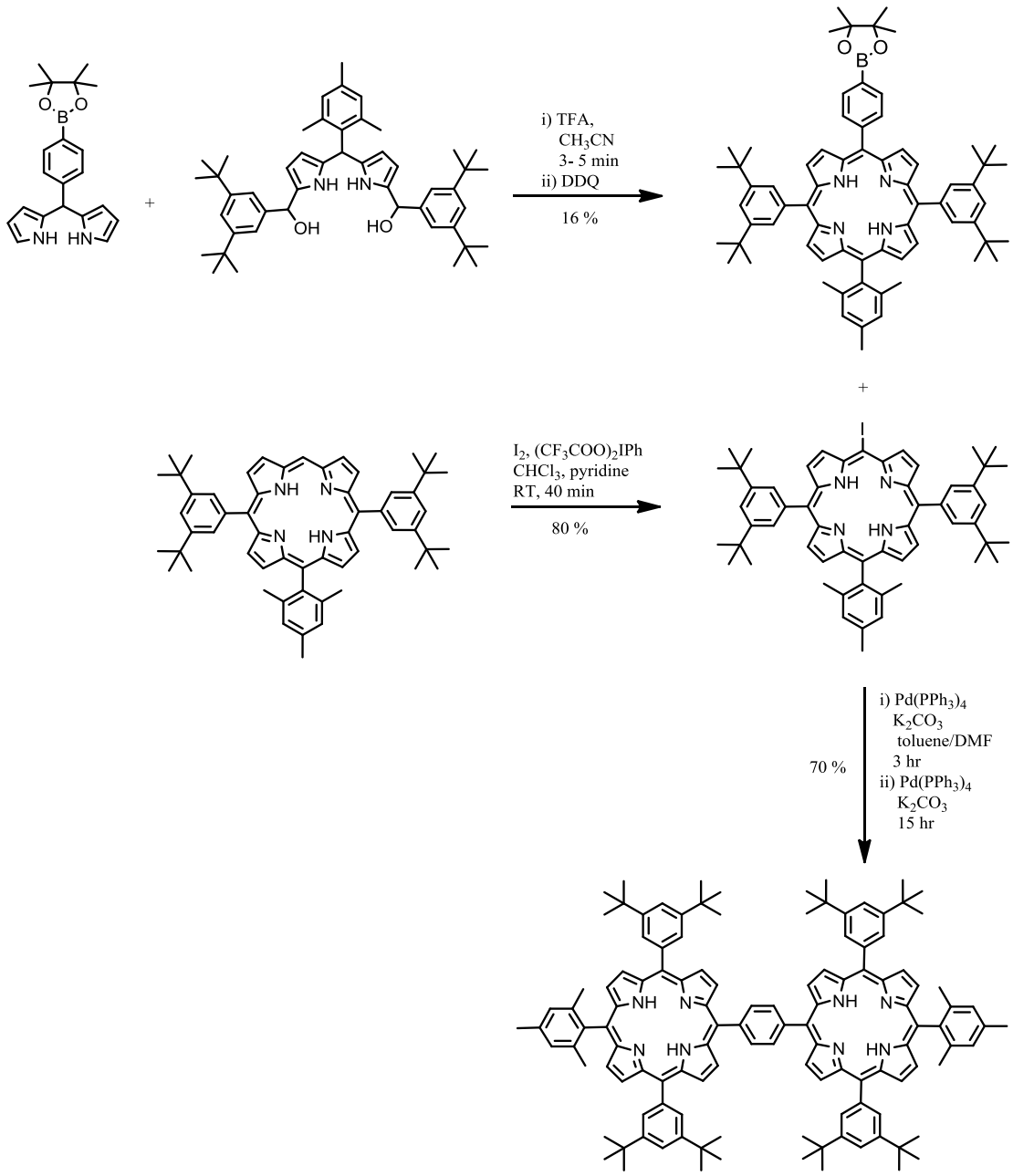

Scheme 54: Porphyrin dimer synthesis.[199]

Yu *et al.*[201] have reported the addition of a boronic ester to the zinc(II) complex of 5-bromo-10,20-dimesitylporphyrin, as illustrated in Scheme 55. A Schlenk flask was charged with 4,4,5,5-tetramethyl-1,3,2-dioxaborolane, triethylamine and dichlorobis(triphenylphosphine)palladium(II), under an inert atmosphere. 1,2-Dichloroethane was added, and the mixture was heated at 85 ^{o}C for 1 hour, with the boronated porphyrin isolated in 93 % yield. The boronated porphyrin was added to bis-(5-(4-iodophenyl)dipyrrinato)palladium(II), barium hydroxide octahydrate and tetra(triphenylphosphine)palladium(0). The reaction vessel was purged with argon and dimethoxyethane and water were added. The reaction was stirred at 80 ^{o}C, for 2 hours,

and following work-up and column chromatography, the target complex was furnished in 50 % yield.

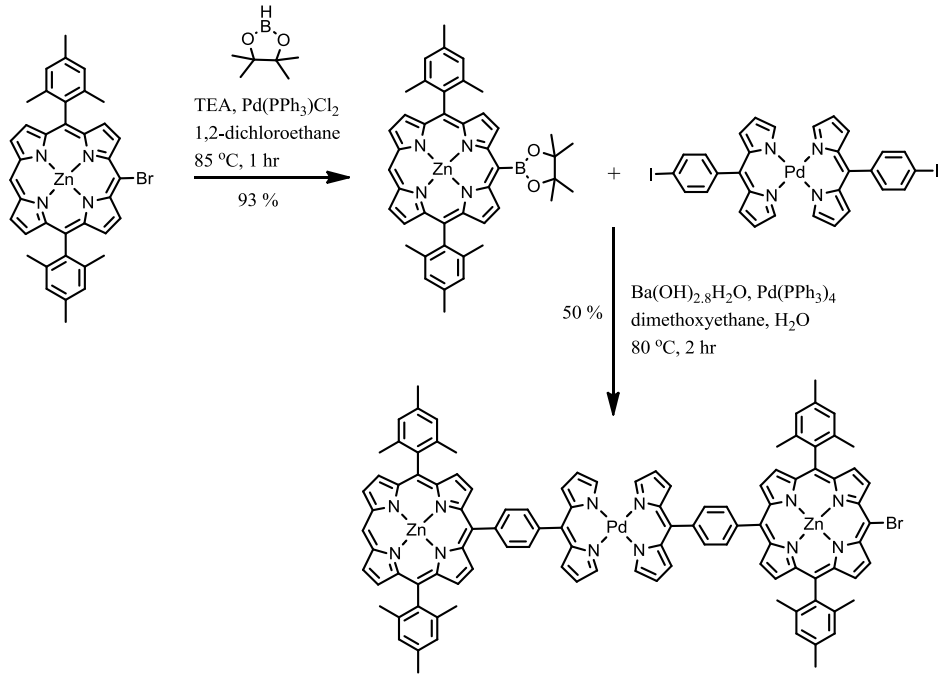

Scheme 55: Synthesis of bis(5-4-(5,15-dimesitylporphyrinatozinc(II)-10-yl)phenyl)dipyrro)palladium (II).[201]

The addition of a boronic ester to a pyridyl derivative bearing a bromo functionality, can be achieved using bis(pinacolato)diboron, as demonstrated by Aspley and Williams.[202] Bis(pinacolato)diborone, 4-(4-bromophenyl)-2,2:6,2-terpyridine, potassium acetate and [1,1′-bis(diphenylphosphino)ferrocene]dichloropalladium(II) were added to a Schlenk flask, under an inert atmosphere. Dry, degassed dimethylsulfoxide was added, and the mixture was stirred at 80 ^{o}C, for 6 hours under an inert atmosphere. The product was extracted into toluene, and following work-up, the boronic ester derivative was isolated in 42 % yield. The reaction conditions were evaluated, with the rate of the reaction increasing in more polar solvents, and stronger bases, such as potassium carbonate, promote further coupling of the desired boronic ester product with the initial halide. Furthermore, the reaction is tolerant towards diverse functionalities such as nitro, cyano and ester groups.[197] Additionally iodo-derivatives react more rapidly than bromo-analogues, producing the corresponding boronated derivatives in higher yields.[203]

The Suzuki coupling strategy has been applied to pyridyl containing porphyrins. A solution of 5,10,15,20-tetra(5-bromo-3-pyridyl)porphyrin in toluene and methanol was

treated with 2-furanboronic acid, tetra(triphenylphosphine)palladium(0) and an aqueous solution of sodium carbonate. After the mixture was stirred at 70 ^{o}C for 20 hours, additional palladium catalyst and 2-furanboronic acid was added, and the reaction was continued for a further 15 hours. The porphyrinic product was isolated in 44 % yield, after work-up and flash chromatography.[170]

Interestingly, a variety of Suzuki couplings has been achieved using metal complexes of 5-(4-bromophenyl)-10,15,20-(4-pyridyl)porphyrin, as depicted in Figure 41. It was found that couplings with the non-metallated porphyrin were unsuccessful and the zinc porphyrin complexes gave the most favourable reaction times and yields.[204]

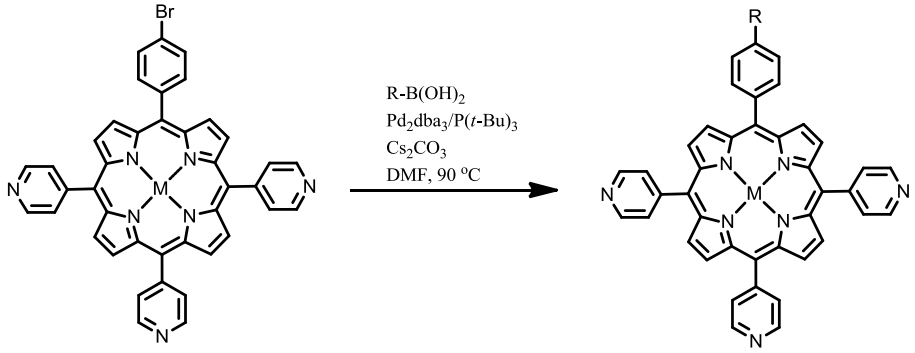

M	R	Time (hours)	Yield (%)
Zn	4-methoxyphenyl	6	65
Ni	4-methoxyphenyl	24	58
Zn	4-acetylphenyl	5	75
Ni	4-acetylphenyl	24	71
Zn	*trans*-1-hexen-1-yl	6	76

Figure 41: Suzuki couplings involving metal complexes of 5-(4-bromophenyl)-10,15,20-(4-pyridyl)porphyrin.[204]

5.2.3 Click chemistry

The criteria describing the concept of 'Click reaction' were first coined in 2001:

' The reaction must be modular, wide in scope, give very high yields, generate only inoffensive by-products that can be removed by non-chromatographic methods, and are stereospecific (but not necessarily enantioselective). The required process characteristics include simple reaction conditions, readily available starting materials and reagents, the use of no solvents or a solvent which is benign or is easily removed, and simple product isolation.[205,206]

At elevated temperatures, the Huisgen 1,3-dipole addition of azide to alkyne derivatives, leads to the formation of a triazole, in the 1,4 and 1,5 regioisomeric forms. It was discovered in 2001 that copper(I) salts accelerate the reaction and leads to the production of the 1,4-regioisomer exclusively, as shown in Figure 42.[205,207] The catalytic cycle requires copper(I), which can be provided by using copper(I) salts or the *in situ* reduction of copper(II) salts, such as copper(II) sulphate pentahydrate using reducing agents such as sodium ascorbate, or the inexpensive copper on charcoal. The catalytic cycle starts with the formation of the active copper acetylide intermediate, thus the presence of base is required.[205] It has been proposed that the [2+3] cycloaddition can then occur directly, or via the step-wise addition of the azide to the copper complex, which subsequently leads to the formation of the 6-membered-copper containing intermediate. A ring contraction then occurs, and protonation results in the production of the triazole product.[207,208]

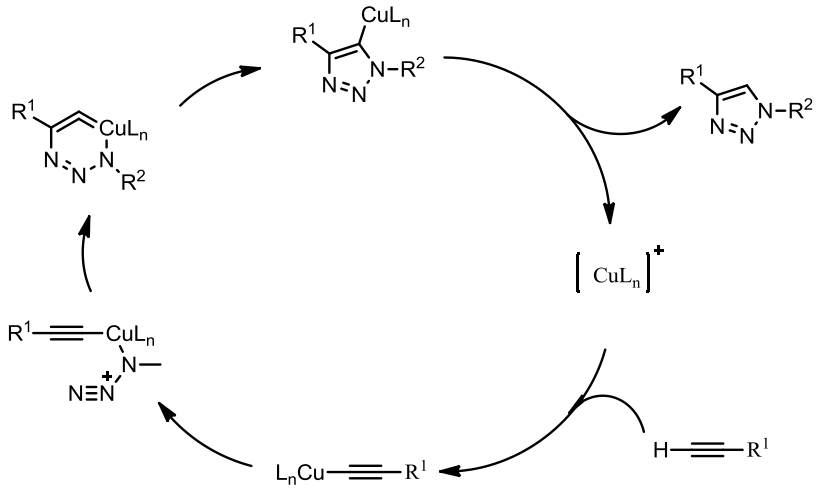

Figure 42: Click catalytic cycle.[207]

The azide moiety is stable towards dimerisation and hydrolysis, hence is considered to be a convenient 1,3 dipolar reagent. However, due to the general toxicity of azides, medicinal chemists utilise the reaction with caution.[206] As azide and alkyne substituents can be incorporated into compounds via a variety of methods, the potential of the [2+3] cycloaddition of azide and alkyne as a Click reaction was realised.[205] From a medicinal point of view, the triazole group is relatively stable due to its aromatic nature, and is therefore inert under many acid/base and oxidative/reductive conditions.[205] Furthermore, the triazole group is stable to hydrolytic cleavage and can therefore be used for biological applications.[208]

Shen *et al*.[209] have demonstrated that the amino group, of the nickel(II) complex of 2-amino-TPP, can be transformed into an azide group, which can subsequently be coupled to a porphyrin which possesses an alkyne group in the *meso*-position. The amino-porphyrin was dissolved in tetrahydrofuran and was treated with a saturated solution of sodium nitrite in a mixture of water and concentrated sulphuric acid, for 30 minutes at ambient temperature. A saturated solution of sodium azide in water was added drop-wise to the stirred mixture. After 20 minutes, the product was extracted into dichloromethane and was chromatographically separated, affording the corresponding azido-porphyrin in 95 % yield. The nickel(II) complex of 5,15-di(phenyl)-10-ethynylporphyrin was added to a mixture of the azido-porphyrin,

copper(II) sulphate pentahydrate, sodium ascorbate dissolved in dimethylformamide, and the resulting mixture was stirred at 50 ^{o}C for 1.5 hours. The product was extracted into dichloromethane, washed with water, dried and purified by flash chromatography, furnishing the dimer in 98 % yield. Interestingly, an intramolecular cyclisation reaction

occurs if the azido-porphyrin is dissolved in toluene, and heated at reflux for 2 hours. A similar approach for synthesising an azido porphyrin has been described for the synthesis of the zinc(II) complex of 5-(4-azidophenyl)-10,15,20-tri(4-tert-butylphenyl)porphyrin, as illustrated in Scheme 56. The diazotisation of the free-base amino porphyrin dissolved in trifluoroacetic acid was achieved by the addition of sodium nitrite in water, and the diazonium salt was then converted into the azide functionality via treatment with sodium azide in water, affording the azido porphyrin in 95 % yield, after purification. The azido porphyrin was then quantitatively converted into the zinc(II) complex, using zinc acetate. An evaluation of the reaction conditions leading to the formation of a porphyrin dimer was then described, using the zinc(II) complexes of the azido-porphyrin and 5-(4-ethynylphenyl)-10,15,20-tri(4-tert-butylphenyl)porphyrin, as shown in Scheme 56. It was reported that the typical click coupling conditions, using copper(II) sulphate pentahydrate and ascorbic acid were unsuccessful, and the coupling was only achieved using more novel copper catalytic systems. The couplings were attempted using free-base porphyrin precursors, which resulted in copper being inserted into the porphyrin core.[210]

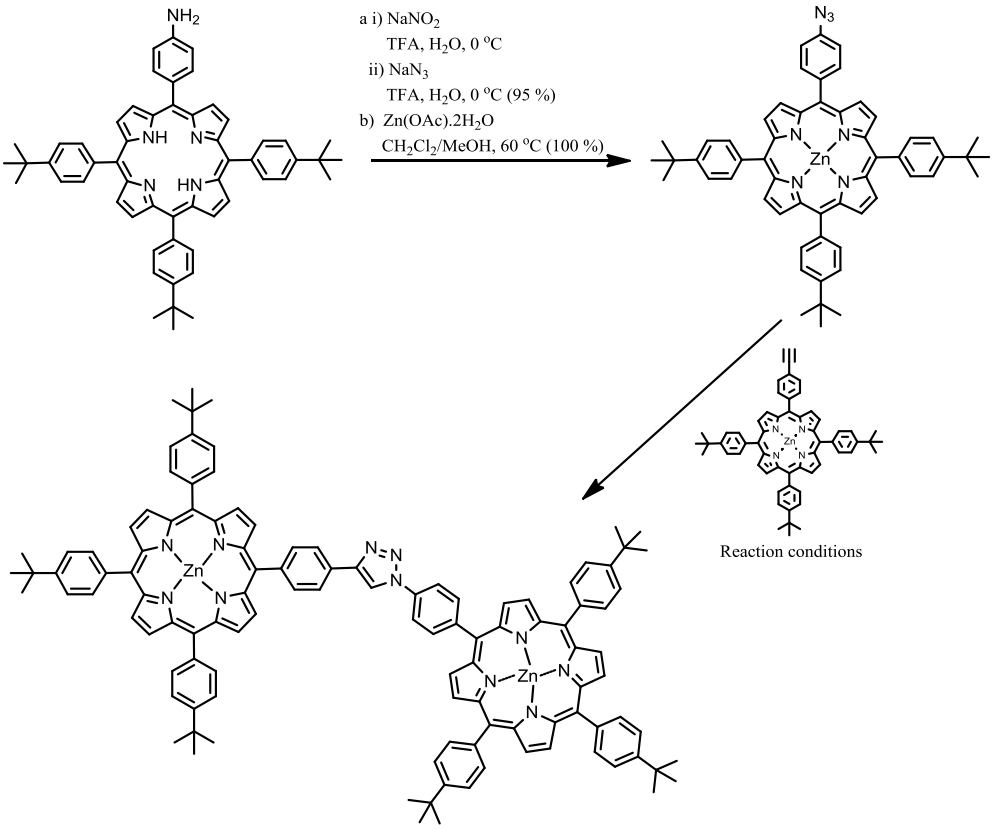

Reaction Conditions	Yield (%)
$CuSO_4$, $4H_2O$, ascorbic acid, DCM, Et_3N (5:1), 60 ^oC, 12 h	0
$CuSO_4$, $4H_2O$, ascorbic acid, 40 ^oC, DMSO/DCM/ Et_3N (10:5:1), 4 hrs	0
CuI, $4H_2O$, 1,6-dimethyl-pyridine, $CHCl_3$, 0 ^oC 12 hrs, then RT 72 hrs	0
$Cu(PPh_3)_3Br$, DIEA/THF (1:5), 50 ^oC, 3 hrs	23
$Cu(P(OEt)_3)I$, DIEA/THF/H_2O (1:1:5), 50 ^oC, 12 hrs	29
(SIMes)CuBr, THF/H_2O (3:1), 45 ^oC, 12 hrs	32
(SIMes)CuBr, THF/H_2O (3:1), 45 ^oC, 60 hrs	44

Scheme 56: Evaluation of different reaction conditions for the synthesis of a porphyrin dimer.[210]

The addition of an azide moiety to a pre-formed porphyrin can also be achieved by the nucleophilic substitution reaction between sodium azide and a alkyl halide bearing porphyrin, as reported by Punidha *et al*.[211] A solution of 5-(4-hydroxyphenyl)-10,15,20-tri(*p*-tolyl)porphyrin and potassium carbonate dissolved in dimethylformamide was treated with a large excess of 1,3-dibromopropane, and the resulting mixture was stirred at room temperature for 10 hours. The 5-(4-(3-bromo)-propyloxyphenyl)-10,15,20-tri(*p*-tolyl)porphyrin was isolated in 88 % yield , after purification. The porphyrin bearing an alkyl halide and sodium azide, were dissolved in acetone, and the mixture was stirred at 80 ^oC for 12 hours. Once the reaction mixture

has been washed with water, dried, and chromatographically separated, the azido porphyrin was isolated in 76 % yield. The article also described the synthesis of a dithiaporphyrin derivative which bore a hydroxyl functionality, which was modified to possess an alkyne group. The dithiaporphyrin and sodium hydride were dissolved in dry tetrahydrofuran. Once the mixture had stirred at ambient temperature for 30 minutes, DABCO and propargyl tosylate were added, and the mixture was stirred for a further 12 hours. The alkyne porphyrin was produced in 52 % yield, after purification. The free-base azido porphyrin and alkyne dithiaporphyrin were dissolved in a mixture of water and acetic acid and copper(II) sulphate pentahydrate and sodium ascorbate were subsequently added, the mixture was then stirred at 80 ^{o}C for 96 hours. The porphyrin-dithiaporphyrin adduct was isolated in 46 % yield, after chromatographic separation, as depicted in Scheme 57.

A hydroxyl group attached to a phenyl group can also be modified to bear an azide moiety. A solution of the hydroxyl/phenyl derivative dissolved in dimethylformamide was treated with potassium carbonate, lithium bromide and 3-azidopropyltosylate; and the reaction mixture was heated at 80 ^{o}C for 96 hours, yielding the azido compound in 33 % yield.[212] Although this approach for the introduction of azido functionality to a hydroxyl group has been achieved, this particular strategy has not been applied to porphyrin chemistry.

Vicente and co-workers,[213] have reported the mono-alkylation of 5,10,15,20-tetra(4-hydroxylphenyl)porphyrin using 3-bromo-1-yne, with the reaction conducted in anhydrous dimethylsulfoxide in the presence of potassium carbonate, at 60 ^{o}C for 15 minutes, under an inert atmosphere. The free base porphyrin was isolated, and converted into the zinc(II) complex, using zinc acetate, giving an overall yield of 28 %. Click reactions were then performed, employing carbohydrates which bore azide functionalities, with the reactions performed using copper(II) sulphate pentahydrate and sodium ascorbate in a mixture of *tert*-butanol and water, with the reaction heated at 70 ^{o}C for 24 hours. The porphyrin-carbohydrate compounds were produced in 92 % and 88 % yields. It was found that the reaction had to be heated to at least 50 ^{o}C for the click reaction to occur. Furthermore, the reactions were attempted using the free-base porphyrin, but failed to produce the target compound.

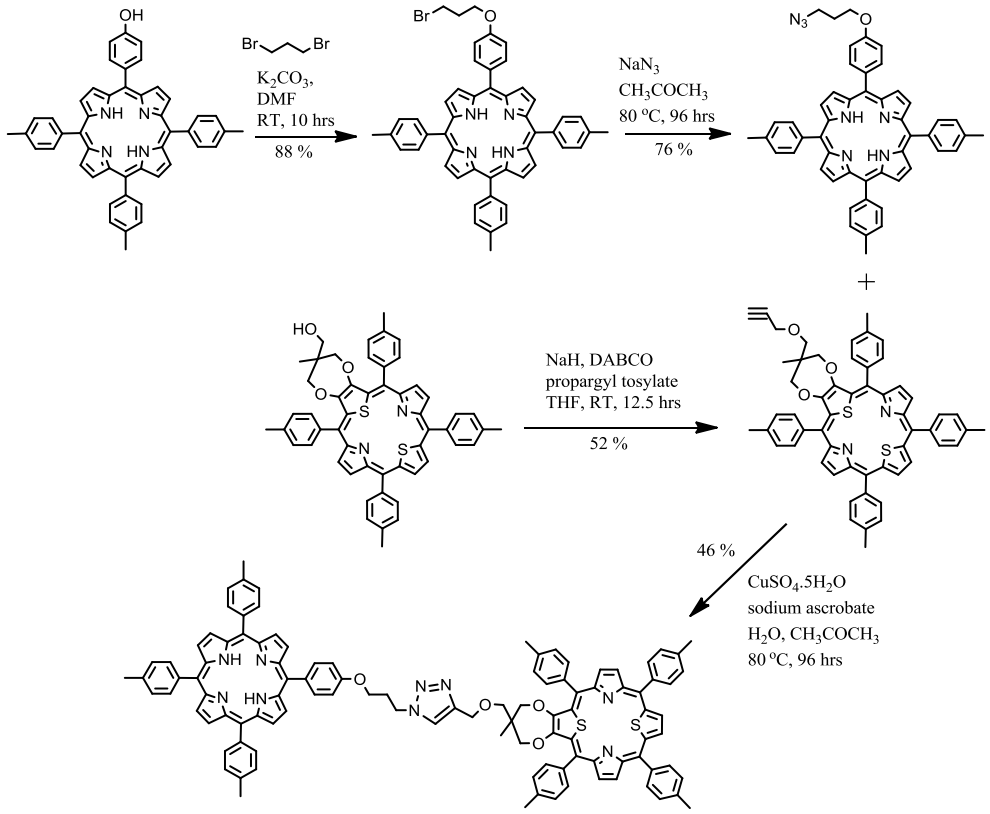

Scheme 57: Syntheses of a porphyrin-thiaporphyrin adduct.[211]

The mono-alkylation of 5,10,15,20-tetra(2,3,4,5,6-pentaflourophenyl)porphyrin has been reported, using propargyl alcohol in the presence of potassium carbonate. The reagents were dissolved in dimethylsulfoxide, and the resulting mixture was heated at 50 °C for 4 hours, furnishing the alkylated porphyrin in 86 % yield. A variety of quinolone derivatives, which bore azide functionalities, were then used to form porphyrin-quinolone conjugates with the modified porphyrin. The porphyrin, quinolone, copper(II) sulphate pentahydrate and ascorbic acid were dissolved in dimethylformamide. The reactions were performed for 8-72 hours, affording the conjugates in 53-93 %.[214]

5.3 *Trans*-substituted porphyrins

The synthesis of a *trans*-porphyrin could be achieved via a mixed aldehyde condensation reaction with pyrrole, using a 1:1 ratio of aldehydes, with pyrrole. Using aldehyde **A** and **B**, the statistical distribution of porphyrins produced under these conditions is: $\mathbf{A}_4$ (6.25 %), $\mathbf{A}_3\mathbf{B}$ (25 %), *cis*-$\mathbf{A}_2\mathbf{B}_2$ (25 %), *trans*- $\mathbf{A}_2\mathbf{B}_2$ (12.5 %), $\mathbf{AB}_3$ (25 %), $\mathbf{B}_4$ (6.25 %), assuming the reactivity's of the aldehydes are the same and no scrambling occurs.[215] Thus, assuming the total yield of the porphyrin is 20 %, only 2.5 % would be the target *trans*-porphyrin.

A 2+2 strategy, using a dipyrromethane-carbinol derivative and a dipyrromethane would also result in the production of a *trans*-porphyrin. However, reactions employing pyridyl-dipyrromethanes tend to lead to lower than expected yields, and the acetamido group is incompatible with the required Grignard reagent, as discussed in Chapter 3.[152,153]

Ravikanth *et al*.[216] have reported the synthesis of 5,15-dimesityl-10-(3-(2-(trimethylsilyl)ethynyl)phenyl)-20-(4-iodophenyl)porphyrin using a condensation reaction between 3-(2-(trimethylsilyl)ethynyl)benzaldehyde and 4-iodobenzaldehyde with 5-mesityldipyrromethane. Firstly, the 3-(2-(trimethylsilyl)ethynyl)benzaldehyde was prepared via a Sonogashira coupling reaction between 4-iodobenzaldehyde and (trimethylsilyl)acetylene, employing tri(dibenzylideneacetone)dipalladium(0) and triphenylarsine in triethylamine, affording the product in 81 % yield. The aldehydes and dipyrromethane were used to produce the porphyrin under Lindsey conditions,[120] affording the *trans*-porphyrin in 14 % yield after purification. Under these conditions, only 3 porphyrins are produced, thus in comparison to a mixed condensation using aldehydes and pyrrole, less chromatographic separation would be required. However, the reaction mixture did exhibit other trace porphyrinic fractions, attributed to scrambling of a polypyrrolic intermediate

Littler *et al*.[217] have investigated the acid catalysed rearrangement, of the poly-pyrrolic intermediate, which occurs during a dipyrromethane and aldehyde condensation, as shown in Figure 43. It was found that reactions employing dipyrromethanes which have sterically hindered substituents in the *meso*-position e.g. mesityl group, exhibit a lower degree of scrambling in comparison to reactions which use sterically unhindered groups, such as phenyl functionalities. The condensation reaction, between 5-mesityldipyrromethane and various aldehydes, was investigated. It was discovered that scrambling can be circumvented if the reaction was performed at ambient temperature,

in dichloromethane, using trifluoroacetic acid at a concentration of 17.8 mM, with 5-mesityldipyrromethane and aldehyde at a concentration of 10 mM. It was also observed that using anhydrous solvents did not affect the porphyrin yield. An extensive study was then conducted, to obtain reaction conditions which suppressed scrambling, for reactions involving sterically un-hindered dipyrromethanes. While analysing the reaction between 5-(4-iodophenyl)dipyrromethane and 4-(2-(trimethylsilyl)ethynyl)benzaldehyde, two sets of reaction conditions were identified which resulted in reasonable yields, with little or no scrambling occurring:

1. A solution of dipyrromethane (10 mM) and aldehyde (10 mM) in acetonitrile, was treated with boron trifluoride etherate (1.0 mM) and ammonium chloride (100 mmol/L) at 0 ^{o}C, for typically 4 hours. Following DDQ oxidation and column chromatography, the *trans*-porphyrin was isolated in 8 % yield.
2. The dipyrromethane (100 mM) and aldehyde (100 mM) was dissolved in dimethylsulfoxide, and in the presence of ammonium chloride (316 mmol/L), the reaction was heated at 90 ^{o}C, for 24 hours, while exposed to air. The porphyrin was insoluble in dimethylsulfoxide and was isolated in 5 % yield, by filtration.

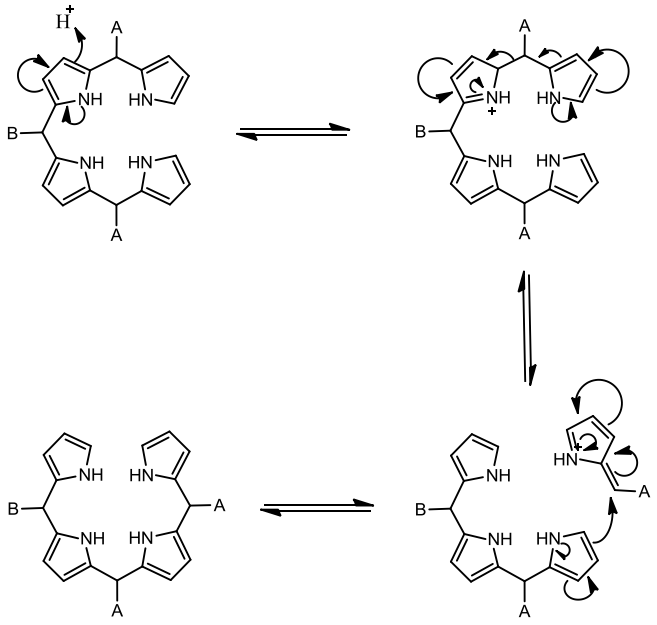

Figure 43: Scrambling of poly-pyrrolic intermediate.[217]

5.4 Synthetic strategy: porphyrin dimer via Suzuki coupling.

A Suzuki coupling approach was selected for the synthesis of the porphyrin dimer, as shown in Scheme 58. One porphyrin would possess three functionalities which could be transformed into water-solubilising groups, e. g. methylated pyridyl groups, and a single functionality enabling coupling to the *trans*-porphyrin. The *trans*-porphyrin would require a functionality which could be transformed into a bioconjugatable group, e g. acetamido, two hydrophilic moieties, and a functionality which would facilitate dimer production. Since Suzuki couplings involving pyridyl porphyrins have been reported,[170,204] it was selected as an appropriate strategy for coupling the two porphyrins together; thus one of the porphyrins would possess a boronic ester or acid, and the other porphyrin would possess a halide. The literature suggests that Suzuki couplings using pyridyl porphyrins requires the porphyrin to be metallated, highly reactive palladium catalysts and strong bases,[204] therefore developing chemistry using TPP derivatives was not attempted, as it was unlikely that the optimised conditions could be transferred to pyridyl porphyrin derivatives. It seemed more relevant to assess the conditions required for the Suzuki coupling between bis(pinacolato)diboron and the zinc(II) complex of 5-(4-bromophenyl)-10,15,20-tri(4-pyridyl)porphyrin. Although it was envisaged that these reaction conditions would not be directly used for coupling the two pyridyl porphyrins together, as a stronger catalytic systems would be required. If the boronic ester was on the tri-pyridyl porphyrin derivative, the *trans*-porphyrin would require a complementary halide, and an acetamido group which could be converted into the maleimide functionality using a literature method,[144] with pyridyl groups in the remaining *meso*-positions. Thus, the *trans*-porphyrin would be the product of the dehydration between 4-acetamidobenzaldehyde and 4-bromobenzaldehyde, with 4-pyridyldipyrromethane, as illustrated in Scheme 58. As it has been reported that scrambling of the poly-pyrrolic intermediate occurs during *trans*-porphyrin formation, conditions which circumvent the scrambling phenomena were employed. Due to the extremely high cost of acetonitrile at this time, the reaction using dimethylsulfoxide, in the presence of ammonium chloride, at 90 ^{o}C, was employed.[217]

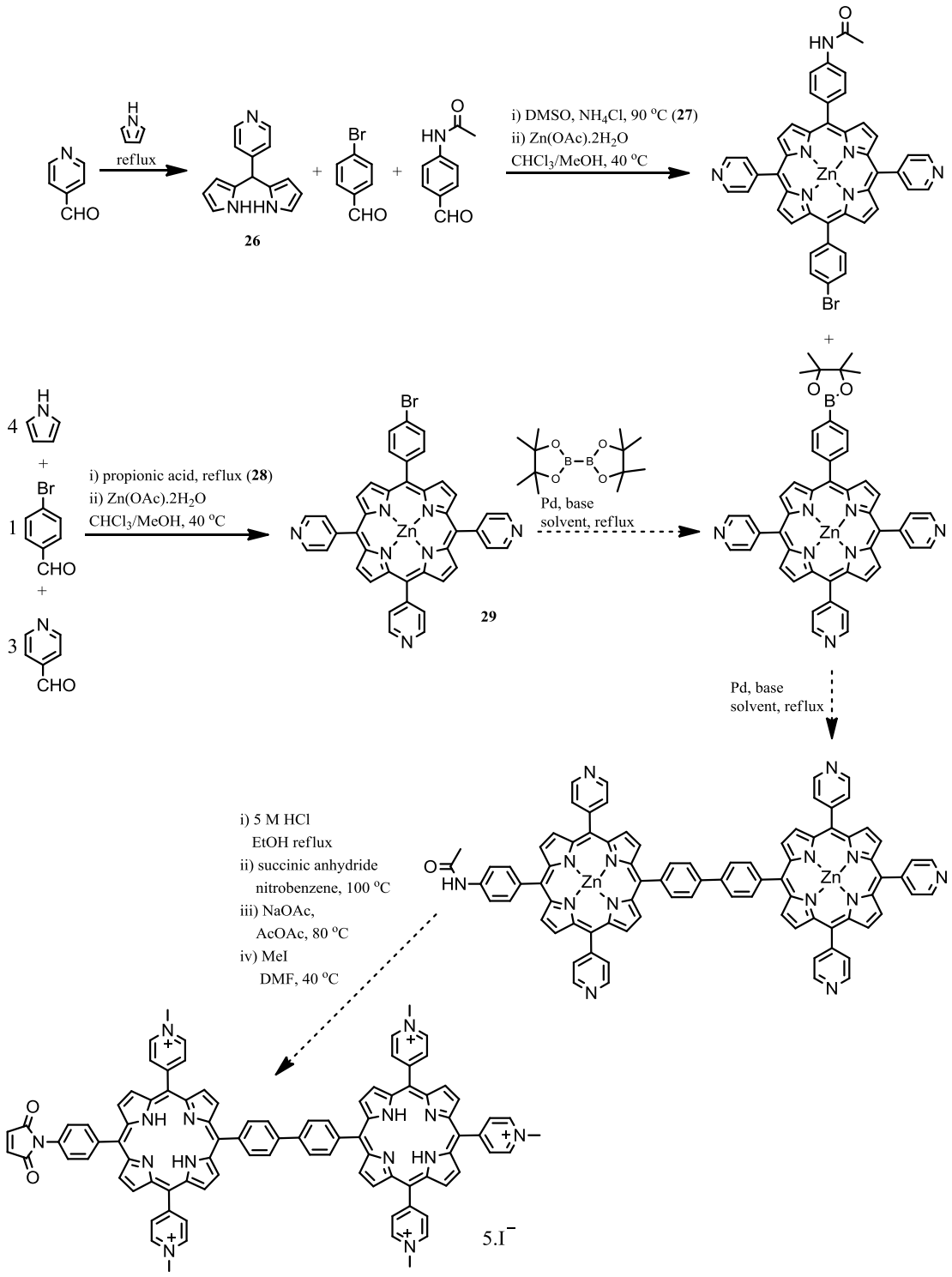

Scheme 58: Proposed synthesis of porphyrin dimer using Suzuki coupling.

5.4.1 Synthesis of 5-(4-acetamidophenyl)-10,20-di-(4-pyridyl)-15-(4-bromophenyl)porphyrin (27)

The literature suggested that the synthesis of 5-(4-pyridyl)dipyrromethane (**26**) via the traditional trifluoroacetic acid catalysed reaction between 4-pyridinecarboxaldehyde and pyrrole, only produced the desired dipyrromethane in relatively low yields; 35 %[218] and 26 %.[219] It has been reported that the reaction can be performed at elevated temperatures (85 ^{o}C), overnight, without the addition of the acid catalyst, and under these conditions **26** has been isolated in 58 % yield.[153] Following Scheme 58, and a known procedure,[153] **26** was isolated in 48 % yield after purification. After 15 hours, the reaction was complete, as indicated by TLC (silica, 30 % hexane/ethyl acetate), thus the excess pyrrole was removed under reduced pressure, and the residue was purified by flash column chromatography (silica, 20 % hexane/ethyl acetate). The fraction containing the crude product was identified and pure **26** was isolated as a white powder, after precipitation from acetone by the addition of hexane.

The assignment of the signals for the ^{1}H NMR spectrum for **26**, was achieved using a combination of 2D COSY and C-H correlation experiments, and was slightly different to reported determinations,[153] although deuterated dimethylsulfoxide was employed for the analysis. The broad singlet at 8.10 ppm coupled to the multiplet at 6.72-6.77 ppm, which in turn coupled to a quartet at 6.17 ppm. Therefore, the broad singlet at 8.10 ppm was assigned the N*H* protons, the multiplet at 6.72-6.77 ppm was designated the 1 and 9-C*H* environments and the quartet at 6.17 ppm was assigned to the 2 and 8-C*H*. The literature determination had the N*H* proton environment at 10.67 ppm.[153] Apart from the position of the N*H* proton signal, the ^{1}H NMR of **26** was in agreement with the published data. The mass spectrum gave the expected 223 *m/z* peak, therefore it was concluded that **26** had been produced.

The synthesis of **27** was performed using a modified procedure.[217] Appropriate stoichiometric quantities of **26**, 4-acetamidobenzaldehyde, 4-bromobenzaldehyde and ammonium chloride were dissolved in dimethylsulfoxide and the resulting mixture was heated to 90 ^{o}C for 24 hours. Once cooled, the mixture was then stirred at ambient temperature for a further 3 hours to ensure that the porphyrinogen had been oxidised. The TLC (silica, eluent: 10 % methanol/dichloromethane) of the reaction mixture exhibited three distinct porphyrin fractions and poly-pyrrolic by-products. The porphyrins appeared to be soluble in dimethylsulfoxide as filtration did not yield any porphyrinic product and the TLC of the filtrate showed the presence of the porphyrins.

Therefore a 5 % methanol/dichloromethane solution was used to extract the porphyrin from the dimethylsulfoxide, which was subsequently washed with copious amounts of water to remove the residual dimethylsulfoxide and ammonium chloride. The crude product was dried over anhydrous sodium sulphate to remove the residual water and the crude mixture was chromatographically separated (silica, eluent: 3 % methanol/dichloromethane). Once the relevant fraction was collected, **27** was isolated as a purple solid in 1 % yield, after precipitation from dichloromethane by the addition of methanol. The concentration of the dipyrromethane used (76 mM) was lower than the optimal concentration of 100 mM, which could have contributed to the low reaction yield. However, isolating the porphyrins from dimethylsulfoxide was the most likely process which led to a diminished yield. The reaction was only attempted once, thus the optimum reaction conditions were not identified.

The relevant section of the ^{1}H NMR spectrum for **27** is shown in Figure 44. All of the proton environments were accounted for; however 2D HMBC, COSY and C-H correlation experiments would have to be performed to reveal the exact assignments. The doublets at 7.84 ppm and 8.00 ppm appear to have a roof-top appearance, as does the doublets at 7.92 ppm and 8.07 ppm; all of which have the same coupling constant: J = 8.36 Hz. However the 2D experiments would provide the conclusive evidence for the signal assignments.

The mass spectrum for **27** is depicted in Figure 45 and shows a typical bromine isotope distribution pattern and exhibits the expected 752 *m/z* peak, therefore there was sufficient evidence that the reaction had occurred as postulated.

The metallation of **27** was not attempted.

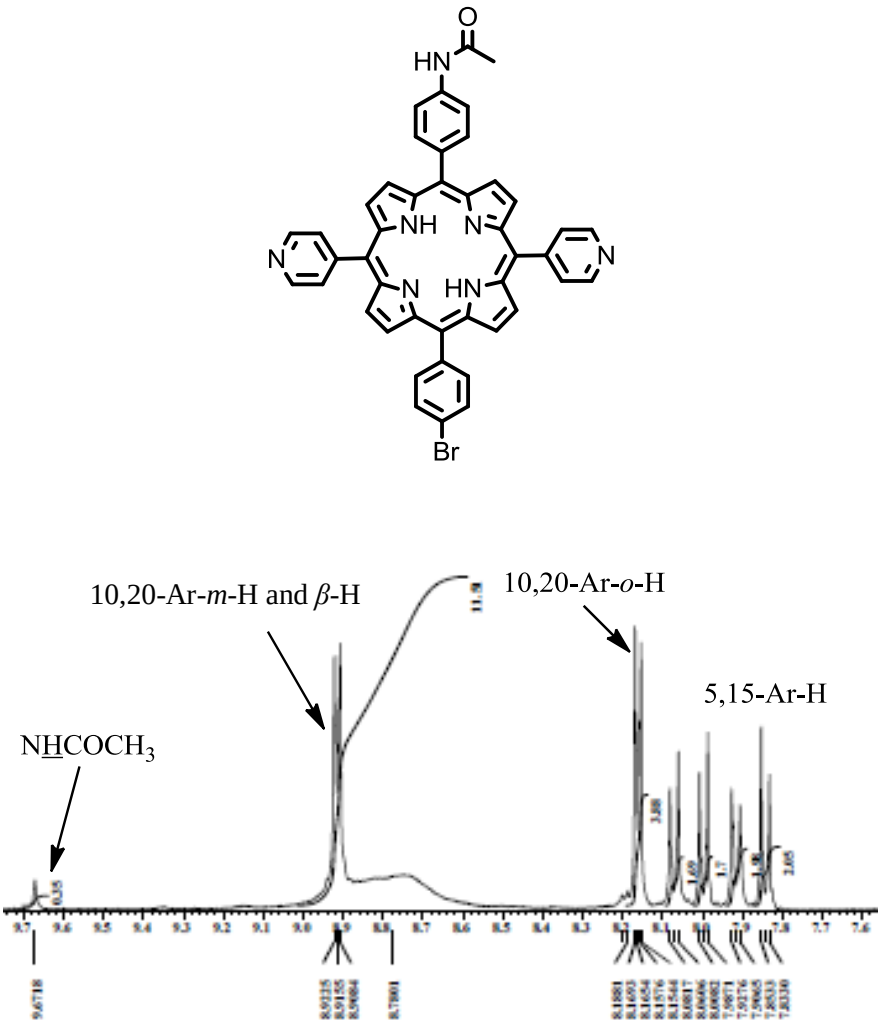

Figure 44: ^{1}H NMR spectrum of **27**.

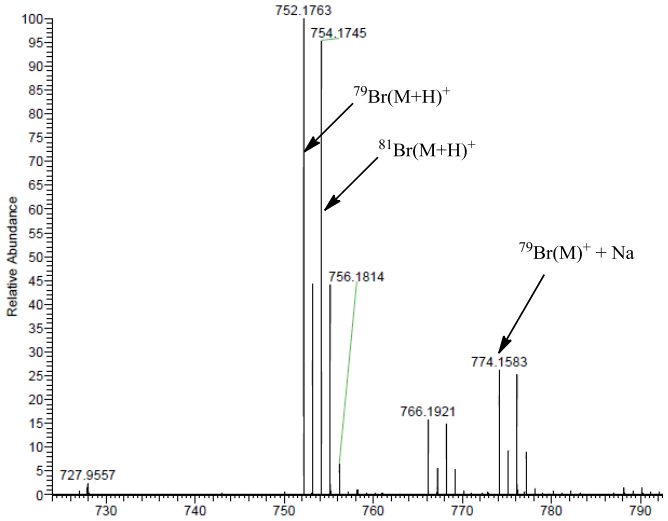

Figure 45: Mass spectrum of **27**.

5.4.2 Attempted synthesis of (5-(4-(4,4,5,5-tetramethyl-1,3,2-dioxaborinan-2-yl)phenyl)-10,15,20-tri-(4-pyridyl)porphyrinato) zinc(II)

5-(4-Bromophenyl)-10,15,20-tri(4-pyridyl)porphyrin (**28**) was synthesised using 4-bromobenzaldehyde, 4-pyridinecaroxaldehyde and pyrrole, under Adler-Longo conditions.[114] Compound **28** was isolated in 4 % yield. Although the ^{1}H NMR of **28** was not as refined as reported data,[220] all the proton environments were accounted for, and the mass spectrum gave the 695 *m/z* $^{79}Br(M)^{+}$ signal, and the expected isotope distribution pattern.

The insertion of zinc into the free-base **28** was achieved using a modified procedure.[221] A solution **28** dissolved in 25 % methanol/chloroform was treated with zinc acetate dihydrate for 2 hours at 40 °C. The solution was subsequently washed with a saturated sodium hydrogen carbonate solution; to remove un-reacted zinc acetate dihydrate and the acetic acid by-product; and water, and the organic layer was dried over anhydrous sodium sulphate; to remove residual water. The solvent was removed under reduced pressure, with **29** isolated in 83 % yield, after precipitation from chloroform by the addition of methanol. The characterisation studies confirmed that **29** had been synthesised.

The reaction between **29** and bis(pinacolato)diboron was attempted multiple times, as tabulated in Table 3, with the initial attempt following a published method.[197] An oven dried Schlenk flask which was cooled under argon, was charged with **29**, bis(diphenylphosphino)ferrocene]dichloropalladium(II), potassium acetate and bis(pinacolato)diborane under an argon atmosphere. The Schlenk flask was flushed with argon to remove residual oxygen. Anhydrous dimethylsulfoxide was degassed with argon to remove oxygen, and was added to the Schlenk flask under an argon atmosphere. The resulting mixture was sonicated to ensure the reagents were in solution. The reaction mixture was then heated at 80 °C, under an argon atmosphere while protected against light. The reaction was monitored over a 24 hour period, by working-up aliquots of the reaction mixture and subsequent analysis by TLC (silica, eluent: tetrahydrofuran), which indicated that no reaction was occurring and recovery of **29**. Therefore additional potassium acetate, bis(pinacolato)diborane and bis(diphenylphosphino)ferrocene]dichloropalladium(II) were added under argon. The reaction was monitored for a further 19 hours by TLC, but only **29** was observed.

The reaction was also attempted in a similar manner using dimethylformamide, heating the reaction at 80 °C, and tetrahydrofuran with heating the reaction at 50 °C. Both reactions were monitored over 48 hours, with **29** being recovered in both reactions, as indicated by TLC.

The conditions required for the palladium catalysed reaction between bis(pinacolato)diborane and a halo-arene were evaluated, and it was found that stronger bases such as potassium phosphate and potassium carbonate, promoted further coupling with the initial halo-arene.[197] As it appeared that no reaction was occurring between **29** and bis(pinacolato)diborane using the weakly basic potassium acetate, stronger bases were employed. Thus the reaction was repeated substituting potassium acetate with potassium carbonate, with the reactions being conducted in either dimethylformamide or dimethylsulfoxide. The reactions were monitored by TLC over a 72 hour period, with almost complete recovery of **29,** and trace polar fractions being observed in both cases. The trace fractions were more prominent for the reaction conducted in dimethylsulfoxide, thus subsequent reaction attempts were performed in dimethylsulfoxide.

The reaction was repeated in a similar manner, employing caesium carbonate or potassium phosphate as the base. Both reactions were monitored by TLC over a 72 hour period, which revealed that mainly **29** had being recovered, and the development of 2 polar trace fractions, which were more prominent for the reaction employing potassium phosphate.

Porphyrin	Palladium catalyst	Base	Solvent
29	$Pd(dppf)Cl_2$	KOAc	DMSO
29	$Pd(dppf)Cl_2$	KOAc	THF
29	$Pd(dppf)Cl_2$	KOAc	DMF
29	$Pd(dppf)Cl_2$	K_2CO_3	DMF
29	$Pd(dppf)Cl_2$	K_2CO_3	DMSO
29	$Pd(dppf)Cl_2$	Cs_2CO_3	DMSO
29	$Pd(dppf)Cl_2$	K_3PO_4	DMSO

Table 3: Attempted Suzuki coupling reactions involving bis(pinacolato)diborane and **29**.

It has been reported that reactions between bis(pinacolato)diborane and iodo-derivatives are more rapid and produce the boronated product in higher yields, in comparison to reactions which used bromo-analogues.[197,203] Thus the reaction was repeated employing the zinc(II) complex of 5-(4-iodophenyl)-10,15,20-tri(4-pyridyl)porphyrin in place of **29**, as illustrated in Scheme 59.

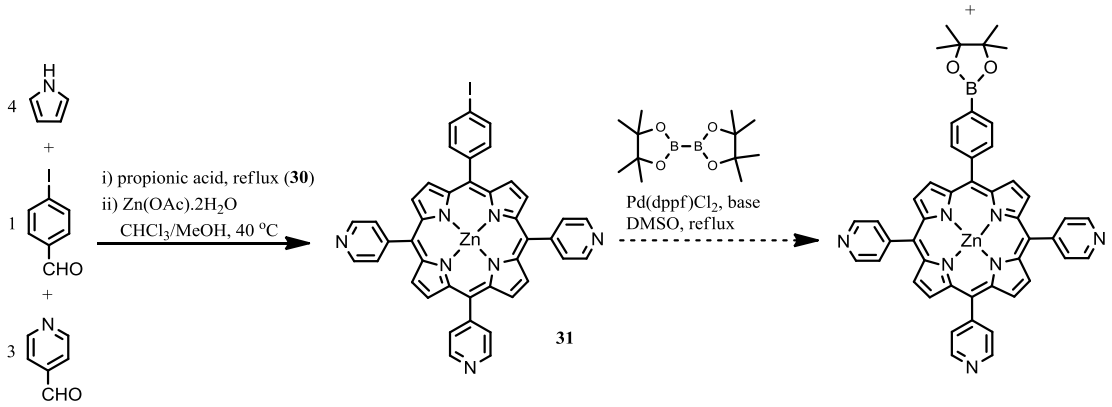

Scheme 59: Attempted Suzuki coupling involving **31**.

Following the Adler procedure,[114] 5-(4-iodophenyl)-10,15,20-tri(4-pyridyl)porphyrin (**30**) was synthesised from the dehydration reaction between 4-iodobenzaldehyde, 4-pyridinecaroxaldehyde and pyrrole. The ^{1}H NMR spectrum of **30** possessed all the expected signals, the UV-visible spectrum was typical for a free-base porphyrin, and the mass spectrum gave the expected 744 *m/z* peak corresponding to the $(M+H)^{+}$ ion. Thus there was sufficient evidence that **30** had been synthesised. The production of the zinc(II) complex of **30** (**31**), was achieved by a modified literature method,[221] affording **31** in 88 % yield, after precipitation form chloroform by the addition of methanol. The characterisation studies suggested that **31** had been produced as postulated. However, **31** was poorly soluble in chlorinated solvents, dimethylsulfoxide and tetrahydrofuran, thus a ^{13}C NMR spectrum was not obtained.

The reaction between bis(pinacolato)diboron and **31** was attempted using a modified literature method,[197] using a different base for each reaction, as shown in Table 4. The reactions were monitored by TLC (silica, eluent: tetrahydrofuran).

Porphyrin	Palladium catalyst	Base	Solvent
31	$Pd(dppf)Cl_2$	KOAc	DMSO
31	$Pd(dppf)Cl_2$	K_3PO_4	DMSO
31	$Pd(dppf)Cl_2$	Cs_2CO_3	DMSO

Table 4: Attempted Suzuki coupling reactions involving bis(pinacolato)diborane and **31**.

The reactions employing potassium acetate and caesium carbonate were monitored over a 96 hour period by TLC, which exhibited nearly total recovery of **31**, with the development of trace polar fractions; hence those reactions were discarded. The reaction using potassium phosphate showed almost complete consumption of **31** within 5 hours, with the development of a newly formed polar fraction, with other more polar trace fractions also being observed; thus the porphyrinic products were extracted into 10 % methanol/dichloromethane. The porphyrinic product only appeared to be partially soluble in the 10 % methanol/dichloromethane solution; using a higher concentration of methanol was attempted, but resulted in dimethylsulfoxide being detected in the organic layer. The organic layer was washed with copious amounts of water, to remove dimethylsulfoxide and potassium phosphate, and dried over anhydrous sodium sulphate to remove residual water. The mixture was chromatographically separated (silica coated preparative TLC plates, eluent: 10 % methanol/chloroform) and the relevant fraction was isolated. The suspected product was isolated after precipitation form 10 % methanol/dichloromethane, by the addition of methanol.

^{1}H NMR analysis of the suspected product proved to be problematic, as the product seemed to precipitate out of chloroform/ methanol solutions and dimethylsulfoxide. Therefore the sample was dissolved in deuterated dimethylsulfoxide, and the solution was filtered prior to the ^{1}H NMR analysis. The relevant sections of the ^{1}H NMR and ^{11}B NMR spectrum's of suspected (5-(4-(4,4,5,5-tetramethyl-1,3,2-dioxaborinan-2-yl)phenyl)-10,15,20-tri-(4-pyridyl)porphyrinato) zinc(II), are shown in Figure 46. The aromatic region of the suspected product was similar to the ^{1}H NMR of **31**, with both exhibiting a doublet at 8.85 ppm corresponding to a β-proton environment, with all the other proton environments accounted for in comparable positions. However, the ^{1}H NMR spectrum of the suspected product did not show a peak in the alkyl region accounting for methyl groups of the boronic pinacol ester, which would be present if the reaction had occurred as postulated. Furthermore, the ^{11}B NMR of the suspected product produced a very weak signal, thus it was inconclusive whether the suspected

product possessed a boron moiety. The strength of the signals for ^{11}B NMR and ^{1}H NMR were similar, indicating that although the ^{11}B NMR signal was extremely weak, it was comparable with the strength of the ^{1}H NMR. As the ^{11}B NMR of the suspected product was inconclusive and the ^{1}H NMR did not have a signal for the methyl groups of the pinacol ester, it was concluded that the reaction had failed and no further characterisation studies were conducted.

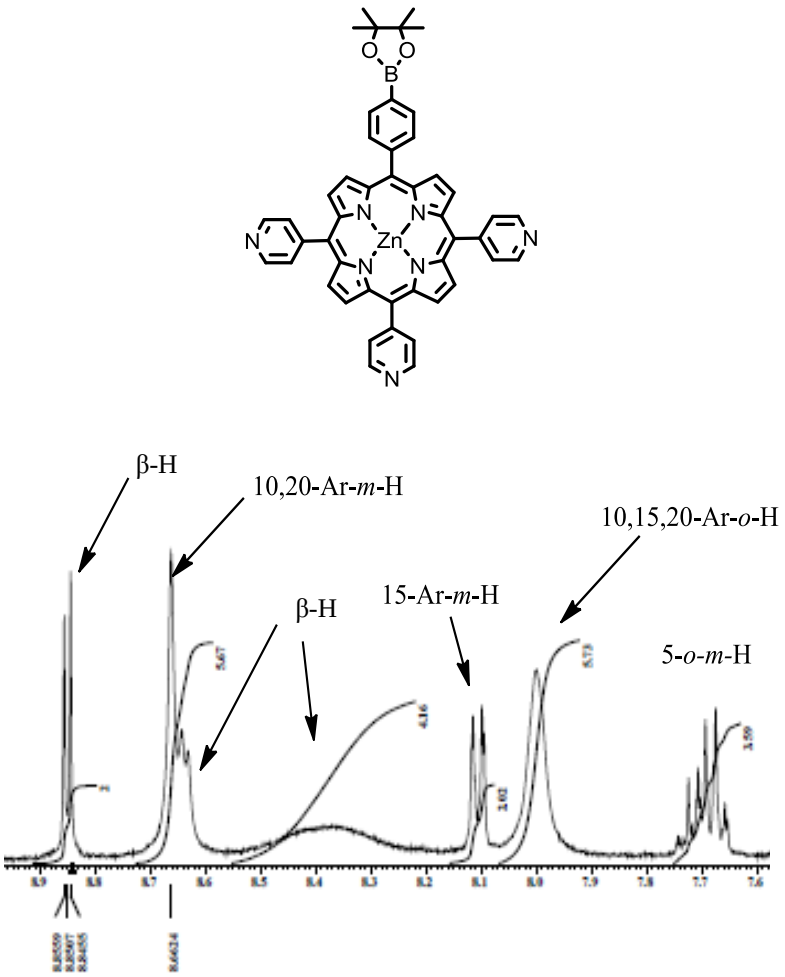

^{1}H NMR

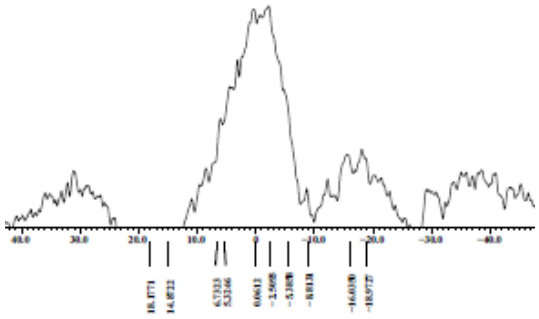

^{11}B NMR

Figure 46: ^{1}H NMR and ^{11}B NMR of spectra of suspected (5-(4-(4,4,5,5-tetramethyl-1,3,2-dioxaborinan-2-yl)phenyl)-10,15,20-tri-(4-pyridyl)porphyrinato) zinc(II).

As the boronation attempts involving bis(pinacolato)diborane were unsuccessful, an alternative boronation strategy was adopted, employing pinacolborane, as depicted in Scheme 60. Following a modified literature procedure,[201] an oven dried Schlenk flask was charged with **29** and bis(diphenylphosphino)ferrocene]dichloropalladium(II), and the residual oxygen was removed form the reaction, under reduced pressure. Under an inert atmosphere, degassed dimethylformamide and triethylamine were added, followed by pinacolborane. The resulting solution was heated at 80 °C overnight, with the TLC (silica, eluent: tetrahydrofuran) of the reaction mixture only showing the presence of **29**. Since the reported reaction was complete after 1 hour,[201] and similar reactions involving pinacolborane and aryl-bromo derivatives,[222] and (5-bromo-10,20-diphenylporphyrinato)zinc(II) the reaction,[223] were complete in 2-6 hours and 45 minutes respectively, it was deemed that the reaction had failed.

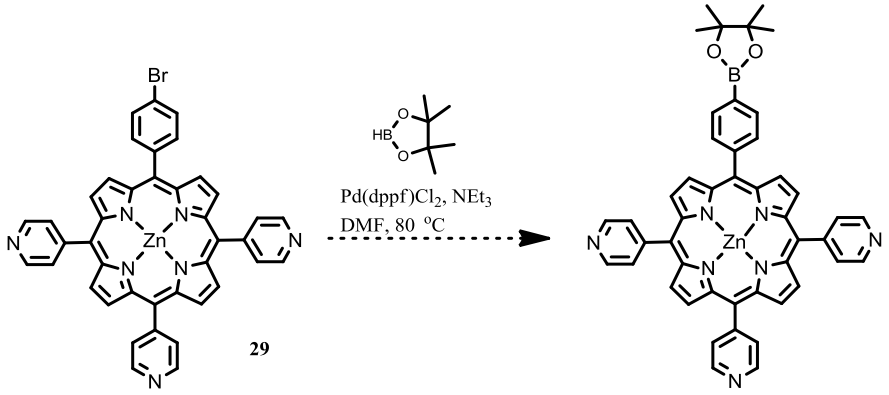

Scheme 60: Attempted boronation of **29**.

It has been reported that Suzuki couplings involving **29** are successful when employing tris(dibenzylideneacetone)dipalladium(0), tri(*tert*-butyl)phosphine and caesium carbonate, however the exact experimental conditions were not published.[204]

It has been reported that porphyrins bearing pyridyl groups can coordinate with zinc metalled porphyrins,[224] and palladium(II),[225] leading to the production of multi-porphyrin systems. Additionally, porphyrins bearing both pyridyl and iodophenyl moieties, can form supramolecular assemblies, where the iodo functionality coordinates to the pyridyl group.[226] The formation of these coordination complexes could hinder or prevent Suzuki reactions involving **29** or **31** from occurring.

5.5 Synthetic strategy: porphyrin dimer by click coupling.

Since the Suzuki coupling attempts involving **29** and **31** were unsuccessful, a click coupling approach was adopted for producing the porphyrin dimer, as shown in Scheme 61. The synthetic strategy was similar to the Suzuki coupling approach, with the exception of the functional groups which facilitate dimer formation; it was required for the porphyrin moieties to possess azido and alkyne groups.

Since it has been reported that porphyrins bearing a single amino group, can be converted into the azido analogue in good yields (95 %),[209,210] it seemed prudent to use similar reaction conditions for the conversion of **17** into the azido derivative. The zinc(II) complex of the azido porphyrin was then produced, as the literature suggested that click reactions involving azido porphyrins are favoured when the porphyrin is in a metalled form,[213] and copper(II) is present in the click reaction mixture which could insert into the porphyrin.[210] Although click reactions utilising a free-base porphyrin has been reported.[211]

Alkyne functionalities can be incorporated into a *trans*-porphyrin structure during the condensation reaction between an alkyne bearing aldehyde and dipyrromethane.[216] The alkyne bearing aldehyde can be produced via the Sonogashira reaction between 4-bromobenzaldehyde and ethynyltrimethylsilane.[227] The literature suggested that there were two sets of reaction conditions which resulted in little or no scrambling of the poly-pyrrolic intermediate prior to *trans*-porphyrin formation.[217] Due to the high cost of acetonitrile, the synthesis of the *trans*-porphyrin was performed in dimethylsulfoxide in the presence of ammonium chloride. Thus, the *trans*-porphyrin was the product of the condensation between 4-((trimethylsilyl)ethynyl)benzaldehyde, **26** and 4-acetamidobenzaldehyde, which was subsequently converted into the zinc(II) complex. The trimethylsilyl protecting group could be removed via treatment with tetrabutylammoniumfluoride, enabling the alkyne to participate in a click reaction with an azido derivative. Once the porphyrin dimer formed, the acetamido group could be removed under acidic conditions, and the amino functionality could then be converted into the maleimide group by a published procedure.[144]

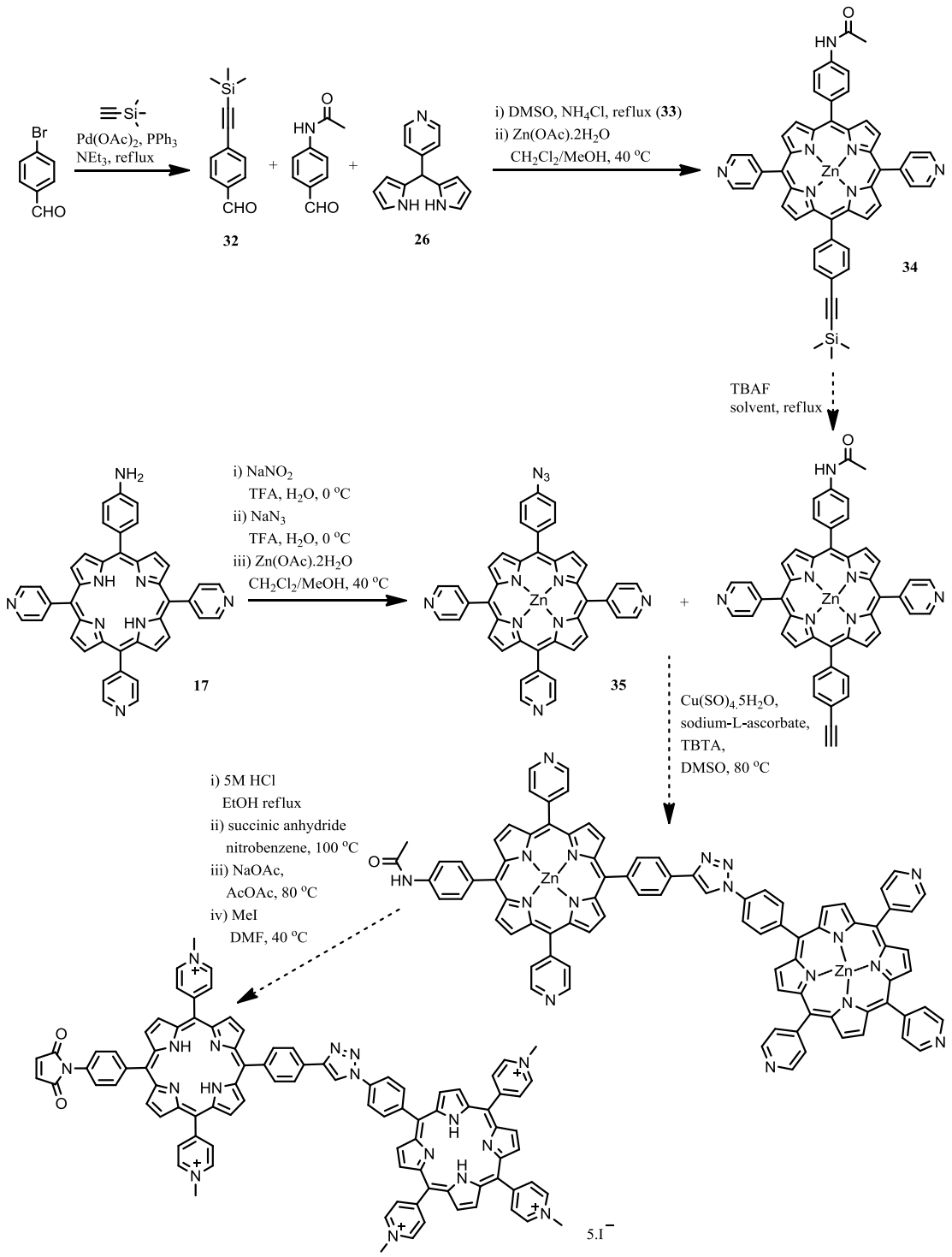

Scheme 61: Proposed synthesis of porphyrin dimer using ‘click’ chemistry.

5.5.1 Synthesis of (5-(4-acetamidophenyl)-10,20-di-(4-pyridyl)-15-(4-((trimethylsilyl)ethynyl)phenyl)porphyrinato) zinc(II) (34)

Following the synthetic sequence outlined in Scheme 61 and a known procedure,[227] a vessel was charged with 4-bromobenzaldehyde, palladium(II) acetate and triphenylphosphine. Freshly distilled triethylamine, which had been degassed with argon, was added and the resulting solution was degassed with argon for a further 5 minutes. Ethynyltrimethylsilane was then added to the solution, which was subsequently heated at reflux for 2 hours. Once the reaction had reached ambient temperature, the mixture was filtered to remove the triethylamine hydrobromide by-product, and the filtrate was collected. The solvent was removed *in vacuo* and the crude thick oil was re-dissolved in 50 % dichloromethane/hexane and was chromatographically separated (silica, eluent: 50 % dichloromethane/hexane). 4-((Trimethylsilyl)ethynyl)benzaldehyde (**32**) was isolated as white/yellow crystals in a reasonable 72 % yield, after recrystalisation from *iso*propanol. The characterisation studies conducted on **32** were comparable to published data,[228] hence it was concluded that **32** had been produced.

Following a modified reported method,[217] 5-(4-acetamidophenyl)-10,20-di-(4-pyridyl)-15-(4-((trimethylsilyl)ethynyl)phenyl)porphyrin (**33**) was synthesised via the condensation reaction between **32** and 4-acetamidobenzaldehyde, with **26**.

A solution of **32**, **26**, 4-acetamidobenzaldehyde and ammonium chloride dissolved in dimethylsulfoxide, was heated to 90 °C for 24 hours. Once cooled to ambient temperature, the mixture was stirred for a further 3 hours, open to air to ensure that the porphyrinogen had been oxidised. The porphyrinic products were extracted into a 5 % methanol/dichloromethane solution and the organic layer was isolated, and washed with copious amounts of water, to remove residual dimethylsulfoxide and ammonium chloride. The organic layer was dried over anhydrous sodium sulphate and the solvent was removed under reduced pressure. The crude product was chromatographically separated (silica, eluent: 3 % methanol/dichloromethane), with **33** isolated as a purple solid after precipitation from dichloromethane by the addition of methanol. The yield of **33** was particularly low (1 %), which could have been due to the extraction from dimethylsulfoxide procedure.

The alkyl region of the ^{1}H NMR spectrum of **33** exhibited a singlet at 0.38 ppm, corresponding to the trimethyl proton environment, and another singlet at 2.38 ppm, from the acetamido protons. The aromatic region showed a pair of doublets at 7.88 ppm

and 7.93 ppm, with both signals having the same coupling constants, J = 8.44 Hz. However, 2D COSY analysis showed that both of the doublets at 7.88 ppm and 7.93 ppm, coupled with the multiplet at 8.11-8.18 ppm, but not with each other. By considering the shielding effect exerted by the porphyrin core, the doublets at 7.88 ppm and 7.93 ppm were assigned the 5,15-*meta*-aromatic protons, with the 5,15-*ortho*-aromatic protons within the 8.11-8.18 ppm multiplet. The 2D COSY also showed that the a proportion of the multiplet at 8.11-8.18 ppm coupled with the multiplet at 8.99-9.07, thus by considering the inductive effect of the pyridyl groups, the multiplet at 8.99-9.07 was assigned the 10,20-*meta*-aromatic protons and a proportion of the multiplet at 8.11-8.18 was assigned the 10,20-*ortho*-aromatic protons. The pair of doublets at 8.86 ppm and 8.93 ppm had J values which were typical for β-protons (J = 4.8 Hz), and the 2D COSY analysis showed that those doublets and the multiplet at 8.78-8.83 ppm exhibited coupling with each other; thus the doublets at 8.86 ppm and 8.93 ppm, and the multiplet at 8.78-8.83 ppm were assigned the β-protons. The UV-visible spectrum of **33** was typical for a free-base porphyrin and the mass spectrum gave the expected 770 *m/z* peak due to the $(M+H)^+$ ion. There was substantial evidence suggesting that **33** had been synthesised as hypothesised.

Following Scheme 61 and a modified reported method,[221] the zinc(II) complex of **33** (**34**) was produced in 84 % yield. The relevant sections of the ^{1}H NMR spectrum of **34**, is shown in Figure 47. The alkyl region of the ^{1}H NMR spectrum of **34** has a singlet at 0.25 ppm (**a**) which corresponds to the trimethyl group, and another singlet at 2.09 ppm (**b**), corresponding to the methyl protons from the acetamido group. The aromatic region of the spectrum contains doublets at 7.72 ppm and 8.04 ppm, both of which having the same coupling constant (J = 7.96 Hz). The 2D COSY analysis indicated that those doublets coupled with each other, thus those doublets were attributed *ortho-meta*-aromatic-protons, located at either the 5 or 15 positions on the porphyrin core. The 2D COSY also showed that the multiplet at 7.88-7.98 ppm coupled with the multiplet at 8.56-8.68 ppm. By considering the inductive effect of the pyridyl groups, the multiplet at 8.56-8.68 ppm was assigned 10,20-*meta*-aromatic-protons and a proportion of the multiplet at 7.88-7.98 was assigned 10,20-*ortho*-aromatic-protons. The multiplet at 7.88-7.98 had an integral of 8, thus the remaining 4 protons were assigned as *ortho-meta*-aromatic-protons, located at either the 5 or 15 positions on the porphyrin core. The remaining signals were assigned as the β-protons. The UV-visible spectrum of **34,** was typical for a metallated porphyrin, and the mass spectrum gave the 832 *m/z* peak; thus it was concluded that **34** had been successfully produced.

The removal of the trimethylsilyl group from **34**, via treatment with tetrabutylammoniumfluoride, was not attempted.

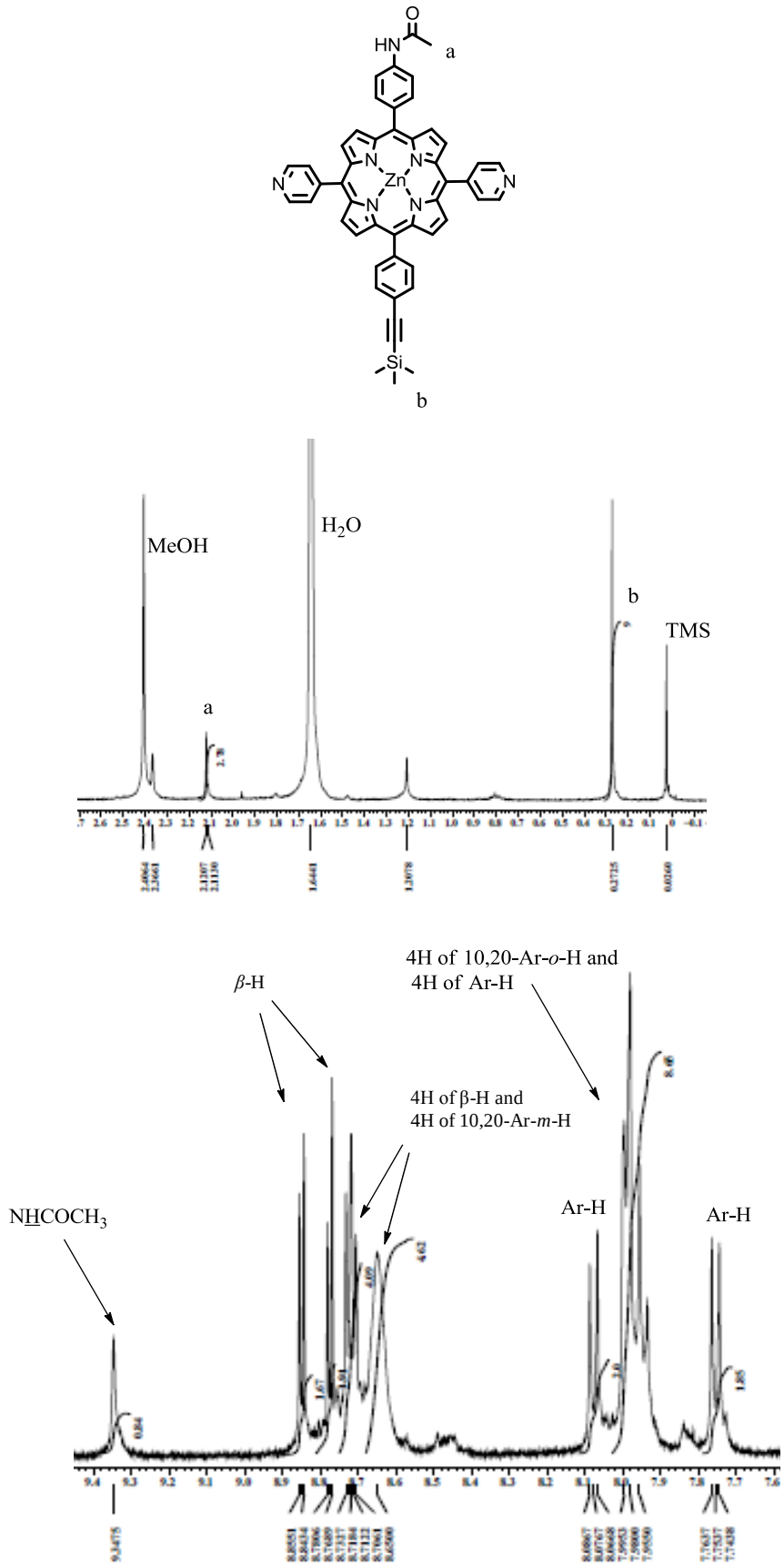

Figure 47: ^{1}H NMR spectrum of **34**.

5.5.2 Synthesis of (5-(4-azidophenyl)-10,15,20-tri-(4-pyridyl)porphyrinato) zinc(II) (35)

Following Scheme 61 and a modified published procedure,[169] a solution of **17** in trifluoroacetic acid was cooled to 0 °C, and was subsequently treated with sodium nitrite dissolved in water. After 15 minutes, sodium azide dissolved in water was added and the reaction mixture was stirred for a 1 hour. Water was added to the reaction mixture and the porphyrinic product was extracted into dichloromethane, with the un-reacted reagents and trifluoroacetic acid retained in the aqueous layer. The organic layer was collected, washed with water to remove residual impurities, and dried over anhydrous sodium sulphate, to remove residual water. TLC analysis (silica, 10 % methanol/dichloromethane) indicated that **17** had been quantitatively converted into the azido analogue. The azido porphyrin intermediate was re-dissolved in dichloromethane and zinc acetate dihydrate dissolved in methanol was added. The resulting mixture was heated at 40 °C for 2 hours. Once cooled to room temperature, the reaction mixture was washed with water to remove zinc acetate dihydrate, dried over anhydrous sodium sulphate to remove residual water, and the solvent was removed under reduced pressure, affording (5-(4-azidophenyl)-10,15,20-tri-(4-pyridyl)porphyrinato) zinc(II) (**35)** as a black solid in 94 % yield. Once the solvent was removed, compound **35** was insoluble in chloroform, acetone, methanol, 5-20 % methanol/chloroform; and was only partially soluble in tetrahydrofuran, dimethylsulfoxide and dimethylformamide, after sonicating the suspensions. Preparative TLC (silica coated prep TLC plates, eluent: tetrahydrofuran) was attempted, but resulted in the porphyrin precipitating on the silica, thus purification of **35** was not achieved. The ^{1}H NMR of **35** was performed in deuterated dimethylsulfoxide, with the sample requiring filtration prior to the analysis. The aromatic region of the ^{1}H NMR spectrum of **35** is depicted in Figure 48. The alkyl region of the spectrum did not possess a broad singlet corresponding to the amino protons of starting material **17**. The aromatic region of the spectrum contained signals for all the proton environments. The sample was not concentrated enough to obtain a ^{13}C NMR. The UV-visible spectrum of **35** was typical for a metalled porphyrin. The mass spectrum of **35** produced a 694.1 *m/z* signal which could be attributed to the $(M+2H-2N)^{+}$ ion, however the HRMS gave a 695.1645 *m/z* peak, which did not correspond to the possible ions which **35** could produce. Although the ^{1}H NMR of **35** indicated that the reaction had occurred as postulated, the mass spectrum was

inconclusive, thus there was not sufficient evidence that the reaction had occurred as hypothesised.

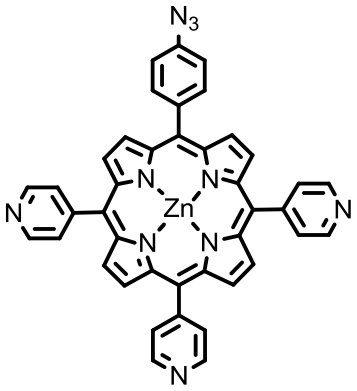

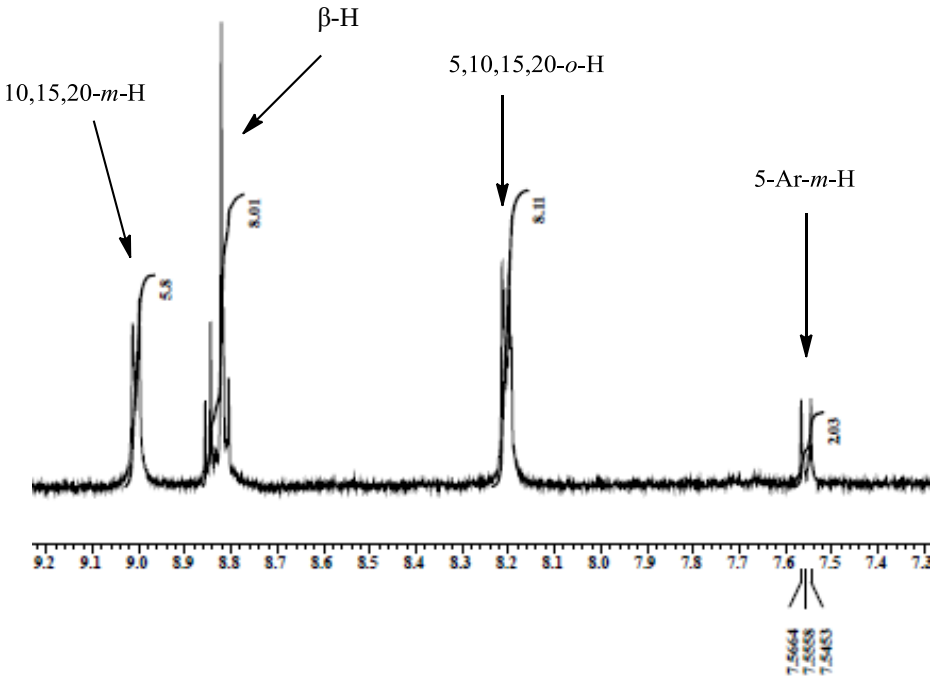

Figure 48: ^{1}H NMR spectrum of **35**.

During the synthesis of **35**, the TLC analysis of the reaction mixture indicated that **17** had been converted into the azido analogue. Hence to ensure the amino group was transformed into the azido functionality, the reaction was repeated without the insertion of zinc, as shown in Scheme 62.

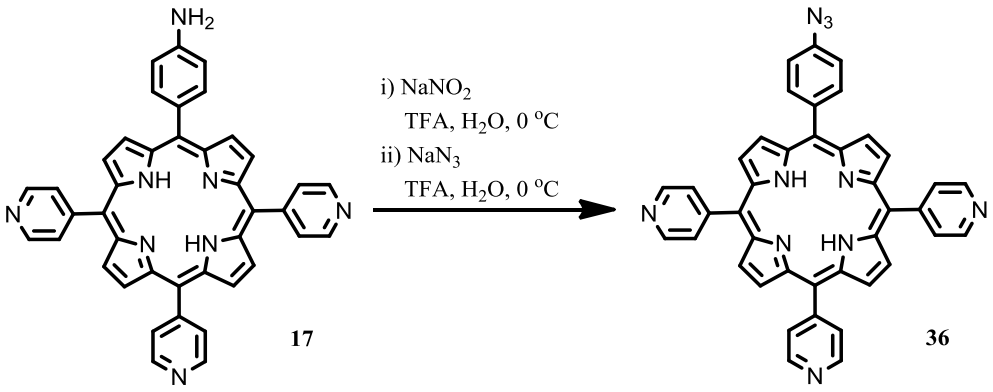

Scheme 62: Synthesis of **36**.

The synthesis of 5-(4-azidophenyl)-10,15,20-tri-(4-pyridyl)porphyrin (**36**) was achieved in a similar manner as described for **35**, except for the zinc dihydrate treatment. The aromatic region of the ^{1}H NMR spectrum of **36** is shown in Figure 49, and was comparable to the ^{1}H NMR spectrum of **35**. The mass spectrum of **36** exhibited a 659.2408 *m/z* peak due to the $(M+H)^{+}$ ion, thus it was concluded that **36** had being successfully produced. As **36** had been synthesised, it was likely the zinc(II) complex (**35**) had also been produced as postulated.

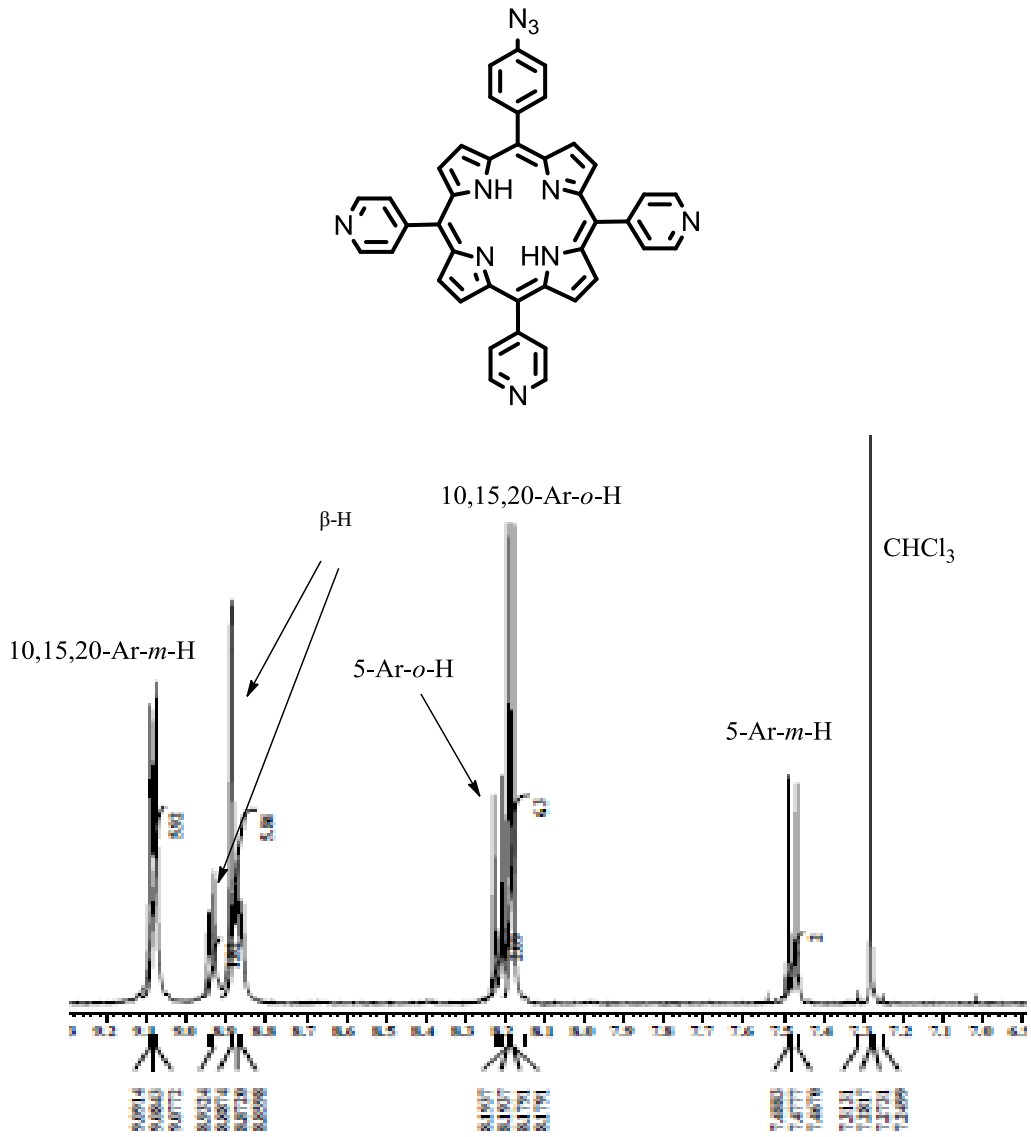

Figure 49: ^{1}H NMR spectrum of **36**.

5.5.3 Attempted synthesis of 5-(4-((4-trimethylsilyl)-1,2,3-triazole)phenyl)-10,15,20-tri-(4-pyridyl)porphyrin

Before attempting a click reaction using **35** and deprotected **34**, a trial reaction was attempted involving **35** and ethynyltrimethylsilane, as illustrated in Scheme 63.
Following a modified procedure,[213] a solution of **35** in dimethylsulfoxide (10 mL) was charged with sodium *L*-ascorbate and copper(II) sulphate pentahydrate suspended in water. It has been reported that additives such as tris((1-benzyl-1*H*-1,2,3-triazol-4-yl)methyl)amine enhances the click reaction by reducing the required copper concentration, or increasing the efficiency of the reaction.[205] Thus tris((1-benzyl-1*H*-1,2,3-triazol-4-yl)methyl)amine was then added to the reaction mixture, which was than heated to 80 °C. The reaction was monitored by TLC (silica, eluent: tetrahydrofuran) over 4 days, with only **36** being detected.

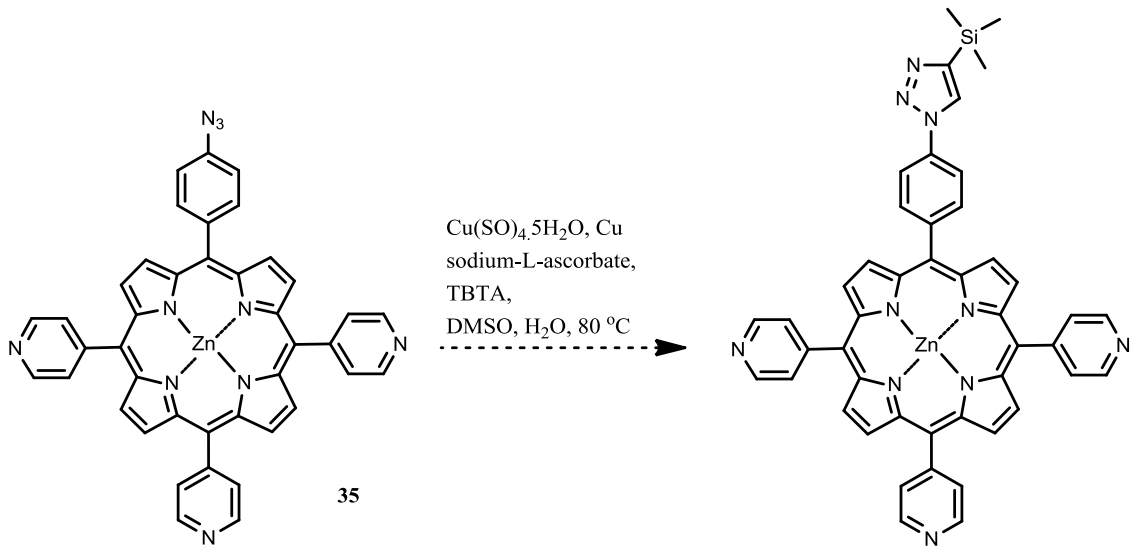

Scheme 63: Attempted 'click' reaction.

Compound **35** was poorly soluble in dimethylsulfoxide, thus the reaction could have failed due to the low concentration of **35** within the reaction mixture. Click reactions have been performed in acetic acid solutions,[211] and as pyridyl groups can be protonated, it would have been prudent to investigate the click reaction using acetic acid in the solvent system.

5.6 Summary/further work

Both the Suzuki and click coupling strategies for producing a porphyrin dimer were unsuccessful. For the Suzuki coupling approach, the zinc(II) complexes of the bromo and iodo pyridyl porphyrins were poorly soluble in the solvent systems used, possibly due to zinc-pyridyl or halide-pyridyl coordination. To suppress the formation of the possible coordination complexes, porphyrins could be produced which have the pyridyl nitrogens located in the 2-postion, opposed to the 4. Suzuki coupling attempts involving the free-base porphyrins should also be attempted.

The click coupling attempt was hindered by the solubility of **35**, thus time permitting, different solvent systems should be investigated, initially using weakly acidic solutions.

Chapter 6: Experimental

Starting reagents were purchased from Fisher Scientific UK (Fisher Scientific UK, Bishop Meadows Road, Loughborough, Leicestershire), Sigma Aldrich (YorLab, 9 The Crescent, Blossom Street, York, Yorkshire) and Strem Chemicals (Strem Chemicals UK, 48 High Street, Orwell, Royston, Hertfordshire) and were used as received unless otherwise stated. Solvents, of either analytical of HPLC grade, were obtained from Fisher Scientific UK. Solvents were dried according to published procedures.[229]

TLC analysis was preformed using aluminium-backed silica gel 60 $F_{254,}$ (Merck plates) or aluminium-backed aluminium oxide 60 F_{254}, (Merck plates) purchased from Sigma Aldrich.

Silica gel chromatography was preformed with silica gel 60 Å (Davisil), bought from Sigma Aldrich. Alumina chromatography was preformed using aluminium oxide 150, purchased from Sigma Aldrich.

NMR studies were conducted using either a JEOL-ECP 400 MHz FT-NMR spectrometer or JEOL-JNM-LA400 FT NMR spectrometer. The chemical shifts were quoted in ppm, with the coupling constants (*J*) quoted in hertz (Hz). The solvent peaks were assigned using literature determinations.[230]

UV-Vis absorption spectra were recorded on Agilent 8453 spectrometer.

.

Mass spectrometry was performed using either a Bruker Reflex IV MALDI TOF mass spectrometer, or a Perkin-Elmer Turbomass quadrupole GC/MS, with a Perkin-Elmer Autosystem XL GC and autosampler.

High resolution mass spectra were provided by:

EPSRC National Mass Spectrometry Service Centre
Chemistry Department
University of Swansea
Wales

With the analyses performed using the following instrumentation:

Applied Biosystems Mariner (Electrospray)
Applied Biosystems Voyager (MALDI-TOF)

6.1 Synthesis of 5,10,15,20-tetraphenylporphyrin (1)

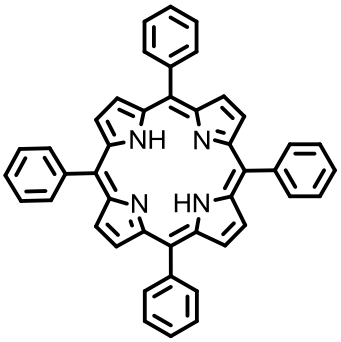

Benzaldehyde (10.6 mL, 100 mmol) was dissolved in propionic acid (400 mL) and the resulting mixture was heated to reflux. Pyrrole (7.9 mL, 100 mmol, 1 equiv. relative to benzaldehyde) was added drop-wise to the refluxing mixture and the resulting solution was heated under reflux conditions for a further 30 minutes, while protected against light. Once cooled to ambient temperature, the dark mixture was filtered to yield a purple solid, which was washed with methanol and hot water to afford **1** (2.7 g, 18 %) as a purple crystalline solid. R*f* = 0.82 (silica, CH_2Cl_2:C_6H_{12}; 3:2); m.p. = >350 °C decomp.

^{1}H N.M.R. [400 MHz, $CDCl_3$], δ (ppm) = −2.77 (s, 2H, N*H*), 7.71-7.81 (m, 12H, 5,10,15,20-Ar-*m*-*p*-*H*), 8.19-8.25 (m, 8H, ,10,15,20-Ar-*o*-*H*), 8.84 (br s, 8H, *β*-*H*)
^{13}C N.M.R. [100 MHz, $CDCl_3$], δ (ppm) = 120.1, 126.7, 127.7, 131.3, 134.6, 142.2
UV/Vis (CH_2Cl_2, nm) λ_{max} = 417, 514, 549, 590, 646
MS (MALDI) *m/z* = 614 $(M)^+$

6.2 Synthesis of (5,10,15,20-tetraphenylporphyrinato)copper(II) (2)

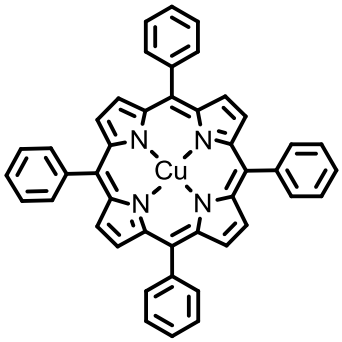

A slurry of copper (II) acetate monohydrate (3.2 g, 16 mmol, 10 equiv. relative to **1**) in methanol-water (50 mL; 6:1) was added to a solution of **1** (1 g, 1.6 mmol) dissolved in chloroform (250 mL) and the resulting mixture was heated at reflux, for 5 hours. The hot solution was applied to a warm neutral alumina oxide pad, and eluted using warm chloroform. The organic layer was collected, dried over magnesium sulphate and the solvent was removed under reduced pressure. The purple product was isolated (1.07 g, 97 %), after precipitation from methanol over chloroform. R*f* = 0.94 (silica, CH_2Cl_2:C_6H_{12}; 3:2); m.p. = >350 °C decomp.

UV/Vis (CH_2Cl_2, nm) λ_{max} = 414, 538, 616

MS (MALDI) *m/z* = 675 $^{63}Cu(M)^+$, 676 $^{63}Cu(M+H)^+$, 677 $^{65}Cu(M)^+$ and $^{63}Cu(M+2H)^+$, 678 $^{65}Cu(M+H)^+$, 679 $^{65}Cu(M+2H)^+$

6 .3 Synthesis of 2-formyl-5,10,15,20-tetraphenylporphyrin (3)

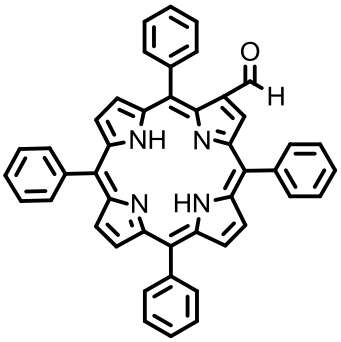

Phosphorus oxychloride (7.91 mL, 84 mmol) was added drop-wise to ice cooled anhydrous dimethylformamide (10 mL, 129 mmol), under an argon atmosphere, while avoiding exposure to moisture. An ice cooled solution of **2** (900 mg, 1.3 mmol) dissolved in anhydrous 1,2-dichloroethane (90 mL) was added to the viscous Vilsmeier complex. The mixture was then allowed to reach room temperature and then was subsequently heated at reflux for 7 hours. Once the reaction mixture had cooled to ambient temperature over night, sulphuric acid (18 M, 17.3 mL, 300 mmol) was added to the stirred solution. The mixture was then poured onto a stirred, ice-cooled solution of sodium hydroxide (0.72 M, 900 mL), and chloroform was added. The organic layer was separated, washed with a saturated solution of sodium hydrogen carbonate and water, and was then dried over anhydrous sodium sulphate. The solvent was removed under reduced pressure and the crude product was isolated by column chromatography (silica, eluent: dichloromethane). Compound **3** (575 mg, 67 %) was isolated as a purple solid after precipitation from dichloromethane by the addition of hexane. R*f* = 0.51 (silica, CH_2Cl_2); m.p. = >350 °C decomp.

^{1}H N.M.R. [400 MHz, $CDCl_3$], δ (ppm) = −2.55 (s, 2H, N*H*), 7.66-7.86 (m, 12H, 5,10,15,20-Ar-*m*-*p*-*H*), 8.13-8.27 (m, 8H, 5,10,15,20-Ar-*o*-*H*), 8.67-9.02 (m, 6H, *β*-*H*), 9.22 (s, 1H, *β*-*H*), 9.41 (s, 1H, C*H*O)

^{13}C N.M.R. [100 MHz, $CDCl_3$], δ (ppm) = 120.0, 120.3, 120.6, 122.6, 126.85, 126.88, 127.4, 128.0, 128.2, 129.0, 134.5, 134.6, 134.7, 135.0, 141.6, 141.8, 142.4, 189.4

UV/Vis (CH_2Cl_2, nm) λ_{max} = 430, 525, 566, 605, 663

MS (MALDI) *m/z* = 642 $(M)^+$

6.4 Attempted synthesis of *tert*-butyl(3-((5,10,15,20-tetraphenylporphyrin-2-ylmethyl)amino)propyl)carbamate

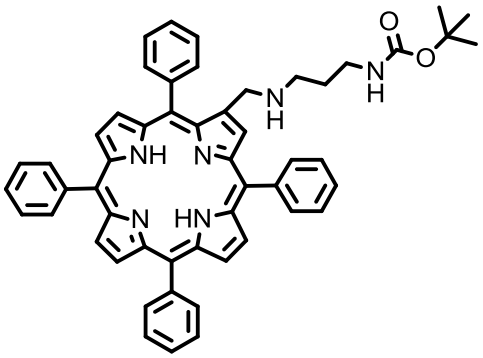

Method 1

A solution of **3** (50 mg, 77 μmol) in anhydrous toluene (35 mL), was charged with *N*-Boc-1,3-diaminopropane hydrochloride (19.6 mg, 93 μmol, 1.2 equiv. relative to **3**), and 1 drop of acetic acid, and the reaction vessel was fitted with a Dean-Stark trap. The reaction mixture was heated to reflux, under an inert atmosphere (N_2), while avoiding exposure to light. After 16 hours, a trace, polar, UV-active fraction was observed by TLC (silica, eluent: 5 % methanol/dichloromethane), with almost all the starting material remaining. A solution of sodium cyanoborohydride (6 mg, 95 μmol, 1.2 equiv. relative to **3**) dissolved in dry methanol (7 mL) was added to the reaction mixture, and heating was continued for a further 14 hours (overnight), until the TLC of the reaction mixture showed almost complete consumption of **3**, and the development of another UV-active fraction (suspected product). Once cooled to room temperature, the solvent was removed under reduced pressure. The crude mixture was re-dissolved in dichloromethane, washed with water, and the organic layer was dried over anhydrous sodium sulphate. Chromatographic separation (silica coated prep TLC plates, eluent: 5 % methanol/dichloromethane) isolated the relevant fractions, however TLC analysis showed the suspected product had decomposed.

The reaction was repeated, with the exception of using a 10 molar excess of *N*-Boc-1,3-diaminopropane hydrochloride (164 mg, 778 μmol, 10 equiv. relative to **3**), and in the presence of activated 3 Å molecular sieves. The reaction proceeded in exactly the same manner as previously described. Decomposition of the suspected product was observed,

following chromatographic separation (silica coated prep TLC plates, eluent: 5 % methanol/dichloromethane).

Method 2

Compound **3** (200 mg, 311 μmol) dissolved in anhydrous toluene (50 mL), was charged with *N*-Boc-1,3-diaminopropane hydrochloride (327 mg, 1.56 mmol, 5 equiv. relative to **3**), 1 drop of acetic acid and activated 3 Å molecular sieves; and the reaction vessel was fitted with a Dean-Stark trap. Sodium cyanoborohydride (23 mg, 370 μmol, 1.2 equiv. relative to **3**) dissolved in dry methanol (15 mL) was added to the reaction mixture, which was subsequently heated to reflux, under an inert atmosphere (N_2) while avoiding exposure to light. After 24 hours (overnight) no further consumption of **3** was observed, as indicated by TLC (silica, eluent: 5 % methanol/dichloromethane), with the reaction mixture exhibiting the presence of a major UV-active fraction (suspected product), and multiple trace UV-active fractions**.** Once cooled to room temperature, the solvent was removed *in vacuo*, the crude mixture was re-dissolved in dichloromethane and washed with a saturated sodium hydrogen carbonate solution, brine and then water. The organic layer was dried over anhydrous sodium sulphate and chromatographic separation (silica coated preparative TLC plates, eluent: 5 % methanol/dichloromethane) isolated the relevant fraction. The suspected product was precipitated from dichloromethane by the addition of hexane. Once dried, the suspected product had degraded as indicated by TLC, therefore the chromatographic and precipitation procedures were repeated. Once isolated, ^{1}H NMR analysis of the suspected product was inconclusive, with the TLC of the ^{1}H NMR sample exhibiting decomposition. The suspected product (11 mg, 14 μmol-assuming suspected product was the imine) was dissolved in anhydrous dichloromethane (5 mL), and was treated with a solution of sodium borohydride (2 mg, 55 μmol, 4. equiv. relative to suspected product) in dry methanol (1 mL). The resulting solution was stirred for 15 minutes, at 0 °C, under an inert atmosphere (N_2). Acetic acid (0.1 mL) was added, and the resulting mixture was washed with water and then dried over anhydrous sodium sulphate. TLC analysis indicated that the sodium borohydride treatment had not affected the suspected product.

Method 3

A solution of sodium cyanoborohydride (6 mg, 93 μmol, 1.2 equiv. relative to **3**) dissolved in dry methanol (6 mL) was added to **3** (50 mg, 77 μmol), *N*-Boc-1,3-diaminopropane hydrochloride (82 mg, 39 μmol, 5 equiv. relative to **3**), 1 drop of acetic acid and activated 3 Å molecular sieves in anhydrous tetrahydrofuran (30 mL). The reaction was heated to reflux, under an inert atmosphere (N_2), while protected against light. After 24 hours (overnight), the TLC (silica, eluent: 5 % methanol/dichloromethane) of the reaction mixture revealed the presence of a major UV-active fraction (suspected product), a minor polar fraction (suspected imine) and a trace amount **3**, therefore the reaction was stopped to avoid possible decomposition. Once cooled to ambient temperature, the solvent was removed under reduced pressure, the crude mixture was re-dissolved in dichloromethane and washed with water. The organic layer was dried over anhydrous sodium sulphate and chromatographic separation (silica coated prep TLC plates, eluent: 5 % methanol/dichloromethane) isolated the relevant fraction. The suspected product was precipitated in hexane over dichloromethane. The suspected product had degraded as indicated by TLC.

6.5 Attempted synthesis of *tert*-butyl(12-((5,10,15,20-tetraphenylporphyrin-2-ylmethyl)-amino)dodecyl)carbamate

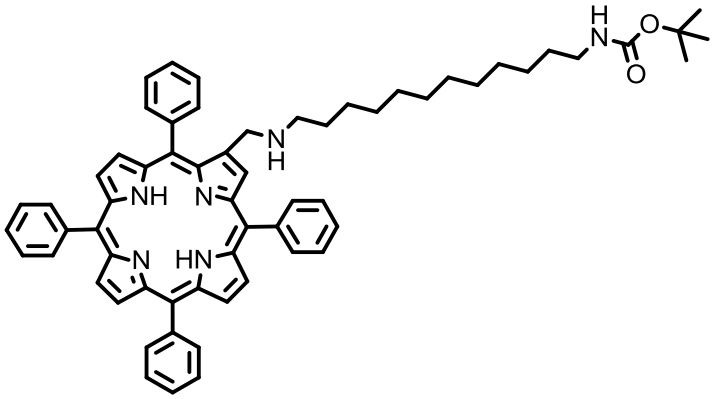

A solution of **3** (50 mg, 77 μmol) in anhydrous toluene (35 mL), was charged with *N*-Boc-1,12-diaminododecane (28 mg, 93 μmol, 1.2 equiv. relative to **3**), 1 drop of acetic acid and activated 3 Å molecular sieves. The reaction vessel was fitted with a Dean-Stark trap and was heated to reflux, under an inert atmosphere (N_2), while avoiding exposure to light. After 16 hours, the reaction mixture showed no change as indicated by TLC (silica, eluent: 5 % methanol/dichloromethane), with recovery of the starting material. A methanolic solution of sodium cyanoborohydride (6 mg, 95 μmol, ≈ 1.2 equiv. relative to **3**) was added to the refluxing mixture. After 14 hours (overnight) the TLC of the reaction mixture exhibited multiple UV-active fractions, including a substantial quantity of **3**, therefore the reaction was discarded.

The reaction was repeated, with the exceptions of using a 10 molar excess of *N*-Boc-1,12-diaminododecane (133 mg, 778 μmol, 10 equiv. relative to **3**) and in the presence of activated 3 Å molecular sieves. The reaction proceeded in exactly the same manner as previously described, with the formation of multiple UV-active fractions, including a substantial quantity of **3**, therefore the reaction mixture was discarded.

6.6 Synthesis of (2-formyl-5,10,15,20-tetraphenylporphyrinato)copper(II) (4)

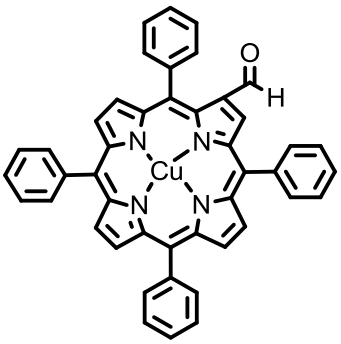

Phosphorus oxychloride (8.8 mL, 96 mmol) was added drop-wise to ice cooled anhydrous dimethylformamide (11.2 mL, 145 mmol), under an argon atmosphere while avoiding exposure to moisture. A cooled solution of **3** (1 g, 1.55 mmol) dissolved in anhydrous 1,2-dichloroethane (100 mL), was then added to the viscous Vilsmeier complex, and the mixture was then allowed to reach ambient temperature, and was then heated at reflux for 7 hours. Once the reaction mixture had cooled to room temperature overnight, it was poured onto a stirred, ice-cooled solution of sodium hydroxide (0.72 M, 1 L). Chloroform was then added, the organic layer was collected, washed with water, dried over anhydrous sodium sulphate and the solvent was removed under reduced pressure. The crude product was isolated by column chromatography (silica, eluent: dichloromethane) and precipitation from dichloromethane by the addition of hexane, affording **4** (771 mg, 74 %) as a red solid. R*f* = 0.67 (silica, CH_2Cl_2); m.p. = >350 °C decomp.

UV/Vis (CH_2Cl_2, nm) λ_{max} = 427, 550, 591

MS (MALDI) *m/z* = 703 $^{63}Cu(M)^+$,705 $^{65}Cu(M)^+$

6.7 Attempted synthesis of *tert*-butyl(3-((((5,10,15,20-tetraphenylporphyrinato)copper(II))-2-ylmethyl)-amino)propyl)carbamate

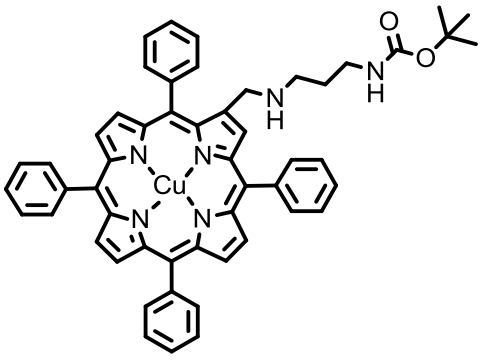

A solution of **4** (50 mg, 71 μmol) in anhydrous toluene (30 mL), was charged with *N*-Boc-1,3-diaminopropane hydrochloride (73 mg, 350 μmol, 5 equiv. relative to **4**), and lanthanum(III) triflate (8 mg, 1.4 μmol, 0.2 equiv. relative to **4**); and the reaction vessel was fitted with a Dean-Stark trap. The reaction was heated to reflux, under an inert atmosphere (N_2), while avoiding exposure to light. The reaction was monitored over a 3 day period by TLC (silica, eluent: dichloromethane), with a trace, polar, UV-active fraction located at the base line being observed, with almost all the starting material remaining. Once cooled to room temperature, the reaction mixture was diluted with dichloromethane, filtered, washed with water and the organic fraction was dried over anhydrous sodium sulphate. The TLC of the reaction mixture revealed that **4** had been recovered, and trace fractions which couldn't be characterised.

The reaction was repeated in a similar manner, in the presence of potassium carbonate (48 mg, 350 μmol, 1 equiv. relative to *N*-Boc-1,3-diaminopropane hydrochloride). The reaction was monitored by TLC (silica, eluent: dichloromethane) over a 3 day period, with the starting material being recovered.

6.8 Attempted synthesis of *tert*-butyl(12-((((5,10,15,20-tetraphenylporphyrinato)copper(II))-2-ylmethyl)-amino)dodecyl)carbamate

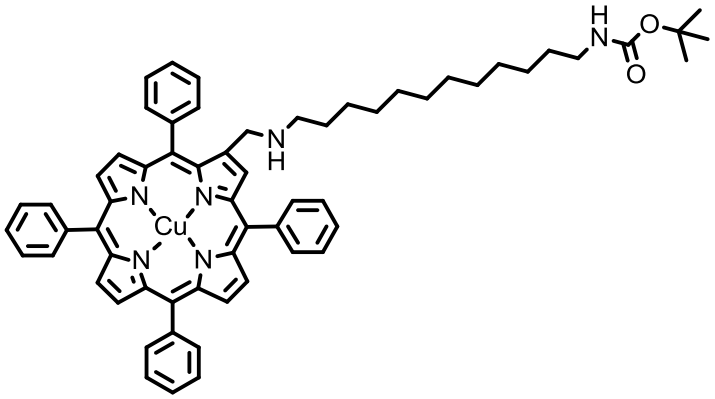

N-Boc-diaminododecane (105 mg, 350 μmol, 5 equiv. relative to **4**), and lanthanum(III) triflate (8 mg, 1.4 μmol, 0.2 equiv. relative to **4**) were added to **4** (50 mg, 71 μmol) dissolved in anhydrous toluene (30 mL). The reaction vessel was fitted with a Dean-Stark trap and was heated to reflux, under an inert atmosphere (N_2), while avoiding exposure to light. The reaction was monitored over a 3 day period, by TLC (silica, eluent: dichloromethane), a trace, polar, UV-active fraction located at the base line was observed with almost all the starting material remaining. Once cooled to room temperature, the reaction mixture was diluted with dichloromethane, filtered, the filtrate was washed and dried over anhydrous sodium sulphate. The TLC of the worked-up reaction mixture revealed that **4** had been recovered.

The reaction was repeated in a similar manner, in the presence of potassium carbonate (48 mg, 350 μmol, 1 equiv. relative to N-Boc-1,3-diaminododecane). The reaction was monitored over a 3 day period by TLC (silica, eluent: dichloromethane), with the starting material being recovered.

6.9 Synthesis of phenyl-(5,10,15,20-tetraphenylporphyrin-2-ylmethyl)amine (5)

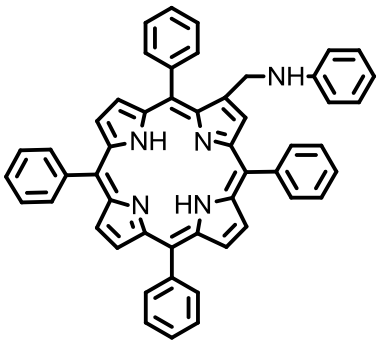

Aniline (0.1 mL, 100 mg, 1.1 mmol, 1.7 equiv. relative to **3**) and 1 drop of acetic acid were added to a solution of **3** (40 mg, 62 μmol) dissolved in anhydrous toluene (30 mL). The reaction vessel was fitted with a Dean-Stark trap and was heated to reflux, under an inert atmosphere (N_2), while avoiding exposure to light. After 24 hours, the reaction mixture showed no further change as indicated by TLC (silica, eluent: dichloromethane), with almost complete consumption of the starting material. A methanolic solution of sodium cyanoborohydride (5 mg, 80 μmol, 1.3 equiv. relative to **3**) was then added to the refluxing mixture. Following 2 hours at reflux, the TLC of the reaction mixture revealed that the reaction had gone to completion. Once cooled to ambient temperature, the solvent was removed under reduced pressure and the crude product was re-dissolved in dichloromethane, washed with water and dried over anhydrous sodium sulphate. The organic layer was concentrated *in vacuo* and was purified by column chromatography (silica, eluent: dichloromethane). The purified **5** (30 mg, 67 %) was isolated as a purple powder after precipitation from dichloromethane by the addition of pentane. R*f* = 0.31 (silica, CH_2Cl_2); m.p. = >350 °C decomp.

^{1}H N.M.R. [400 MHz, $CDCl_3$], δ (ppm) = not observed (s, 2H, N*H*), 4.26 (br s, 1H, PhN*H*), 4.51 (s, 2H, C*H*$_2$NH), 6.51-6.56 (m, 2H, NH-Ar-*m*-*H*), 6.68-6.73 (m, 1H, NH-Ar-*p*-*H*), 7.09-7.15 (m, 2H, NH-Ar-*o*-*H*), 7.65-7.80 (m, 12H, 5,10,15,20-Ar-*m*-*p*-*H*), 8.09- 8.16 and 8.18-8.23 (2m, 8H, 5,10,15,20-Ar-*o*-*H*), 8.65 (d, *J* = 4.77 Hz, 1H, *β*-*H*), 8.75-8.87 (m, 6H, *β*-*H*)

^{13}C N.M.R. [100 MHz, $CDCl_3$], δ (ppm) = 44.2, 113.3 (NH-Ar-*m*-*C*), 117.6, 119.4, 120.2, 120.6, 126.6, 127.3, 127.6, 127.7, 128.5, 129.0 (NH-Ar-*o*-*C*), 133.2, 134.5 (5,10,15,20-Ar-*o*-*C*), 134.58 (5,10,15,20-Ar-*o*-*C*), 134.64 (5,10,15,20-Ar-*o*-*C*), 141.9, 142.0, 142.2, 142.3, 148.1

UV/Vis (CH_2Cl_2, nm) λ_{max} = 419, 515, 549, 590, 645

MS (MALDI) *m/z* = 720 $(M+H)^+$

6.10 Synthesis of succinimidyl-4-aminobenzoate (6)

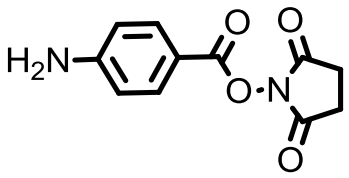

4-Aminobenzoic acid (2.0 g, 15 mmol), *N*-hydroxysuccinimide (1.68 g, 15 mmol, 1 equiv. relative to 4-aminobenzoic acid), *N,N'*-dicyclohexylcarbodiimide (3.0 g, 15 mmol, 1 equiv. relative to 4-aminobenzoic acid) were dissolved in dry dimethylformamide (18 mL). The reaction mixture was cooled using an ice bath and was stirred for 24 hours, while protected against moisture, until complete consumption of 4-aminobenzoic acid was observed by TLC (silica, eluent: 40 % dichloromethane/ethyl acetate). The reaction mixture was filtered, the filtrate was collected and the solvent was removed *in vacuo*. The crude mixture was dissolved in ethyl acetate, washed with water, dried over anhydrous sodium sulphate, and the solvent was removed under reduced pressure. The crude mixture was re-dissolved in 40 % dichloromethane/ethyl acetate and was chromatographically separated (silica, eluent: 40 % dichloromethane/ethyl acetate). Once the relevant fraction had been collected, the solvent was removed under reduced pressure. The white crystalline **6** (2.04 g, 58 %) was precipitated from 40 % dichloromethane/ethyl acetate by the addition of hexane. R*f* = 0.25 (silica, $C_2H_5CO_2CH_3$:C_6H_{12}; 1:1); m.p. = 177-180 °C.

^{1}H N.M.R. [400 MHz, $CDCl_3$], δ (ppm) = 2.89 (br s, 4H, 2 x CH_2), 4.27 (br s, 2H, NH_2), 6.66 and 7.93 (AB, *J* = 8.77 Hz, 4H, Ar-*H*)

^{13}C N.M.R. [100 MHz, $CDCl_3$], δ (ppm) = 25.8 (2 x *C*H_2), 113.7, 114.0 (Ar-*C*), 133.1 (Ar-*C*), 152.6, 161.7, 169.7

HRMS (ES): calculated for $C_{11}H_{10}N_2O_4Na$ $(M+Na)^+$ 257.0533, found: 257.0536

6.11 Synthesis of *tert*-butyl(3-(4-aminobenzamido)propyl)carbamate (7)

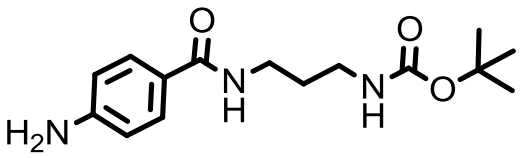

N-Boc-1,3-diaminopropane hydrochloride (135 mg, 640 µmol, 2 equiv. relative to **6**) and diisopropylethylamine (0.2 mL, 1.28 mmol, 2 equiv. relative to *N*-Boc-1,3-diaminopropane hydrochloride) were added to **6** (75 mg, 320 µmol) dissolved in anhydrous dimethylformamide (20 mL). The reaction mixture cooled with an ice-water mixture and was stirred under an inert atmosphere (N_2) for 24 hours (overnight), until complete consumption of **6** was observed, as indicated by TLC (silica, 40 % dichloromethane/ethyl acetate). The solvent was removed under reduced pressure, the crude mixture was dissolved in ethyl acetate, washed with water, dried over anhydrous sodium sulphate, and the solvent was removed under reduced pressure. The crude product was re-dissolved in a mixture of 25 % dichloromethane/ 0.5 % methanol/ 75 % ethyl acetate and was chromatographically separated (silica, eluent: 25 % dichloromethane/ethyl acetate). The product **7** (62 mg, 66 %) was isolated as a yellow powder after precipitation in hexane over ethyl acetate. R*f* = 0.23 (silica, $C_2H_5CO_2CH_3$:C_6H_{12}; 7:3); m.p. = 155-156 °C .

^{1}H N.M.R. [400 MHz, $(CD_3)_2SO$], δ (ppm) = 1.37 (s, 9H, 3 × C*H*$_3$), 1.56 (quintet, *J* = 6.5 Hz, 2H, -CH_2C*H*$_2$$CH_2$-), 2.94 (q, *J* = 6.5 Hz, 2H, NHC*H*$_2$$CH_2$), 3.18 (q, *J* = 6.5 Hz, 2H, NH-C*H*$_2$-CH_2), 5.59 (br s, 2H, N*H*$_2$), 6.52 and 7.54 (AB, *J* = 8.43 Hz, 4H, Ar-*H*), 6.81 (t, *J* = 5.6 Hz, 1H, N*H*), 7.96 (t, *J* = 5.6 Hz, 1H, N*H*)

^{13}C N.M.R. [100 MHz, $(CD_3)_2SO$], δ (ppm) = 28.3 (3 × *C*H_3), 29.9 (-CH_2-*C*H_2-CH_2-), 36.6 (NH-*C*H_2-CH_2), 37.7 (NH-*C*H_2-CH_2), 77.5, 112.5 (Ar-*C*), 121.2, 128.6 (Ar-*C*), 151.5, 155.6, 166.2

HRMS (ES): calculated for $C_{15}H_{24}N_3O_3$ $(M+H)^+$ 294.1812, found: 294.1815

6.12 Synthesis of *tert*-butyl(12-(4-aminobenzamido)dodecyl)carbamate (8)

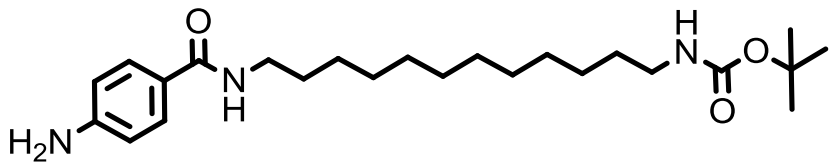

A solution of **6** (100 mg, 427 μmol) in dry dimethylformamide (50 mL) was charged with *N*-Boc-1,12-diaminododecane (256 mg, 854 μmol, 2 equiv. relative to **6**) and diisopropylethylamine (0.3 mL, 1.71 mmol, 2 equiv. relative to *N*-Boc-1,12-diaminododecane). The reaction mixture was cooled using ice-water and was stirred under an inert atmosphere (N_2), for 24 hours (overnight), until complete consumption of **6** was observed as shown by TLC (silica, 40 % dichloromethane/ethyl acetate). The solvent was removed under reduced pressure, and the crude product was re-dissolved in a mixture of 25 % dichloromethane/ 75 % ethyl acetate, and was chromatographically separated (silica, eluent: 25 % dichloromethane/ethyl acetate). Compound **8** (135 mg, 76 %) was isolated after precipitation from ethyl acetate by the addition of hexane. R*f* = 0.53 (silica, $C_2H_5CO_2CH_3$:C_6H_{12}; 7:3); m.p. = 122-123 °C.

^{1}H N.M.R. [400 MHz, ($(CD_3)_2SO$)], δ (ppm) = 1.16-1.25 (m, 18H, 9 × C*H*$_2$), 1.35 (s, 9H, 3 × C*H*$_3$), 1.45 (quintet, *J* = 6.60 Hz, 2H, $CH_2C\underline{H_2}CH_2$), 2.94 (q, *J* = 6.60 Hz, 2H, C*H*$_2$), 3.16 (q, *J* = 6.60 Hz, 2H, C*H*$_2$), 5.55 (br s, 2H, N*H*$_2$), 6.51 (d, *J* = 8.61 Hz, 2H, Ar-*H*), 6.75 (t, *J* = 5.41 Hz, 1H, N*H*), 7.53 (d, *J* = 8.61 Hz, 2H, Ar-*H*), 7.93 (t, *J* = 5.5 Hz, 1H, N*H*)

^{13}C N.M.R. [100 MHz, ($(CD_3)_2SO$)], δ (ppm) = 26.2, 26.5, 28.2, 28.7, 28.8, 28.95, 29.0, 29.4, 29.5, the signals corresponding to the NH-*C*H_2 were not observed, 77.3, 112.5, 121.5, 128.6, 151.4, 155.5, 166.0

HRMS (ES): calculated for $C_{24}H_{42}N_3O_3$ $(M+H)^+$ 420.3221, found: 420.3221

6.13 Attempted synthesis of *tert*-butyl(3-(4-((5,10,15,20-tetraphenylporphyrin-2-ylmethyl)-amino)benzamido)propyl)carbamate

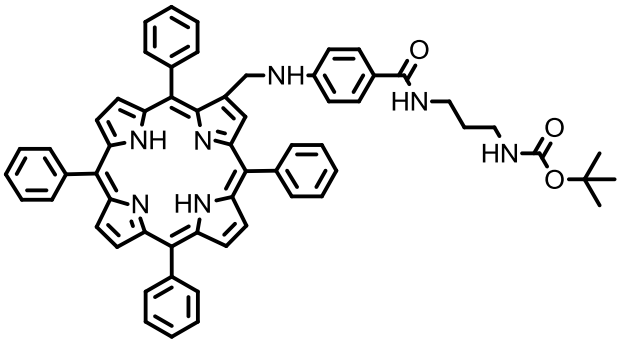

A solution of sodium cyanoborohydride (6 mg, 95 μmol, 1.6 equiv. relative to **3**) in methanol (3 mL), was added to **3** (38 mg, 59 μmol), **7** (35 mg, 119 μmol, 2 equiv. relative to **3**), 1 drop of acetic acid and activated 3 Å molecular sieves in anhydrous tetrahydrofuran (15 mL). The reaction was heated to reflux, under an inert atmosphere (N_2), while protected against light.

After 24 hours, the reaction was not progressing any further, with the TLC (silica, eluent: 5 % methanol/dichloromethane) of the reaction mixture revealing the presence of a newly formed UV-active fraction (suspected product) and **3**. A solution of sodium cyanoborohydride (6 mg, 95 μmol, 1.6 equiv. relative to **3**) in methanol (3 mL), was added. After 4 hours, the composition of the reaction mixture had remained unchanged as indicated by TLC. Once cooled to room temperature, the solvent was removed under reduced pressure, the crude mixture was re-dissolved in dichloromethane, washed with water and the organic layer was dried over anhydrous sodium sulphate. Chromatographic separation (silica coated prep TLC plates, eluent: 5 % methanol/dichloromethane) isolated the relevant fraction. The TLC of the suspected product exhibited decomposition, therefore the reaction was discarded.

6.14 Attempted synthesis of *tert*-butyl(12-(4-((5,10,15,20-tetraphenylporphyrin-2-ylmethyl)-amino)benzamido)dodecyl)carbamate

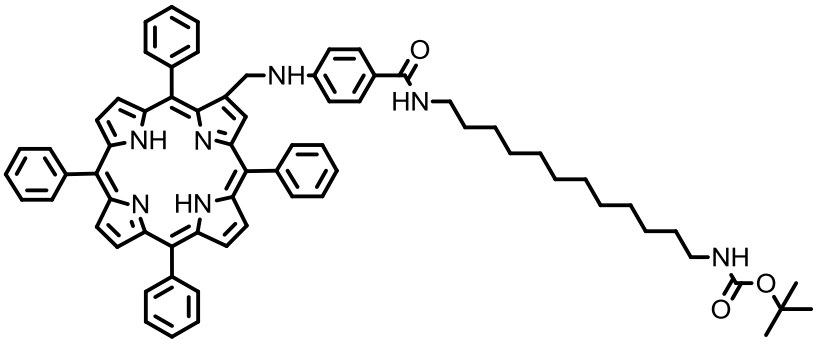

Compound **3** (80 mg, 124 μmol) dissolved in anhydrous tetrahydrofuran (30 mL), was charged with **8** (104 mg, 247 μmol, 2 equiv. relative to **3**), 1 drop of acetic acid and activated 3 Å molecular sieves. Sodium cyanoborohydride (12 mg, 190 μmol, 1.5 equiv. relative to **3**) dissolved in dry methanol (7 mL) was added to the reaction mixture, which was subsequently heated to reflux, under an inert atmosphere while avoiding exposure to light. After 24 hours (overnight) no further consumption of **3** was observed, as indicated by TLC (silica, eluent: 5 % methanol/dichloromethane), thus an additional methanolic solution of sodium cyanoborohydride (12 mg, 190 μmol, 1.5 equiv. relative to **3**) was added. After 13 hours (overnight) the reaction mixture had remained unchanged as indicated by TLC. Once cooled to room temperature, the solvent was removed *in vacuo*, the crude mixture was re-dissolved in dichloromethane and washed with a saturated sodium hydrogen carbonate solution and water. The organic layer was collected and dried over anhydrous sodium sulphate and chromatographic separation (silica coated prep TLC plates, eluent: 5 % methanol/dichloromethane) isolated the relevant fraction. The suspected product had degraded, therefore the suspected product was isolated again by chromatography (silica coated prep TLC plates, eluent: 5 % methanol/dichloromethane) and a crude ^{1}H NMR was conducted. The suspected product had decomposed and was discarded.

6.15 Attempted synthesis of *tert*-butyl(3-(4-((((5,10,15,20-tetraphenylporphyrinato)copper(II))-2-ylmethyl)-amino)benzamido)propyl)carbamate

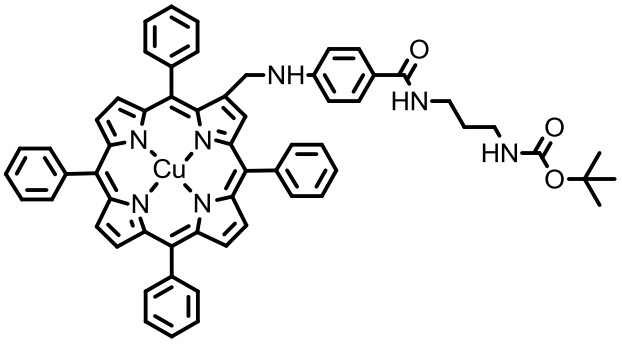

Compound **7** (17 mg, 57 μmol, 2 equiv. relative to **4**), and lanthanum(III) triflate (2 mg, 3.4 μmol, 8 equiv. relative to **4**) were added to a solution of **4** (20 mg, 28 μmol) dissolved in anhydrous tetrahydrofuran (15 mL). Activated molecular sieves were added and the reaction mixture was heated to reflux, under an inert atmosphere (N_2), while avoiding exposure to light. The reaction was monitored over a 3 day period by TLC (silica, eluent: dichloromethane), with only the starting material being observed.

6.16 Attempted synthesis of *tert*-butyl(12-(4-((((5,10,15,20-tetraphenylporphyrinato)copper(II))-2-ylmethyl)-amino)benzamido)dodecyl)carbamate

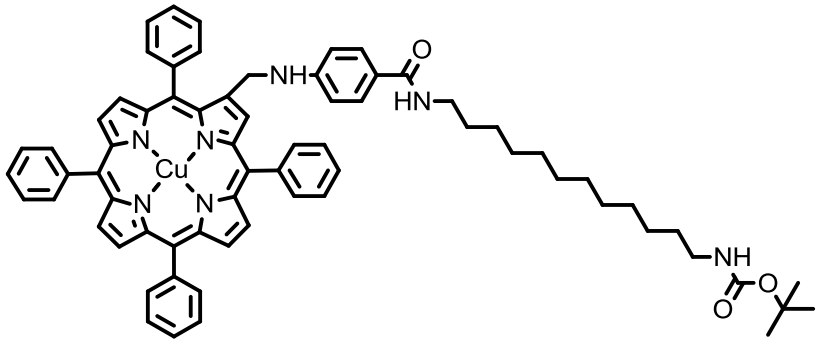

A solution of **4** (20 mg, 28 μmol) in anhydrous tetrahydrofuran (15 mL), was charged with **8** (24 mg, 57 μmol, 2 equiv. relative to **4**), lanthanum(III) triflate (2 mg, 3.4 μmol, 8 equiv. relative to **4**) and activated 3 Å molecular sieves. The reaction was heated to reflux, under an inert atmosphere (N_2), while avoiding exposure to light. The reaction was monitored over a 3 day period by TLC (silica, eluent: dichloromethane), which revealed that no reaction had occurred, with recovery of **4**.

6.17 Synthesis of methyl 4-((((5,10,15,20-tetraphenylporphyrinato)copper(II))-2-ylmethyl)amino)benzoate (9)

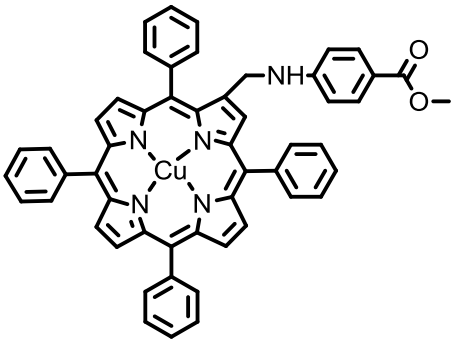

Compound **4** (500 mg, 711 μmol) dissolved in anhydrous tetrahydrofuran (150 mL) was charged with methyl 4-aminobenzoate (315 mg, 2 mmol, 2.9 equiv. relative to **4**), lanthanum(III) triflate (80 mg, 136 μmol, 0.19 equiv. relative to **4**) and activated 3 Å molecular sieves. The reaction was heated to reflux, under an inert atmosphere (N_2), while avoiding exposure to light. The reaction was monitored over a 44 hour period until the reaction mixture showed no further change as indicated by TLC (silica, eluent: dichloromethane). Once cooled to room temperature, the solvent was removed under reduced pressure and the crude mixture was re-dissolved in dichloromethane. The solution was passed through a silica plug column, washed with water and the organic layer was dried over anhydrous sodium sulphate. The volume was reduced (100 mL) *in vacuo*, and was added to a stirred, ice cooled solution of sodium borohydride (108 mg, 2.8 mmol, 4 equiv. relative to **4**) in dry methanol (100 mL), under an inert atmosphere (N_2), while protected against light. After 15 minutes, acetic acid (1.3 mL) was added, and the resulting mixture was washed with water and then dried over anhydrous sodium sulphate. The solvent was removed under reduced pressure and the crude product was re-dissolved in dichloromethane and was then chromatographically separated (silica, eluent: dichloromethane). Compound **9** (388 mg, 65 %) was isolated as a red powder after precipitation from dichloromethane by the addition of pentane. R*f* = 0.18 (silica, CH_2Cl_2:C_6H_{12}; 6:4); m.p. = >350 ^oC decomp.

UV/Vis (CH_2Cl_2, nm) λ_{max} (log ε) = 415 (5.63), 539 (4.72)

MS (MALDI) *m/z* = 838 $(M)^+$

HRMS (ESI): calculated for $C_{53}H_{37}CuN_5O_2Na$ $(M+Na)^+$ 861.2135, found: 861.2134

6.18 Synthesis of methyl 4-((5,10,15,20-tetraphenylporphyrin-2-ylmethyl)amino)benzoate (10)

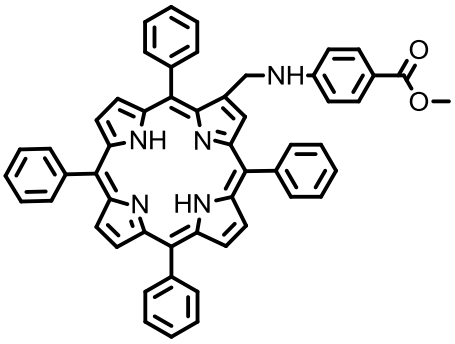

Method 1

Methyl 4-aminobenzoate (50 mg, 331 μmol, 1.5 equiv. relative to **3**) and 1 drop of acetic acid were added to a solution of **3** (142 mg, 221 μmol) dissolved in anhydrous tetrahydrofuran (60 mL). The reaction mixture was heated to reflux, under an inert atmosphere (N_2), while avoiding exposure to light. After 6 hours, sodium cyanoborohydride (21 mg, 339 μmol, 1.5 equiv. relative to **3**) dissolved in dry methanol (12 mL) was added to the reaction. After 40 hours, the composition of the reaction mixture exhibited no further change, as indicated by TLC (silica, eluent: dichloromethane). Once cooled to ambient temperature, the solvent was removed under reduced pressure and the crude product was re-dissolved in dichloromethane, washed with water and dried over anhydrous sodium sulphate. The organic layer was concentrated *in vacuo* and was purified by column chromatography (silica, eluent: dichloromethane). The purified **10** (45 mg, 26 %) was isolated as a purple powder after precipitation from dichloromethane by the addition of methanol.

Method 2

A stirred solution of **9** (172 mg, 204 μmol) dissolved in chloroform (20 mL), was treated with concentrated sulphuric acid (20 mL) for 5 minutes, while protected against light. The solution was carefully poured onto a vigorously stirred, ice cooled saturated sodium hydrogen carbonate solution (500 mL). Dichloromethane was added, and the organic layer was washed with water and was then dried over anhydrous sodium sulphate. The solvent was removed under reduced pressure, the crude product was re-dissolved in dichloromethane and was chromatographically separated (silica, eluent: dichloromethane). The purified **10** (98 mg, 62 %) was isolated as a purple powder after precipitation in methanol over dichloromethane. R*f* = 0.33 (silica, CH_2Cl_2); m.p. = >350 °C decomp.

^{1}H N.M.R. [400 MHz, $CDCl_3$], δ (ppm) = −2.84 (s, 2H, N*H*), 3.78 (s, 3H, OCH_3), 4.45 (d, *J* = 5 Hz, 2H, CH_2NH), 4.53 (t, *J* = 5 Hz, 1H, CH_2N*H*), 6.38 (d, *J* = 8.9 Hz, 2H, NH-Ar-*m*-*H*), 7.56-7.71 (m, 12H, 5,10,15,20-Ar-*m*-*p*-*H*), 7.74 (d, *J* = 8.9 Hz, 2H, NH-Ar-*o*-*H*), 8.01-8.07 and 8.10-8.16 (2m, 8H, 5,10,15,20-Ar-*o*-*H*), 8.58 (d, *J* = 4.69 Hz, 1H, *β*-*H*), 8.66-8.78 (m, 6H, *β*-*H*)

^{13}C N.M.R. [100 MHz, $CDCl_3$], δ (ppm) = 42.5 (*C*H_2NH), 50.5 (O*C*H_3), 110.9 (NH-Ar-*m*-*C*), 117.5, 118.3, 118.5, 119.3, 119.6, 125.61, 125.64, 125.7, 126.2, 126.70, 126.74, 127.5, 130.3 (NH-Ar-*o*-*C*), 132.2 (5,10,15,20-Ar-*o*-*C*), 133.5 (5,10,15,20-Ar-*o*-*C*) , 133.6 (5,10,15,20-Ar-*o*-*C*), 140.8, 140.9, 141.1, 141.2, 150.7, 166.4

UV/Vis (CH_2Cl_2, nm) λ_{max} (log ε) = 419 (5.84), 515 (4.58), 550 (4.09), 591 (4.05), 645 (3.81)

HRMS (ESI): calculated for $C_{53}H_{40}N_5O_2$ $(M+H)^+$ 778.3177, found: 778.3171

6.19 Synthesis of 4-((5,10,15,20-tetraphenylporphyrin-2-ylmethyl)amino)benzoic acid (11)

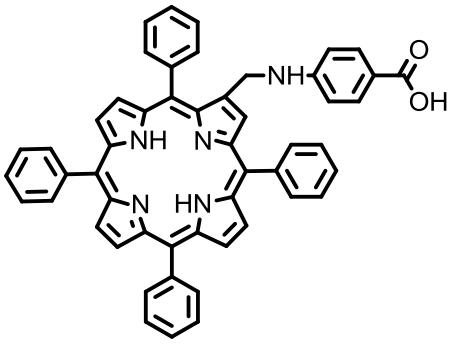

p-Toluenesulfonic acid monohydrate (30 mg, 160 μmol, 4.equiv. relative to **10)** was added to **10** (31 mg, 40 μmol) dissolved in sulphuric acid (4 M, 25 mL) and the subsequent mixture was heated to reflux. After 20 hours, complete consumption of **10** was observed by TLC (silica, eluent: dichloromethane) and the reaction mixture was cooled to ambient temperature. The vigorously stirred reaction mixture was cooled further on ice, and sodium hydroxide (1 M) was carefully added until neutralisation had occurred. The crude product was extracted with dichloromethane, which was subsequently washed with a saturated sodium hydrogen carbonate solution, then water, and the organic layer was dried over anhydrous sodium sulphate. The solvent was removed *in vacuo* and column chromatography (silica, eluent: 3 % methanol/dichloromethane) was used to isolate the relevant fraction. Product **11** (22 mg, 73 %) was isolated as a purple powder after precipitation from dichloromethane by the addition of hexane. R*f* = 0.55 (silica, CH_2Cl_2:CH_3OH; 10:1); m.p. = >350 °C decomp.

^{1}H N.M.R. [400 MHz, $(CD_3)_2SO$], δ (ppm) = −2.92 (br s, 2H, N*H*), 4.41 (d, *J* = 5 Hz, 2H, CH_2NH), 6.51 (d, *J* = 8.8 Hz, 2H, NH-Ar-*m*-*H*), 7.27 (t, *J* = 5 Hz, 1H, CH_2N*H*), 7.63 (d, *J* = 8.8 Hz, 2H, NH-Ar-*o*-*H*), 7.65-7.89 (m, 12H, 5,10,15,20-Ar-*m*-*p*-*H*), 8.03-8.09 and 8.19-8.26 (2m, 8H, 5,10,15,20-Ar-*o*-*H*), 8.64 (d, *J* = 4.7 Hz, 1H, *β*-*H*), 8.70-8.89 (m, 6H, *β*-*H*), 12.02 (br s, 1H, CO_2H)

^{13}C N.M.R. [100 MHz, $CDCl_3$/CD_3OD], δ (ppm) = 43.1, 111.3, 111.7, 126.45, 126.52, 126.6, 127.2, 127.6, 128.4, 131.5, 133.0, 134.4, 151.9, 169.2

UV/Vis (CH_2Cl_2:CH_3OH; 2:1, nm) λ_{max} (log ε) = 418 (5.5), 515 (4.22), 549 (3.75), 589 (3.73), 645 (3.48)

HRMS (ESI) calculated for $C_{52}H_{38}N_5O_2$ $(M + H)^+$ 764.3020, found: 764.3013

6.20 Synthesis of 5,10,15,20-tetra-(4-pyridyl)porphyrin (12)

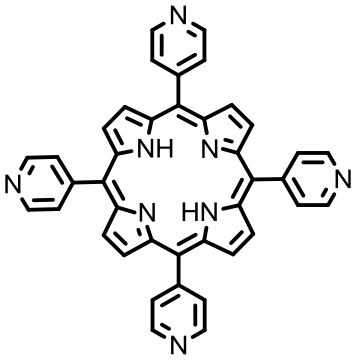

4-Pyridinecarboxaldehyde (4 mL, 42 mmol) was dissolved in propionic acid (100 mL) and the resulting pale yellow mixture was heated to reflux. Pyrrole (2.9 mL, 42 mmol, 1 equiv. relative to 4-pyridinecarboxaldehyde) was added drop-wise to the refluxing mixture and the resulting solution was left under reflux conditions for 30 minutes, while protected against light. Once cooled to ambient temperature, the mixture was filtered to yield a dark purple solid. The crude product was washed with methanol and hot water to afford a purple solid.

The propionic acid solvent was removed under reduced pressure and the black tarry crude mixture was dissolved in dichloromethane and methanol, which was subsequently washed with a saturated sodium hydrogen carbonate solution and water. The organic layer was dried over magnesium sulphate and the solvent was removed by evaporation *in vacuo*. The crude product was re-dissolved in 5 % methanol/dichloromethane and was purified by gravitational column chromatography (silica, eluent: 5 % methanol/dichloromethane), the relevant fraction was collected and was combined with the previously isolated purple solid. The purple crystalline **12** (0.75 g 11 %) was isolated after precipitation from chloroform by the addition of methanol. R*f* = 0.55 (silica, CH_2Cl_2:CH_3OH; 10:1); m.p. = >350 °C decomp.

^{1}H N.M.R. [400 MHz, $CDCl_3$/CD_3OD], δ (ppm) = −2.92 (s, 2H, N*H*), 8.16 (dd, *J* = 1.68 Hz, *J* = 4.21 Hz, 8H, 5,10,15,20-Ar-*o*-*H*), 8.87 (br s, 8H, *β*-*H*), 9.07 (dd, *J* = 1.68 Hz, *J* = 4.21 Hz, 8H, 5,10,15,20-Ar-*m*-*H*)

^{13}C N.M.R. [100 MHz, $CDCl_3$/CD_3OD], δ (ppm) = 117.1, 129.3, 147.2, 150.3

UV/Vis (CH_2Cl_2, nm) λ_{max} = 416, 513, 546, 587, 643

MS (MALDI) *m/z* = 619 $(M+H)^+$

6.21 Synthesis of (5,10,15,20-tetra(4-pyridyl)porphyrinato) copper(II) (13)

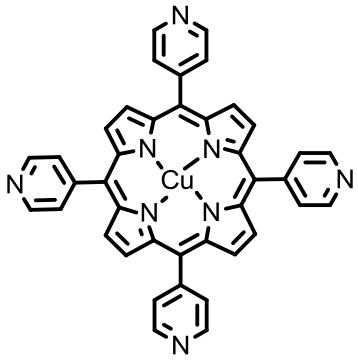

A slurry of copper(II) acetate monohydrate (770 mg, 39 mmol) in methanol-water (10 mL; 6:1) was added to compound **12** (600 mg, 971 μmol) dissolved in chloroform (100 mL), and the resulting mixture was heated to reflux. After 5 hours, the hot solution was poured onto a warm neutral alumina oxide pad and eluted using hot chloroform. The red band was collected and dried over magnesium sulphate, and the solvent was removed under reduced pressure yielding **13** as a red powder (612 mg, 93 %); R*f* = 0.60 (silica, CH_2Cl_2:CH_3OH; 10:1); m.p. = >350 °C decomp.

UV/Vis (CH_2Cl_2, nm) λ_{max} = 415, 495, 538
MS (MALDI) *m/z* = 679 $^{63}Cu(M)^+$, 681 $^{65}Cu(M)^+$

6.22 Attempted synthesis of 2-formyl-5,10,15,20-tetra(4-pyridyl)porphyrin

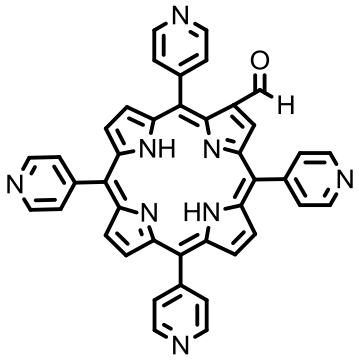

Phosphorus oxychloride (0.95 mL, 10 mmol) was added drop-wise to ice cooled, dry dimethylformamide (15 mL, 15 mmol), under an argon atmosphere while avoiding exposure to moisture. An ice cooled solution of **13** (100 mg, 147 μmol) dissolved in anhydrous 1,2-dichloroethane (10 mL), was then added to the viscous Vilsmeier complex, and the mixture was then allowed to reach room temperature, and was then heated at reflux for 7 hours. Once cooled to room temperature over night, the reaction mixture was poured onto an ice-cooled, stirred solution of sodium hydroxide (0.29 M, 300 mL). Chloroform was then added, the organic layer was collected, washed with saturated sodium hydrogen carbonate solution and then water. The organic layer was then dried over anhydrous sodium sulphate and the solvent was removed under reduced pressure. TLC analysis (silica, eluent: 5 % methanol/dichloromethane) of the reaction mixture showed only the presence of **12**.

6.23 Synthesis of 5,10,15,20-tetra(3,5-dimethoxyphenyl)porphyrin (14)

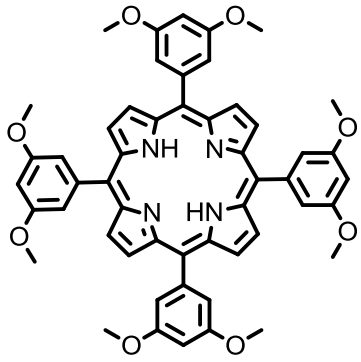

3,5-Dimethoxybenzaldehyde (18.46 g, 111 mmol) was dissolved in propionic acid (300 mL) and the resulting colourless mixture was heated to reflux. Pyrrole (7.69 mL, 111 mmol, 1 equiv. relative to 3,5-dimethoxybenzaldehyde) was added drop-wise to the refluxing mixture and the resulting dark solution was left under reflux conditions for 30 minutes, while protected against light. Once the dark mixture was cooled to room temperature, the mixture was filtered to yield a purple solid product. The crude product was washed with methanol and hot water; and was then dried under vacuum to afford the purple crystalline **14** (3.54 g, 15 %). R*f* = 0.81 (silica, CH_2Cl_2:CH_3OH; 150:1); m.p. = >350 °C decomp.

^{1}H N.M.R. [400 MHz, $CDCl_3$], δ (ppm) = −2.84 (s, 2H, N*H*), 3.96 (s, 24H, 8 × OCH_3), 6.90 (t, *J* = 2.15 Hz, 4H, 5,10,15,20-Ar-*p*-*H*), 7.40 (d, *J* = 2.15 Hz, 8H, 5,10,15,20-Ar-*o*-*H*), 8.94 (br s, 8H, *β*-*H*)

^{13}C N.M.R. [100 MHz, $CDCl_3$], δ (ppm) = 55.7, 100.2, 113.9, 119.8, 144.0, 158.9

UV/Vis (CH_2Cl_2, nm) λ_{max} = 421, 516, 549, 589, 645

MS (MALDI) *m/z* = 855 $(M+H)^+$

6.24 Synthesis of (5,10,15,20-tetra(3,5-dimethoxyphenyl)porphyrinato) copper(II) (15)

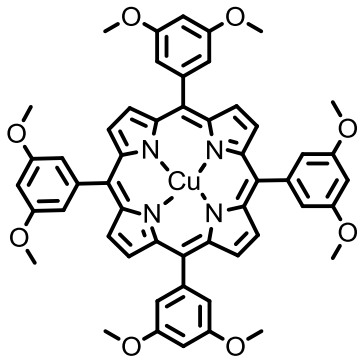

Compound **14** (350 mg, 409 μmol) dissolved in chloroform (40 mL) and a slurry of copper(II) acetate monohydrate (326 mg, 1.64 mmol, 4. equiv. relative to **14**) in methanol-water (7 mL, 6:1) was heated to reflux for 5 hours. The hot solution was poured onto a warm silica pad and eluted using hot chloroform. The red band was collected, dried over magnesium sulphate and the solvent was removed *in vacuo*. The red-purple crystalline product **15** (356 mg, 95 %) was precipitated in methanol over chloroform. R*f* = 0.86 (silica, CH_2Cl_2:CH_3OH; 150:1); m.p. = >350 °C decomp.

UV/Vis (CH_2Cl_2, nm) λ_{max} = 417, 485, 539
MS (MALDI) *m/z* = 915.348 $^{63}Cu(M)^+$, 917.352 $^{65}Cu(M)^+$ and $^{63}Cu(M+2H)^+$

6.25 Attempted synthesis of 2-formyl-5,10,15,20-tetra(3,5-dimethoxyphenyl)porphyrin

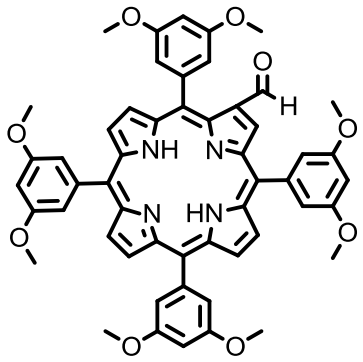

A Vilsmeier complex, formed by the drop-wise addition of phosphorus oxychloride (0.95 mL, 10 mmol) to ice cooled, anhydrous dimethylformamide (1.15 mL, 15 mmol), under an argon atmosphere while avoiding exposure to moisture, was added to a cooled solution of **15** (140 mg, 153 μmol) in dry 1,2-dichloroethane (15 mL). The reaction mixture was then allowed to reach room temperature, and then heated at reflux for 7 hours, while protected against moisture and light. Once the reaction mixture had cooled to ambient temperature over night, it was poured onto a stirred, ice-cooled solution of sodium hydroxide (0.29 M, 300 mL). Chloroform was then added, the organic layer was collected, washed with saturated sodium hydrogen carbonate solution and then water. The organic layer was then dried over anhydrous sodium sulphate. The TLC (silica, eluent: dichloromethane) of the reaction mixture exhibited no UV-active fraction.

6.26 Synthesis of 5-(4-acetamidophenyl)-10,15,20-tri(4-pyridyl)porphyrin (16)

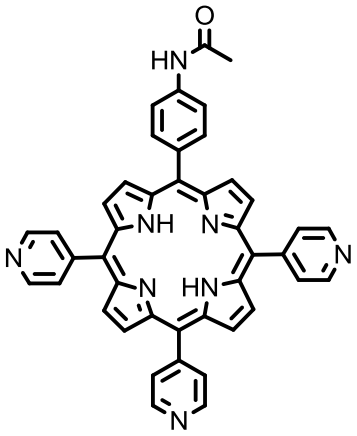

4-Acetamidobenzaldehyde (4.08 g, 25 mmol) and 4-pyridinecarboxaldehyde (7.2 mL, 75 mmol, 3 equiv. relative to 4-acetamidobenzaldehyde) were dissolved in propionic acid (400 mL), and the resulting pale yellow mixture was heated to reflux. Pyrrole (6.9 mL, 100 mmol, 4 equiv. relative to 4-acetamidobenzaldehyde) was added drop-wise to the refluxing mixture and the resulting solution was left under reflux conditions for 60 minutes, while avoiding exposure to light. Once the dark mixture was cooled to room temperature, the propionic acid was removed under reduced pressure to yield a crude dark purple, tarry solid. Gravitation column chromatography (silica, eluent: 5 % methanol/dichloromethane) was used to isolated the relevant fraction, and **16** was furnished a purple solid (849 mg, 5 %) after precipitation from dichloromethane by the addition of methanol. R*f* = 0.24 (silica, CH_2Cl_2: CH_3OH; 10:1); m.p. = >350 °C decomp.

^{1}H N.M.R. [400 MHz, $CDCl_3/CD_3OD$], δ (ppm) = −2.90 (br s, 2H, N*H*), 2.35 (s, 3H, NHCOC*H*$_3$), 8.00 and 8.15 (AB, 4H, *J* = 8.55 Hz, 5-Ar-*m*-*o*-*H*), 8.19-8.23 (m, 6H, 10,15,20-Ar-*o*-*H*), 8.71-9.08 (m, 14H, 8H of *β*-*H* and 6H of 10,15,20-Ar-*m*-*H*), 9.49 (br s, N*H*$COCH_3$)

^{13}C N.M.R. [100 MHz, $CDCl_3/CD_3OD$], δ (ppm) = 24.2, 116.8, 117.3, 117.7, 118.3, 118.4, 121.7, 129.8, 135.2, 137.0, 138.7, 147.9, 148.0, 150.7, 150.8, 170.3

UV/Vis (CH_2Cl_2, nm) λ_{max} = 418, 514, 549, 589, 646

MS (MALDI) *m/z* = 675$(M+H)^+$

6.27 Synthesis of 5-(4-aminophenyl)-10, 15, 20-tri-(4-pyridyl)porphyrin (17)

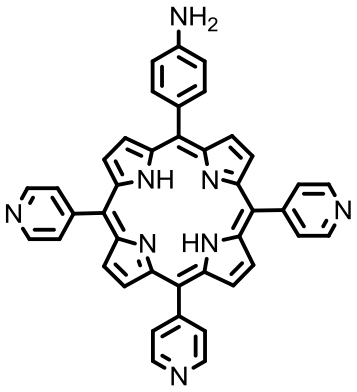

Hydrochloric acid (5 M, 100 mL) was added to **16** (136 mg, 833 μmol) in ethanol (14 mL) and the mixture was heated to reflux for 3 hours. Once the solution had cooled to room temperature, the hydrochloric acid was removed *in vacuo*. The crude was dissolved in a mixture of chloroform (20 mL) and triethylamine (2 mL), and the resulting solution was stirred at room temperature for 10 minutes. The solution was washed with a dilute citric acid solution and water. The organic layer was collected, dried over magnesium sulphate and the solvent was reduced *in vacuo*. Gravity percolation chromatography (silica, eluent: 5 % methanol/dichloromethane) was used to purify the crude product, with **17** (116 mg, 91 %) isolated as a purple/red solid after precipitation from chloroform by the addition of methanol. R*f* = 0.35 (silica, $CHCl_3$:CH_3OH; 19:1); m.p. = >350 °C decomp.

^{1}H N.M.R. [400 MHz, $CDCl_3/CD_3OD$], δ (ppm) = −2.84 (s, 2H, N*H*), not observed (NH_2), 7.13 (d, *J* = 8.4 Hz, 2H, 5-Ar-*m*-*H*), 7.99 (d, *J* = 8.4 Hz, 2H, 5-Ar-*o*-*H*), 8.17-8.22 (m, 6H, 10,15,20-Ar-*o*-*H*) 8.74-9.07(m, 14H, 8H of *β*-*H* and 6H of 10,15,20-Ar-*m*-*H*)

^{13}C N.M.R. [100 MHz, $CDCl_3/CD_3OD$], δ (ppm) = 113.7, 116.5, 117.1, 122.8, 129.6, 131.6, 135.9, 146.5, 147.99, 148.04, 148.1, 150.5, 150.6

UV/Vis (CH_2Cl_2, nm) λ_{max} = 420, 516, 554, 591, 648

MS (MALDI) *m/z* = 633 $(M+H)^+$

6.28 Attempted synthesis of 5-(4-((*N*-maleimidomethyl)cyclohexane-1-amido)phenyl)-10,15,20-tri(4-pyridyl)porphyrin

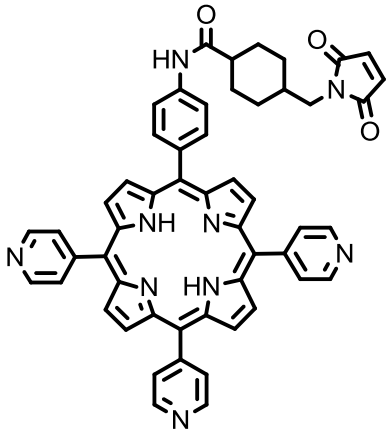

SMCC (10 mg, 30 μmol, ≈ 2 equiv. relative to **17**) was added to **17** (10 mg, 16 μmol) dissolved in dry dichloromethane (10 mL), and the resulting solution was stirred at 30 °C, while protected against light and moisture. After 2 hours, TLC analysis (silica, eluent: 10 % methanol/dichloromethane) indicated only the presence of **17**, therefore a drop of diisopropylethylamine was added. After 16 hours (overnight) the TLC of the reaction mixture remained unchanged.

The reaction was repeated in a similar manner, employing chloroform (5 mL), with diisopropylethylamine being added at the start of the reaction. The reaction was monitored over a 6 day period, with no reaction occurring, as shown by TLC.

The reaction was also repeated using pyridine (4 mL) as solvent, without the addition diisopropylethylamine. The reaction was monitored over a 4 days, with no reaction being observed, as indicated by TLC.

6.29 Synthesis of 5-(4-carboxyphenyl)-10,15,20-tri-(4-pyridy)porphyrin (18)

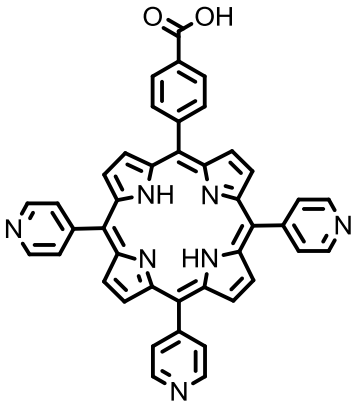

Pyrrole (4 mL, 58 mmol) was added drop-wise to a refluxing mixture of 4-carboxybenzaldehyde (2.54 g, 17 mmol, 0.29 equiv. relative to pyrrole) and 4-pyridinecarboxaldehyde (4 mL, 42 mmol, 0.72 equiv. relative to pyrrole) dissolved in propionic acid (250 mL), while avoiding exposure to light. After 30 minutes at reflux, the reaction mixture was cooled to room temperature and the propionic acid was removed *in vacuo*. Gravity column chromatography (silica, eluent: 7 % methanol/dichloromethane) was used to obtain the relevant fraction and precipitation from dichloromethane, by the addition of methanol afforded the purple crystalline **18** (516 mg, 6 %). R*f* = 0.42 (silica,CH_2Cl_2: CH_3OH; 9:1); m.p. = >350 °C decomp.

^{1}H N.M.R. [400 MHz, $CDCl_3/CD_3OD$], δ (ppm) = −2.89 (s, 2H, N*H*), 8.23-8.27 (m, 6H, 10,15,20-Ar-*o*-*H*), 8.31 and 8.49 (AB, *J* = 8 Hz, 2H, 5-Ar-*m*-*o*-*H*), 8.74-9.09 (m, 14H, 6H of 10,15,20-Ar-*m*-*H* and 8H of *β*-*H*), not observed (CO_2H)

^{13}C N.M.R. [100 MHz, $CDCl_3/CD_3OD$], δ (ppm) = 116.7, 117.0, 120.3, 128.1, 129.5, 130.2, 134.2, 145.7, 147.3, 150.6, 168.6

UV/Vis ($CHCl_3$, nm) λ_{max} = 418, 514, 548, 588, 657

MS (MALDI) *m/z* = 662 $(M+H)^+$

6.30 Synthesis of 5-(4-(succinimidyl-*N*-oxycarbonyl)phenyl)-10,15,20-tri-(4-pyridyl)porphyrin (19)

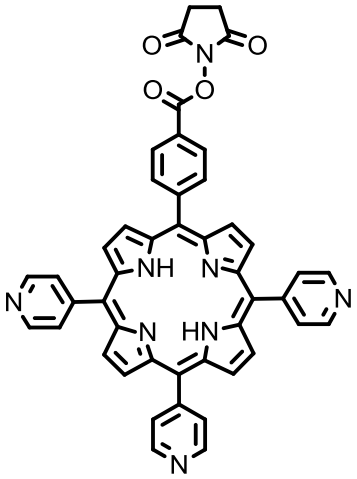

Thionyl chloride (0.1 mL, 1.37 mmol, 18 equiv. relative to **18**) was slowly added to a stirred solution of **18** (51 mg, 77 μmol) in anhydrous pyridine (5 mL) and the reaction was then stirred at 50 °C, while protected from light and atmospheric moisture. After 30 minutes, *N*-hydroxysuccinimide (200 mg, 1.74 mmol, 22.6 equiv. relative to **19**) was added, and the mixture was stirred for a further 3 hours. Once cooled to room temperature, the solvent was removed *in vacuo*, and the crude mixture was re-dissolved in dichloromethane and washed with a saturated solution of sodium hydrogen carbonate and then water. The organic layer was dried over anhydrous sodium sulphate and the solvent was removed under reduced pressure. The pure **19** (52 mg, 90 %) was isolated as a brown/red solid after precipitation in hexane over chloroform. R*f* = 0.82 (Silica, CH_2Cl_2: CH_3OH; 9:1). m.p. = >350 °C decomp.

^{1}H N.M.R. [400 MHz, $CDCl_3$], δ (ppm) = −2.90 (br s, 2H, N*H*), 3.03 (br s, 4H, 2 x CH_2), 8.17 (dd, *J* = 1.6 Hz, *J* = 4.3 Hz, 6H, 10,15,20-Ar-*o*-*H*), 8.37 (d, *J* = 6.5 Hz, 2H, 5-Ar-*m*-*H*), 8.57 (d, *J* = 6.5 Hz, 2H, 5-Ar-*o*-*H*), 8.85 (d, *J* = 4.8 Hz, 2H, *β*-*H*), 8.86-8.90 (m, 6H, *β*-*H*), 9.06 (dd, *J* = 1.6 Hz, *J* = 4.3 Hz, 6H, 10,15,20-Ar-*m*-*H*)

^{13}C N.M.R. [100 MHz, $CDCl_3$], δ (ppm) = 25.8 (2x*C*H_2), 117.7, 117.8, 119.2, 124.9, 129.1, 129.3, 131.5, 134.8, 148.5, 149.8, 162.0, 169.3 (2 x *C*O)

UV/Vis (CH_2Cl_2), λ_{max} (log ε) = 418 (5.66), 513 (4.43), 547 (3.93), 588 (3.91), 644 (3.50)

HRMS (ESI): calculated for $C_{46}H_{31}N_8O_4$ $(M + H)^+$ 759.2463, found: 759.2446

6.31 Synthesis of 5-(4-((6-*tert*-butylcarbamate)hexyl-1-amino-*N*-carbonyl)phenyl)10,15,20-tri-(4-pyridyl)porphyrin (20)

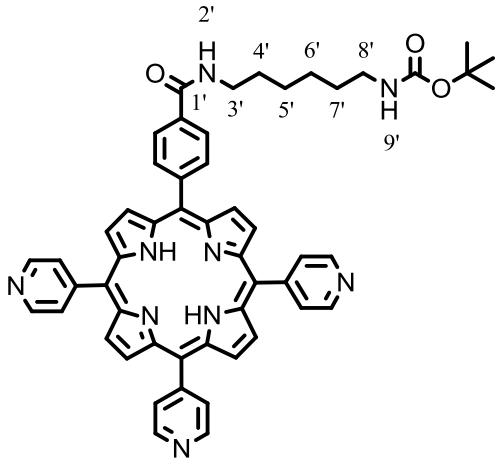

To a stirred solution of **19** (51 mg, 67 μmol) in anhydrous dimethylsulfoxide (6 mL) it was added *N*-Boc-1,6-diaminohexane hydrochloride (43 mg, 170 μmol, 2.5 equiv. relative to **19**) and potassium carbonate (58 mg, 420 μmol, 2.5 equiv. relative to *N*-Boc-1,6-diaminohexane hydrochloride). The reaction mixture was stirred at 40 °C, while protected against atmospheric moisture and light. After 40 minutes, full consumption of the starting porphyrin was achieved as indicated by TLC (silica, eluent: 10 % methanol/dichloromethane) and the reaction mixture was diluted with dichloromethane and washed with water. The organic layer was dried over anhydrous sodium sulphate and the solvent was removed under reduced pressure. The pure **20** was obtained (47 mg, 82 %) after purification by flash chromatography (silica, eluent: 6 % methanol/dichloromethane) and precipitation from dichloromethane by the addition of hexane. R*f* = 0.67 (Silica, CH_2Cl_2: CH_3OH; 9:1); m.p. = >350 °C decomp.

^{1}H N.M.R. [400 MHz, $CDCl_3$], δ (ppm) = −2.94 (br s, 2H, N*H*), 1.37-1.47 (m, 11H, -$CO_2C(CH_3)_3$ and 6'-CH_2), 1.48-1.58 (m, 4H, 5'-CH_2 and 7' -CH_2), 1.75 (quintet, *J* = 6.9 Hz, 2H, 4'-CH_2), 3.06-3.18 (m, 2H, 8'-CH_2), 3.58 (t, *J* = 6.9 Hz, 2H, -NHC$\underline{H_2}$ (3'-CH_2), 5.09 (br s, 1H, 9'-N*H*), 7.68 (br s, 1H, 2'-N*H*), 8.11-8.29 (m, 10H, 5-Ar-*o*-*m*-*H* and 10,15,20-Ar-*o*-*H*), 8.63-9.08 (m, 14H, 10,15,20-Ar-*m*-*H* and *β*-*H*)

^{13}C N.M.R. [100 MHz, $CDCl_3$], δ (ppm) = 25.9, 26.1, 28.2 (3 x CH_3), 29.1, 29.5, 29.7, 39.7, 39.8, 116.6, 117.0, 120.1, 120.7, 125.5, 129.7 (10,15,20-Ar-*o*-*C*), 134.2, 134.4, 142.2, 146.9 (10,15,20-Ar-*m*-*C*), 151.2, 151.3, 156.5 (-NH$CO_2{}^t$Bu), 167.9 (1'-*C*)

UV/Vis (CH_2Cl_2, nm), λ_{max} (log ε) = 417 (5.66), 513 (4.38), 547 (3.89), 589 (3.87), 644 (3.51)

HRMS (ESI): calculated for $C_{53}H_{50}N_9O_3$ $(M + H)^+$ 860.4031, found: 860.4029

6.32 Synthesis of 5-(4-(6-(4-(*N*-maleimidomethyl)cyclohexane-1-amido)hexyl-1-amino-*N*-carbonyl)phenyl)-10,15,20-tri-(4-pyridyl)porphyrin (21)

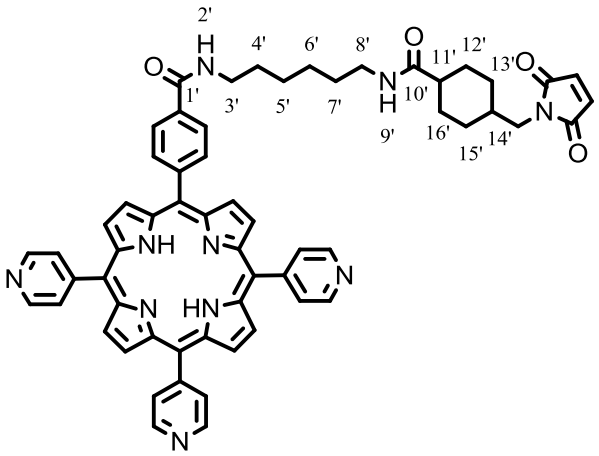

Trifluoroacetic acid (6 mL) was added to a stirred solution of porphyrin **20** (35 mg, 41 μmol) in dry dichloromethane (6 mL). The mixture was then kept under stirring at room temperature, while protected against light and moisture, for 50 minutes, until complete consumption of **20** had occurred as indicated by TLC (silica, eluent: 10 % methanol/chloroform). The mixture was then poured into an ice cooled aqueous solution of sodium hydrogen carbonate containing ice and the organic layer was collected, then washed with water and dried over anhydrous sodium sulphate. The solvent was then removed under reduced pressure and the resulting mixture was promptly dissolved in anhydrous dimethylformamide (4 mL). To the resulting solution was added SMCC (16.5 mg, 48 μmol, 1.2 equiv. relative to **20**) and diisopropylethylamine (35 μL, 204 μmol, 4.1 equiv. relative to SMCC) and the reaction mixture was stirred for 1 hour, at ambient temperature, while protected against light and moisture. After this period, the porphyrinic material was precipitated with diethyl ether and hexane. The precipitate was dissolved in dichloromethane and purified by flash chromatography (silica, eluent: 5 % methanol/chloroform). Precipitation from dichloromethane by the addition of hexane furnished porphyrin **21** (34 mg, 85 %). R*f* = 0.52 (Silica, CH_2Cl_2: CH_3OH; 9:1); m.p. = >350 °C decomp.

^{1}H N.M.R. [400 MHz, $CDCl_3$], δ (ppm) = −2.90 (s, 2H, N*H*), 0.94-1.09 (m, 2H, 1H of 13'-CH_2 and 1H of 15'-CH_2); 1.40-1.51, 1.52-1.63 and 1.64-1.88 (3m, 11H, 5 x CH_2 + 1C*H*); 1.89-1.99 (m, 2H, CH_2), 2.00-2.11 (m, 1H, 11'-*H*), 3.28-3.42 (m, 4H, 8'-CH_2, CH_2-mal), 3.63 (q, *J* = 6.1 Hz, 2H, 3'-CH_2), 5.62 (t, *J* = 5.9 Hz, 1H, 9'-N*H*), 6.62 (s,

2H, COC*H*=C*H*CO), 6.89 (t, *J* = 6.1 Hz, 1H, 2'-N*H*), 8.10-8.21 (m, 6H, 10,15,20-Ar-*o*-*H*), 8.23 and 8.29 (AB, *J* = 8.1 Hz, 4H, 5-Ar-*o*-*m*-*H*), 8.84 (d, *J* = 4.6 Hz, 2H, *β*-*H*), 8.85-8.87 (m, 4H, *β*-*H*), 8.88 (d, *J* = 4.6 Hz, 2H, *β*-*H*), 8.98-9.16 (m, 6H, 10,15,20-Ar-*m*-*H*)

^{13}C N.M.R. [100 MHz, $CDCl_3$], δ (ppm) = 25.6 (*C*H_2), 25.8 (*C*H_2), 29.0 (13'and 15' *C*H_2), 29.5, 29.6, 29.7, 29.9, 36.4, 38.5 (*C*H_2), 39.5 (*C*H_2-mal), 43.6, 45.4, 117.4, 117.6, 120.3, 125.5 (5-Ar-*m*-*C*), 129.4 (10,15,20-Ar-*o*-*C*), 131.3 (*β*-*C*), 133.9 (CO*C*H=*C*HCO), 134.5, 134.6 (5-Ar-*o*-*C*), 144.6, 148.4(10,15,20-Ar-*m*-*C*), 149.9, 167.5 (1'-*C*O), 171.0 (*C*OCH=CH*C*O), 175.8(10'-*C*O)

UV/Vis (CH_2Cl_2, nm), λ_{max} (log ε) = 417 (5.51), 513 (4.23), 547 (3.83), 588 (3.81), 644 (3.43)

HRMS (ESI) calculated for $C_{60}H_{55}N_{10}O_4$ $(M + H)^+$ 979.4402, found: 979.4398

6.33 Synthesis of 5-(4-(6-(4-(*N*-maleimidomethyl)cyclohexane-1-amido)hexyl-1-amino-*N*-carbonyl)phenyl)-10,15,20-tri-(4-*N*-methyl-pyridyniumyl)porphyrin triiodide (22)

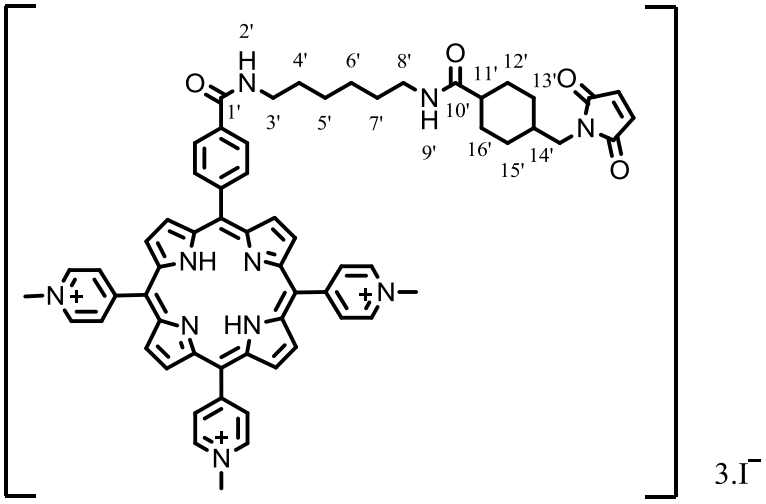

A solution of porphyrin **21** (21 mg, 20 μmol) in anhydrous dimethylformamide (2.6 mL) was charged with a large excess of methyl iodide (0.2 mL, 3.21 mmol, 160 equiv. relatively to **21**) and the resulting mixture was stirred at 40 °C for 4 hours, while protected against light. Once cooled to room temperature, the porphyrinic material was precipitated with ice cooled diethyl ether and hexane (50:1) and washed thoroughly with cold diethyl ether. The methylated porphyrin was obtained as a lustrous purple solid (24 mg, 80 %). m.p. = >350 °C decomp.

^{1}H N.M.R. [400 MHz, $(CD_3)_2SO$], δ (ppm) = −3.03 (s, 2H, N*H*), 0.83-0.97 (m, 2H, 1H of 13'-CH_2 and 1H of 15'-CH_2), 1.20-1.36 (m, 2H, 1H of 12'-CH_2 and 16'-CH_2), 1.37-1.54 (m, 7H, 3 x CH_2 and 14'-*H*), 1.59-1.78 (m, 6H, 4'-CH_2 and 1H of 12'-CH_2, 1H of 16'-CH_2, 1H of 13'-CH_2 and 1H of 15'-CH_2), 1.98-2.10 (m, 1H, 11'-*H*), 3.02-3.10 (m, 2H, 8'-CH_2), 3.23 (d, *J* = 6.9 Hz, 2H, C$\underline{H}_2$-mal), 3.41-3.47 (m, 2H, 3'-CH_2), 4.72 and 4.73 (2s, 6H+3H, 3 × CH_3), 6.97 (s, 2H,-COC$\underline{H}$=C$\underline{H}$CO-), 7.72 (t, *J* = 5.5 Hz, 1H, 9'-N*H*), 8.32 and 8.35 (AB, *J* = 8.4 Hz, 4H, 5-Ar-*o*-*m*-*H*), 8.87 (t, *J* = 5.6 Hz, 1H, 2'-N*H*), 8.95-9.06 (m, 8H, 2H of *β*-*H* and 6H of 10,15,20-Ar-*o*-*H*), 9.06-9-08 (m, 2H, *β*-*H*), 9.19-9.24 (m, 4H, *β*-*H*), 9.48 (d, *J* = 6.9 Hz, 6H, 10,15,20-Ar-*m*-*H*)

^{13}C N.M.R. [100 MHz, $((CD_3)_2SO)$], δ (ppm) = 26.1 (12'-CH_2 and 16'-CH_2), 26.2 (14'-CH_2), 28.6 (CH_2), 29.2, 29.4 (13'-CH_2 and 15'-CH_2), 36.1 (14'-CH), 43.1 (8'-CH_2), 43.8 (CH_2-mal), 47.9 (CH_3), 48.5, 114.7, 115.3 (10,15,20-*C*), 126.0 (5-Ar-*m*-*C*), 132.1

(10,15,20-Ar-*o*-*C*), 134.1 (5-Ar-*o*-*C*), 134.3 (-CO*C*H=*C*HCO-), 134.6, 142.9, 144.2 (10,15,20-Ar-*m*-*C*), 156.5, 165.8 (1'-*C*O), 171.2 (-*C*OCH=CH*C*O-), 174.8 (10'-*C*O)

UV/Vis (H_2O, nm), λ_{max} (log ε): 424 (5.32), 519 (4.18), 555 (3.81), 588 (3.78), 643 (3.31)

HRMS (ESI) calculated for $[C_{63}H_{63}N_{10}O_4\ (M)^{3+} - 3.I]$ 341.1672, found: 341.1675

6.34 5-(4-(23-(*tert*-butylcarbamate)-3,6,9,12,15,16,21-heptaoxadocosyl-1-amino-*N*-cabonyl)phenyl)-10,15,20-tri(4-pyridyl)porphyrin (23)

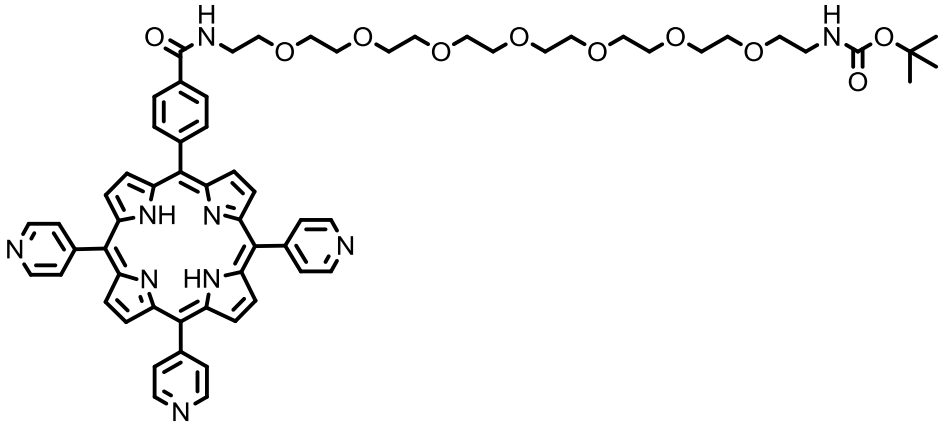

Compound **19** (68 mg, 89 μmol), *O*-(2-aminoethyl)-*O*'-[2-(Boc-amino)ethyl]-hexaethylene glycol (110 mg, 230 μmol, 2.6 equiv. relative to **19**) and anhydrous potassium carbonate (50 mg, 360 μmol, 1.6 equiv. relative to the *O*-(2-aminoethyl)-*O*'-[2-(Boc-amino)ethyl]-hexaethylene glycol) were dissolved in dry dimethylsulfoxide (7 mL). The reaction mixture was protected from light and atmospheric moisture, and kept under stirring at 40 ^{o}C, for 5 days, until complete consumption of **19** was observed as shown by TLC (silica, eluent: 10 % methanol/dichloromethane). The reaction was allowed to cool to ambient temperature, diluted with dichloromethane and the organic layer was washed with copious amounts of water, and dried over anhydrous sodium sulphate. The solvent was then removed under reduced pressure and the mixture was purified by flash column chromatography (silica, eluent: 8 % methanol/dichloromethane). Porphyrin **23** was obtained as a purple solid (54 mg, 53 %), after precipitation from hexane over dichloromethane and ethyl acetate. R*f* = 0.43 (Silica, CH_2Cl_2: CH_3OH; 9:1); m.p. = >350 °C decomp.

^{1}H N.M.R. [400 MHz, $CDCl_3$], δ (ppm) = −2.89 (br s, 2H, N*H*), 1.40 (s, 9H, -$CO_2C(C\underline{H}_3)_3$), 3.24 (q, *J* = 5.0 Hz, 2H, -$OCH_2C\underline{H}_2NHCO_2{}^tBu$), 3.44 (t, *J* = 5.0 Hz, 2H, -$OC\underline{H}_2CH_2NHCO_2{}^tBu$); 3.47-5.51, 3.52-3.58, 3.59-3.66, 3.67-3.73 and 3.74-3.80 (5m, 24H, -$(OC\underline{H}_2C\underline{H}_2)_6$-), 3.81-3.90 (m, 4H, -$CONHC\underline{H}_2C\underline{H}_2O$-), 5.10 (br s, 1H, -$OCH_2CH_2N\underline{H}CO_2{}^tBu$), 7.55 (br s, 1H, -$CON\underline{H}CH_2CH_2O$-), 8.17 (d, *J* = 5.9 Hz, 6H, 10,15,20-Ar-*o*-*H*), 8.27-8.29 (m, 4H, 5-Ar-*o*-*m*-*H*), 8.84 (d, *J* = 4.7 Hz, 2H, *β*-*H*), 8.86-8.88 (m, 4H, *β*-*H*), 8.89 (d, *J* = 4.7 Hz, 2H, *β*-*H*), 9.06 (d, *J* = 5.9 Hz, 6H, 10,15,20-Ar-*m*-*H*)

^{13}C N.M.R. [100 MHz, $CDCl_3$], δ (ppm) = 28.4 (3 x *C*H_3), 40.1 (-CONH*C*H_2*C*H_2O-), 40.3 (-OCH_2*C*H_2NH$CO_2{}^t$Bu); 70.11, 70.13, 70.2, 70.3, 70.4, 70.47, 70.50, 70.53, 70.59 and 70.61 (-CONHCH_2CH_2(O*C*H_2*C*H_2)$_6$O*C*H_2CH_2NH$CO_2{}^t$Bu); 117.4, 117.6, 120.4, 125.8 (5-Ar-*m*-*C*), 129.4 (10,15,20-Ar-*o*-*C*), 131.3 (*β*-*C*), 134.4, 134.5 (5-Ar-*o*-*C*), 144.6, 148.4 (10,15,20-Ar-*m*-*C*), 149.9, 156.0 (-NH*C*$O_2{}^t$Bu), 167.4 (-*C*ONHCH_2CH_2O-)

UV/Vis (CH_2Cl_2, nm), λ_{max} (log ε): 417 (5.90), 513 (4.52), 548 (3.98), 588 (3.95), 644 (3.56)

HRMS (ESI) calculated for $C_{63}H_{70}N_9O_{10}$ $(M + H)^+$ 1112.5240, found: 1112.5228

6.35 5-(4-(23-(4-(*N*-maleimidomethyl)cyclohexane-1-amido)-3,6,9,12,15,18,21-heptaoxadocosyl-1-amino-*N*-cabonyl)phenyl)-10,15,20-tri(4-pyridyl)porphyrin (24)

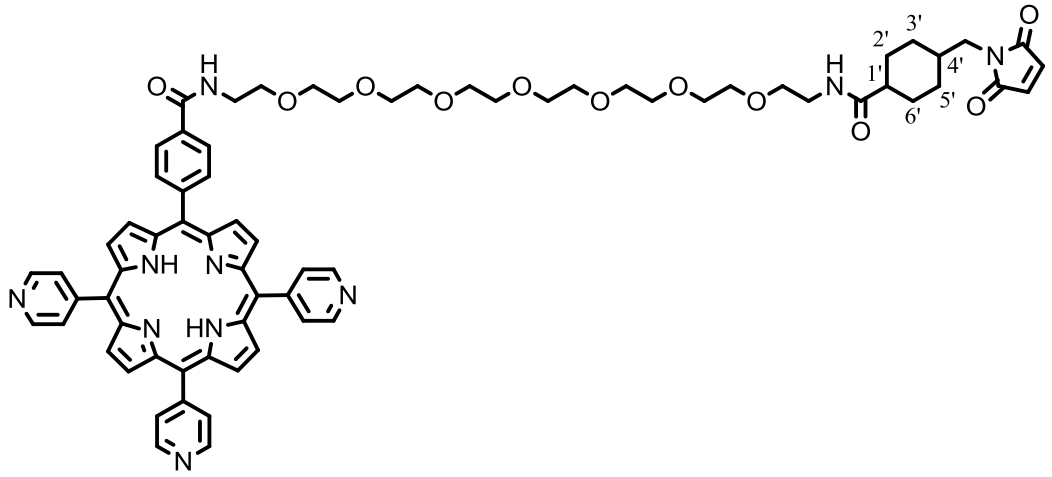

Trifluoroacetic acid (9 mL) was added to a solution of **23** (99 mg, 89 μmol) dissolved in dry dichloromethane (9 mL). The mixture was stirred at room temperature for 50 minutes, while avoiding exposure to light and moisture. Once the reaction was complete as indicated by TLC (silica, eluent: 8 % methanol/dichloromethane), the reaction mixture was poured onto a saturated sodium hydrogen carbonate solution containing ice. The organic layer was washed with water and dried over anhydrous sodium sulphate. The solvent was removed under reduced pressure to afford the porphyrin intermediate.

SMCC (36 mg, 108 μmol, 1.2 equiv. relative to **23**) and diisopropylethylamine (0.1 mL, 574 μmol, 5.3 equiv. relative to SMCC) were added to a stirred solution of the porphyrin intermediate dissolved in anhydrous dimethylformamide (10 mL). The solution was stirred at ambient temperature for 14 hours (overnight), while protected from moisture and light. After this period, the porphyrinic material was precipitated with diethyl ether (50 mL) and hexane (5 mL). Compound **24** (60 mg, 55 %) was isolated by flash chromatography (silica, eluent: 8 % methanol/dichloromethane) and precipitation in diethyl ether and hexane over dichloromethane. R*f* = 0.35 (Silica, CH_2Cl_2:CH_3OH; 9:1); m.p. = >350 °C decomp.

^{1}H N.M.R. [400 MHz, $CDCl_3$], δ (ppm) = the singlet corresponding to the 2H of the inner NH groups was not observed, 0.83-0.94 (m, 2H, 1H of 3'-C*H*$_2$ and 1H of 5'-C*H*$_2$), 1.25-1.38 (m, 2H, 1H of 2'-C*H*$_2$ and 1H of 6'-C*H*$_2$), 1.49-1.66 (m, 3H, 4'-C*H*, 1H of 3'-

C*H*$_2$ and 1H of 5'-C*H*$_2$), 1.67-1.80 (m, 2H, 1H of 2'-C*H*$_2$ and 1H of 6'-C*H*$_2$), 1.88-1.95 (m, 1H, 1'-C*H*), 3.19 (d, *J* = 7.0 Hz, 2H, C*H*$_2$-mal), 3.24 (t, *J* = 5.0 Hz, 2H, PEG-C*H*$_2$), 3.38 (t, *J* = 5.0 Hz, 2H, PEG-C*H*$_2$), 3.42-3.53 (m, 20H, 10 x PEG-C*H*$_2$), 3.53-3.59 (m, 4H, 2 x PEG-C*H*$_2$), 3.60-3.66 (m, 4H, 2 x PEG-C*H*$_2$), 6.56 (s, 2H, COC*H*=C*H*CO), 8.15-8.25 (m, 10H, 4H of 5-Ar-*o*-*m*-*H* and 6H of 10,15,20-Ar-*o*-*H*), 8.62-8.91 (m, 8H, *β*-*H*), 8.97 (d, *J* = 5.5 Hz, 6H, 10,15,20-Ar-*m*-*H*)

^{13}C N.M.R. [100 MHz, $CDCl_3$], δ (ppm) = 28.5 (2'-*C*H_2 and 6'-*C*H_2), 29.6 (3'-*C*H_2 and 5'-*C*H_2), 38.8 (4'-*C*H), 43.4 (*C*H_2-mal), 44.7 (1'-*C*H); 69.6, 69.8, 69.9, 70.0, 70.16, 70.22, 70.25, 70.29 and 70.30(*C*H_2-PEG); 116.7, 117.0, 120.7, 125.7 (5-Ar-*m*-*C*), 129.7(10,15,20-Ar-*o*-*C*), 133.8 (CO*C*H=*C*HCO), 134.1, 134.4 (5-Ar-*o*-*C*), 144.3, 146.9 (10,15,20-Ar-*m*-*C*), 151.3, 167.98 (1''-*C*O), 171.0 (*C*OCH=CH*C*O), 176.5 (10''-*C*O)

UV/Vis (CH_2Cl_2, nm), λ_{max} (log ε):417 (5.75), 513 (4.40), 548 (3.94), 588 (3.91), 644 (3.61)

HRMS (ESI) calculated for $C_{70}H_{75}N_{10}O_{11}$ $(M + H)^+$ 1231.5611, found: 1231.5575

6.36 5-(4-(23-(4-(*N*-maleimidomethyl)cyclohexane-1-amido)-3,6,9,12,15,18,21-heptaoxadocosyl-1-amino-*N*-cabonyl)phenyl)-10,15,20-tri(4-*N*-methyl-pyridyniumyl)porphyrin triiodide (25)

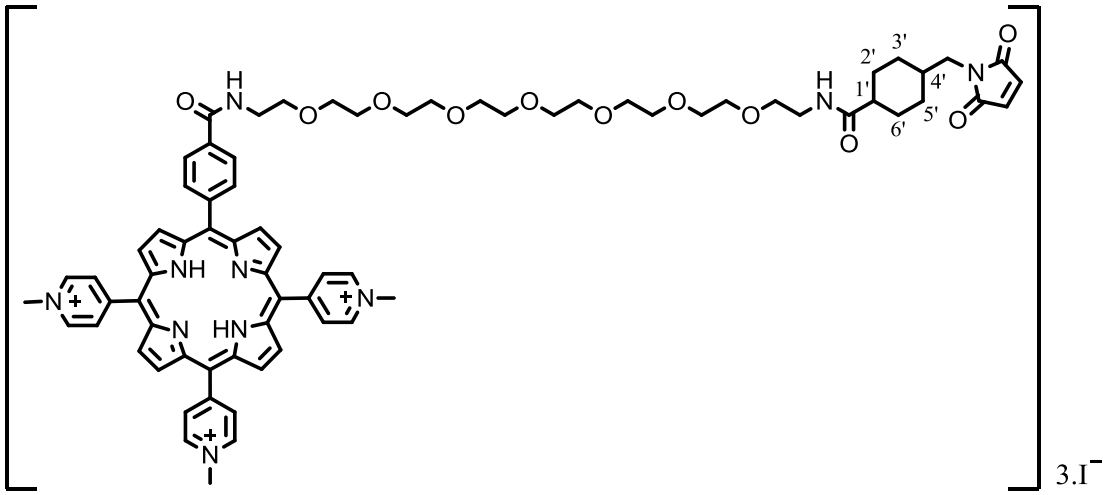

Methyl iodide (1.5 mL, 2.4 mmol, 100 equiv. relative to **24**) was added to a stirred solution of **24** (30 mg, 24 μmol) dissolved in anhydrous dimethylformamide (3 mL). The reaction mixture was stirred at 40 ^{o}C for 4 hours, whilst avoiding exposure to moisture and light. Ice cooled diethyl ether and hexane (50:1) was added to promote precipitation, yielding the crude methylated porphyrin product, which was washed with cold diethyl ether to afford **25** (30 mg, 75 %) as a lustrous purple solid. m.p. = >350 °C decomp.

^{1}H N.M.R. [400 MHz, $(CD_3)_2SO$], δ (ppm) = −3.02 (s, 2H, N*H*), 0.76-0.92 (m, 2H, 1H of 3'-*H* and 1H of 5'-*H*), 1.22-1.28 (m, 2H, 1H of 2'-*H* and 6'-*H*), 1.40-1.52 (m, 1H, 4'-*H*), 1.52-1.60 (m, 2H, 1H of 3'-*H* and 1H of 5'-*H*), 1.61-1.70 (m, 2H, 1H of 2'-*H* and 6'-*H*), 1.94-2.06 (m, 1H, 1'-*H*), 3.07-3.13 (m, 2H, -NHC*H*$_2$CH$_2$O-), 3.15 (d, *J* = 7.3 Hz, 2H, C*H*$_2$-mal), 3.29-3.33 (m, 2H, -NHCH$_2$C*H*$_2$O-), 3.44-3.75 (m, 28H, PEG- C*H*$_2$), 4.73 and 4.74 (2s, 6H + 3H, 3 × C*H*$_3$), 6.80 (s, 2H,-COC*H*=C*H*CO-), 7.72 (t, *J* = 5.6 Hz, 1H, 9 N*H*), 8.35 and 8.38 (AB, *J* = 8.4 Hz, 4H, 5-Ar-*o*-*m*-*H*), 8.98 (t, *J* = 5.6 Hz, 1H, N*H*), 9.00-9.06 (m, 8H, 2H of *β*-*H* and 10,15,20-Ar-*o*-*H*), 9.07-9.12 (m, 2H, *β*-*H*), 9.14-9.25 (m, 4H, *β*-*H*), 9.50 (d, *J* = 6.6 Hz, 6H, 10,15,20-Ar-*m*-*H*)

^{13}C NMR [100 MHz, $(CD_3)_2SO$], δ (ppm) = 28.5, 29.4, 34.4 (4'-*C*H), 38.3 (*C*H$_2$-mal), 43.0 (-NH*C*H$_2$CH$_2$O-), 47.8 (3 x *C*H$_3$); 69.0, 69.5, 69.6, 69.70, 69.72, 69.74, 69.75, 69.80, and 69.82 (*C*H$_2$-PEG); 114.7, 115.4, 121.9, 126.1 (5-Ar-*m*-*C*), 132.1 (10,15,20-

Ar-*o*-*C*), 134.2, 134.3 (-CO*C*H=*C*HCO-), 143.0 (5-Ar-*o*-*C*), 144.2 (10,15,20-Ar-*m*-*C*), 156.5, 166.0 (*C*O), 171.2 (-*C*OCH=CH*C*O-), 175.0 (*C*O).

UV/Vis (H_2O), λ_{max} (log ε): 425 (5.28), 519 (4.16), 556 (3.77), 589 (3.74), 645 (3.29)

MS (MALDI) *m/z* = 1276.5 $(M+H)^+$ -3I

6.37 Synthesis of 5-(4-pyridyl)dipyrromethane (26)

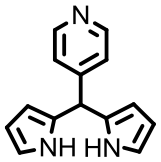

A mixture of a large excess of pyrrole (60 mL, 865 mmol) and pyridine-4-carboxaldehyde (1.9 mL, 20 mmol) was stirred and degassed (N_2) for 20 minutes. The mixture was then heated to 85 °C, for 15 hours, under an inert atmosphere (N_2), while avoiding exposure to light. The excess pyrrole was removed *in vacuo* and the resulting crude mixture was chromatographically separated (silica, 20 % hexane/ethyl acetate). Precipitation of the crude product from acetone by the addition of hexane yields **26** (2.14 g, 48 %) as a white powder. R*f* = 0.94 (Silica, $CH_3CO_2CH_3$: C_6H_{12}; 8:2); m.p. = 137-140 °C decomp.

^{1}H N.M.R. [400 MHz, $CDCl_3$], δ (ppm) = 5.46 (s, 1H, 5-C*H*), 5.87-5.93 (m, 2H, 3 and 7-C*H*), 617 (q, *J* = 2.9 Hz, 2H, 2 and 8-C*H*), 6.72-6.77 (m, 2H, 1 and 9-C*H*), 7.13 (dd, *J* = 1.63 Hz, *J* = 4.4 Hz, 2H, Ar-*o*-*H*), 8.10 (br s, 2H, N*H*$_2$), 8.48-8.55 (dd, *J* = 1.63 Hz, *J* = 4.4 Hz, 2H, Ar-*m*-*H*)

^{13}C N.M.R. [100 MHz, $CDCl_3$], δ (ppm) = 43.5 (5-*C*H), 107.8 (3 and 7-*C*H), 108.8 (2 and 8-*C*H), 118.0 (1 and 9-*C*H), 123.7 (Ar-*o*-*C*), 130.7, 150.1 (Ar-*m*-*C*), 151.2

MS (GC-MS) *m/z* = 223 $(M)^+$

6.38 Synthesis of 5-(4-acetamidophenyl)-10,20-di-(4-pyridyl)-15-(4-bromophenyl)porphyrin (27)

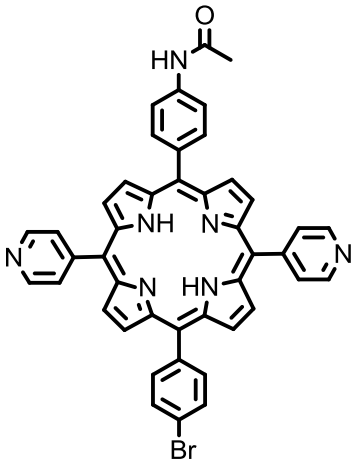

Compound **26** (850 mg, 3.8 mmol), 4-acetamidobenzaldehyde (310 mg, 1.9 mmol), 4-bromobenzaldehyde (352 mg, 1.9 mmol) and ammonium chloride (850 mg, 16 mmol) were dissolved in dimethylsulfoxide (50 mL) and the resulting mixture was heated to 100 °C for 24 hours, while avoiding exposure to light. Once cooled, the mixture was stirred at ambient temperature for a further 3 hours. A 5 % methanol/dichloromethane solution was added, and the organic layer was washed with copious amounts of water. The organic layer was dried over anhydrous sodium sulphate and the solvent was removed under reduced pressure. The crude product was obtained by chromatographic separation (silica, eluent: 3 % methanol/dichloromethane). The crude product was re-dissolved in dichloromethane and addition of methanol initiated precipitation, affording **27** (35 mg, 1 %) as a purple solid. R*f* = 0.66 (Silica, CH_2Cl_2: CH_3OH; 9:1); m.p. = >350 °C decomp.

^{1}H N.M.R. [400 MHz, $CDCl_3$], δ (ppm) = −2.88 (br s, 2H, N*H*), 2.34 (s, 3H, NHCOC*H*$_3$), 7.84 (d, *J* = 8.36 Hz, 2H, Ar-*m*-*H*), 7.92 (d, *J* = 8.36 Hz, 2H, Ar-*H*), 8.00 (d, *J* = 8.36 Hz, 2H, Ar-*H*), 8.07 (d, *J* = 8.36 Hz, 2H, Ar-*H*), 8.17 (d, *J* = 5.78 Hz, 4H, 10,15-Ar-*o*-*H*), 8.53-9.02 (m, 12H, 4H of 10,15-Ar-*m*-*H* and 8H of *β*-*H*), 9.67 (br s, 1H, N*H*$COCH_3$)

^{13}C N.M.R. [100 MHz, $CDCl_3$], δ (ppm) = 23.6 (NHCO*C*H_3), 116.4, 118.0, 119.1, 120.9, 122.6, 129.6, 129.8, 134.8, 135.6, 136.7, 138.4, 140.2, 147.1, 151.1, 170.3

UV/Vis (CH_2Cl_2:CH_3OH; 2:1, nm) λ_{max} (log ε) = 418 (5.6), 514 (4.3), 549 (3.9), 590 (3.8), 645 (3.5)

MS (MALDI) *m/z* = 753 $^{79}Br(M+2H)^+$ and/or $^{81}Br(M)^+$

HRMS (ESI): calculated for $C_{44}H_{31}N_7O^{79}Br$ $(M+H)^+$ 752.1786, found: 752.1763

6.39 Synthesis of 5-(4-bromophenyl)-10,15,20-tri-(4-pyridyl)porphyrin (28)

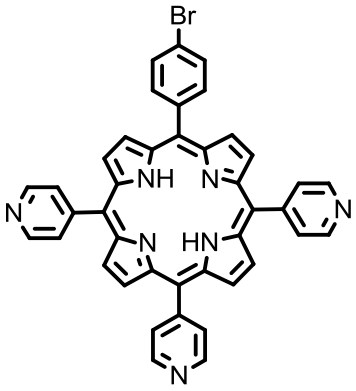

4-Bromobenzaldehyde (6.62 g, 36 mmol) and 4-pyridinecarboxaldehyde (10.2 mL, 108 mmol, 3 equiv. relative to 4-bromobenzaldehyde) were added to propionic acid (400 mL) while avoiding exposure to light. Pyrrole (10 mL, 144 mmol, 4 equiv. relative to 4-bromobenzaldehyde) was added drop-wise to the refluxing mixture. After 40 minutes at reflux, the reaction mixture was cooled to room temperature, and the propionic acid was removed *in vacuo*. Gravity column chromatography (silica, eluent: 2 % methanol/dichloromethane) was used to obtain the crude product. Precipitation of the crude product from dichloromethane by the addition of methanol, furnished **28** (1.03 g, 4 %). R*f* = 0.91 (silica, CH_2Cl_2: CH_3OH; 9:1); m.p. = >350 °C decomp.

^{1}H N.M.R. [400 MHz, $CDCl_3/CD_3OD$], δ (ppm) = −2.92 (br s, 2H, N*H*), 7.94 and 8.08 (AB, 4H, *J* = 8.28 Hz, 5-Ar-*o*-*m*-*H*), 8.19-8.25 (m, 6H, 10, 15, 20-Ar-*o*-*H*), 8.75-9.11 (m, 14H, 6H of 10,15,20-Ar-*m*-*H* and 8H of *β*-*H*)

^{13}C N.M.R. [100 MHz, $CDCl_3/CD_3OD$], δ (ppm) = 116.8, 117.1, 120.0, 122.7, 129.5, 129.9, 135.6, 140.1, 147.5, 150.5

UV/Vis (CH_2Cl_2:CH_3OH; 2:1, nm) λ_{max} = 417, 513, 547, 588, 644

MS (MALDI) *m/z* = 695 $^{79}Br(M)^+$, 696.142 $^{79}Br(M+H)^+$, 697.142 $^{79}Br(M+2H)^+$ and/or $^{81}Br(M)^+$

6.40 Synthesis of (5-(4-bromophenyl)-10,15,20-tri-(4-pyridyl)porphyrinato) zinc(II) (29)

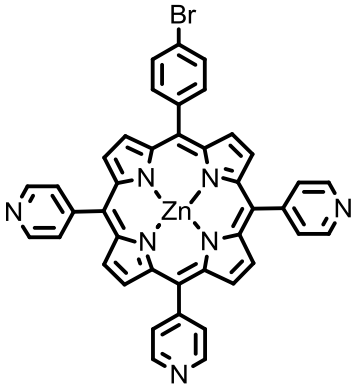

Compound **28** (167 mg, 239 μmol) and zinc acetate dihydrate (1.26 g, 5.7 mmol, 24 equiv. relative to **28**) were dissolved in chloroform (30 mL) and methanol (10 mL) and the resulting mixture was stirred at 40 ^{o}C for 2 hours, while avoiding exposure to light. The solvents where removed under reduced pressure and the crude product was re-dissolved in chloroform (30 mL) and methanol (10 mL), and was washed with a saturated sodium hydrogen carbonate solution and water. The organic layer was dried over anhydrous sodium sulphate and the solvent was removed *in vacuo*. The crude product was dissolved in the minimum volume of chloroform and methanol was added to initiate precipitation, furnishing the purple crystalline product (151 mg, 83 %). R*f* = 0.63 (Silica, C_4H_8O); m.p. = >350 °C decomp.

^{1}H N.M.R. [400 MHz, $CDCl_3/CD_3OD$], δ (ppm) = = 7.82 and 7.99 (AB, *J* = 8.3 Hz, 4H, 5-Ar-*o*-*m*-*H*), 8.03-8.07 (m, 6H, 10,15,20-Ar-*o*-*H*), 8.50-8.63 (m, 6H, 10,15,20-Ar-*o*-*H*), 8.68-8.73 (m, 6H, *β*-*H*), 8.83 (d, *J* = 4.69 Hz, 2H, *β*-*H*)

^{13}C N.M.R. [100 MHz, $(CD_3)_2SO$], δ (ppm) = 111.2, 114.2, 117.0, 119.9, 130.3, 132.4, 132.6, 133.0, 133.2, 133.8, 136.4, 140.1, 148.6, 148.8, 149.0, 150.5, 158.4, 158.8, 159.1, 159.5

UV/Vis (C_4H_8O, nm) λ_{max} = 423, 555, 595

MS (MALDI) *m/z* = 759 $(M+2H)^+$

6.41 Synthesis of 5-(4-iodophenyl)-10,15,20-tri-(4-pyridyl)porphyrin (30)

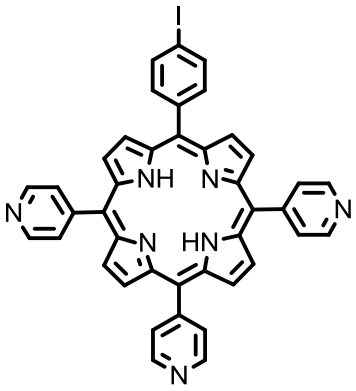

Pyrrole (4.7 mL, 68 mmol, 4 equiv. relative to 4-iodobenzaldehyde) was added drop-wise to a stirred refluxing solution of 4-iodobenzaldehyde (4.00 g, 17 mmol) and pyridine-4-carboxaldehyde (4.7 mL, 49 mmol, 3 equiv. relative to 4-iodobenzaldehyde) dissolved in propionic acid 250 mL. The mixture was stirred under reflux conditions for 40 minutes, while avoiding exposure to light. Once the reaction had reached ambient temperature, the solvent was removed *in vacuo*. Compound **30** (539 mg, 4 %) was isolated as a dark purple solid after gravity column chromatography (silica, 2 % methanol/dichloromethane) and precipitation form chloroform by the addition of methanol. R*f* = 0.88 (silica, CH_2Cl_2:CH_3OH; 9:1); m.p. = >350 °C decomp.

^{1}H N.M.R. [400 MHz, $CDCl_3$], δ (ppm) = −2.91 (br s, 2H, N*H*), 7.84-7.96 (m, 2H, 5-Ar-*m*-*H*), 8.02-8.20 (m, 8H, 5,10,20,15-Ar-*o*-*H*), 8.74-8.95 (m, 8H, *β*-*H*), 8.95-9.10 (m, 6H, 10,15,20-Ar-*m*-*H*)

^{13}C N.M.R. [400 MHz, $CDCl_3$], δ (ppm) = 94.6, 117.3, 117.6, 120.0, 129.3, 131.2, 136.06, 136.07, 141.0, 148.4, 149.85, 149.87

UV/Vis (CH_2Cl_2:CH_3OH; 2:1, nm) λ_{max} = 417, 513, 547, 588, 643

MS (MALDI) *m/z* = 744 $(M+H)^+$

6.42 Synthesis of (5-(4-iodophenyl)-10,15,20-tri-(4-pyridyl)porphyrinato) zinc(II) (31)

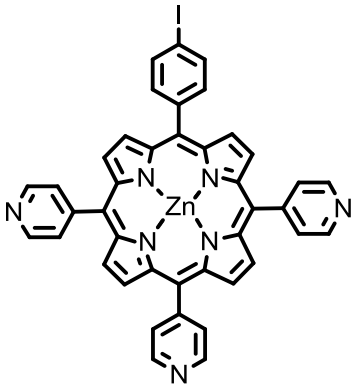

Zinc acetate dihydrate (100 mg, 456 μmol, 6.8 equiv. relative to **30**) and compound **30** (50 mg, 67 μmol) were dissolved in chloroform (15 mL) and methanol (5 mL), and the resulting mixture was stirred at 40 °C for 2 hours, while avoiding exposure to light. The solution was subsequently washed with a saturated sodium hydrogen carbonate solution and then water. The organic layer was dried over anhydrous sodium sulphate and the solvent was removed *in vacuo*. Precipitation from chloroform by the addition of methanol afforded **31** (48 mg, 88 %). R*f* = 0.63 (Silica, C_4H_8O); m.p. = >350 °C decomp.

^{1}H N.M.R. [400 MHz, $CDCl_3/CD_3OD$], δ (ppm) = 7.86 and 8.02 (AB, 4H, *J* = 8.13 Hz, 5-Ar-*m*-*o*-*H*), 8.10 (d, *J* = 5.32 Hz, 6H, 10,20,15-Ar-*m*-*H*), 8.67-8.76 (m, 12H, 6H of 10,20,15-Ar-*o*-*H* and 6H of *β*-*H*), 8.85 (d, *J* = 4.69 Hz, 2H, *β*-*H*)

^{13}C N.M.R. [400 MHz, $CDCl_3/CD_3OD$], δ (ppm) = (sample was not concentrated enough to obtain a complete spectrum)

UV/Vis (C_4H_8O, nm) λ_{max} = 422, 555, 595

MS (MALDI) *m/z* = 805 $(M)^+$

6.43 Attempted synthesis of (5-(4-(4,4,5,5-tetramethyl-1,3,2-dioxaborinan-2-yl)phenyl)-10,15,20-tri-(4-pyridyl)porphyrinato) zinc(II)

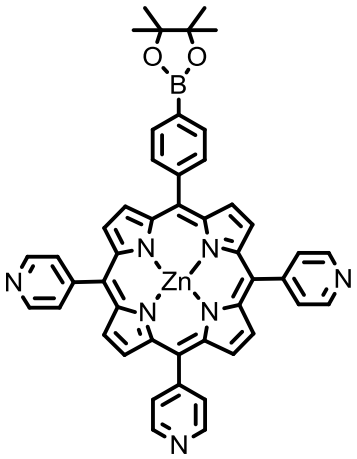

General method 1

An oven dried, argon flushed Schlenk flask was charged with porphyrin, bis(pinacolato)diborane, bis(diphenylphosphino)ferrocene]dichloropalladium(II) and base, under an inert atmosphere (Ar). Degassed (Ar), anhydrous solvent was added, and the mixture was degassed (Ar) and sonicated. The stirred reaction mixtures were heated, under an inert atmosphere, while protected against light. The reactions were monitored by TLC (silica, eluent: tetrahydrofuran).

The series of reactions attempted are tabulated in Table 5.

For the reaction employing **31** and potassium phosphate: the porphyrinic product was extracted into 10 % methanol/dichloromethane and the solution was then washed with water, dried over anhydrous sodium sulphate, and the solvent was removed *in vacuo*. The mixture was chromatographically separated (silica coated prep TLC plates, eluent: 10 % methanol/dichloromethane) and the relevant fraction was isolated.

Porphyrin	**bis(pinacolato)diborane**	**Palladium Catalyst**	**Base**	**Solvent**	**Temperature**	**Reaction time**
29 (50 mg, 66 μmol)	1) 18 mg 1.05 equiv. relative to **29** 2) 18 mg 1.05 equiv. relative to **29**	1) $Pd(dppf)Cl_2$ (4 mg, 0.03 equiv. relative to **29**) 2) $Pd(dppf)Cl_2$ (4 mg, 0.03 equiv. relative to **29)**	1) KOAc (20 mg, 3 equiv. relative to **29**) 2) KOAc (20 mg, 3 equiv. relative to **29**)	DMSO (7 mL)	80 °C	1) 24 hrs 2) 19 hrs
29 (30 mg, 39 μmol)	11 mg, 1.05 equiv. relative to **29**	$Pd(dppf)Cl_2$ (3 mg, 0.03 equiv. relative to **29)**	KOAc (12 mg, 3 equiv. relative to **29**)	THF (4 mL)	50 °C	48 hrs
29 (30 mg, 39 μmol)	11 mg, 1.05 equiv. relative to **29**	$Pd(dppf)Cl_2$ (3 mg, 0.03 equiv. relative to **29)**	KOAc (12 mg, 3 equiv. relative to **29**)	DMF (4 mL)	80 °C	48 hrs
29 (30 mg, 39 μmol)	12 mg, 1.2 equiv. relative to **29**	$Pd(dppf)Cl_2$ (1.5 mg, 0.05 equiv. relative to **29**)	K_2CO_3 (27 mg, 5 equiv. relative to **29**)	DMF (5 mL)	80 °C	72 hrs
29 (30 mg, 39 μmol)	12 mg, 1.2 equiv. relative to **29**	$Pd(dppf)Cl_2$ (1.5 mg, 0.05 equiv. relative to **29**)	K_2CO_3 (27 mg, 5 equiv. relative to **29**)	DMSO (5 mL)	80 °C	72 hrs
29 (30 mg, 39 μmol)	30 mg, 3 equiv. relative to **29**	$Pd(dppf)Cl_2$ (3 mg, 0.1 equiv. relative to **29**)	Cs_2CO_3 (128 mg, 10 equiv. relative	DMSO (5 mL)	80 °C	72 hrs

			to **29**)			
29 (30 mg, 39 μmol)	30 mg, 3 equiv. relative to **29**	$Pd(dppf)Cl_2$ (3 mg, 0.1 equiv. relative to **29**)	K_3PO_4 (84 mg, 10 equiv relative to **29**)	DMSO (5 mL)	80 °C	72 hrs
31 (20 mg, 24 μmol)	8 mg, 1.2 equiv. relative to **31**	$Pd(dppf)Cl_2$ (2 mg, 0.1 equiv. relative to **31**)	KOAc (24 mg, 10 equiv. relative to **31**)	DMSO (4 mL)	80 °C	96 hrs
31 (30 mg, 37 μmol)	12 mg, 1.2 equiv. relative to **31**	$Pd(dppf)Cl_2$ (3 mg, 0.1 equiv. relative to **31**)	K_3PO_4 (77 mg, 10 equiv. relative to **31**)	DMSO (5 mL)	80 °C	5 hrs
31 (20 mg, 24 μmol)	8 mg, 1.2 equiv. relative to **31**	$Pd(dppf)Cl_2$ (2 mg, 0.1 equiv. relative to **31**)	K_2CO_3 (34 mg, 10 equiv. relative to **31**)	DMSO (4 mL)	80 °C	96 hrs

Table 5: Attempted boronation reactions involving **29** or **31** and bis(pinacolato)diborane.

Method 2

A dried, degassed (Ar) Schlenk flask was charged with **29** (30 mg, 39 μmol), and bis(diphenylphosphino)ferrocene]dichloropalladium(II) (3 mg, 4.1 μmol, 0.1 equiv. relative to **29**) under an inert atmosphere (Ar), while protected against light. The residual moisture/air was then removed under reduced pressure. Degassed (Ar), dimethylformamide (8 mL), triethylamine (240 μL, 1.7 mmol, 415 equiv. relative to bis(diphenylphosphino)ferrocene]dichloropalladium(II)) and 4,4,5,5-tetramethyl-1,3,2-dioxaborolane (100 μL, 690 μmol, 17.7 equiv. relative to **29**) were added under an inert atmosphere. The resulting reaction mixture was stirred at 80 °C overnight. The TLC (silica, eluent: tetrahydrofuran) of the reaction mixture only exhibited **29**, thus the reaction was discarded.

6.45 Synthesis of 4-((trimethylsilyl)ethynyl)benzaldehyde (32)

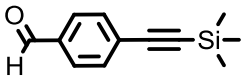

4-Bromobenzaldehyde (6.37 g, 22 mmol), palladium(II) acetate (78 mg, 0.01 equiv. relative to 4-bromobenzaldehyde) and triphenylphosphine (260 mg, 991 μmol, 2.9 equiv. relative to palladium(II) acetate) were added to freshly distilled and degassed (Ar) triethylamine (80 mL), and the resulting solution was degassed (Ar) for a further 5 minutes. Ethynyltrimethylsilane (7.6 mL, 53 mmol, 1.6 equiv. relative to 4-bromobenzaldehyde) was added and the mixture, which was subsequently heated to reflux for 2 hours. Once the reaction had reached ambient temperature, the mixture was filtered, the filtrate was collected and the solvent was removed *in vacuo*. The crude mixture was dissolved in dichloromethane/hexane (1:1) and was chromatographically separated (silica, eluent: 50 % dichloromethane/hexane). Compound **32** (5.05 g, 72 %) was isolated as white/yellow crystals after recrystalisation from isopropanol. R*f* = 0.4 (Silica, $CH_3CO_2CH_3$: C_6H_{12}; 8:2); m.p. = 69-70 °C.

^{1}H N.M.R. [400 MHz, $CDCl_3$], δ (ppm) = 0.27 (s, 9H, Si(CH_3)$_3$), 7.60 (d, *J* = 8.3 Hz, 2H, Ar-*H*), 7.82 (d, *J* = 8.3 Hz, 2H, Ar-*H*), 10.0 (s, 1H, C*H*O)

^{13}C N.M.R. [100 MHz, $CDCl_3$], δ (ppm) = 99.2, 104.0, 129.6, 129.7, 132.7, 135.8, 191.7

MS (GC-MS) *m/z* = 202 $(M)^+$

6.46 Synthesis of 5-(4-acetamidophenyl)-10,20-di-(4-pyridyl)-15-(4-((trimethylsilyl)ethynyl)phenyl)porphyrin (33)

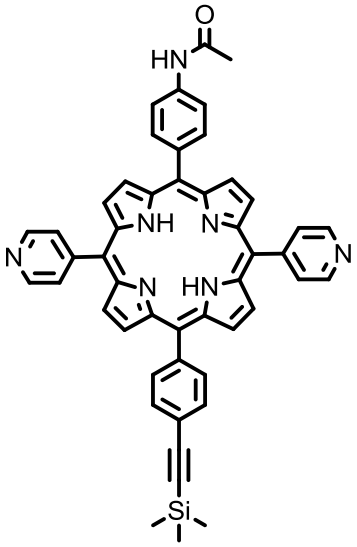

A solution of **32** (1.01 g, 5 mmol), and 4-acetamidobenzaldehyde (815 mg, 5 mmol, 1 equiv. relative to **32**) dissolved in dimethylsulfoxide (100 mL) was charged with **26** (2.23 g, 10 mmol, 2 equiv. relative to **32**) and ammonium chloride (1.69 g, 31.6 mmol, 6 equiv. relative to **32**) and the resulting mixture was heated to 90 °C for 24 hours, while avoiding exposure to light. Once cooled, the mixture was stirred at room temperature for a further 3 hours. A 5 % methanol/dichloromethane solution was added, and the organic layer was washed with copious amounts of water. The organic layer was dried over anhydrous sodium sulphate and the solvent was removed under reduced pressure. The crude product was chromatographically separated (silica, eluent: 3 % methanol/dichloromethane). Compound **33** (46.4 mg, 1 %) was isolated as a purple solid after precipitation from dichloromethane by the addition of methanol. R*f* = 0.68 (silica, CH_2Cl_2:CH_3OH; 9:1); m.p. = >350 °C decomp.

^{1}H N.M.R. [400 MHz, $CDCl_3$], δ (ppm) = −2.87 (br s, 2H, N*H*), 0.38 (s, 9H, Si(CH_3)$_3$), 2.38 (s, 3H, NHCOC*H*$_3$), 7.59 (br s, 1H, N*H*COCH$_3$, 7.88 (d, *J* = 8.44 Hz, 2H, Ar-*m*-*H*), 7.93 (d, *J* = 8.44 Hz, 2H, Ar-*m*-*H*), 8.11-8.18 (m, 8H, 5,10,15,20-Ar-*o*-*H*), 8.78-8.83 (m, 4H, *β*-*H*), 8.86 (d, *J* = 4.8 Hz, 2H, *β*-*H*), 8.93 (d, *J* = 4.8 Hz, 2H, *β*-*H*), 8.99-9.07 (m, 4H, 10,20-Ar-*m*-*H*)

^{13}C N.M.R. [100 MHz, $CDCl_3$], δ (ppm) = 1.1 ($Si(\underline{C}H_3)_3$, 25.0 ($NHCO\underline{C}H_3$), 96.0, 104.9, 117.3, 118.2, 120.0, 120.6, 123.0, 129.4, 130.5, 134.5, 135.2, 137.6, 138.0, 141.8, 142.0, 148.4 (10,20-Ar-*m*-*C*), 148.5, 150.0, 150.2, 168.7

UV/Vis (CH_2Cl_2:CH_3OH; 2:1, nm) λ_{max} (log ε) = 419 (5.63), 514 (4.327), 549 (3.97), 590 (3.84), 645 (3.59)

MS (MALDI) *m/z* = 769 $(M)^+$

HRMS (ESI) calculated for $C_{49}H_{40}N_7OSi$ $(M+H)^+$ 770.3058, found: 770.3052

6.47 Synthesis of (5-(4-acetamidophenyl)-10,20-di-(4-pyridyl)-15-(4-((trimethylsilyl)ethynyl)phenyl)porphyrinato) zinc(II) (34)

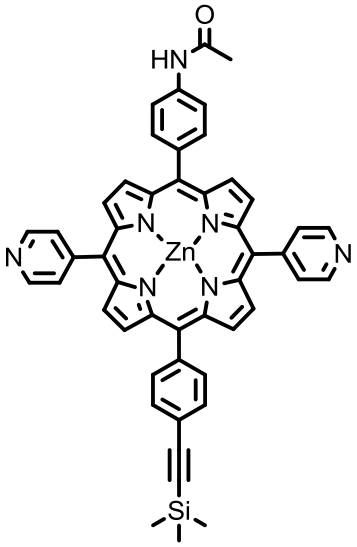

Compound **33** (21 mg, 27 μmol) and excess zinc acetate dihydrate (40 mg, 182 μmol, 6.7 equiv. relative to **33**) were dissolved in dichloromethane (9 mL) and methanol (3 mL), and the resulting mixture was stirred at 40 °C for 2 hours, while avoiding exposure to light. The crude product was washed with a saturated sodium hydrogen carbonate solution and water. The organic layer was dried over anhydrous sodium sulphate and the solvent was removed *in vacuo*. TLC analysis (silica, eluent: 20 % methanol/dichloromethane) indicated complete consumption of **33**. The crude product was dissolved in the minimum volume of chloroform and methanol was added to initiate precipitation, yielding **34** (19 mg, 84 %). R*f* = 0.73 (Silica, C_4H_8O); m.p. = >350 °C decomp.

^{1}H N.M.R. [400 MHz, $(CD_3)_2SO$], δ (ppm) = 0.25 (s, 9H, Si(CH_3)$_3$), 2.09 (s, 3H, NHCOC$\underline{H}_3$), 7.72 (d, *J* = 7.96 Hz, 2H, Ar-*H*), 7.88-7.98 (m, 8H, 4H of 10,20-Ar-*o*-*H* and 4H of Ar-*H*) 8.04 (d, *J* = 7.96 Hz, 2H, Ar-*H*), 8.56-8.68 (m, 4H, 10,20-Ar-*m*-*H*), 8.69-8.71 (m, 4H of *β*-*H*), 8.74 (d, *J* = 4.69 Hz, 2H, *β*-*H*), 8.82 (d, *J* = 4.69 Hz, 2H, *β*-*H*), 9.32 (br s, 1H, N$\underline{H}$COCH$_3$)

^{13}C N.M.R. [100 MHz, $(CD_3)_2SO$], δ (ppm) = 1.0, 24.0, 95.5, 116.8, 118.0, 120.6, 121.5, 122.4, 129.5, 130.2, 130.8, 131.0, 132.3, 132.7, 134.5, 135.0, 138.2, 138.5, 143.4, 145.4, 148.6, 148.7, 150.1, 150.7, 152.4, 170.5

UV/Vis (C_4H_8O, nm) λ_{max} = 425 (5.85), 557 (4.45), 597 (3.96)

HRMS (ESI): calculated for $C_{49}H_{38}N_7OSiZn$ $(M+H)^+$ 832.2193, found: 832.2187

6.48 Synthesis of (5-(4-azidophenyl)-10,15,20-tri-(4-pyridyl)porphyrinato) zinc(II) (35)

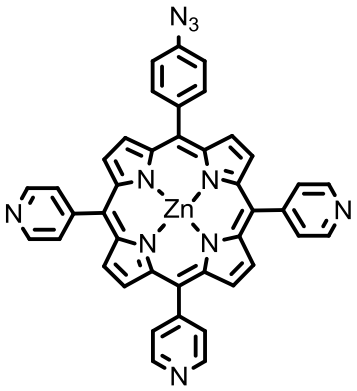

Sodium nitrite (7 mg, 101 μmol, ≈ 2.2 equiv. relative to **17**) dissolved in water (0.2 mL) was added to a stirred solution of **17** (30 mg, 47 μmol) in trifluoroacetic acid (0.8 mL) at 0 °C, while avoiding exposure to light. After 15 minutes, sodium azide (10 mg, 153 μmol, ≈ 3.3 equiv. relative to **17**) dissolved in water (0.2 mL) was added. After 1 hour, the reaction mixture was partitioned between water and dichloromethane, and the organic layer was collected, washed with water and dried over anhydrous sodium sulphate. Complete consumption of **17** had occurred as indicated by TLC (silica, 10 % methanol/dichloromethane). The porphyrinic intermediate was re-dissolved in dichloromethane and an excess of zinc acetate dihydrate (250 mg, 1 mmol) dissolved in methanol was added. The resulting mixture was heated at 40 °C for 2 hours. Once cooled to room temperature the reaction mixture was washed with water, dried over anhydrous sodium sulphate and the solvent was removed under reduced pressure; affording **35** (32 mg, 94 %) as a black solid. R*f* = 0.63 (Silica, C_4H_8O); m.p. = >350 °C decomp.

^{1}H N.M.R. [400 MHz, $(CD_3)_2SO$], δ (ppm) = 7.55 (d, *J* = 8.44 Hz, 2H, 5-Ar-*m*-*H*), 8.18-8.22 (m, 8H, 5,10,15,20-Ar-*o*-*H*), 8.80-8.86 (m, 8H, *β*-*H*), 8.98-9.02 (m, 6H, 10,15,20-Ar-*m*-*H*)

^{13}C N.M.R. [100 MHz, $(CD_3)_2SO$], δ (ppm) = spectrum not obtained

UV/Vis ($(CH_3)_2SO$, nm) λ_{max} = 428 (5.63), 560 (4.33), 600 (3.84)

MS (MALDI) *m/z* = 694 $(M+2H-2N)^+$

6.49 Synthesis of 5-(4-azidophenyl)-10,15,20-tri-(4-pyridyl)porphyrin (36)

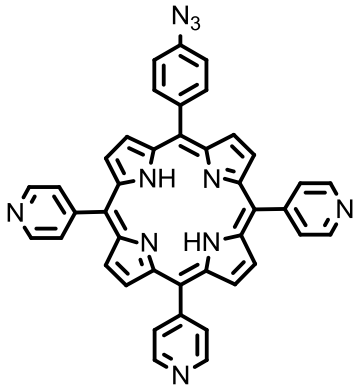

Compound **17** (38 mg, 60 μmol) dissolved in trifluoroacetic acid (1.5 mL) was treated with a solution of sodium nitrite (12 mg, 174 μmol, 2.9 equiv. relative to **17**) dissolved in water (0.3 mL). The resulting mixture was stirred at 0 °C, while avoiding exposure to light, for 15 minutes. Sodium azide (18 mg, 277 μmol, ≈ 4.6 equiv. relative to **17**) dissolved in water (0.3 mL) was then added and the reaction was stirred for a further 1 hour. The reaction mixture was partitioned between water and dichloromethane and the organic layer was dried over anhydrous sodium sulphate. Compound **36** (26 mg, 73 %) was isolated after gravity column chromatography (silica, eluent: 10 % methanol/dichloromethane) and precipitation from hexane over dichloromethane. R*f* = 0.58 (Silica, CH_2Cl_2: CH_3OH; 9:1); m.p. = >350 °C decomp.

^{1}H N.M.R. [400 MHz, $CDCl_3$], δ (ppm) = −2.89 (s, 2H, N*H*), 7.45 (dd, *J* = 2.05 Hz, J = 6.45 Hz, 2H, 5-Ar-*m*-*H*), 8.14-8.17 (m, 6H, 10,15,20-Ar-*o*-*H*), 8.19 (dd, *J* = 2.05 Hz, J = 6.45 Hz, 2H, 5-Ar-*o*-*H*), 8.81-8.93 (m, 8H, *β*-*H*), 9.03-9.07 (m, 6H, 10,15,20-Ar-*m*-*H*)

^{13}C N.M.R. [100 MHz, $CDCl_3$], δ (ppm) = 117.2, 117.55, 117.63, 120.4, 129.3 (5-Ar-*o*-*C*), 131.2 (*β*-*C*), 135.7, 138.2, 140.4, 148.4, 148.5, 149.86, 149.9

UV/Vis (CH_2Cl_2:CH_3OH; 2:1, nm) λ_{max} (log ε) = 417 (5.79), 513 (4.37), 548 (3.86), 588 (3.82), 644 (3.46)

HRMS (ESI): calculated for $C_{41}H_{27}N_{10}$ $(M+H)^+$ 659.2415, found: 659.2408

6.50 Attempted synthesis of 5-(4-((4-trimethylsilyl)-1,2,3-triazole)phenyl)-10,15,20-tri-(4-pyridyl)porphyrin

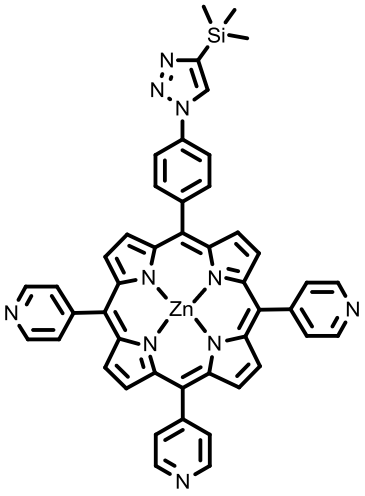

A solution of **35** (20 mg, 28 µmol) and ethynyltrimethylsilane (20 µL, 144 µmol, 5 equiv. relative to **35**) in dimethylsulfoxide (10 mL) was charged with sodium *L*-ascorbate (2.7 mg, 13.8 µmol, 0.5 equiv. relative to **35**) and copper(II) sulphate pentahydrate (1.7 mg, 6.9 µmol, 0.25 equiv. relative to **35**) suspended in water (1 mL). A micro-spatula of tris((1-benzyl-1H-1,2,3-triazol-4-yl)methyl)amine was added to the stirred mixture which was subsequently was heated to 80 °C. The reaction was monitored by TLC (silica, eluent: tetrahydrofuran) over 4 days, with only **35** being detected.

References

[1] Bonnett R. *Chem. Soc. Rev.* 1995; 19-33.
[2] Macdonald IJ and Dougherty TJ. *J. Porphyrins Phthalocyanines* 2001; **5**: 105-129.
[3] Moghissi K and Dixon K. *Photodiagnosis Photodynamic Ther*. 2008; **5**: 10-18.
[4] Kûbler AC. *Med. Laser Appl.* 2005; **20**: 37-45.
[5] Kaiserman I, Kaiserman N, Elhayany A and Vinker S. *Am. J. Ophthalmol.* 2006; **142**: 441-447.
[6] O'Riordan K, Akilov OE and Hasan T. *Photodiagnosis Photodynamic Ther.* 2005; **2**: 247-262.
[7] Litvack F, Grundfest WS, Forrester JS, Fishbein MC, Swan HJC, Corday E, Rider DM, McDermid IS, Pacala TJ and Laudenslager JB. *Am. J. Cardiol.* 1985; **56**: 667-671.
[8] Mitra A and Stables GI, *Photodiagnosis Photodynamic Ther.* 2006; **3**: 116-127.
[9] Brown SB, Brown EA and Walker I. *Lancet. Oncol.* 2004; **5**: 497-508.
[10] Sternberg ED and Dolphin D. *Tetrahedron* 1998; **54**: 4151-4202.
[11] Allison RR, Sibata CH, Downie GH and Cuenca RE. *Photodiagnosis Photodynamic Ther.* 2006; **3**: 214-226.
[12] Sharman WM, Allen CM and van Lier JE. *Therapeutic Focus* 1999; **4**: 507-517.
[13] Sobolev AS, Jans DA and Rosenkranz AA. *Prog. Biophys. Mol. Biol.* 2000; **73**: 51-90.
[14] DeRosa MC and Crutchley RJ. *Coord. Chem. Rev*. 2002; **233-234**: 351-371.
[15] Castano AP, Demidova TN and Hamblin MR. *Photodiagnosis Photodynamic Ther.* 2004; **1**: 279-293.
[16] Castano AP, Demidova TN and Hamblin MR. *Photodiagnosis Photodynamic Ther.* 2005; **2**: 1-23.
[17] Castano AP, Demidova TN and Hamblin MR. *Photodiagnosis Photodynamic Ther.* 2005; **2**: 91-106.
[18] Nowis D, Stoklosa T, Legat M, Issat T, Jabóbisiak M and Goląb J. *Photodiagnosis Photodynamic Ther.* 2005; **2**: 283-298.
[19] Berg K, Selbo PK, Weyergang A, Dietze A, Prasmickaite L, Bonsted A, Engesaeter BØ, Angellpetersen E, Warloe T, Frandsen N and Høgset A. *J. Microscopy* 2005; **218**: 133-147.
[20] Fuhrhop J-H. *Angew. Chem. Int. Ed*. 1974; **13**: 321-335.
[21] Anderson HL. *Chem. Commun.* 1999; 2323-2330.
[22] Wijesekera TP and Dolphin D. *Metalloporphyrins in Catalytic Oxidations* ed. Sheldon RA. Dekker NY, 2004; 193-239.
[23] Nyman ES and Hynninen PH. *J. Photochem. Photobiol. B: Biol.* 2004; **73**: 1-28.
[24] Hooper L. *Lancet Oncol*. 2000; **1**: 212-219.
[25] Kongshaug M. *Int. J. Biochem*. 1992; **24**: 1239-1265.
[26] Konan YN, Gurny R and Allémann E. *J. Photochem. Photobiol. B: Biol.* 2002; **66**: 89-106.
[27] Alonso C and Boyle RW. *Handbook of porphyrin science* ed. Kadish KM, Smith KM and Guilard R. World Scientific, 2010; **4**: 121-190.
[28] Sharman WM, van Lier JE and Allen CM. *Adv. Drug Deliv. Rev.* 2004; 5**6**: 53-76.
[29] Köhler G and Meilstein C. *Nature* 1975; **256**: 495-497.
[30] Hudson H and Boyle RW. *J. Porphyrins Phthalocyanines* 2004; **8**: 954-975.
[31] Kretzschmar T and von Rüden T. *Curr. Opin. Biotechnol.* 2002; **13**: 598-602.
[32] van Dongen GAMS, Visser GWM and Vrouenraets MB. *Adv. Drug Deliv. Rev.* 2004; **56**: 31-52.
[33] Weisser NE and Hall JC. *Biotechnol. Adv.* 2009; **27**: 502-520.
[34] Batra SK, Jain M, Wittel UA, Chauhan SC and Colcher D. *Curr. Opin. Biotechnol.* 2002; **13**: 603-608.
[35] de Bree R, Roos JC, Quak JJ, den Hollander W, Wilhelm AJ, van Lingen A, Snow GB and van Dongen GAMS. *Clin. Cancer Res.* 1995; **1**: 277-286.
[36] Borsi L, Balza E, Bestagno M, Castellani P, Carnemolla B, Biro A, Leprini A, Sepulveda J, Burrone O, Neri D and Zardi L. *Int. J. Cancer* 2002; **102**: 75-85.
[37] Jain RK. *Cancer Res.* 1990; **50**: 814-819.
[38] Vrouenraets MB, Visser GWM, Stewart FA, Stigter M, Oppelaar H, Postmus PE, Snow GB and van Dongen GAMS. *Cancer Res.* 1999; **59**: 1505-1513.
[39] Berndorff D, Borkowski S, Sieger S, Rother A, Friebe M, Viti F, Hilger CS, Cyr JE and Dinkelborg LM. *Clinc. Cancer Res.* 2005; **11**: 7053-7063.
[40] Albrecht H, Burke PA, Natarajan A, Xiong C-Y, Kalicinsky M, DeNardo GL and DeNardo SJ. *Bioconj. Chem.* 2004; **15**: 16-26.
[41] Mew D, Wat C-K, Towers GHN and Levy JG. *J. Immunol.* 1983; **130**: 1473-1477.
[42] Mew D, Lum V, Wat C-K, Towers GHN, Sun C-HC, Walter RJ, Wright W, Berns MW and Levy JG. *Cancer Res.* 1985; **45**: 4380-4386.
[43] Pogrebniak HW, Matthews W, Black C, Russo A, Mitchell JB, Smith P, Roth JA and Pass HI. *Surg. Oncol*. 1993; **2**: 31-42.
[44] Berki T and Németh P. *Cancer Immunol. Immunother.* 1992; **35**: 69-74.
[45] Linares R, Pacheco JR and Good TA. *J. Photochem. Photobiol. B: Biol*. 2004; **77**: 17-26.

[46] Martsez SP, Preygerzon VA, Mel'nikova YI, Kravchuk ZI, Ponomarev GV, Lunev VE and Savitsky AP. *J. Immuno. Meth*. 1995: **186**: 293-304.
[47] Clarke OJ and Boyle RW. *Chem. Commun.* 1999; **21**: 2231-2232.
[48] Soukos NS, Hamblin MR, Keel S, Fabian RL, Deutsch TF and Hasan T. *Cancer Res.* 2001; **61**: 4490-4496.
[49] Fabbrini M, Trachsel E, Soldani P, Bindi S, Alessi P, Bracci L, Kosmehl H, Zardi L, Neri D and Neri P. *Int. J. Cancer* 2006; **118**: 1805-1813.
[50] Savellano MD and Hasan T. *Photochem. Photobiol*. 2003; **77**: 431-439.
[51] Savellano MD and Hasan T. *Clin. Cancer Res.* 2005; **11**: 1658-1668.
[52] Savellano MD, Pogue BW, Hoopes PJ, Vitette ES and Paulsen KD. *Cancer Res.* 2005; **65**: 6371-6379.
[53] Kuimova MK, Bhatti M, Deonarain M, Yahioglu G, Levitt JA, Stamati I, Suhling K and Phillips D. *Photochem. Photobiol. Sci*. 2007; **6**: 933-939.
[54] Bhatti M, Yahioglu G, Milgrom LR, Garcia-Maya M, Chester KA and Deonarian MP. *Int. J. Cancer* 2008; **122**: 1155-1163.
[55] Carcenac M, Larroque C, Langlosis R, van Lier JE, Artus J-C and Pèlegrin A. *Photochem. Photobiol*. 1999; **70**: 930-936.
[56] Carcenac M, Dorvillius M, Gamambois V, Glaussel F, Larroque C, Langlosis R, van Lier JE and Pèlegrin A. *Br. J. Cancer* 2001; **85**: 1787-1793.
[57] Brasseur N, Langlois R, La Madeleine C, Ouellet R and van Lier JE. *Photochem. Photobiol*. 1999; **69**: 345-352.
[58] Halime Z, Michaudet L, Lachkar M, Brossier P and Boitrel B. *Bioconj. Chem.* 2004; **15**: 1193-1200.
[59] Collman JP, Bröring M, Fu L, Rapta M, Schwenninger R and Straumanis A. *J. Org. Chem*. 1998; **63**: 8082-8083.
[60] Vrouenraets MB, Visser GWM, Stigter M, Oppelaar H, Snow GB and van Dongen GAMS. *Cancer Res*. 2001; **61**: 1970-1975.
[61] Vrouenraets MB, Visser GWM, Stigter M, Oppelaar H, Snow GB and van Dongen GAMS. *Int. J. Cancer* 2002; **98**: 793-798.
[62] Vrouenraets MB, Visser GWM, Loup C, Meunier B, Stigter M, Oppelaar H, Stewart FA, Snow GB and van Dongen GAMS. *Int. J. Cancer* 2000; **88**: 108-114.
[63] Casas C, Saint-Jalmes B, Loup C, Lacey CJ and Meunier B. *J. Org. Chem*. 1993; **58**: 2913-2917.
[64] Lu X-M, Fischman AJ, Stevens E, Lee TT, Strong L, Tompkins RG and Yarmush ML. *J. Immuno. Meth.* 1992; **156**: 85-99.
[65] Thorpe WP, Toner M, Ezzell RM, Tompkins RG and Yarmush ML. *Biophys. J*. 1995; **68**: 2198-2206.
[66] Wolfort SF, Reiken SR, Berthiaume F, Tompkins RG and Yarmush ML. *J. Surg. Res.* 1996; **62**: 17-22.
[67] Strong LH, Berthiaume F and Yarmush ML. *Laser Surg. Med.* 1997; **21**: 235-247.
[68] Sutton JM, Clarke OJ, Fernandez N and Boyle RW. *Bioconj. Chem.* 2002; **13**: 249-263.
[69] Malatesti N, Smith K, Savoie H, Greenman J and Boyle RW. *Int. J. Oncol.* 2006; **28**: 1561-1569.
[70] Hudson R, Carcenac M, Smith K, Madden L, Clarke OJ, Pèlegrin A, Greenman J and Boyle RW. *Br. J. Cancer* 2005; **92**: 1442-1449.
[71] Staneloudi C, Smith KA, Hudson R, Malatesti N, Savoie H, Boyle RW and Greenman J. *Immunol.* 2007; **120**: 512-517.
[72] Millgrom LR and O'Neill F. *Tetrahedron* 1995; **51**: 2137-2144.
[73] Oseroff AR, Ohuoha D, Hasan T, Bommer JC and Yarmush ML. *Proc. Natl. Acad. Sci. USA* 1986; **83**: 8744-8748.
[74] Oseroff AR, Ara G, Ohuoha D, Aprille J, Bommer JC, Yarmush ML, Foley J and Cincotta L. *Photochem. Photobiol*. 1987; **46**: 83-96.
[75] Rakestraw SL, Tompkins RG and Yarmush ML. *Bioconj. Chem.* 1990; **1**: 212-221.
[76] Rakestraw SL, Tompkins RG and Yarmush ML. *Proc. Natl. Acad. Sci. USA* 1990; **87**: 4217-4221.
[77] Rakestraw SL, Ford WE, Tompkins RG, Rodgers MAJ, Thorpe WP and Yarmush ML. *Biotechnol. Prog.* 1992; **8**: 30-39.
[78] Jiang FN, Jiang S, Liu D, Richter A and Levy JG. *J. Immunol. Meth.* 1990; **134**: 139-149.
[79] Jiang FN, Liu D, Richter A, Neyndorff H, Chester M, Jiang S and Levy JG. *J. Natl. Cancer Inst.* 1991; **83**: 1218-1225.
[80] Jiang FN, Allison B, Liu D and Levy JG. *J. Control Release* 1992; **19**: 41-58.
[81] Jiang FN, Liu D, Richter AM, Jain AK, Levy JG and Smits C. *Biotechnol. Ther*. 1993; **4**: 43-61.
[82] Hemming AW, Davis NL, Dubois B, Quenville NF and Finley RJ. *Surg. Oncol.* 1993; **2**: 187-196.
[83] Hamblin MR, Miller JL, Hasan T. *Cancer Res.* 1996; **56**: 5205-5210.
[84] Duska LR, Hamblin MR, Bamberg MP and Hasan T. *Br. J. Cancer* 1997; **75**: 837-844.
[85] Duska LR, Hamblin MR, Miller JL and Hasan T. *J. Natl. Cancer Inst.* 1999; **91**: 1557-1563.
[86] Molpus KL, Hamblin MR, Rizvi I, Hasan T. *Gynecol. Oncol.* 2000; **76**: 397-404.
[87] Governatore MD, Hamblin MR, Piccinini EE, Ugolini G and Hasan T. *Br. J. Cancer* 2000; **82**: 56-64.

[88] Hamblin MR, Governatore MD, Rizvi I and Hasan T. *Br. J. Cancer* 2000; **83**: 1544-1551.
[89] Governatore MD, Hamblin MR, Shea CR, Rizvi I, Molpus KG, Tanabe KK and Hasan T. *Cancer Res.* 2000; **60**: 4200-4205.
[90] Kopeček J, Kopečková P, Minko T and Lu Z-R. *Eur. J. Pharm. Biopharm.* 2000; **50**: 61-81.
[91] Omelyanenko V, Kopečková P, Gentry C, Shiah J-G and Kopeček J. *J. Drug Target.* 1996; **3**: 357-373.
[92] Omelyanenko V, Gentry C, Kopečková P and Kopeček J. *Int. J. Cancer* 1998; **75**: 600-608.
[93] Shiah J-G, Sun Y, Kopečková P, Peterson CM, Straight RC and Kopeček J. *J. Control Release* 2001; **74**: 249-253.
[94] Shiah J-G, Sun Y, Peterson CM and Kopeček J. *J. Control Release* 1999; **61**: 145-157.
[95] Lu Z-R, Kopečková P and Kopeček J. *Nature Biotechnol.* 1999; **17**: 1101-1104.
[96] Lu Z-R, Shiah J-G, Kopečková P and Kopeček J. *J. Control Release* 2001; **74**: 263-268.
[97] Houen G and Jensen OM. *J. Immunol. Meth.* 1995; **181**: 187-200.
[98] Winger TM, Ludovice PJ and Chaikof EL. *Biomat.* 1996; **17**: 437-441.
[99] Maurel F, Debart F, Cavelier F, Thierry AR, Lebleu B, Vasseur J-J and Vivès E. *Bioorg. Med. Chem. Lett.* 2005; **15**: 5084-5087.
[100] Endo M, Fujitsuka M and Majima T. *Tetrahedron* 2008; **64**: 1839-1846.
[101] Karapitta CD, Xenakis A, Papadimitriou A and Sotiroudis TG. *Chinica Chimica Acta* 2001; **308**: 99-106.
[102] Jain AK, Awasthi SK and Tandon V. *Bioorg. Med. Chem.* 2006; **14**: 6444-6452.
[103] Harapanhalli RS, Matalka KZ, Jones PL, Mahmood A, Adelstein SJ and Kassis AI. *Nuclear Med. Biol.* 1998; **25**: 267-278.
[104] Yoshitake S, Yamada Y, Ishikawa E and Masseyeff R. *Eur. J. Biochem.* 1979; **101**: 395-399.
[105] Harokopakis E, Childers NK, Michalek SM, Zhang SS and Tomasi M. *J. Immunol. Meth.* 1995; **185**: 31-42.
[106] Walker MA. *J. Org. Chem.* 1995; **60**: 5352-5355.
[107] Veronese FM and Morpurgo M. *IL Farmaco* 1999; **54**: 497-516.
[108] Hermanson GT. *Bioconjugation techniques*, Acedemic Press Inc, 1996; 148.
[109] Merritt JE and Loening KL. *Eur. J. Biochem.* 1980; **108**: 1-30.
[110] L. Milgrom. *The Colours of Life: An Introduction to the Chemistry of Porphyrins and Related Compounds*, Oxford University Press, 1997; 66-99.
[111] Rothemund P. *J. Am. Chem. Soc*. 1936; **58**: 625-627.
[112] Thomas DW and Martell AE. *J. Am. Chem. Soc.* 1956; **78**: 1335-1338.
[113] Fleischer EB. *Inorg. Chem.* 1962; **1**: 493-495.
[114] Adler AD, Longo FR, Finarelli JD, Goldmacher J, Assour J and Korsakoff L. *J. Org. Chem.* 1967; **32**: 476.
[115] Adler AD, Longo FR and Shergalis W. *J. Am. Chem. Soc*. 1964; **86**: 3145-3149.
[116] Adler AD, Sklar L, Longo FR, Finarelli JD and Finarelli MG. *J. Heterocycl. Chem.* 1968; **5**: 669-678.
[117] Little RG. *J. Heterocycl. Chem.* 1981; **18**: 833-834.
[118] Rousseau K and Dolphin D. *Tetrahedron Lett.* 1974; **48**: 4251-4254.
[119] Amaravathi M, Murthy KSK, Rao MK, and Reddy BS. *Tetrahedron Lett.* 2001; **42**: 6745-6747.
[120] Lindsey JS, Schreiman IC, Hsu HC, Kearney PC and Marguerettaz AM. *J. Org. Chem.* 1987; **52**: 827-836.
[121] Geier III GR and Lindsey JS. *Tetrahedron* 2004; **60**: 11435-11444.
[122] Giraudeau A, Callot HJ, Jordan J, Ezhar I and Gross M. *J. Am. Chem. Soc*. 1979; **101**: 3857-3862.
[123] Liu C, Shen D-M and Chen Q-Y. *Chem. Commun.* 2006; 770-772.
[124] Ali H and van Lier JE. *Tetrahedron Lett.* 1991; **32**: 5015-5018.
[125] Hombrecher HK, Gherdan VM, Ohm S, Cavaleiro JAS, Neves MGPMS and Condesso MF. *Tetrahedron* 1993; **49**: 8569-8578.
[126] Catalano MM, Crossley MJ, Harding MM and King LG. *J. Chem. Soc. Chem. Commun.* 1984; 1535-1536.
[127] Shea KM, Jaquinod L and Smith KM. *J. Org. Chem.* 1998; **63**: 7013-7021.
[128] Vodzinskii SV, Malinovskii VL, Ishkov YV, Zhilina ZI and Kirichenko AM. *Russ. J. Org. Chem.* 1997; **34**: 933-936.
[129] Catalano MM, Crossley MJ and King LG. *J. Chem. Soc. Chem. Commun.* 1984; 1537-1538.
[130] Bonfantini EE, Burrell AK, Campbell WM, Crossley MJ, Gosper JJ, Harding MM, Officer DL and Reid DCW. *J. Poprhyrins Phthalocyanines* 2002; **6**: 708-719.
[131] Momenteau M, Loock B, Bisagni E and Rougee M. *Can. J. Chem.* 1979; **57**: 1804-1813.
[132] Callot HJ, Schaeffer E, Cromer R, Metz F. *Tetrahedron* 1990; **46**: 5253-5262.
[133] Santos J, Illescas BM, Wielopolski M, Silva AMG, Tomé AC, Guldi DM and Martín N. *Tetrahedron* 2008; **64**: 11404-11408.
[134] Stephenson AWI, Wagner P, Partridge AC, Jolley KW, Filichev V, and Officer DL. *Tetrahedron Lett.* 2008; **49**: 5632-5635.

[135] Silva AMG, Tomé AC, Neves MGPMS, Silva AMS and Cavaleiro JAS. *J. Org. Chem.* 2002; **67**: 726-732.
[136] Silva AMG, Lacerda PSS, Tomé AC, Neves MGPMS, Silva AMS, Cavaleiro JAS, Makarova EA and Lukyanets EA. *J. Org. Chem.* 2002; **71**: 8352-8356.
[137] Welch C, Achibald SJ and Boyle RW. *Synthesis* 2009; **4**: 551-556.
[138] Brodney MA, Cole ML, Freemont JA, Kyl S, Junk PC, Padwa A, Riches AG and Ryan JH. *Tetrahedron Lett.* 2007; **48**: 1939-1943.
[139] Abedel-Magid AF, Carson KG, Harris BD, Maryanoff CA and Shah RD. *J. Org. Chem.* 1996; **61**: 3849-3862.
[140] Franek M, Diblikova I, Cernoch I, Vass M and Hruska K. *Anal. Chem.* 2006; **78**: 1559-1567.
[141] Tan K, Jaquinod L, Paolesse R, Nardis S, Di Natale C, Di Carlo A, Prodi L, Montalti M, Zaccheroni N and Smith K. *Tetrahedron* 2004; **60**: 1099-1106.
[142] Yamaguchi H, Tsubouchi K, Kawaguchi K, Horita E and Harada A. *Chem. Eur. J.* 2004; **10**: 6179-6186.
[143] Walter MG, Wamser CC, Ruwitch J, Zhao Y, Braden D, Stevens M, Denman A, Pi R, Rudine A and Pessiki PJ. *J. Porphyrin Phthalocyanines* 2007; **11**: 601-612.
[144]Alonso CMA, Palumbo A, Bullous AJ, Pretto F, Neri D and Boyle RW. *Bioconj. Chem.* 2010; **21**: 302-313.
[145] Takeuchi M, Chin Y, Imada T and Shinkai S. *Chem. Commun.* 1996; 1867-1868.
[146] Gust D, Moore TA, Moore AL, Legget L, Lin S, DeGraziano JM, Hermant RM, Nicodem D, Craig P, Seely GR and Nieman RA. *J. Phys. Chem.* 1993; **97**: 7926-7931.
[147] Würthner F, Vollmer MS, Effenberger F, Emele P, Meyer DU, Port H and Wolf HC. *J. Am. Chem. Soc.* 1995; **117**: 8090-8099.
[148] Frydman L, Olivieri AC, Diaz LE, Valasinas A and Frydman B. *J. Am. Chem. Soc.* 1988; **110**: 5651-5661.
[149] Oulmi D, Maillard P, Guerquin-kern J-L, Huel C and Momenteau M. *J. Org. Chem.* 1995; **60**: 1554-1564.
[150] Arsenault GP, Bullock E and MacDonald SF. *J. Am. Chem. Soc.* 1960; **82**: 4384-4389.
[151] Rao PD, Dhanalekshmi S, Littler BJ and Lindsey JS. *J. Org. Chem.* 2000; **65**: 7323-7344.
[152] Rao PD, Littler BJ, Geier III R and Lindsey JS. *J. Org. Chem.* 2000; **65**: 1084-1092.
[153] Gryko D and Lindsey JS. *J. Org. Chem.* 2000; **65**: 2249-2252.
[154] Yang Q, Streb KK and Borhan B. *Tetrahedron Lett.* 2005; **46**: 6737-6740.
[155] Fungo F, Otero LA, Sereno L, Silber JJ and Durantini EN. *Dyes and Pigments* 2001; **50**: 163-170.
[156] Milanesio ME, Morán FS, Yslas EI, Alvarez MG, Rivarola V and Durantini EN. *Bioorg. Med. Chem.* 2001; **9**: 1943-1949.
[157] Wang HM, Jiang JQ, Xiao JH, Gao RL, Lin FY and Liu XY. *Chemico-Biol. Interact.* 2008; **172**: 154-158.
[158] Liu X, Liu J, Jin K, Yang X, Peng Q and Sun L. *Tetrahedron* 2005; **61**: 5655-5662.
[159] Flamigni L, Ventura B, Tasior M and Gryko DT. *Inorg. Chim. Acta* 2007; **360**: 803-813.
[160] Feng X and Senge MO. *J. Chem. Soc. Perkin Trans*. 2001: 1030-1038.
[161] Biron E and Voyer N. *Chem. Commun.* 2005; **37**: 4652-4654.
[162] Ishikawa Y, Yamashita A and Uno T. *Chem. Pharm. Bull.* 2001; **49**: 287-293.
[163] *http://www.sigmaaldrich.com/catalog*
[164] Schuster DI, MacMahon S, Guldi DM, Echegoyen L and Braslavsky SE. *Tetrahedron* 2006; **62**: 1928-1936.
[165] Balaz M, Holmes AE, Benedetti M, Proni G and Berova N. *Bioorg. Med. Chem.* 2005; **13**: 2413-2421.
[166] Habadas J and Boduszek B. *J. Pept. Sci.* 2009; **15**: 305-311.
[167] Schneider R, Schmitt F, Frochot C, Fort Y, Lourette N, Guillemin F, Müller J-F and Barberi-Heyob M. *Bioorg. Med. Chem.* 2005; **13**: 2799-2808.
[168] Tomé JPC, Neves MGPMS, Tomé AC, Cavaleiro JAS, Soncin M, Magaraggia M, Ferro S and Jori G. *J. Med. Chem*. 2004; **47**: 6649-6652.
[169] Fazio MA, Lee OP and Schuster DI. *Org. Lett.* 2008; **10**: 4979-4982.
[170] Shi D-F, Wheelhouse RT, Sun D and Hurley LH. *J. Med. Chem.* 2001; **44**: 4509-4523.
[171] Zhou S. *J. Chromatogr. B* 2003; **797**: 63-90.
[172] Jin L-T and Choi J-K. *Electrophoresis* 2004; **25**: 2429-2438.
[173] Huber A, Demartis S and Neri D. *J. Mol. Recognit.* 1999; **12**: 198-216.
[174] Rich RL and Myszka DG. *J. Mol. Recognit*. 2001; **14**: 223-228.
[175] Borissevitch JE and Gandini SCM. *J. Photochem. Photobiol. B: Biol.* 1998; **43**: 112-120.
[176] Roberts MJ, Bently MD and Harris JM. *Adv. Drug Deliv.* 2002; **54**: 459-476.
[177] Thompson MS, Vadala TP, Valala ML, Lin Y and Riffle JS. *Polymer* 2008; **49**: 345-373.
[178] Zhang M, Li XH, Gong YD, Zhao NM and Zhang XF. *Biomaterials* 2002; **23**: 2641-2648.
[179] Hamblin MR, Miller JL, Rizvi I, Ortel B, Maytin EV and Hasan T. *Cancer Res.* 2001; **61**: 7155-7162.

[180] Sibrian-Vazquez M, Jenson TJ and Vicente GH. *J. Photochem. Photobiol. B: Biol*. 2007; **86**: 9-21.
[181] Sibrian-Vazquez M, Jenson TJ, Hammer RP and Vicente GH. *J. Med. Chem.* 2006; **49**: 1364-1372.
[182] Sibrian-Vazquez M, Jenson TJ and Vicente GH. *Bioconj. Chem.* 2007; **18**: 1185-1193.
[183] Nawalany K, Kozik B, Kepczynski M, Zapotoczny S, Kumorek M, Nowakowska M and Jachimska B. *J. Phys. Chem. B* 2008; **112**: 12231-12239.
[184] Zhang J-L, Huang J-S and Che C-M. *Chem. Eur. J*. 2006; **12**: 3020-3031.
[185] Mewis RE, Savoie H, Archibald SJ and Boyle RW. *Photodiag. Photodyn. Ther.* 2009; **6**: 200-206.
[186] Siejak A, Wróbel D, Laskowska B and Avlasevich YS. *Spec. Acta A–Mol. Biomol. Spec.* 2009; **74**: 148-153.
[187] Avlasevich YS, Kulinkovich OG, Knyukshto VN and Solov'ev N. *J. Appl. Spectro*. 1999; **66**: 597-601.
[188] Kim J-O, Lee Y-A, Jin B, Park T, Song R and Kim SK. *Biophys. Chem.* 2004; **111**: 63-71.
[189] Felix AM and Bandaranayake RM. *J. Peptide Res.* 2004; **63**: 85-90.
[190] Faustino MAF, Neves MGPMS, Vicente GH, Cavaleiro JAS, Neumann M, Brauer H-D and Jori G. *Photochem. Photobiol*. 1997; **66**: 405-412.
[191] Wang K, Fu S, Wu L and Li Z. *Mendeleev Commun.* 2007: **17**: 37-39.
[192] Sol V, Chaleix V, Champavier Y, Granet R, Huang Y-M and Krausz P. *Bioorg. Med. Chem*. 2006; **14**: 7745-7760.
[193] Sol V, Chaleix V, Granet R and Krausz P. *Tetrahedron* 2008; **64**: 364-371.
[194] Screen TEO, Blake IM, Rees LH, Clegg W, Borwick SJ and Anderson HL. *J. Chem. Soc. Pekin Trans.* 2002; **1**: 320-329.
[195] Suzuki A. *J. Organomet. Chem.* 1999; **576**: 147-168.
[196] Genet JP and Savignac M. *J. Organomet. Chem.* 1999; **576**: 305-317.
[197] Ishiyama T, Murata M and Miyaura N. *J. Org. Chem.* 1995; **60**: 7508-7510.
[198] Zhou X and Chan KS. *J. Org. Chem.* 1998; **63**: 99-104.
[199] Yu L and Lindsey JS. *Tetrahedron* 2001; **57**: 9285-9298.
[200] Tong LH, Pascu SI, Jarrosson T and Saunders JKM. *Chem. Commun.* 2006; 1085-1087.
[201] Yu L, Muthukumaran K, Sazanovich IV, Kirmaier C, Hindin E, Diers JR, Boyle PD, Bocian DF, Holten D and Lindsey JS. *Inorg. Chem*. 2003; **42**: 6629-6647.
[202] Aspley CJ and Williams JAG. *New J. Chem*. 2001; **25**: 1136-1147.
[203] Ishiyama T, Ishida K and Miyaura N. *Tetrahedron* 2001; **57**: 9813-9816.
[204] Tremblay-Morin J-P, Ali H and van Lier JE. *Tetrahedron Lett*. 2006; **47**: 3043-3046.
[205] Tron GC, Pirali T, Billington RA, Canonico PL, Sorba G and Genazzani AA. *Med. Res. Rev*. 2008; **28**: 278-308.
[206] Kolab HC, Finn MG and Sharpless KB. *Angew. Chem. Int. Ed*. 2001; **40**: 2004-2021.
[207] Rostovtsev VV, Green LG, Fokin VV and Sharpeless KB. *Angew. Chem. Int. Ed*. 2002; **41**: 2596-2599.
[208] Bock VD, Hiemstra H and and van Maarseveen JH. *Eur. J. Org. Chem*. 2006; **12**: 51-68.
[209] Shen D-M, Liu C and Chen Q-Y. *Eur. J. Org. Chem.* 2007; 1419-1422.
[210] Séverac M, Le Pleux L, Scarpaci A, Blart E and Odobel F. *Tetrahedron Lett*. 2007; **48**: 6518-6522.
[211] Punidha S, Sinha J, Kumar A and Ravikanth M. *J. Org. Chem*. 2008; **73**: 323-326.
[212] Iehl J, Osinska I, Louis R, Holler M and Nierengarten J-F. *Tetrahedron Lett*. 2009; **50**: 2245-2248.
[213] Hao E, Jenson TJ and Vicente GH. *J. Porphyrins Phthalocyanines* 2009; **13**: 51-59.
[214] Santos FC, Cunha AC, de Souza MCBV, Tomé AC, Neves MGPMS, Ferreira VF and Cavaleiro JAS. *Tetrahedron Lett.* 2008; **49**: 7268-7270.
[215] Lindsey JS. Synthesis *of meso-substituted porphyrins, The Porphyrin Handbook,* Academic Press, London, 2000; 53.
[216] Ravikanth M, Strachan J-P, Li F and Lindsey JS. *Tetrahedron* 1998; **54**: 7721-7734.
[217] Littler BJ, Ciringh Y and Lindsey JS. *J. Org. Chem.* 1999; **64**: 2864-2872.
[218] Ka J-W and Lee C-H. *Tetrahedron Lett*. 2000; **41**: 4609-4613.
[219] Maeda H, Hasegawa M and Ueda A. *Chem. Commun*. 2007; 2726-2728.
[220] Ikeda T, Shinkai S, Sada K and Takeuchi M. *Tetrahedron Lett.* 2009; **50**: 2006-2009.
[221] Wagner RW, Johnson TE, Li F and Lindsey JS. *J. Org. Chem*. 1995; **60**: 5266-5273.
[222] Murata M, Watanabe S and Masuda Y. *J. Org. Chem.* 1997; **62**: 6458-6459.
[223] Hyslop AG, Kellett MA, Iovine PM and Therien MJ. *J. Am. Chem. Soc*. 1998; **120**: 12676-12677.
[224] Mulder A, Huskens J and Reinhoudt DN. *Org. Biomol. Chem*. 2004; **2**: 3409-3424.
[225] Drain CM and Lehn J-M. *J. Chem. Soc. Chem. Commun*. 1994; 2313-2315.
[226] Lipstman S, Muniappan S and Goldberg I. *Cryst. Growth Des*. 2008; **8**: 1682-1688.
[227] Austin WB, Bilow N, Kelleghan WJ and Lau KSY. *J. Org. Chem*. 1981; **46**: 2280-2286.
[228] Mahmud IM, Zhou N, Wang L and Zhao Y. *Tetrahedron* 2008; **64**: 11420-11432.
[229] Leonard J, Lygo B and Procter G. *Advanced Practical Organic Chemistry second edition,* Stanely Thornes Ltd, 1998.

[230] Gottlieb HE, Kotlyar V and Nudelman A. *J. Org. Chem.* 1997; **62**: 7512-7515.